Regulation of biosynthesis and transport of strigolactones and their effect on plant development

Wouter Kohlen

Regulation of biosynthesis and transport of strigolactones and their effect on plant development

Wouter Kohlen

Thesis committee

Thesis supervisor
Prof. dr. ir. H.J. Bouwmeester
Professor of Plant Physiology
Wageningen University

Thesis co-supervisor
Dr. ir. C.P. Ruyter-Spira
Researcher at the Laboratory of Plant Physiology
Wageningen University

Other members
Prof. dr. H.M.O. Leyser, Cambridge University, UK
Prof. dr. A.H.J. Bisseling, Wageningen University
Prof. dr. C. Mariani, Radboud Universtiy Nijmegen
Dr. W.H. Vriezen, Nunhems BV, Haelen

This research was conducted under the auspices of the Graduate School of Experimental Plant Sciences

Regulation of biosynthesis and transport of strigolactones and their effect on plant development

Wouter Kohlen

Thesis
submitted in fulfilment of the requirements for the degree of doctor
at Wageningen University
by the authority of the Rector Magnificus
Prof. dr. M.J. Kropff,
in the presence of the
Thesis Committee appointed by the Academic Board
to be defended in public
on Friday 7 October 2011
at 4 p.m. in the Aula.

Wouter Kohlen
Regulation of biosynthesis and transport of strigolactones and their effect on plant development
192 pages.

Thesis Wageningen University, Wageningen, NL (2011)
With references, with summaries in English and Dutch

ISBN 978-94-6173-014-5

The research for this thesis was funded by the Netherlands Organization for Scientific Research (NWO; Vici grant, 865.06.002, and Equipment grant, 834.08.001, to Harro Bouwmeester) and was co-financed by the Centre for BioSystems Genomics (CBSG) which is part of the Netherlands Genomics Initiative/Netherlands Organisation for Scientific Research.

Financial support from Wageningen University, the Haselderheide foundation and Waters Corporation for printing this thesis is gratefully acknowledged.

"I'm a scientist and I know what constitutes proof. But the reason I call myself by my childhood name is to remind myself that a scientist must also be absolutely like a child. If he sees a thing, he must say that he sees it, whether it was what he thought he was going to see or not. See first, think later, then test. But always see first. Otherwise you will only see what you were expecting. Most scientists forget that. The reason I call myself Wonko the Sane is so that people will think I am a fool. That allows me to say what I see when I see it. You can't possibly be a scientist if you mind people thinking that you're a fool."

John Watson (Douglas Adams)

Contents

In loving memory of

Marjorie Kohlen-Janssen
(June 16, 1948 - November 18, 2008)
&
Henry John Deutschendorf, Jr
(December 31, 1943 - October 12, 1997)

Chapter 1

General introduction

This is an adapted version of:
Wouter Kohlen, Carolien Ruyter-Spira and Harro J. Bouwmeester, 2011. Strigolactones. A new musician in the orchestra of plant hormones. Accepted by Botany

Chemical communication

Communication between individuals belonging to the same species, as well as communication between individuals of different species is essential for all life on earth. Although plants are not able to speak, hear or see they communicate with their environment on a large scale. For this, plants use so-called secondary metabolites. An example of this communication can be seen when plants attract pollinating insects to their flowers by using specific fragrances. Although underground communication might be hard to imagine, the ability of a plant to adequately communicate in the rhizosphere is of vital importance. For instance, a plant needs to be able to attract nematodes to pray on insects feeding on its root system (Rasmann et al., 2005) or establish symbiosis with the nitrogen fixing bacteria *Rhizobium* (Albrecht and Bisseling, 1998; Limpens and Bisseling, 2003). In these signaling processes precise regulation is mandatory as nematodes only need to be attracted when the root system of a plant is being preyed upon and *Rhizobium* is only able to colonizes roots of specific legumes.

Root parasitic plants of the *Orobanchaceae*

Parasitic plants are plants that obtain some or all of their assimilates, water and nutrients from another plant (the host). In the plant kingdom parasitism has evolved several different times, leading to approximately 4100 species divided over roughly 19 families of flowering plants (Nickrent and Musselman, 2004). Parasitic plants display great phenotypic plasticity, have a wide environmental tolerance and can attach to their host on several different organs. Root parasites are parasitic plants that attach to the roots of their host. The family of *Orobanchaceae* consists of 90 genera (e.g. *Orobanche spp*, *Phelipanche spp* and *Striga spp*) and totals approximately 1800 species (Nickrent and Musselman, 2004). These species can be divided into two types of parasites, hemi- and holoparasites depending on their ability to produce chlorophyll. Hemiparasites contain chlorophyll and - to some extent – can perform photosynthesis. However most of their carbohydrates are derived from their host. Holoparasites on the other hand have no chlorophyll and as a consequence they are completely dependent on their host (Nickrent and Musselman, 2004). Only their attachment to the root system of a suitable host plant enables them to get access to the nutrients needed for completion of their lifecycle, which they steal from their host.

The parasitic plant problem

Some of the root parasites mentioned above are among the most damaging pests in agriculture known to date. For example from the *Striga spp*. *Striga hermonthica* (figure 1a), *S. asiatica* (figure 1b), *S. aspera* and *S. forbesii* parasitize cereal crops such as rice, sorghum and maize (Parker and Riches, 1993; Oswald, 2005). Although *Striga spp*. are hemiparasites - and thus have green leaves - they are unable to perform sufficient photosynthesis for their survival (Shah *et al.*, 1987) and are therefore dependent on their host plant for obtaining most of their carbohydrates (Press et al., 1987; Press and Gurney, 2000). In addition, these parasites exhibit elevated transpiration rates enabling them to obtain even larger quantities of water and nutrients from their host (Musselman, 1980). The Food and Agricultural Organization of the United Nations (FAO) (http://www.fao.org/) estimated that 40%

Figure 1: Striga spp growing on rice **(a)** Striga hermonthica, **(b)** Striga asiatica (photographs taken by Peter Tóth)

of the land used for cereal production in Africa is infested with *Striga*, negatively affecting the lives of hundreds of millions of people (Scholes and Press, 2008; Parker, 2009). Some experts even believe that the Striga infection is the biggest obstacle for achieving a stable food production in Africa and is therefore responsible for the famine of millions.

In addition, from the more than 100 *Orobanche/Phelipanche spp* only *Phelipanche* (*Orobanche*) *ramosa* (figure 2a) (Joel, 2009), *Orobanche cumana* (figure 2b), *Orobanche crenata* (figure 2c) and *Orobanche aegyptiaca* (figure 2d) parasitise agricultural crops such as legumes, solanaceae and brassicaceae (Parker, 1994; Bouwmeester et al., 2003). The most notorious of these parasites is *P. ramosa*. It is known to parasitize on plants from eleven different dicot families - including species like carrot (*Daucus carota*), aubergine (*Solanum melongena*), hemp (*Cannabis sativa*), lentil (*Lens culinaris*), potato (*Solanum tuberosum*), tomato (*Solanum lycopersicum*) and tobacco (*Nicotiana tabacum*) (Parker and Riches, 1993; Musselman, 1994; Buschmann et al., 2005) - which is more than any other broomrape. Most host plants of the *Orobanche/Phelipanche spp* are of great economic importance. As such, *Orobanche/Phelipanche* infestation is not threatening basic food production and should be considered more of an economical problem.

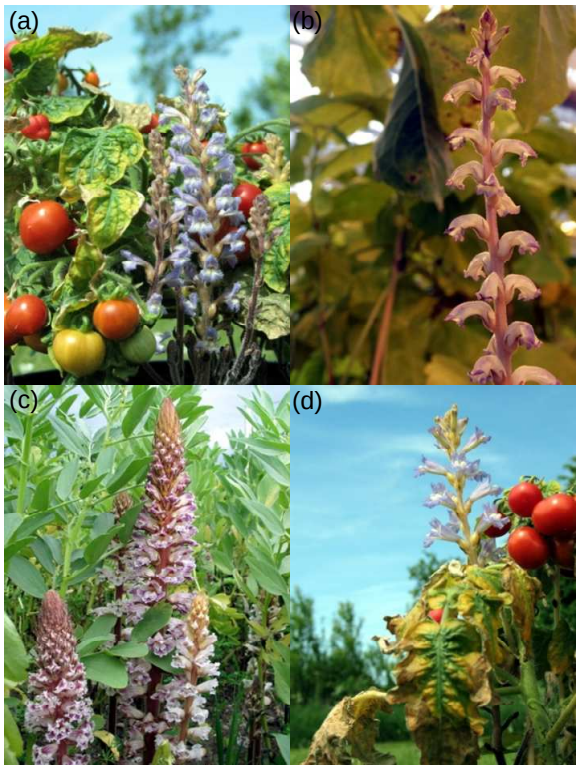

Figure 2: Orobanche/Phelipanche spp (photographs taken by Peter Tóth) **(a)** Phelipanche ramosa growing on tomato, **(b)** Orobanche Cumana growing on sunflower, **(c)** Orobanche crenata growing on faba bean, **(d)** Orobanche aegyptiaca growing on tomato

Germination of root parasites

One of the important phases in the lifecycle of these parasitic plants is the germination of their seeds. These seeds are very small and contain only minimal reserves. After germination, attachment to the root of a host plant needs to be established within days or the seedling will perish. To accomplish this, root parasites have evolved an elegant strategy, enabling them to cope with his dilemma. Their germination is unconditionally dependent on compounds secreted by the roots of the host plants. In the early sixties of the last century it was discovered that these germination stimulants are strigolactones (Cook et al., 1966; Cook et al., 1972). The seeds of root parasites are extremely sensitive to strigolactones as they are able to induce germination of parasitic plant seeds in minute concentrations (10^{-8} to 10^{-12} M) (Bouwmeester et al., 2003; Hirsch et al., 2003; Bouwmeester et al., 2007).

Why do host-plants produce strigolactones?

Strigolactones have been detected in the root extracts and exudates of many monocot as well as dicot plant species (Yoneyama et al., 2007; Goldwasser et al., 2008; Gomez-Roldan et al., 2008; López-Ráez et al., 2008; Umehara et al., 2008). The first evolutionary advantage for the conservation of these seemingly disadvantageous rhizosphere signaling molecules was identified only 40 years later when it was discovered that strigolactones are the pre-symbiotic branching factors for

arbuscular mycorrhizal (AM) fungi (Akiyama *et al.*, 2005; Besserer *et al.*, 2006). This discovery suggests that the beneficial role of the strigolactones in attracting AM fungi outweighs the negative consequences of the attraction of the parasitic plants and shows that the strigolactones have a dual role in rhizosphere communication (Bouwmeester et al., 2007).

In the same year as the discovery of the AM fungi hyphal branching activity of the strigolactones, it was demonstrated that the strigolactones biosynthetically originate from the carotenoids (Matusova *et al.*, 2005). The authors postulated that oxidative cleavage by a carotenoid cleavage dioxygenase (CCD) or 9-*cis*-epoxycarotenoid dioxygenase (NCED) followed by intra-molecular rearrangement and functionalization by one or more cytochrome P450s and/or other enzymes are involved in the biosynthesis of the strigolactones known at that moment (Matusova *et al.*, 2005) (figure 3). Intriguingly, right about at the same time the plant research community was trying to identify a novel unknown carotenoid-derived plant hormone involved in the inhibition of shoot branching (Turnbull et al., 2002; Sorefan et al., 2003; Booker et al., 2004; Booker et al., 2005; Auldridge et al., 2006). This elusive new plant growth regulator was shown to be a mobile, long-distance signal, which moves acropetally (Turnbull et al., 2002; Sorefan et al., 2003; Booker et al., 2005). In Arabidopsis (*Arabidopsis thaliana*) four genes were found to be involved in the formation and downstream signaling of this novel plant hormone. The carotenoid cleavage dioxygenase *MORE AXILLARY GROWTH3* (*MAX3*; *AtCCD7*), *MAX4* (*AtCCD8*), and the cytochrome P450 *MAX1* (*AtCyp711A1*) were shown to be involved in its biosynthesis (Turnbull et al., 2002; Sorefan et al., 2003; Booker et al., 2004; Booker et al., 2005; Auldridge et al., 2006), whereas the leucine rich repeat (LRR) F-box protein MAX2 was shown to have a role in the perception of the signal (Stirnberg et al., 2002; Stirnberg et al., 2007). Orthologs for all *MAX* genes, except *MAX1*, were found in other plant species e.g. *Pisum sativum* (pea; *RMS1 (PsCCD8), RMS5 (PsCCD7)* and *RMS4 (F-box)* (Beveridge *et al.*, 1996; Morris *et al.*, 2001), *Oryza sativa* (rice; *D10 (OsCCD8), HTD1 (OsCCD7)* and *D3 (F-Box*) (Zou et al., 2006; Arite et al., 2007; Yan et al., 2007) and *Petunia hybrida* (*DAD1 (PhCCD8)* and *DAD3 (PhCCD7) (Simons et al., 2007)*.

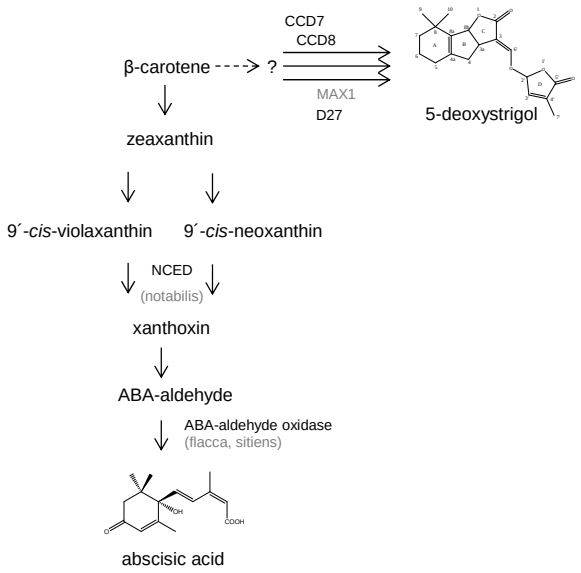

Figure 3. Schematic representation of the abscisic acid and strigolactone biosynthetic pathways. Abbreviations: ?, unidentified carotenoid substrate; CCD7 and CCD8, carotenoid cleavage dioxygenase 7 and 8; MAX1, more axillary growth 1; D27, DWARF27; NCED, 9-*cis*-epoxycarotenoid dioxygenase; ABA, abscisic acid (adapted from López-Raéz et al., 2010).

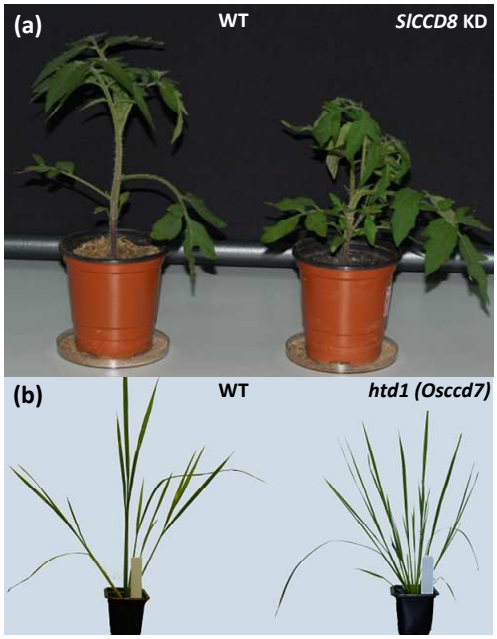

Figure 4: Branching phenotype of strigolactone deficient mutants **(a)** Tomato CV Craigella and *SlCCD8* KD (photograph taken by Juan Antonio López Raéz) **(b)** Rice WT and *htd1/Osccd7* (photograph taken by Muhammad

Plants mutated in any of these genes all display increased numbers of shoot branches (Figure 4a) or tillers (in rice, Figure 4b). The efforts to elucidate the strigolactone biosynthetic pathway and the search for the unknown branching inhibiting signal merged in 2008, when strigolactones – or their derivatives – were shown to be this elusive branching inhibiting signal (Gomez-Roldan *et al.*, 2008; Umehara *et al.*, 2008).

Strigolactone biosynthesis, what do we know?

The first steps in strigolactone biosynthesis were identified in 2008. It was demonstrated by MRM-LC-MS/MS analysis that *ccd8* and *ccd7* mutants in pea and rice produced no or strongly reduced levels of strigolactones. The branching phenotype of the mutants could be complemented by exogenous application of the synthetic strigolactone analogue GR24. This work hence identified CCD7 and CCD8 as part of the strigolactone biosynthetic pathway (Gomez-Roldan et al., 2008; Umehara et al., 2008)(Figure 3). The highly branched phenotype of Arabidopsis plants mutated in *MAX1* (Stirnberg et al., 2002; Booker et al., 2005), could also be rescued by GR24 application (Gomez-Roldan et al., 2008). However, the authors did not provide analytical proof for the involvement of MAX1 in strigolactone biosynthesis. Interestingly, no *MAX1* orthologs have been identified in other species than Arabidopsis whereas orthologs for *MAX3 (CCD7)* and *MAX4 (CCD8)* have been identified in several other monocot and dicot species (Snowden et al., 2005; Zou et al., 2006; Arite et al., 2007; Ledger et al., 2010; Vogel et al., 2010; Proust et al., 2011). This could imply that in other species *MAX1* is not a single copy gene. This possible redundancy would make *MAX1* identification through genetics approaches difficult. Indeed, in rice several putative *MAX1* homologs were reported (Nelson et al., 2004; Umehara et al., 2010). Moreover, a *MAX1* homolog was found in the unicellular green algae *Chlamydomonas reinhardtii* (Nelson et al., 2004). However, it has been reported that in the moss *Physcomitrella patens* genome no *MAX1* homolog can be found (Proust et al., 2011).

A fourth step in the biosynthetic pathway, encoded by *DWARF27* (*D27*), was identified in 2009. Although the precise function of this iron containing protein remains unknown, no strigolactones were detected in lines mutated in this gene (Lin et al., 2009). At the moment no *D27* ortholog has been identified in any other plant species, but homologous sequences were found in the National Center for Biotechnology Information (NCBI) database and The Institute for Genomic Research (TIGR) plant transcript assemblies for many plant species (Lin et al., 2009).

Considering the complexity of the strigolactone molecules it is likely that more genes than the four discussed above are required for their biosynthesis. An example is the putative D-ring coupling enzyme postulated by Matusova et al (2005) for which so far no candidate has been identified. Indeed, no additional biosynthesis mutants have been reported in any plant species. Considering the absence of ortholog mutants in the strigolactone model species rice and pea, in the proven biosynthetic gene *MAX1*, it is not unlikely that there is also redundancy in additional strigolactone biosynthesis genes, making their identification through reverse genetics difficult. 5-Deoxystrigol and 2'-epi-5-deoxystrigol are believed to be the first true strigolactones in the biosynthetic pathway from which all other strigolactones can be derived by hydroxylation, acetylation and/or oxidation (Figure 5) (Matusova et al., 2005; Humphrey et al., 2006; Rani et al., 2008). However, also these enzymes so far remain unknown. It has been reported that there is variation in biological activity between structurally different strigolactones in AM fungi hyphal branching (Akiyama et al., 2010) and germination of root parasitic plants (García-Garrido et al., 2009; Yoneyama et al., 2009; Xie et al., 2010) and similar claims were made for shoot branching (Yamaguchi, 2010 IPGSA conference) so the elucidation of the functionalizing enzymes downstream of 5-deoxystrigol and 2'-epi-5-deoxystrigol is highly relevant.

The strigolactones are biosynthetically derived from the carotenoids (Matusova et al., 2005).

Carotenoids are tetraterpenoid organic pigments that are naturally occurring in the chloroplasts and chromoplasts of plants and some other photosynthetic organisms like algae (Walter and Strack, 2011). CCD7, CCD8 and D27 are functioning in the plastids (Schwartz et al., 2004; Lin et al., 2009),

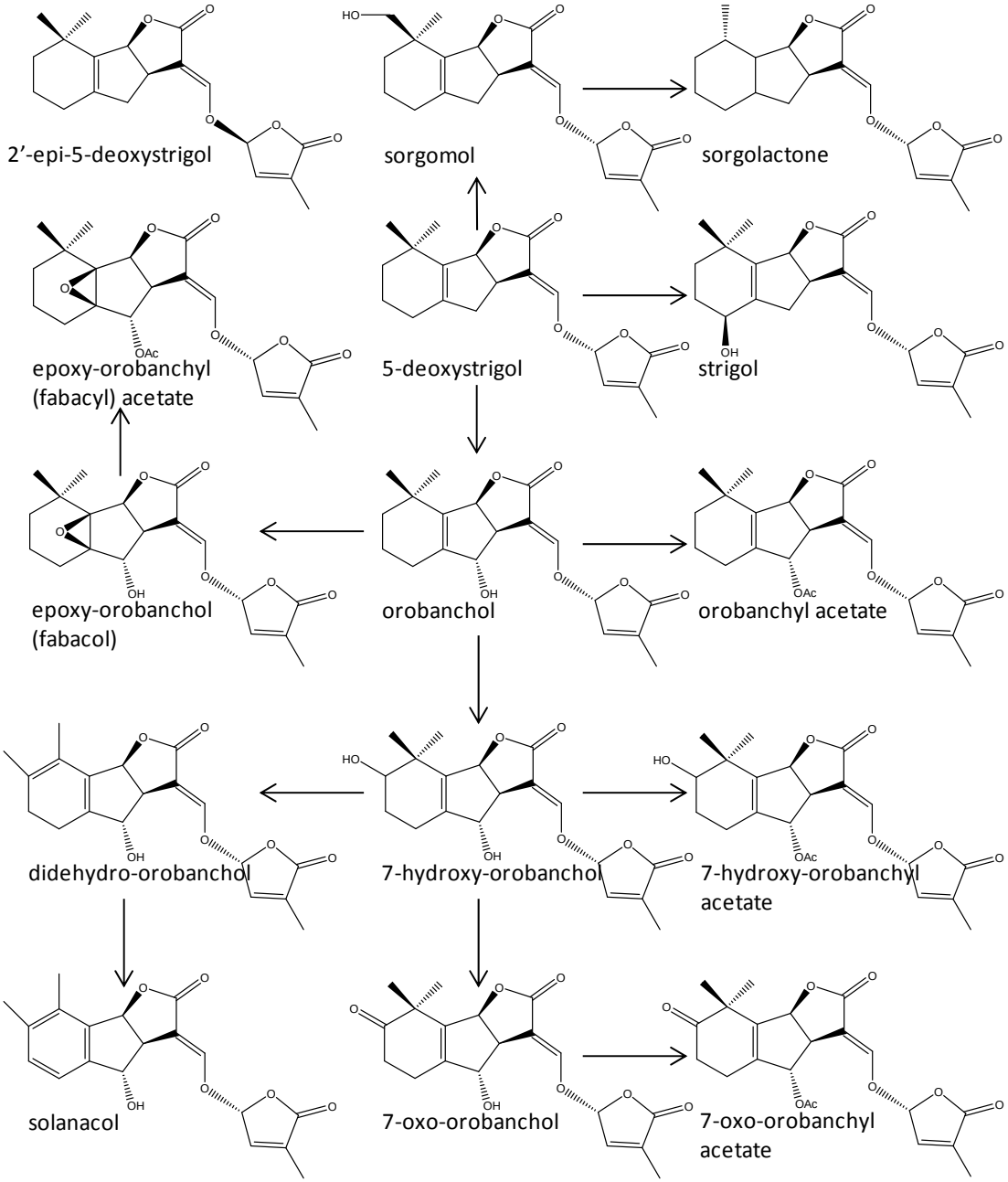

Figure 5: Some of the strigolactones identified up to date and postulated biosynthetic relationships. (adapted from Rani et al., 2008 and Xie et al., 2010). The D-ring can also be coupled 2'-epi, leading to a series of 2'-epi-isomers such as 2'-epi-strigol, 2'-epi-orobanchol, etc (only 2'-epi-5-deoxystrigol shown) (see Xie et al., 2010).

whereas MAX1 is likely bound to the cytoplasmic surface of the endoplasmic reticulum (ER), where most cytochrome P450 enzymes are believed to be located (Mizutani and Ohta 2010). The tissue localization of strigolactone biosynthesis, however, remains elusive. It is thought that a part of the total strigolactones pool is synthesized in the roots and that they are either exuded into the rhizosphere or transported to the shoot where they exert their inhibitory effect on shoot branching. However, biosynthesis of the strigolactones – of which we assume they function in the shoot - is not limited to the root system as grafting studies indicate that inter stock grafting with only a small part

of the wild-type hypocotyl is sufficient to restore branching in biosynthetic mutants to near wild-type (Foo et al., 2001). The expression of strigolactone biosynthesis genes is also not limited to the root system (Sorefan et al., 2003; Booker et al., 2004; Booker et al., 2005), leaving the exact origin of strigolactones present in the shoot unknown. Still, transport through the plant is definitely required and the xylem is likely to be involved.

Strigolactone signaling

A strigolactone signaling mutant is fully capable of strigolactone biosynthesis. However, it is unable to perceive or respond to strigolactones. So far two genes involved in strigolactone signaling have been identified, *MAX2* and *D14*. The highly branched Arabidopsis *max2* mutant could not be complemented by GR24 application (Gomez-Roldan et al., 2008; Umehara et al., 2008) and strigolactone levels in Arabidopsis *max2* and the ortholog mutants in both rice (*d3*) and pea (*rms4*) were not reduced (Gomez-Roldan et al., 2008; Umehara et al., 2008; Kohlen et al., 2011). On the contrary, the strigolactone levels in *max2* and *d3* were significantly higher than in the corresponding wild-types (Umehara et al., 2008), suggesting feedback up-regulation of strigolactone biosynthesis through MAX2. Indeed, in the Arabidopsis *max* mutants, *CCD7* and *CCD8* expression were up-regulated and these elevated expression levels could be reduced by GR24 application in all lines except *max2* (Mashiguchi et al., 2009). As mentioned above, *MAX2* encodes a member of the large family of LRR F-box proteins which suggests MAX2 participates in an SCF complex (Stirnberg et al., 2002; Stirnberg et al., 2007). An SCF complex is a receptor complex that consists of several proteins e.g. SKP, CULLIN and an F-box protein. This complex - after being activated by the specific plant hormone - targets repressors of gene expression for degradation enabling the RESPONSE FACTORs (RFs) to initiate the appropriate transcriptional response. Similar complexes have been identified in the perception of other plant hormones e.g SCF^{TIR1} for auxin and SCF^{GID2} for gibberellic acid (Gomi et al., 2004; Dharmasiri et al., 2005). The fact that the *max2* phenotype cannot be complemented by GR24 and that MAX2 is an F-box protein belonging to the same protein family as the auxin receptor TIR1 (Dharmasiri et al., 2005) makes *max2* a strigolactone signaling mutant and MAX2 a candidate for the strigolactone receptor. However, no proof for this has been published to date.

The second putative strigolactone receptor encoding gene was identified in rice. In cv. Lansheng, *DWARF14* (*D14*) and the allelic *DWARF88* (*D88*) in cv Shiokari were identified to be part of the strigolactone signaling pathway (Arite et al., 2009; Gao et al., 2009). The gene was cloned and identified as a member of the α/β-hydrolase superfamily with putative esterase activity. Two *D14* homologs (At3g03990, At4g37470) were found in Arabidopsis based on sequence homology (Arite et al., 2009). Similar to *d3/max2*, elevated strigolactone levels were detected in *d14* and exogenous application of GR24 or strigol could not restore the branching phenotype (Arite et al., 2009), placing D14 downstream of strigolactone biosynthesis. Arite et al. (2009) postulated that *D14* is part of the signaling cascade leading towards strigolactone response as other members of this α/β-hydrolase family have been shown to be directly involved in the binding and perception of gibberellic acid (Ueguchi-Tanaka et al., 2005) . However, if an unidentified strigolactone derivative is the biologically active compound in the inhibition of shoot branching, D14 could also be involved in the biosynthesis of this derivative, rather than in signaling. Grafting of a *d14* scion on wild-type roots would have provided evidence for the exact role of *D14*, but due to technical limitations these experiments were not conducted (Arite et al., 2009). Hence, even though the exact function of D14 so far remains unknown it is a candidate for the strigolactone receptor just as MAX2.

Strigolactone function in shoot architecture, two hypotheses to test

Seeds plants are able to adapt their architecture in order to cope with changing environmental

conditions. To a large extent this plasticity is achieved by post-embryonic initiation of axillary meristems. These meristems recapitulate the function of the shoot apical meristem by initiating several leaf primordia, resulting in the formation of axillary buds, which either grow out or remain dormant, depending on their position along the shoot axis, the developmental phase of the plant and environmental factors (Bennett and Leyser, 2006). As mentioned above, strigolactones were recently identified as the branch-inhibiting signal (Gomez-Roldan et al., 2008; Umehara et al., 2008). They are believed to interact with auxin in regulating apical dominance, a process which also involves cytokinins (Ferguson and Beveridge, 2009). There are two main hypotheses on how strigolactones can be integrated into the apical dominance theory; the canalization (Figure 6a) and the second messenger (Figure 6b) hypothesis. Both hypotheses have their pros and cons (Brewer et al., 2009; Crawford et al., 2010).

The canalization hypothesis

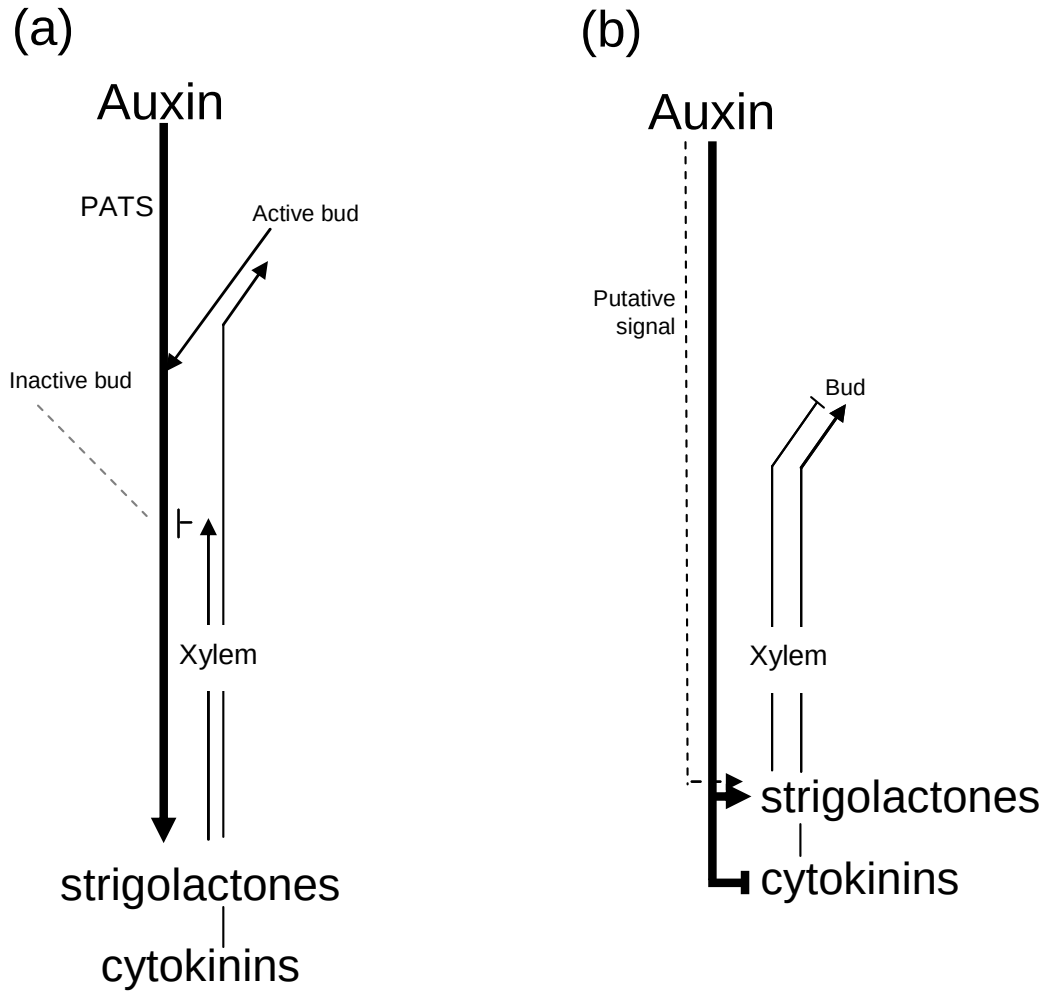

Figure 6: Hypotheses for strigolactone integration in the control of shoot branching. **(a)** canalization hypothesis **(b)** second messenger hypothesis.

This hypothesis states that the limited capacity of the polar auxin transport system (PATS) to transport auxin from the shoot apical meristem to the root system is sufficient to control the outgrowth of lateral buds, as the buds cannot export auxin and hence remain dormant ((Leyser, 2009; Domagalska and Leyser, 2011)). When auxin transport capacity becomes available and buds can export auxin this will result in bud outgrowth. This occurs when the apical auxin source is

removed, the apical auxin production decreases or the transport capacity of the PATS increases. When the auxin can be exported from the bud a sequence of events is triggered that leads to the connection of the bud to the main vascular system, enabling outgrowth. In the canalization hypothesis cytokinins promote bud outgrowth but can only enter the bud when the connection to the main vascular system has been established (Stirnberg et al., 2010). The canalization hypothesis is based on the observation that in the highly branched *max* mutants PIN mediated auxin transport is elevated and that the branching phenotype can be rescued by application of the auxin transport inhibitor 1-N-naphthylphthalamic acid (NPA) (Bennett et al., 2006). PIN (PIN-FORMED) proteins comprise a family of membrane bound auxin efflux carriers that facilitate the directional cell to cell transport of auxin (Friml et al., 2002; Friml et al., 2003; Blilou et al., 2005).
In favor of the canalization hypothesis, computer modeling showed that it is possible to fully explain the outgrowth of lateral buds with auxin transport capacity (Prusinkiewicz et al., 2009). Furthermore, it was demonstrated that polar auxin transport can be reduced by GR24 application or by induced endogenous strigolactone biosynthesis in a *max1* background and that this leads to a competition in bud outgrowth of Arabidopsis mediated through differences in auxin transport capacity (Crawford et al., 2010). Combined, these results indicate a direct correlation between strigolactone levels, auxin transport capacity and bud outgrowth.
It has been suggested that the observed increase in auxin transport in strigolactone mutants is the consequence of their higher auxin level (Bainbridge et al., 2005; Dun et al., 2006; Arite et al., 2007). Indeed, GR24 application to the roots of Arabidopsis seedlings led to a reduction in free auxin levels in the leaves (Ruyter-Spira et al., 2011) and auxin is known to induce its own transport (Vieten et al., 2005). However, changes in pPIN1::PIN1-GFP intensities in the stem were observed in Arabidopsis within 6 h after GR24 application (Crawford et al., 2010) making it less likely that strigolactones regulate the PATS through auxin biosynthesis. Indeed, auxin accumulation after the application of the auxin transport inhibitor NPA also led to reduced auxin biosynthesis through negative feedback, eventually reducing auxin levels (Ljung et al., 2001).

The second messenger hypothesis
This second hypothesis assumes that auxin induces the biosynthesis of a second messenger (strigolactones) that inhibits bud outgrowth directly (Brewer et al., 2009). The inhibiting effect of strigolactones on bud outgrowth can also occur in the presence of cytokinins, making the integration of these plant hormones into the model slightly different. In this model strigolactones are believed to act downstream of auxin and the ratio between strigolactones and cytokinins determine the buds fate (Brewer et al., 2009). A reduction in the auxin level will lead to a reduced concentration of the second messenger enabling lateral buds to grow out (Brewer et al., 2009). In line with this hypothesis, *CCD8* expression is up-regulated when auxin is applied to both pea and Arabidopsis (Sorefan et al., 2003; Bainbridge et al., 2005). However, direct (analytical) evidence for the up-regulation of strigolactone biosynthesis by auxin is not only absent, this auxin mediated up-regulation is also required in the canalization hypothesis. In order to make the second messenger hypothesis work, a third, rapid, signal has been proposed to exist. This signal is sent from the shoot to the root immediately after decapitation initiating - within one hour – to initiate the appropriate responses, including the decreased expression of the strigolactone biosynthesis genes. The signal has been proposed to be electrochemical as auxin is assumed to move too slow to be this signal (Morris et al., 2005; Ferguson and Beveridge, 2009). Most recently it was demonstrated that depletion of auxin by stem girdling alone does not lead to lateral shoot outgrowth, whereas decapitation always does (Ferguson and Beveridge, 2009) supporting the existence of an additional signal besides auxin. However, no direct evidence has been presented for the existence of this additional signal (Waldie et

al., 2010). The strongest evidence supporting the second messenger hypothesis is the fact that in pea the growth of branches up to five centimeters in length can be arrested by GR24 application even though canalization is already completed (Brewer et al., 2009). Furthermore, exogenous application of auxin to wild-type plants demonstrated that the auxin transport capacity in these plants was not saturated, a condition assumed to be necessary in the canalization theory (Brewer et al., 2009). However, in contradiction of the second messenger hypothesis, solitary buds receiving an excessive amount of GR24 were not inhibited in their growth (Crawford et al., 2010), suggesting that strigolactones by themselves are not able to keep a bud dormant.

Many of the experiments that are done to obtain evidence for one hypothesis seem to produce results that refute the other. The exact role of strigolactones in this aspect of plant development will probably be solved in the near future, as many resources are being devoted to solving this outstanding dispute. Final proof for the second messenger hypothesis can only come from detection of strigolactones – or their derivatives - in dormant buds, but so far this has not been demonstrated. Perhaps it will turn out that neither of the hypotheses is wrong as they are perhaps not mutually exclusive.

Outline of this thesis

The objective of the research presented in this thesis was to get a detailed insight in the hormonal regulation of strigolactone biosynthesis. Our working hypothesis was that by understanding the regulation of strigolactone biosynthesis we would be able to find new methods to control the root parasitic plant problem. With the discovery of their hormonal properties - in 2008 – a new dimension was added to the complexity of this problem. To alter strigolactone biosynthesis without seriously compromising plant development our understanding of how and where strigolactones function became vital. For this reason our objectives were expanded, broadening the scope of this thesis to the regulation of strigolactone biosynthesis, including their transport and function in the plant as – considering their new endogenous role - for control of the root parasitic plant problem not only the biosynthesis of strigolactones should be controlled but also their movement in and out of the plant.

Chapter 1 introduces the root parasitic plants of the Orobanchaceae family and the problems they cause in agriculture. Rhizosphere communication is addressed as the role of strigolactones in the lifecycle of root parasite as well as in arbuscular-mycorrhiza symbiosis is highlighted. In addition, their function in shoot architecture, biosynthesis and hormonal signaling as well as two theories how to integrate strigolactones into the apical dominance theory are described. A modified version of this work has been accepted for publication by Botany. **Kohlen W**, Ruyter-Spira C and Bouwmeester HJ (2011) Strigolactones. A new musician in the orchestra of plant hormones.

Chapter 2 describes strigolactone biosynthesis in tomato. Here we focus on the hypothesis that all strigolactones are derived from 5-deoxystrigol and especially emphasize the biosynthesis of tetradehydro-orobanchol (solanacol). Submission of a modified version of this work is in preparation. **Kohlen W**, Charnikhova T, Hooft van der J, López-Ráez JA, Liu W, Mulder P, Zwanenburg B, Geurts R, Vervoort J and Bouwmeester HJ (2011).

Chapter 3 presents the effect of *SlCCD8* knock-down on strigolactone levels, rhizosphere interactions (with arbuscular mycorrhiza fungi and *P. ramosa*), vegetative and generative development, and the interplay of strigolactones and auxin are assessed. In addition, the cloning of the tomato CAROTENOID CLEAVAGE DIOXYGENASE 8 is described. A modified version of this work has been

submitted to the Plant Journal. **Kohlen W**, López-Ráez JA, Pollina T, Lammers M, Toth P, Charnikhova T, Maagd de R, Pozo MJ, Bouwmeester HJ and Ruyter-Spira C (2011) The tomato *CAROTENOID CLEAVAGE DIOXYGENASE8 (SlCCD8)* is regulating, rhizosphere signaling, plant architecture and reproductive development through strigolactone biosynthesis.

Chapter 4 addresses the question if the other carotenoid derived phytohormone abscisic acid (ABA) has a role in the regulation of strigolactone biosynthesis. For this - the well described - ABA deficient tomato mutants; *notabilis*, *flacca* and *sitiens* are analyzed for their strigolactone content. In addition, inhibitors for ABA (abamineSG) and strigolactone (D2) biosynthesis are used to investigate their short term effect on strigolactone biosynthesis. This work has been published as López-Ráez JA, **Kohlen W**, Charnikhova T, Mulder P, Undas AK, Sergeant MJ, Verstappen F, Bugg TDH, Thompson AJ, Ruyter-Spira C, Bouwmeester HJ (2010) Does abscisic acid affect strigolactone biosynthesis? New Phytologist 187: 343-354

Chapter 5 presents a study on transcription factors - the symbiotic GRAS-type transcription factors NODULATION SIGNALING PATHWAY1 (NSP1) and NSP2 - in strigolactone biosynthesis. These transcription factors are essential for rhizobium root nodule formation in legumes. We identified *MtDWARF27* and demonstrate its transcriptional regulation under nutrient deficiency. For this we introduce *Medicago truncatula* as a model plant for strigolactone analysis. A modified version of this work has been accepted for publication by the Plant Cell. Liu W, **Kohlen W**, Lillo A, Camp op den R, Ivanov S, Hartog M, Limpens E, Jamil M, Smaczniak C, Kaufmann K, Yang WC, Hooiveld G, Charnikhova T, Bouwmeester HJ, Bisseling T and Geurts R (2011) Strigolactone biosynthesis requires the sybiotic gras-type transcription factors NSP1 and NSP2.

Chapter 6 presents a study on strigolactone biosynthesis in *Arabidopsis thaliana*. The role of MAX1 and MAX4 in strigolactone biosynthesis was investigated using analytical tools. In addition the relation between phosphate starvation, strigolactone biosynthesis and plant architecture was assessed as well as the role of the xylem in strigolactone transport. This work was published as **Kohlen W**, Charnikhova T, Qing L, Bours R, Domagalska MA, Beguerie S, Verstappen F, Leyser O, Bouwmeester HJ, Ruyter-Spira C (2010) Strigolactones are transported through the xylem and play a key role in shoot architectural response to phosphate deficiency in non-AM host Arabidopsis thaliana. Plant physiology 155(2): 974-987

Chapter 7 presents a study on the role of strigolactones in root architecture in *Arabidopsis thaliana*. For this, primary and lateral root development of the strigolactone deficient Arabidopsis mutants *max1,2,4* and their corresponding wild-type (col-0) is analyzed. Both under phosphate-sufficient as limited conditions. The effect of GR24 application on root development, PIN levels and auxin content in the shoot are investigated. This work has been published as Ruyter-Spira C, **Kohlen W**, Charnikhova T, Zeijl van A, Bezouwen van L, de Ruijter N, Cardoso C, López-Ráez JA, Matusova R, Bours R, Verstappen F, Bouwmeester HJ (2010) Physiological effects of the synthetic strigolactone analogue GR24 on root system architecture in Arabidopsis: Another below-ground role for strigolactones? Plant physiology 155(2): 721-734.

Chapter 8 summarizes and discusses the most important results from this thesis. In this chapter we also consider future perspectives of strigolactone research.

References

Akiyama K, Matsuzaki K, Hayashi H (2005) Plant sesquiterpenes induce hyphal branching in arbuscular mycorrhizal fungi. Nature **435:** 824-827

Akiyama K, Ogasawara S, Ito S, Hayashi H (2010) Structural requirements of strigolactones for hyphal branching in AM fungi. Plant and Cell Physiology **51:** 1104-1117

Albrecht C, Bisseling T (1998) Signaling during legume root symbiosis. *In* F LoSchiavo, RL Last, G Morelli, NV Raikhel, eds, Cellular Integration of Signalling Pathways in Plant Development, Vol 104, pp 289-296

Arite T, Iwata H, Ohshima K, Maekawa M, Nakajima M, Kojima M, Sakakibara H, Kyozuka J (2007) DWARF10, an RMS1/MAX4/DAD1 ortholog, controls lateral bud outgrowth in rice. The Plant Journal **51:** 1019-1029

Arite T, Umehara M, Ishikawa S, Hanada A, Maekawa M, Yamaguchi S, Kyozuka J (2009) *d14*, a strigolactone-insensitive mutant of rice, shows an accelerated outgrowth of tillers. Plant and Cell Physiology **50:** 1416-1424

Auldridge ME, Block A, Vogel JT, Dabney-Smith C, Mila I, Bouzayen M, Magallanes-Lundback M, DellaPenna D, McCarty DR, Klee HJ (2006) Characterization of three members of the Arabidopsis carotenoid cleavage dioxygenase family demonstrates the divergent roles of this multifunctional enzyme family. The Plant Journal **45:** 982-993

Bainbridge K, Sorefan K, Ward S, Leyser O (2005) Hormonally controlled expression of the Arabidopsis *MAX4* shoot branching regulatory gene. The Plant Journal **44:** 569-580

Bennett T, Leyser O (2006) Something on the side: axillary meristems and plant development. Plant Molecular Biology **60:** 843-854

Bennett T, Sieberer T, Willett B, Booker J, Luschnig C, Leyser O (2006) The Arabidopsis MAX pathway controls shoot branching by regulating auxin transport. Current Biology **16:** 553-563

Besserer A, Puech-Pagès V, Kiefer P, Gomez-Roldan V, Jauneau A, Roy S, Portais J-C, Roux C, Bécard G, Séjalon-Delmas N (2006) Strigolactones stimulate arbuscular mycorrhizal fungi by activating mitochondria. PLoS Biol **4:** e226

Beveridge CA, Ross JJ, Murfet IC (1996) Branching in pea (action of genes *RMS3* and *RMS4*). Plant Physiology **110:** 859-865

Blilou I, Xu J, Wildwater M, Willemsen V, Paponov I, Friml J, Heidstra R, Aida M, Palme K, Scheres B (2005) The PIN auxin efflux facilitator network controls growth and patterning in Arabidopsis roots. Nature **433:** 39-44

Booker J, Auldridge M, Wills S, McCarty D, Klee H, Leyser O (2004) MAX3/CCD7 is a carotenoid cleavage dioxygenase required for the synthesis of a novel plant signaling molecule. Current Biology **14:** 1232-1238

Booker J, Sieberer T, Wright W, Williamson L, Willett B, Stirnberg P, Turnbull C, Srinivasan M, Goddard P, Leyser O (2005) MAX1 encodes a cytochrome P450 family member that acts downstream of MAX3/4 to produce a carotenoid-derived branch-inhibiting hormone. Developmental Cell **8:** 443-449

Bouwmeester HJ, Matusova R, Zhongkui S, Beale MH (2003) Secondary metabolite signalling in host-parasitic plant interactions. Current Opinion in Plant Biology **6:** 358-364

Bouwmeester HJ, Roux C, López-Ráez JA, Bécard G (2007) Rhizosphere communication of plants, parasitic plants and AM fungi. Trends in Plant Science **12:** 224-230

Brewer PB, Dun EA, Ferguson BJ, Rameau C, Beveridge CA (2009) Strigolactone acts downstream of auxin to regulate bud outgrowth in pea and arabidopsis. Plant Physiology **150:** 482-493

Buschmann H, Gonsior G, Sauerborn J (2005) Pathogenicity of branched broomrape (Orobanche ramosa) populations on tobacco cultivars. Plant Pathology **54:** 650-656

Cook C, Whichard L, Wall M, Egley G, Coggon P, Luhan P, McPhail A (1972) The structure of strigol, a potent seed germination stimulant for witchweed *(Striga lutea* Lour.). Journal of the American Chemical Society **94**

Cook CE, Whichard LP, Turner B, Wall ME, Egley GH (1966) Germination of witchweed (*Striga lutea Lour.*): isolation and properties of a potent stimulant. Science **154:** 1189-1190

Crawford S, Shinohara N, Sieberer T, Williamson L, George G, Hepworth J, Müller D, Domagalska MA, Leyser O (2010) Strigolactones enhance competition between shoot branches by dampening auxin transport. Development **137:** 2905-2913

Dharmasiri N, Dharmasiri S, Estelle M (2005) The F-box protein TIR1 is an auxin receptor. Nature **435:** 441-445

Domagalska MA, Leyser O (2011) Signal integration in the control of shoot branching. Nature Reviews Molecular Cell Biology **12:** 211-221

Dun EA, Ferguson BJ, Beveridge CA (2006) Apical dominance and shoot branching. Divergent opinions or divergent mechanisms? Plant Physiology **142:** 812-819

Ferguson BJ, Beveridge CA (2009) Roles for auxin, cytokinin, and strigolactone in regulating shoot branching. Plant Physiology **149:** 1929-1944

Foo E, Turnbull CGN, Beveridge CA (2001) Long-distance signaling and the control of branching in the *rms1* mutant of pea. Plant Physiology **126:** 203-209

Friml J, Vieten A, Sauer M, Weijers D, Schwarz H, Hamann T, Offringa R, Jürgens G (2003) Efflux-dependent auxin gradients establish the apical-basal axis of Arabidopsis. Nature **426:** 147-153

Friml J, Wiśniewska J, Benková E, Mendgen K, Palme K (2002) Lateral relocation of auxin efflux regulator PIN3 mediates tropism in

Arabidopsis. Nature **415:** 806-809

Gao Z, Qian Q, Liu X, Yan M, Feng Q, Dong G, Liu J, Han B (2009) *Dwarf 88*, a novel putative esterase gene affecting architecture of rice plant. Plant Molecular Biology **71:** 265-276

García-Garrido J, Lendzemo V, Castellanos-Morales V, Steinkellner S, Vierheilig H (2009) Strigolactones, signals for parasitic plants and arbuscular mycorrhizal fungi. Mycorrhiza **19:** 449-459

Goldwasser Y, Yoneyama K, Xie X, Yoneyama K (2008) Production of strigolactones by *Arabidopsis thaliana* responsible for *Orobanche aegyptiaca* seed germination. Plant Growth Regulation **55:** 21-28

Gomez-Roldan V, Fermas S, Brewer PB, Puech-Pages V, Dun EA, Pillot J-P, Letisse F, Matusova R, Danoun S, Portais J-C, Bouwmeester H, Becard G, Beveridge CA, Rameau C, Rochange SF (2008) Strigolactone inhibition of shoot branching. Nature **455:** 189-194

Gomi K, Sasaki A, Itoh H, Ueguchi-Tanaka M, Ashikari M, Kitano H, Matsuoka M (2004) GID2, an F-box subunit of the SCF E3 complex, specifically interacts with phosphorylated SLR1 protein and regulates the gibberellin-dependent degradation of SLR1 in rice. The Plant Journal **37:** 626-634

Hirsch AM, Bauer WD, Bird DM, Cullimore J, Tyler B, Yoder JI (2003) Molecular signals and receptors: Controlling rhizosphere interactions between plants and other organisms. Ecology **84:** 858-868

Humphrey AJ, Galster AM, Beale MH (2006) Strigolactones in chemical ecology: waste products or vital allelochemicals? Natural Product Reports **23:** 592-614

Joel DM (2009) The new nomenclature of *Orobanche* and *Phelipanche*. Weed Research **49:** 6-7

Kohlen W, Charnikhova T, Liu Q, Bours R, Domagalska MA, Beguerie S, Verstappen F, Leyser O, Bouwmeester H, Ruyter-Spira C (2011) Strigolactones are transported through the xylem and play a key role in shoot architectural response to phosphate deficiency in nonarbuscular mycorrhizal host Arabidopsis. Plant Physiology **155:** 974-987

Ledger SE, Janssen BJ, Karunairetnam S, Wang T, Snowden KC (2010) Modified CAROTENOID CLEAVAGE DIOXYGENASE8 expression correlates with altered branching in kiwifruit (*Actinidia chinensis*). New Phytologist **188:** 803-813

Leyser O (2009) The control of shoot branching: an example of plant information processing. Plant, Cell & Environment **32:** 694-703

Limpens E, Bisseling T (2003) Signaling in symbiosis. Current Opinion in Plant Biology **6:** 343-350

Lin H, Wang R, Qian Q, Yan M, Meng X, Fu Z, Yan C, Jiang B, Su Z, Li J, Wang Y (2009) DWARF27, an iron-containing protein required for the biosynthesis of strigolactones, regulates rice tiller bud outgrowth. Plant Cell **21:** 1512-1525

Ljung K, Bhalerao RP, Sandberg G (2001) Sites and homeostatic control of auxin biosynthesis in Arabidopsis during vegetative growth. Plant Journal **28:** 465-474

López-Ráez JA, Charnikhova T, Gómez-Roldán V, Matusova R, Kohlen W, Vos RD, Verstappen F, Puech-Pages V, Bécard G, Mulder P, Bouwmeester H (2008) Tomato strigolactones are derived from carotenoids and their biosynthesis is promoted by phosphate starvation. New Phytologist **178:** 863-874

Mashiguchi K, Sasaki E, Shimada Y, Nagae M, Ueno K, Nakano T, Yoneyama K, Suzuki Y, Asami T (2009) Feedback-Regulation of Strigolactone Biosynthetic Genes and Strigolactone-Regulated Genes in Arabidopsis. Bioscience Biotechnology and Biochemistry **73:** 2460-2465

Matusova R, Rani K, Verstappen FWA, Franssen MCR, Beale MH, Bouwmeester HJ (2005) The strigolactone germination stimulants of the plant-parasitic *Striga* and *Orobanche spp*. are derived from the carotenoid pathway. Plant Physiology **139:** 920-934

Morris SE, Cox MCH, Ross JJ, Krisantini S, Beveridge CA (2005) Auxin dynamics after decapitation are not correlated with the initial growth of axillary buds. Plant Physiology **138:** 1665-1672

Morris SE, Turnbull CGN, Murfet IC, Beveridge CA (2001) Mutational analysis of branching in pea. evidence that *RMS1* and *RMS5* regulate the same novel signal. Plant Physiology **126:** 1205-1213

Musselman L (1994) Parasitic weeds of the world: Biology and controls. Economic Botany **48:** 332-332

Musselman LJ (1980) The biology of *Striga*, *Orobanche*, and other root-parasitic weeds. Annual Review of Phytopathology **18:** 463-489

Nelson DR, Schuler MA, Paquette SM, Werck-Reichhart D, Bak S (2004) Comparative Genomics of Rice and Arabidopsis. Analysis of 727 Cytochrome P450 Genes and Pseudogenes from a Monocot and a Dicot. Plant Physiology **135:** 756-772

Nickrent D, Musselman L (2004) Introduction to parasitic flowering plants. The Plant Health Instructor

Oswald A (2005) Striga control - technologies and their dissemination. Crop Protection **24:** 333-342

Parker C (1994) The present state of the Orobanche problem,

Parker C (2009) Observations on the current status of *Orobanche* and *Striga* problems worldwide. Pest Management Science **65:** 453-459

Parker C, Riches CR (1993) Parasitic weeds of the world: Biology and control. CAB International, Wallingford

Press M, Gurney A (2000) Plant eats plant: sap-feeding witchweeds and other parasitic angiosperms. . Biologist (London) **47** 189-193

Press MC, Shah N, Tuohy JM, Stewart GR (1987) Carbon isotope ratios demonstrate carbon flux from C4 host to C3 parasite. Plant Physiology **85:** 1143-1145

Proust H, Hoffmann B, Xie X, Yoneyama K, Schaefer DG, Yoneyama K, Nogué F, Rameau C (2011) Strigolactones regulate protonema branching and act as a quorum sensing-like signal in the moss *Physcomitrella patens*. Development **138:** 1531-1539

Prusinkiewicz P, Crawford S, Smith RS, Ljung K, Bennett T, Ongaro V, Leyser O (2009) Control of bud activation by an auxin transport switch. Proceedings of the National Academy of Sciences **106:** 17431-17436

Rani K, Zwanenburg B, Sugimoto Y, Yoneyama K, Bouwmeester HJ (2008) Biosynthetic considerations could assist the structure elucidation of host plant produced rhizosphere signalling compounds (strigolactones) for arbuscular mycorrhizal fungi and parasitic plants. Plant Physiology and Biochemistry **46:** 617-626

Rasmann S, Kollner TG, Degenhardt J, Hiltpold I, Toepfer S, Kuhlmann U, Gershenzon J, Turlings TCJ (2005) Recruitment of entomopathogenic nematodes by insect-damaged maize roots. Nature **434:** 732-737

Ruyter-Spira C, Kohlen W, Charnikhova T, van Zeijl A, van Bezouwen L, de Ruijter N, Cardoso C, López-Ráez JA, Matusova R, Bours R, Verstappen F, Bouwmeester H (2011) Physiological effects of the synthetic strigolactone analog GR24 on root system architecture in Arabidopsis: Another belowground role for strigolactones? Plant Physiology **155:** 721-734

Scholes JD, Press MC (2008) *Striga* infestation of cereal crops - an unsolved problem in resource limited agriculture. Current Opinion in Plant Biology **11:** 180-186

Schwartz SH, Qin XQ, Loewen MC (2004) The biochemical characterization of two carotenoid cleavage enzymes from Arabidopsis indicates that a carotenoid-derived compound inhibits lateral branching. Journal of Biological Chemistry **279:** 46940-46945

Shah N, Smirnoff N, Stewart GR (1987) Photosynthesis and stomatal characteristics of *Striga hermonthica* in relation to its parasitic habit. Physiologia Plantarum **69:** 699-703

Simons JL, Napoli CA, Janssen BJ, Plummer KM, Snowden KC (2007) Analysis of the *DECREASED APICAL DOMINANCE* genes of petunia in the control of axillary branching. Plant Physiology **143:** 697-706

Snowden KC, Simkin AJ, Janssen BJ, Templeton KR, Loucas HM, Simons JL, Karunairetnam S, Gleave AP, Clark DG, Klee HJ (2005) The *Decreased apical dominance 1/petunia hybrida carotenoid cleavage dioxygenase8* gene affects branch production and plays a role in leaf senescence, root growth, and flower development. Plant Cell **17:** 746-759

Sorefan K, Booker J, Haurogné K, Goussot M, Bainbridge K, Foo E, Chatfield S, Ward S, Beveridge C, Rameau C, Leyser O (2003) *MAX4* and *RMS1* are orthologous dioxygenase-like genes that regulate shoot branching in Arabidopsis and pea. Genes & Development **17:** 1469-1474

Stirnberg P, Furner IJ, Leyser HMO (2007) MAX2 participates in an SCF complex which acts locally at the node to suppress shoot branching. The Plant Journal **50:** 80-94

Stirnberg P, van de Sande K, Leyser HMO (2002) MAX1 and MAX2 control shoot lateral branching in Arabidopsis. Development **129:** 1131-1141

Stirnberg P, Ward S, Leyser O (2010) Auxin and strigolactones in shoot branching: Intimately connected? Biochemical Society Transactions**:** 717-722

Turnbull CGN, Booker JP, Leyser HMO (2002) Micrografting techniques for testing long-distance signalling in Arabidopsis. The Plant Journal **32:** 255-262

Ueguchi-Tanaka M, Ashikari M, Nakajima M, Itoh H, Katoh E, Kobayashi M, Chow T-y, Hsing Y-iC, Kitano H, Yamaguchi I, Matsuoka M (2005) *GIBBERELLIN INSENSITIVE DWARF1* encodes a soluble receptor for gibberellin. Nature **437:** 693-698

Umehara M, Hanada A, Magome H, Takeda-Kamiya N, Yamaguchi S (2010) Contribution of strigolactones to the inhibition of tiller bud outgrowth under phosphate deficiency in rice. Plant and Cell Physiology**:** 1118-1126

Umehara M, Hanada A, Yoshida S, Akiyama K, Arite T, Takeda-Kamiya N, Magome H, Kamiya Y, Shirasu K, Yoneyama K, Kyozuka J, Yamaguchi S (2008) Inhibition of shoot branching by new terpenoid plant hormones. Nature **455:** 195-200

Vieten A, Vanneste S, Wiśniewska J, Benková E, Benjamins R, Beeckman T, Luschnig C, Friml J (2005) Functional redundancy of PIN proteins is accompanied by auxin-dependent cross-regulation of PIN expression. Development **132:** 4521-4531

Vogel JT, Walter MH, Giavalisco P, Lytovchenko A, Kohlen W, Charnikhova T, Simkin AJ, Goulet C, Strack D, Bouwmeester HJ, Fernie AR, Klee HJ (2010) SlCCD7 controls strigolactone biosynthesis, shoot branching and mycorrhiza-induced apocarotenoid formation in tomato. The Plant Journal **61:** 300-311

Waldie T, Hayward A, Beveridge CA (2010) Axillary bud outgrowth in herbaceous shoots: How do strigolactones fit into the picture? Plant Molecular Biology **73:** 27-36

Walter MH, Strack D (2011) Carotenoids and their cleavage products: Biosynthesis and functions. Natural Product Reports **28:** 663-692

Xie X, Yoneyama K, Yoneyama K (2010) The strigolactone story. Annual Review of Phytopathology **48:** 93-117

Yan H, Saika H, Maekawa M, Takamure I, Tsutsumi N, Kyozuka J, Nakazono M (2007) Rice tillering dwarf mutant *dwarf3* has increased leaf longevity during darkness-induced senescence or hydrogen peroxide-induced cell death. Genes & Genetic Systems **82:** 361-366

Yoneyama K, Xie X, Yoneyama K, Takeuchi Y (2009) Strigolactones: structures and biological activities. Pest Management Science **65:** 467-470

Yoneyama K, Yoneyama K, Takeuchi Y, Sekimoto H (2007) Phosphorus deficiency in red clover promotes exudation of orobanchol, the signal for mycorrhizal symbionts and germination stimulant for root parasites. Planta **225:** 1031-1038

Zou J, Zhang S, Zhang W, Li G, Chen Z, Zhai W, Zhao X, Pan X, Xie Q, Zhu L (2006) The rice *HIGH-TILLERING DWARF1* encoding an ortholog of Arabidopsis *MAX3* is required for negative regulation of the outgrowth of axillary buds. The Plant Journal **48:** 687-698

Chapter 2

Strigolactone biosynthesis in tomato

Tatsiana Charnikhova, Wouter Kohlen, Patrick Mulder, Juan Antonio López-Ráez, Binne Zwanenburg, Harro J. Bouwmeester

Submission in preparation

Abstract

Strigolactones are plant signaling molecules that induce the germination of parasitic plants, initiate host plant - arbuscular mycorrhizal (AM) fungus symbiosis and act as inhibitors of shoot branching. So far only a limited number of different chemical structures have been described for the strigolactones, but several new strigolactones of yet unknown structure have been reported in plants and many new strigolactones and new functions for this class of plant hormones are expected. The precursor for all known strigolactones is thought to be 5-deoxystrigol, with all other strigolactones postulated to be derived from this compound through a number of different enzymatic and/or non-enzymatic steps. Solanacol, that occurs in the root exudates of tomato (*Solanum lycopersicum)*, contains an aromatic A-ring and therefore its biosynthesis from the precursor 5-deoxystrigol is not obvious. On the basis of the presence of other strigolactones in tomato root extracts and root exudates - orobanchol, orobanchyl acetate, two 7-hydroxy-orobanchol isomers, 7-oxo-orobanchol and four didehydro-orobanchol isomers - we postulate how solanacol is derived from 5-deoxystrigol through a series of enzymatic hydroxylation-dehydroxylation reactions with migration of a methyl group and double bonds.

Keywords: *Solanum lycopersicum*, biosynthetic pathway, LC-MS/MS, strigolactones, solanacol, orobanchol, orobanchyl acetate, 7-hydroxy-orobanchol, 7-oxo-orobanchol, didehydro-orobanchol.

Introduction

The new group of plant hormones, the strigolactones, especially known as germination stimulants for the seeds of parasitic plants of the genera *Striga, Phelipanche* and *Orobanche* have been isolated from many plant species (maize, sorghum, tomato, millet, cotton, red clover, cowpea, etc.) in varying amounts and combinations (Yoneyama et al., 2009; Yoneyama et al., 2010). Strigolactones are exuded by plant roots and induce germination of parasitic plant seeds. Only upon this signal parasitic plant seeds start to germinate, thus making the response to these signaling molecules a crucial event in the parasitic plant lifecycle (Bouwmeester *et al.*, 2003; Bouwmeester *et al.*, 2007; Xie *et al.*, 2010) Besides their role as parasitic plant germination stimulants, strigolactones also act as hyphal branching factors for arbuscular mycorrhizal (AM) fungi making them a critical component in the establishment of the symbiosis between plants and AM fungi (Akiyama et al., 2005; Yoneyama et al., 2008; Akiyama et al., 2010). More recently, the strigolactones were shown to regulate shoot branching or tillering in the host plant, an effect that classifies them as a new class of plant hormones

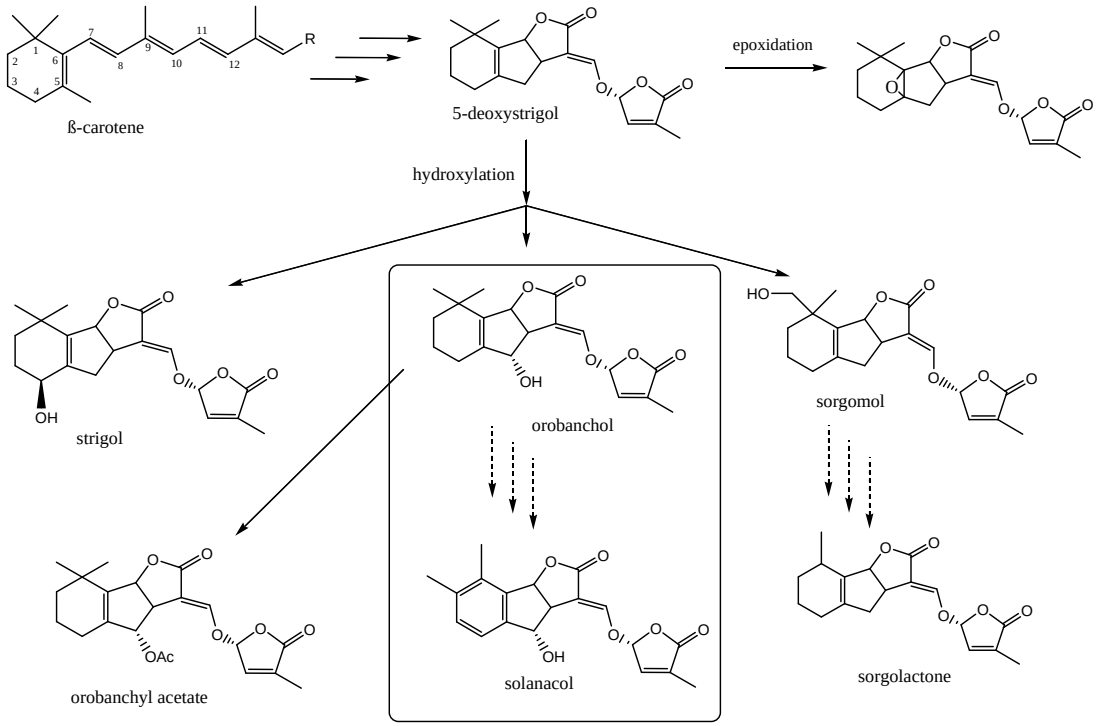

Figure 1: Postulated biosynthetic scheme for strigolactones formation from carotenoids.

(Gomez-Roldan et al., 2008; Umehara et al., 2008). The strigolactones discovered so far all have a similar basic chemical structure, suggesting that they all have the same biosynthetic origin - the carotenoids - and hence belong to one chemical class of compounds - the apocarotenoids - (Matusova et al., 2005) (Figure 1). The latter authors suggested that the ABC-part of the strigolactones is derived from the carotenoids by cleavage either by a 9-*cis*-epoxycarotenoid dioxygenase (NCED) or by a carotenoid cleavage dioxygenase (CCD) enzyme, followed by several enzymatic conversions that could lead to the production of the strigolactones that were then known (Matusova et al., 2005; Rani et al., 2008). Recently it was shown that indeed not only one but two CCDs (CCD7 and CCD8) – which were already known to be involved in the biosynthesis of the elusive shoot branching inhibiting signal (Sorefan et al., 2003; Booker et al., 2004) - are involved in the biosynthesis of strigolactones (Gomez-Roldan et al., 2008; Umehara et al., 2008). These authors showed that mutants of pea *ramosus5* (*rms5*) and *ramosus 1* (*rms1*) and rice *high-tillering dwarf 1* or *dwarf 17* (*htd1* or *d17*) and *dwarf 10* (*d10*) for CCD7 and CCD8, respectively, had strongly decreased

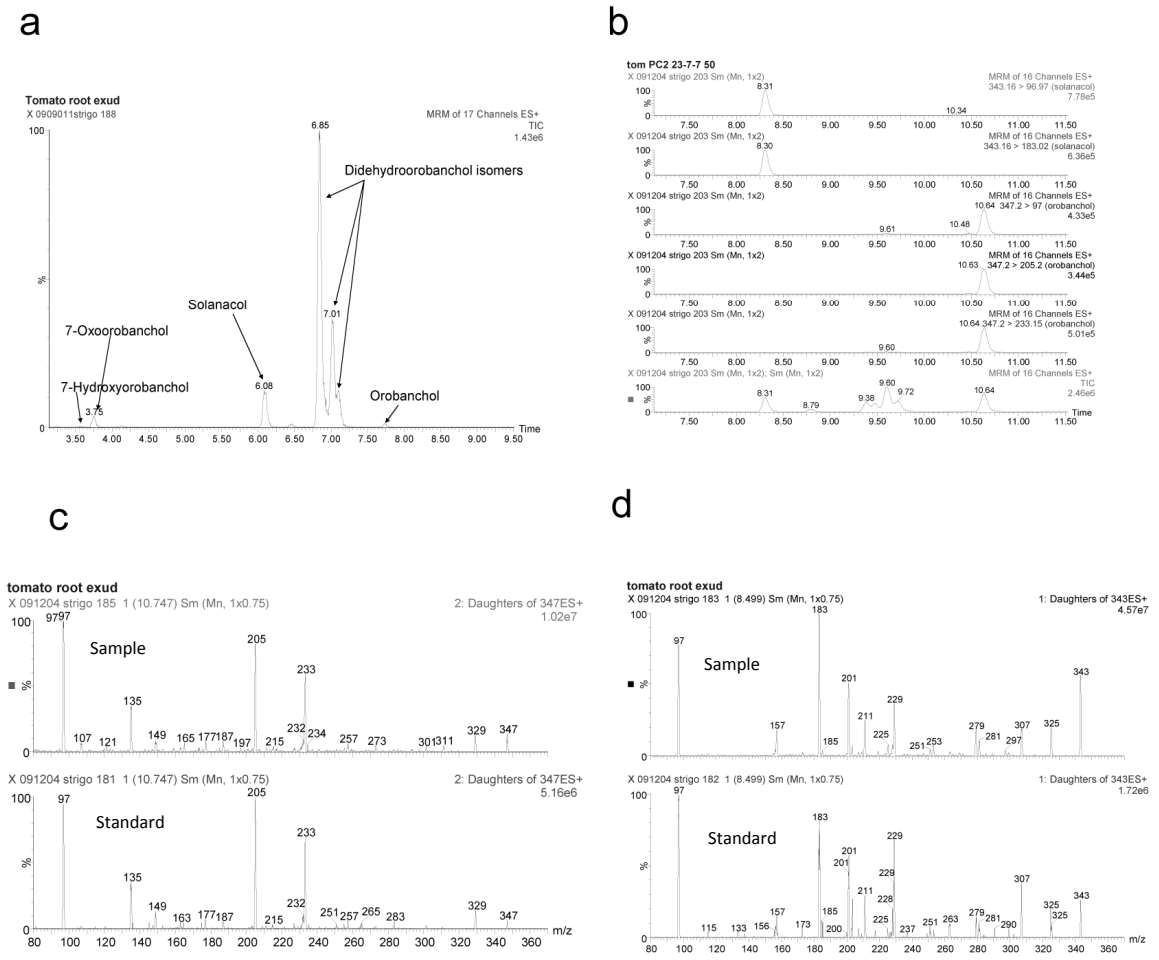

Figure 2: LC-MS/MS analysis of tomato root exudates, **(a)** Total ion current (TIC) chromatogram of tomato Moneymaker crude root exudates, using the standard LC gradient, **(b)** The MRM transitions for orobanchol and solanacol obtained for tomato Moneymaker root exudates using the optimized LC gradient, **(c)** MS/MS fragmentation spectra obtained for orobanchol (10.7 min) at a collision energy of 18 eV, **(d)** MS/MS fragmentation spectra for solanacol (8.5 min) at a collision energy of 20 eV.

strigolactone production compared with the corresponding wild-type. The unusual excessive branching or tillering phenotype of these mutants in combination with complementation experiments with the synthetic strigolactone analogue GR24 also gave the first evidence of the hormonal role of strigolactones – in shoot branching/tillering control - inside the plant. Also MAX1, a cytochrome P450, which upon mutation yields a branching phenotype in Arabidopsis (Booker et al., 2004) was verified by LC-MS/MS analysis to be involved in strigolactone formation (Kohlen et al., 2011). Although the exact function of this P450 in strigolactone biosynthesis is unknown, the involvement of cytochrome P450s is very likely and was already postulated by Matusova et al. (2005). The fourth gene that has been postulated to be part of strigolactone biosynthesis is the rice *DWARF 27* (*D27*) (Lin et al., 2009). How the latter protein contributes to strigolactone biosynthesis or perception/signal transduction is also unknown. Hence, the complete elucidation of the strigolactone biosynthetic pathway is still a challenge.

So far even less is known about the later steps in the pathway – the functionalization of the strigolactone backbone resulting in all the different strigolactones. Although most of these putative enzymatic steps - such as hydroxylation, acetylation and methylation - on paper look very common, a more challenging problem is the biosynthesis of the aromatic A-ring of solanacol (Takikawa et al., 2009). It has been postulated that solanacol is derived from orobanchol (Rani et al., 2008;

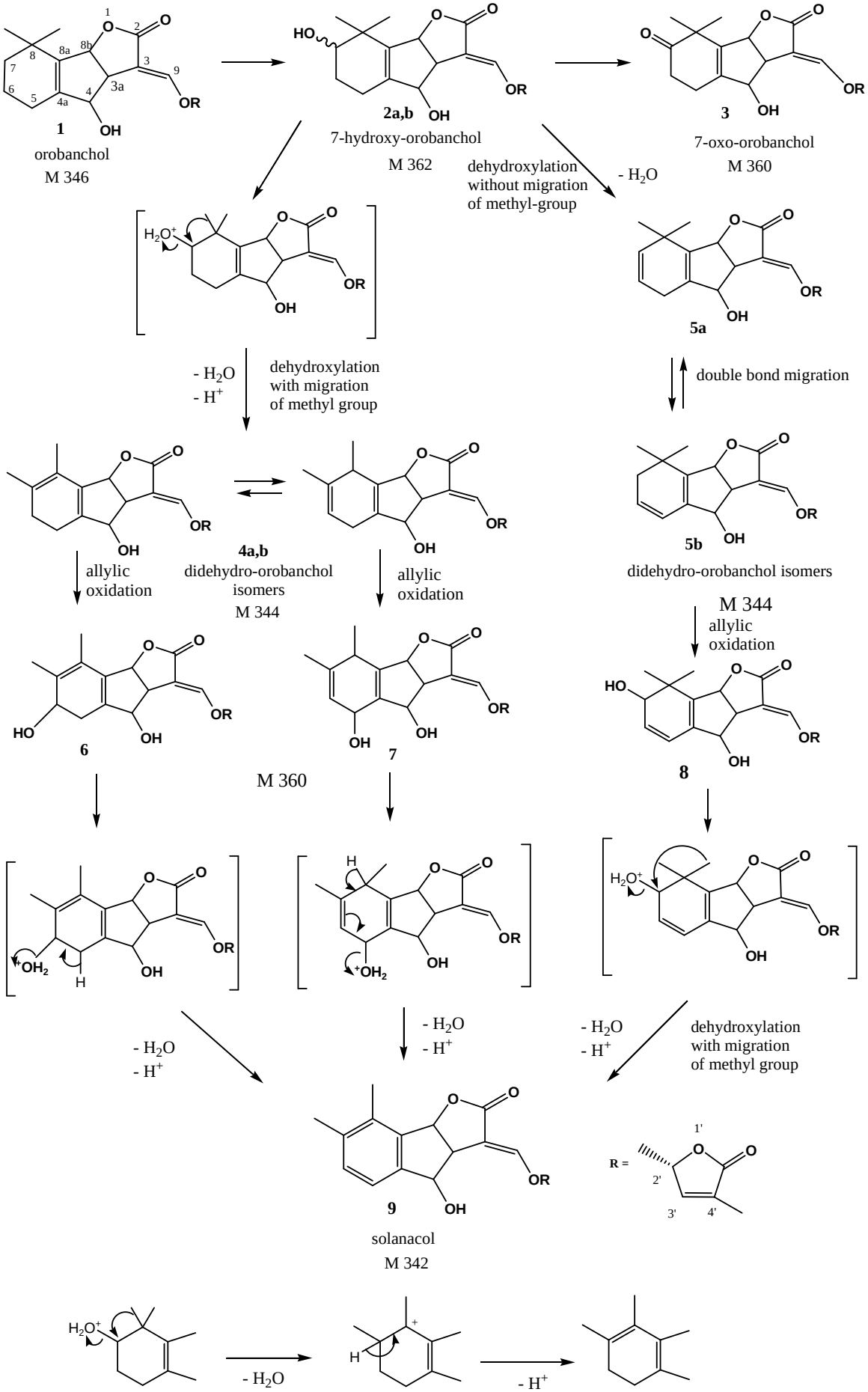

Figure 3: Postulated biosynthetic scheme for the formation of the aromatic strigolactone solanacol from orobanchol.

Zwanenburg et al., 2009; Xie et al., 2010). However, the presence of the aromatic A-ring in solanacol cannot easily be explained. So far no carotenoids with aromatic rings, which could be possible precursors for solanacol biosynthesis, have been reported in higher plants. Aromatic carotenoids do occur in green photosynthetic and non-photosynthetic bacteria (Moshier and Chapman, 1973). Thus, biosynthetic conversion of ß-carotene to aromatic carotenoids in the green photosynthetic bacterium *Streptomyces griseus* via a desaturation/methyltransfer mechanism has been reported (Krugel et al., 1999; Krubasik and Sandmann, 2000; Graham and Bryant, 2008; Maresca et al., 2008).
Recently we have described the presence of strigolactones - orobanchol and solanacol, and two putative didehydro-orobanchol isomers - in tomato (*Solanum lycopersicum*) root exudates and extracts (López-Ráez et al., 2008; López-Ráez et al., 2008). Based on reported spectral features and the chemical structure of all known natural strigolactones (Figure 1) we hypothesized the presence of new strigolactones that may be intermediates in the biosynthesis of solanacol from orobanchol. In the present study we report on the occurrence of these strigolactones in tomato and discuss their possible involvement as intermediates in the biosynthesis of the aromatic strigolactone solanacol.

Results and discussion

Identification of tomato strigolactones

In order to elucidate the biosynthesis of solanacol we analyzed the strigolactones present in tomato root exudates and root extracts in more detail looking for possible intermediates in the biosynthetic pathway. We already reported the presence in tomato of orobanchol, solanacol and two proposed didehydro-orobanchol isomers, although the
latter two could not be characterized (López-Ráez et al., 2008; López-Ráez et al., 2008). Liquid chromatography tandem mass spectrometry (LC-MS/MS) analysis of a crude tomato root exudate indeed showed the presence of solanacol, orobanchol and the two diddehydro-orobanchol isomers, plus one additional isomer (Figure 2). Assuming that orobanchol is the precursor for solanacol, the didehydro-orobanchol isomers could be intermediates in this biosynthetic pathway. If so, we can also predict intermediates between orobanchol and the didehydro-orobanchol isomers having a hydroxy- or an oxo-function in the A-ring, as shown in Figure 3.

For the identification of new strigolactones in tomato, pooled root exudates from about 100 4-wks

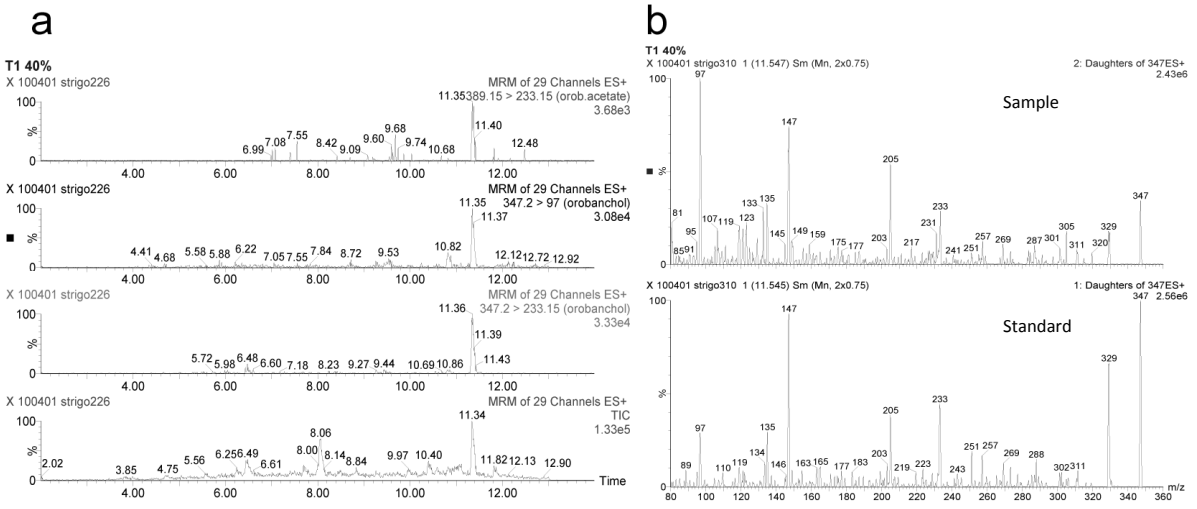

Figure 4: LC-MS/MS analysis of orobanchyl acetate in tomato root exudates, **(a)** The MRM transitions for orobanchyl acetate in tomato root exudates fraction 4, **(b)** MS/MS fragmentation spectra of orobanchyl acetate (11.35 min) at a collision energy of 18 eV.

old plants were concentrated and purified using silica gel column chromatography. Fractions obtained after column chromatography were analyzed using liquid chromatography tandem mass spectrometry (LC-MS/MS). The MRM transitions used to screen the fractions for the presence of strigolactones are shown in table 1. Orobanchol **1** and solanacol **9** were present in fractions 5, 6 and 7 corresponding to 50-70% of ethyl acetate. Orobanchyl acetate(Figure 1), which was not reported to be present in tomato so far, was present in fraction 4 corresponding to 40% of ethyl acetate. Its identity was confirmed by comparison with an authentic standard (Figure 4, a and b). 7-Oxo-orobanchol **3** and the two isomers of 7-hydroxy-orobanchol **2a,b** were detected in fractions 8 and 9, corresponding to 80-90% of ethyl acetate (Figure 5). The low levels of orobanchyl acetate, 7-hydroxy-orobanchols **2a,b** and 7-oxo-orobanchol **3** in tomato root exudates and tissue is likely the reason why they have not been detected before in crude tomato root exudates and extracts.

The chemical structure of compounds **2a,b** and **3** was verified by comparison of their retention times (*Rt*) in the LC-MS/MS (MRM) chromatograms and their MS/MS fragmentation spectra with those of authentic standards of 7α-hydroxy-orobanchol, 7α- and 7ß-hydroxy-orobanchyl acetates (personal communication Prof. dr. Yoneyama) and 7-oxo-orobanchol (Xie et al., 2009) (Figure 5a-f). The retention time of 3.93 min (Figure 5a) in all the corresponding channels on the MRM chromatograms and MS/MS fragmentation spectra obtained at collision energies of 5, 10, 15, 20 and 25 eV of one of the 7-hydroxy-orobanchol isomers, **2a,** were identical to those of an authentic standard of 7α-hydroxy-orobanchol (Figure 5, c and f) and similar to an authentic standard of 7α-hydroxy-orobanchyl acetate (Figure 5c), identifying this compound as 7α-hydroxy-orobanchol. MS/MS fragmentation spectra of the less polar 7-hydroxy-orobanchol isomer, **2b** (*Rt* 4.49 min, Figure 5a) were very similar to those of the authentic standard of 7α-hydroxy-orobanchol and 7ß-hydroxy-orobanchyl acetate (Figure 5d). Therefore, compound **2b** is likely 7ß-hydroxy-orobanchol. The retention times of the two 7-hydroxy-orobanchol isomers differ by approx. 0.5 min, a similar difference as for 7α- and 7ß-hydroxy-orobanchyl acetate (data not shown), which indirectly suggests their structural similarity.

Compound **3** was identified as 7-oxo-orobanchol, based on comparison of its retention time 5.06 min and MS/MS fragmentation spectra with those of an authentic standard of 7-oxo-orobanchol (Figure 5, a, b and e). Standard addition of authentic 7α-hydroxy-orobanchol and 7-oxo-orobanchol to the samples further confirmed their presence in the tomato root exudates (Figure 5, e and f).

In the biosynthetic pathway between orobanchol (an unsaturated molecule with one double bond in the A-ring) and solanacol (an aromatic molecule), we can also expect one or more intermediates with two double bonds in the A-ring (Figure 3). Previously we have reported the presence of two putative didehydro-orobanchol isomers in tomato root exudates (López-Ráez et al., 2008). The fragmentation spectra of these two isomers were very similar, yielding the major fragments *m/z* 231, 203, 175 and 97. Based on the common fragmentation patterns for strigolactones, *m/z* 97 was identified as the protonated D-ring ($C_5H_5O_2$), due to breakdown of the "weak" O-$C^{2'}$ bond in the enol-ether bridge of the molecule and *m/z* 231 corresponds to ($[M + H - H_2O$ – D-ring$]^+$). Further fragmentation of the "ABC-fragments" will depend on the initial chemical structure of the strigolactone, and may consist of several losses of water and CO molecules (Sato et al., 2003). The two other fragments, *m/z* 203 and *m/z* 175, could have been formed by the consecutive loss of two CO molecules. The didehydro-orobanchol isomers were prominent strigolactones in all tomato root exudates investigated (López-Ráez et al., 2008; López-Ráez et al., 2008; López-Ráez et al., 2010).

Using our optimized chromatographic gradient, in fact four closely eluting isomeric

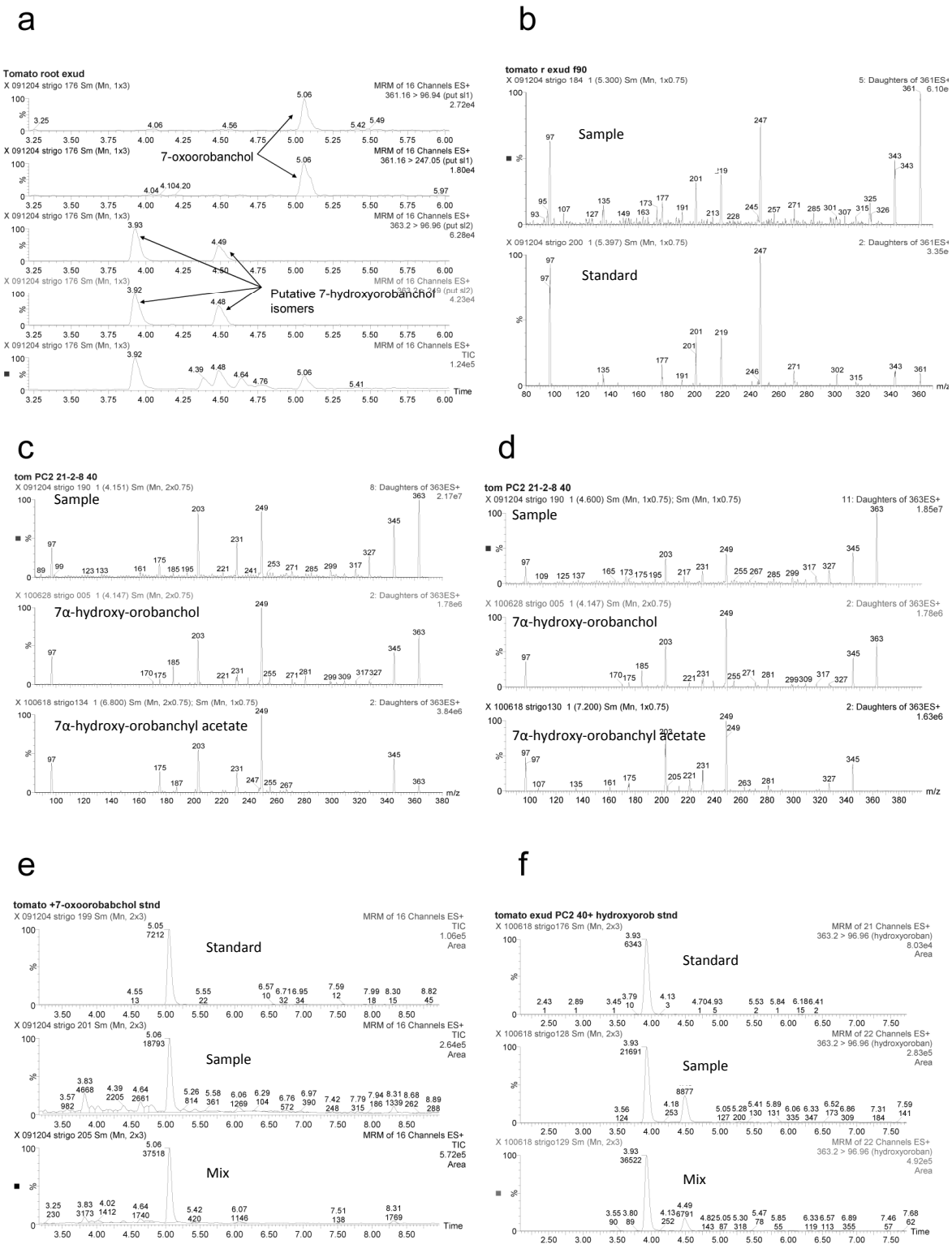

Figure 5: LC-MS/MS analysis of 7-oxo-orobanchol and 7-hydroxy-orobanchol isomers in tomato root exudates, **(a)** The MRM transitions for 7-oxo-orobanchol and two 7-hydroxy-orobanchol isomers obtained for tomato root exudates using the optimized LC gradient, **(b)** MS/MS fragmentation spectrum obtained for 7-oxo-orobanchol during online separation of a tomato root exudates fraction and authentic 7-oxo-orobanchol at a collision energy of 15 eV, **(c)** MS/MS fragmentation spectra of the putative 7-hydroxyoorbanchol isomer (M^+ 363, Rt 4.15 min) in tomato root exudates, authentic 7α-hydroxy-orobanchol and 7α-hydroxy-orobanchyl acetate at a collision energy of 15 eV, **(d)** MS/MS fragmentation spectra of the 7-hydroxyoorbanchol isomer (M^+ 363, Rt 4.5 min) in tomato root exudates, authentic 7α-hydroxy-orobanchol and 7ß–hydroxy-orobanchyl acetate at a collision energy of 15 eV, **(e)** MRM chromatograms of 7-oxo-orobanchol standard, tomato root exudates (fraction 70-80%) and tomato root exudates with addition of authentic 7-oxo-orobanchol standard, **(f)** MRM chromatograms of 7-hydroxyrobanchol standard, tomato root exudates (fraction 90%) and tomato root exudates with addition of

compounds with *m/z* 345 were now detected (Figure 6a) in column chromatography fractions 6 and 7. The accurate mass for the protonated molecular ions $[M + H]^+$ of all four isomeric compounds was determined using a LC-LTQ/Orbitrap-MS. For all isomers a mass of *m/z* 345.1333 was found, which is

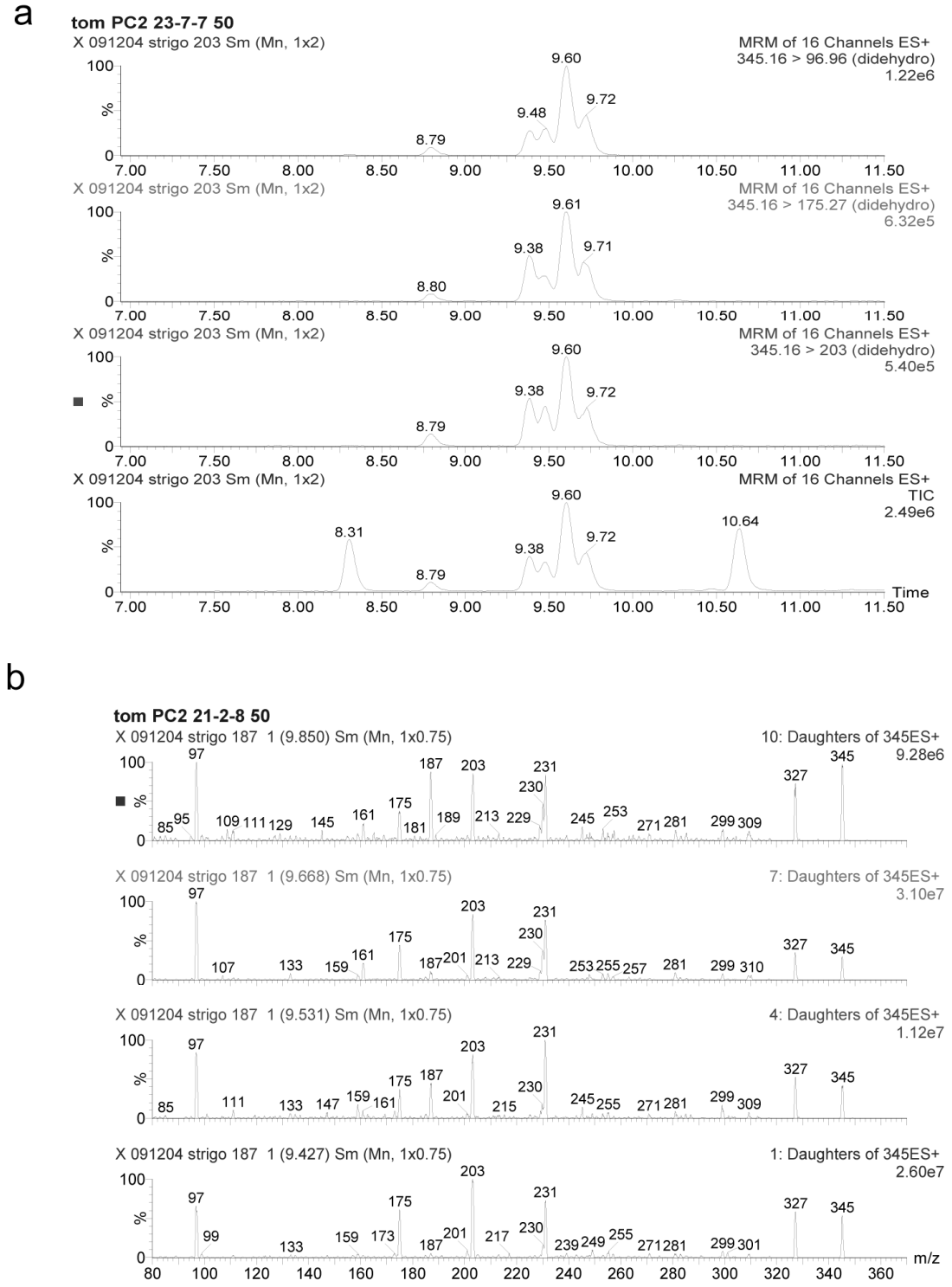

Figure 6: LC-MS/MS analysis of the didehydro-orobanchol isomers detected in tomato root exudates, **(a)** The MRM transitions showing four didehydro-orobanchol isomers in the tomato Moneymaker root exudates, **(b)** MS/MS fragmentation spectra of the four putative didehydro-orobanchol isomers (RT 9.4 min, 9.5 min, 9.7 min and 9.8 min) recorded during online separation of a

in accordance with the theoretically calculated mass for $C_{19}H_{21}O_6$, *m/z* 345.1338 (data not shown). The collision induced fragmentation spectra of the protonated molecular ions of all four isomers, obtained with triple quad MS, are shown in Figure 6b. Upon fragmentation the $[M + H]^+$ ion is converted to an ion with *m/z* 327 $[M + H - H_2O]^+$ with loss of water and with further loss of the D-ring to give the ion at *m/z* 231 $[M + H - H_2O - D\text{-ring}]^+$. Several consecutive losses of water, CO and/or acetylene lead to the ions at *m/z* 203, 187, 175, 161 (Figures 6b, 7). The abundance of most of these fragments is similar for all four isomers. The main difference between the isomers is the fragment with *m/z* 187, which is present in two of the isomers previously reported (López-Ráez et al., 2008) and (practically) absent in the other two. Based on these parameters it seems likely that all four compounds are didehydro-orobanchol isomers and their possible chemical structures are shown in Figure 3. The confirmation of the proposed chemical structures of the compounds **4a,b** and **5a,b** is in progress.

Tomato strigolactone biosynthetic pathway

In order to see whether the different strigolactones present in tomato are conserved, the root exudates from several tomato cultivars - Moneymaker, Manapal, Micro-Tom, Craigella, Rheinlands Ruhm and Ailsa Craig, were examined. All strigolactones reported above were detected in all the cultivars tested, albeit in slightly different levels and ratios. The same combination of strigolactones - in lower concentrations then in the corresponding wild-type - were found in root exudates of the tomato *high pigment-2^{dg}*, also called *darkgreen*, mutant (cv Manapal), in the abscisic acid (ABA) deficient mutants *notabilis* and *flacca* (cv Ailsa Craig) and in *sitiens* (cv. Reinlands Rhum) in agreement with (López-Ráez et al., 2008; López-Ráez et al., 2008; López-Ráez et al., 2010)

In all root extracts examined (Moneymaker, Manapal, Micro-Tom, Craigella, Rheinlands Ruhm, Ailsa Craig) the same set of strigolactones was detected as in the root exudates, although in different concentrations. The observation that the same strigolactones are present in all analyzed tomato root exudates and extracts supports our hypothesis that all these strigolactones are the products and/or intermediates of the same biosynthetic pathway and that this pathway is conserved in tomato. Thus, orobanchol **1** is very likely the precursor for all the strigolactones found in tomato, *viz.* 7-hydroxy-orobanchols **2a,b**, 7-oxo-orobanchol **3**, didehydro-orobanchol isomers **4a,b** and **5a,b**, and the aromatic solanacol **9** (Figure 3). Hydroxylation of orobanchol **1** in position *7* leads to the two isomers of 7-hydroxy-orobanchol **2**. The hydroxylation of the homo-allylic C*7*-position (corresponding to C-5' in ABA) has been reported for the catabolism of ABA (Kikuzaki et al., 2004; Zaharia et al., 2005) and in the biosynthesis of gibberellins (Hedden and Kamiya, 1997).

Dehydrogenation of 7-hydroxy-orobanchols **2a,b** yields 7-oxo-orobanchol **3**. This process is similar to the dehydrogenation of xanthoxin to abscisic aldehyde or the dehydrogenation of 4-dihydrotrisporine to trisporic acid (Schwartz et al., 2003; Schachtschabel et al., 2008). Analogous

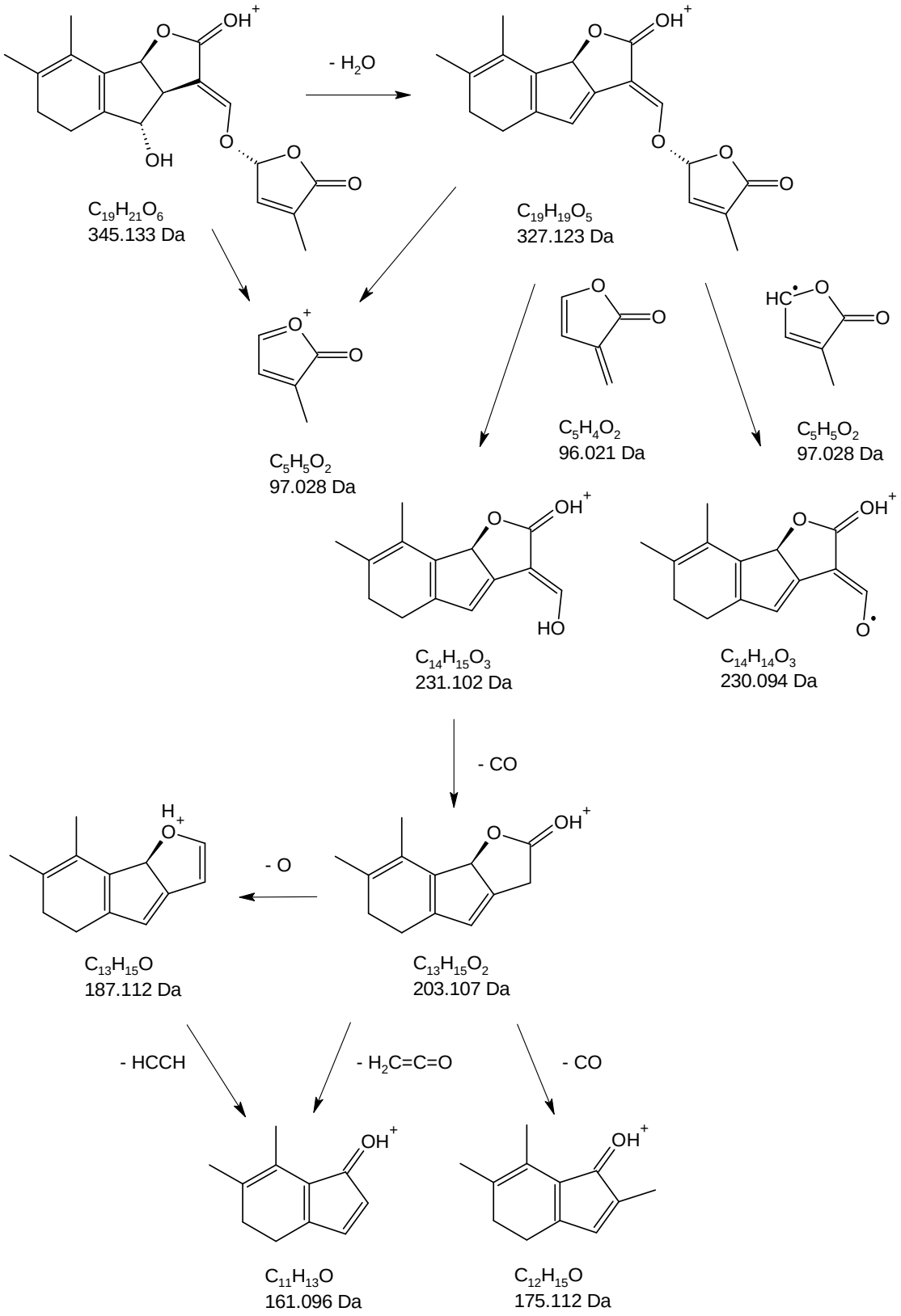

Figure 7: Putative CID fragmentation scheme for the protonated molecular ion of one of the didehydro-orobanchol isomers. For the other three isomers similar fragmentation schemes can be proposed.

reactions were also reported for 4-ketocarotenoid biosynthesis in the flowers of *Adonis aestivalis* (Cunningham and Gantt, 1998, 2005). Analysis of the products of 4-ketolase catalyzed conversion of ß-carotene revealed the production of 4-ketocarotenoids without the expected intermediate 4-hydroxycarotenoids. According to Cunningham and co-authors, 4-ketolases do not only hydroxylate substrates – which should lead to 4-hydroxy-ß-rings if ß-carotene is used as substrate - but can also introduce a 3,4-double bond in the ß-ring of the carotenoid substrate. The 4-keto-ß-ring formation is then the result of keto-enol tautomerisation. This reaction mechanism could also be responsible for the direct oxidation of C7 in orobanchol **1** to 7-oxo-orobanchol **3**, but it seems plausible that the 7-hydroxy-orobanchols **2a,b** are intermediates in this reaction. Dehydration of 7-hydroxy-orobanchol **2** with concomitant migration of the methyl group to the *ortho*-position 7 then leads to two didehydro-orobanchol isomers **4a,b.** This conversion can occur through a desaturation/methyl-transfer mechanism which has recently been reported for the biosynthesis of aromatic carotenoids from ß-carotene via ß-isorenieratene by the new enzyme CrtU (carotene desaturase/methyltransferase) from *S. griseus*, which converts ß-rings to aromatic rings (Krugel et al., 1999; Krubasik and Sandmann, 2000; Graham and Bryant, 2008). Dehydration of compound **2** without methyl migration yields didehydro-orobanchol isomer **5a** and – after further migration of the double bond – didehydro-orobanchol isomer **5b**. Allylic hydroxylation of didehydro-orobanchol isomers **4a,b** in position 5 or 6, giving putative strigolactones **6** and **7,** followed by elimination of water then results in aromatization of the A-ring to give solanacol **9.** Allylic hydroxylation of didehydro-orobanchol isomer **5b** in position 7 results in putative strigolactone **8,** and elimination of water with simultaneous migration of the methyl group to *ortho*-position 7 also leads to aromatization of the A-ring to give solanacol **9.** The putative hydroxyl-didehydro-orobanchols **6, 7** and **8** are expected to be reactive, short-living compounds, which would explain why we have not observed them so far.

Conclusion

More and more strigolactones are being discovered and it can be assumed that strigolactone biosynthesis is ubiquitous in the plant kingdom. It has been reported that structural differences between strigolactones lead to differential activity on AM branching (Akiyama et al., 2010) and parasitic seed germination (Yoneyama et al., 2009). Similar claims were made for their role in controlling shoot branching (Yamaguchi, 2010 IPGSA conference) Indicating that the functionalisation of strigolactones is important in determining their activity in the different biological processes in which they are involved. However, not much is known about these later steps in strigolactone biosynthesis in which the core ABCD structure is decorated. Here, for the first time we describe a multi-step functionalization pathway of the strigolactone backbone with identification of all the intermediates involved. The identification of the strigolactones orobanchol, two 7-hydroxy-orobanchol isomers, 7-oxo-orobanchol and four didehydro-orobanchol isomers in tomato allowed us to propose that the aromatic strigolactone solanacol that is also present in tomato is derived from orobanchol through a series of enzymatic hydroxylation/dehydroxylation reactions with migration of a methyl group and double bonds. These results will be instrumental for the biochemical and molecular characterization of these later steps in strigolactone biosynthesis, which should in the end lead to the possibility to tune strigolactone composition for optimized biological activity and possibly breeding a plant that produces root exudates that do induce AM branching but is not parasites seed germination.

Materials and methods

Plant material and chemicals

Seeds of tomato (*Solanum lycopersicum* L.) cultivar Manapal (LA3007) and *hp-2*^{dg} mutant (LA2451) were originally provided by R.T. Chetelat (Tomato Genetics Cooperative, UC Davis, USA). Seeds of tomato *sitiens* (LA0574) and its parental isogenic cv. Rheinlands Ruhm, and *flacca* (LA3613) and corresponding parental isogenic cv. Ailsa Craig (LA2838a), were obtained from the Tomato Genetics Resource Center (TGRC) at the University of California, Davis, CA, USA. Seeds of cv. Ailsa Craig (LA2838a) and *notabilis* (LA3614) were kindly provided by Wim Vriezen (Department of Plant Cell Biology, Radboud University, Nijmegen, the Netherlands). Seeds of tomato cv. Craigella (LA3247) were kindly provided by Ruud de Maagd (Plant Research International, Wageningen, the Netherlands). Seeds of cv. Micro-tom (LA3911) were kindly provided by Jules Beekwilder (Plant Research International, Wageningen, the Netherlands). Seeds of tomato cv. Moneymaker were provided by Fien Meijer (Laboratory of Plant Breeding. Wageningen University, the Netherlands). Silica gel 60 (70-230 mesh ASTM) was purchased from Merck (Germany).

Growth conditions and experiments

Tomato seedlings from all cultivars were grown under controlled conditions in a greenhouse at 16h light/8h dark, 23°C/20°C, and 60% relative humidity in pots with sand/vermiculate. Phosphate starvation and root exudates collection were carried out as previously described (López-Ráez et al., 2008). For a more detailed investigation of the strigolactone composition the root exudates collected from roughly 100 tomato plants from each cultivar were loaded on a C18-SPE cartridge (GracePure C18-Fast 5000 mg / 20 ml). The strigolactones were eluted with 100% acetone and the acetone was subsequently evaporated in vacuum. The resulting solid material (20-30 mg) was re-dissolved in ethyl acetate and loaded on a column containing 2500 mg of Silica gel 60 (Merck, Germany). Fifteen ml fractions were eluted using an hexane/ethyl acetate gradient (from 0 to 100% ethyl acetate). In total ten fractions were collected. The solvent was evaporated in vacuum and the residue was dissolved in acetonitrile-water (25:75). Aliquots from each fraction were used for LC–MS/MS analysis. MS/MS fragmentation spectra were recorded from the compounds of interest in each of the fractions.

Extraction of germination stimulants from roots

In addition to root exudates, 500 mg root samples collected from phosphate starved plants (López-Ráez et al., 2008) were used to extract the germination stimulants from the tomato roots. The roots were ground in a mortar and pestle with liquid nitrogen and then extracted twice with 2 ml of ethyl acetate in a 10 ml glass tube. The tubes were vortexed and sonicated for 10 min in a Branson 3510 ultrasonic bath (Branson Ultrasonics, Danbury, CT, USA). Samples were centrifuged for 10 min at 1350 x *g* in an MSE Mistral 2000 centrifuge (Mistral Instruments, Leicester, UK), and the organic phase was carefully transferred to 4 ml glass vials, after which the solvent was evaporated. The residue was dissolved in acetonitrile-water (25:75) and aliquots from each fraction were used for LC–MS/MS analysis.

Strigolactone detection and identification by liquid chromatography tandem mass spectrometry (LC–MS/MS)

Analysis was performed as described by López-Ráez et al. (2008b) with some modifications. A Waters Xevo tandem mass spectrometer (Waters, Milford, MA, USA) equipped with an electrospray ionization (ESI) source and coupled to an Acquity UPLC system (Waters, USA) was used. Chromatographic separation was achieved on an Acquity UPLC BEH C_{18} column (150 x 2.1 mm, 1.7

µm) (Waters) by applying a acetonitrile-water (MeCN-H_2O) gradient to the column, starting from 5% MeCN for 0.5 min and rising to 27% MeCN at 1.0 min, followed by a 6.5 min gradient to 40% MeCN, followed by a 4.5 min gradient to 65% MeCN, which was maintained for 0.1 min, followed by a 0.4 min gradient to 90% MeCN, which was maintained for 0.2 min, before going back to 5% MeCN using a 0.3 min gradient, prior to the next run. Then column was equilibrated for 3 min, using this solvent composition. This gradient was used for the analysis of crude tomato root exudates and SPE fractions.. To obtain a better separation of closely eluting isomers, and for on-line recording of MS/MS fragmentation spectra, an optimized gradient was used, starting from 5% MeCN for 1.0 min and rising to 25% MeCN at 2.0 min, followed by a 7.5 min gradient to 35% MeCN, followed by a 2.5 min gradient to 65% MeCN, followed by a 1 min gradient to 90% acetonitrile which was maintained for 1.7 min before going back to 5% MeCN using a 0.3 min gradient, prior to the next run. The column was equilibrated for 3 min, using this solvent composition. The column was operated at 50 ºC with a flow-rate of 0.4 ml min^{-1}. Sample injection volume was 15 µl. The mass spectrometer was operated in positive ESI mode. Cone and desolvation gas flows were set to 50 and 1000 l h^{-1}, respectively. The capillary voltage was set at 3.0 kV, the source temperature at 150ºC and the desolvation temperature at 650ºC. The cone voltage was optimized for each strigolactone standard using the IntelliStart MS Console. Argon was used for fragmentation by collision induced dissociation (CID). Multiple reaction monitoring (MRM) was used for identification of strigolactones in tomato root exudates and extracts by comparing retention times and MRM mass transitions with those of available strigolactone standards such as orobanchol, 2'-epi-orobanchol, 5-deoxystrigol, 2'-epi-5-deoxystrigol, sorgolactone, strigol, solanacol, sorgomol, orobanchyl acetate, 7-oxo-orobanchol, 7-oxo-orobanchyl acetate and 7-hydroxy-orobanchol. MRM transitions were optimized for each standard using the IntelliStart MS Console. The MRM transitions for putative didehydro-orobanchol (and didehydro-strigol) isomers were optimized using the MS/MS fragmentation spectra of these compounds, by injection of tomato root exudates (López-Ráez et al., 2008).
MRM-transitions for all relevant strigolactones and intermediates were incorporated in the MRM-method (Table1). Data acquisition and analysis were performed using MassLynx 4.1 software (Waters).

Table 1. MS/MS conditions for strigolactones analysis of the tomato root exudates and extracts.

Compound	**Precursor Ion (*m/z*)**	**Cone Voltage (V)**	**Collision energy (eV)**	**Daughter Ion (*m/z*)**
Solanacol	343.16	15.0	25.0	96.97
			20.0	183.02
Didehydro-orobanchol	345.16	18.0	22.0	96.96
			20.0	175.27
			16.0	203.00
Orobanchol	347.20	18.0	22.0	97.00
			18.0	205.20
			12.0	233.15
7-Oxo-orobanchol	361.16	15.0	20.0	96.94
			15.0	247.05
7-Hydroxy-orobanchol	363.20	15.0	20.0	96.96
			10.0	249.00
Orobanchyl acetate	389.20	22.0	12.0	233.15
			10.0	347.20

Accurate mass determinations with LC–LTQ/Orbitrap–MS.

The accurate mass for the protonated molecular ions $[M + H]^+$ of four didehydro-orobanchol isomers was determined using a LTQ/Orbitrap XL hybrid mass spectrometer (Thermo Scientific, Bremen, Germany) equipped with an electrospray ionization (ESI) source coupled to an Accela U HPLC system (pump and auto sampler) equipped with an Accela PDA with a 1 cm lightPipe flow cell (Thermo Scientific).

Chromatographic separation was achieved on an HPLC Luna 3u C18(2) 100A column (150 x 2.0 mm, particle size 3.2 µm) (Phenomenex, Torrance, CA, USA) by applying an acetonitrile- water-formic acid (0.1%) gradient to the column, starting from 5% MeCN rising to 75% MeCN in 45.0 min, followed by a 2.0 min gradient to 90% MeCN, which was then maintained for 5.0 min before going back to 5% MeCN using a 3.0 min gradient. Finally, the column was equilibrated for 5.0 min, using this solvent composition. The column was operated at 40 ºC with a flow-rate of 190 µl min^{-1}. Sample injection volume was 5 µl. The mass spectrometer was operated in positive ESI mode. Sheath, Auxiliary and Sweep gas flows were set to 50, 5 and 5 l h^{-1}, respectively. The source voltage and capillary voltage were set at 4.5 kV and 38.0 V, respectively. The capillary temperature was set at 295ºC.

Data acquisition and analysis were performed using Xcalibur software (Thermo Scientific).

Acknowledgements

We acknowledge funding by The Netherlands Organization for Scientific Research (NWO; VICI-grant to HB) and the European Commission (Intra-European Marie Curie postdoctoral fellowship FP6-MEIF-CT-2005-024345 and Reintegration Grant PERG-02-2007-224751 from the Marie Curie program to Juan A. López-Ráez). JAL-R is supported by a postdoctoral contract (JAE-Doc) from the Spanish Research Council (CSIC). This project was co-financed by the Centre for BioSystems Genomics (CBSG) which is part of the Netherlands Genomics Initiative/Netherlands Organization for Scientific Research.

References

Akiyama K, Matsuzaki K, Hayashi H (2005) Plant sesquiterpenes induce hyphal branching in arbuscular mycorrhizal fungi. Nature **435:** 824-827

Akiyama K, Ogasawara S, Ito S, Hayashi H (2010) Structural requirements of strigolactones for hyphal branching in AM fungi. Plant and Cell Physiology **51:** 1104-1117

Booker J, Auldridge M, Wills S, McCarty D, Klee H, Leyser O (2004) MAX3/CCD7 is a carotenoid cleavage dioxygenase required for the synthesis of a novel plant signaling molecule. Current Biology **14:** 1232-1238

Bouwmeester HJ, Matusova R, Zhongkui S, Beale MH (2003) Secondary metabolite signalling in host-parasitic plant interactions. Current Opinion in Plant Biology **6:** 358-364

Bouwmeester HJ, Roux C, López-Ráez JA, Bécard G (2007) Rhizosphere communication of plants, parasitic plants and AM fungi. Trends in Plant Science **12:** 224-230

Cunningham FX, Gantt E (1998) Genes and enzymes of carotenoid biosynthesis in plants. Annual Review of Plant Physiology and Plant Molecular Biology **49:** 557-583

Cunningham FX, Gantt E (2005) A study in scarlet: enzymes of ketocarotenoid biosynthesis in the flowers of Adonis aestivalis. Plant Journal **41:** 478-492

Gomez-Roldan V, Fermas S, Brewer PB, Puech-Pages V, Dun EA, Pillot J-P, Letisse F, Matusova R, Danoun S, Portais J-C, Bouwmeester H, Becard G, Beveridge CA, Rameau C, Rochange SF (2008) Strigolactone inhibition of shoot branching. Nature **455:** 189-194

Graham JE, Bryant DA (2008) The biosynthetic pathway for synechoxanthin, an aromatic carotenoid synthesized by the euryhaline, unicellular cyanobacterium *Synechococcus sp* strain PCC 7002. Journal of Bacteriology **190:** 7966-7974

Hedden P, Kamiya Y (1997) Gibberellin biosynthesis: Enzymes, genes and their regulation. Annual Review of Plant Physiology and Plant Molecular Biology **48:** 431-460

Kikuzaki H, Kayano S, Fukutsuka N, Aoki A, Kasamatsu K, Yamasaki Y, Mitani T, Nakatani N (2004) Abscisic acid related compounds and

lignans in prunes (*Prunus domestica L*.) and their oxygen radical absorbance capacity (ORAC). Journal of Agricultural and Food Chemistry **52:** 344-349

Kohlen W, Charnikhova T, Liu Q, Bours R, Domagalska MA, Beguerie S, Verstappen F, Leyser O, Bouwmeester H, Ruyter-Spira C (2011) Strigolactones are transported through the xylem and play a key role in shoot architectural response to phosphate deficiency in nonarbuscular mycorrhizal host Arabidopsis. Plant Physiology **155:** 974-987

Krubasik P, Sandmann G (2000) A carotenogenic gene cluster from Brevibacterium linens with novel lycopene cyclase genes involved in the synthesis of aromatic carotenoids. Molecular and General Genetics **263:** 423-432

Krugel H, Krubasik P, Weber K, Saluz HP, Sandmann G (1999) Functional analysis of genes from Streptomyces griseus involved in the synthesis of isorenieratene, a carotenoid with aromatic end groups, revealed a novel type of carotenoid desaturase. Biochimica Et Biophysica Acta-Molecular and Cell Biology of Lipids **1439:** 57-64

Lin H, Wang R, Qian Q, Yan M, Meng X, Fu Z, Yan C, Jiang B, Su Z, Li J, Wang Y (2009) DWARF27, an iron-containing protein required for the biosynthesis of strigolactones, regulates rice tiller bud outgrowth. Plant Cell **21:** 1512-1525

López-Ráez JA, Charnikhova T, Gómez-Roldán V, Matusova R, Kohlen W, Vos RD, Verstappen F, Puech-Pages V, Bécard G, Mulder P, Bouwmeester H (2008) Tomato strigolactones are derived from carotenoids and their biosynthesis is promoted by phosphate starvation. New Phytologist **178:** 863-874

López-Ráez JA, Charnikhova T, Mulder P, Kohlen W, Bino R, Levin I, Bouwmeester H (2008) Susceptibility of the tomato mutant high pigment-2dg (hp-2dg) to *Orobanche spp*. infection. Journal of Agricultural and Food Chemistry **56:** 6326-6332

López-Ráez JA, Kohlen W, Charnikhova T, Mulder P, Undas AK, Sergeant MJ, Verstappen F, Bugg TDH, Thompson AJ, Ruyter-Spira C, Bouwmeester H (2010) Does abscisic acid affect strigolactone biosynthesis? New Phytologist **187:** 343-354

Maresca JA, Romberger SP, Bryant DA (2008) Isorenieratene biosynthesis in green sulfur bacteria requires the cooperative actions of two carotenoid cyclases. Journal of Bacteriology **190:** 6384-6391

Matusova R, Rani K, Verstappen FWA, Franssen MCR, Beale MH, Bouwmeester HJ (2005) The strigolactone germination stimulants of the plant-parasitic *Striga* and *Orobanche spp*. are derived from the carotenoid pathway. Plant Physiology **139:** 920-934

Moshier SE, Chapman DJ (1973) Biosynthetic studies on aromatic carotenoids - Biosynthesis of chlorobactene. Biochemical Journal **136:** 395-404

Rani K, Zwanenburg B, Sugimoto Y, Yoneyama K, Bouwmeester HJ (2008) Biosynthetic considerations could assist the structure elucidation of host plant produced rhizosphere signalling compounds (strigolactones) for arbuscular mycorrhizal fungi and parasitic plants. Plant Physiology and Biochemistry **46:** 617-626

Sato D, Awad AA, Chae SH, Yokota T, Sugimoto Y, Takeuchi Y, Yoneyama K (2003) Analysis of strigolactones, germination stimulants for *Striga* and *Orobanche*, by high-performance liquid chromatography/tandem mass spectrometry. Journal of Agricultural and Food Chemistry **51:** 1162-1168

Schachtschabel D, David A, Menzel KD, Schimek C, Woestemeyer J, Boland W (2008) Cooperative biosynthesis of trisporoids by the (+) and (-) mating types of the zygomycete *Blakeslea trispora*. Chembiochem **9:** 3004-3012

Schwartz SH, Qin XQ, Zeevaart JAD (2003) Elucidation of the indirect pathway of abscisic acid biosynthesis by mutants, genes, and enzymes. Plant Physiology **131:** 1591-1601

Sorefan K, Booker J, Haurogné K, Goussot M, Bainbridge K, Foo E, Chatfield S, Ward S, Beveridge C, Rameau C, Leyser O (2003) *MAX4* and *RMS1* are orthologous dioxygenase-like genes that regulate shoot branching in Arabidopsis and pea. Genes & Development **17:** 1469-1474

Takikawa H, Jikumaru S, Sugimoto Y, Xie X, Yoneyama K, Sasaki M (2009) Synthetic disproof of the structure proposed for solanacol, the germination stimulant for seeds of root parasitic weeds. Tetrahedron Letters **50:** 4549-4551

Umehara M, Hanada A, Yoshida S, Akiyama K, Arite T, Takeda-Kamiya N, Magome H, Kamiya Y, Shirasu K, Yoneyama K, Kyozuka J, Yamaguchi S (2008) Inhibition of shoot branching by new terpenoid plant hormones. Nature **455:** 195-200

Xie X, Yoneyama K, Yoneyama K (2010) The strigolactone story. Annual Review of Phytopathology **48:** 93-117

Xie XN, Yoneyama K, Kurita JY, Harada Y, Yamada Y, Takeuchi Y (2009) 7-oxoorobanchyl acetate and 7-oxoorobanchol as germination stimulants for root parasitic plants from flax (*Linum usitatissimum*). Bioscience Biotechnology and Biochemistry **73:** 1367-1370

Yoneyama K, Awad AA, Xie X, Yoneyama K, Takeuchi Y (2010) Strigolactones as germination stimulants for root parasitic plants. Plant and Cell Physiology **51:** 1095-1103

Yoneyama K, Xie X, Sekimoto H, Takeuchi Y, Ogasawara S, Akiyama K, Hayashi H (2008) Strigolactones, host recognition signals for root parasitic plants and arbuscular mycorrhizal fungi, from Fabaceae plants. New Phytologist **179:** 484-494

Yoneyama K, Xie X, Yoneyama K, Takeuchi Y (2009) Strigolactones: structures and biological activities. Pest Management Science **65:** 467-470

Zaharia LI, Walker-Simmon MK, Rodriguez CN, Abrams SR (2005) Chemistry of abscisic acid, abscisic acid catabolites and analogs. Journal of Plant Growth Regulation **24:** 274-284

Zwanenburg B, Mwakaboko AS, Reizelman A, Anilkumar G, Sethumadhavan D (2009) Structure and function of natural and synthetic signalling molecules in parasitic weed germination. Pest Management Science **65:** 478-491

Chapter 3

The tomato *CAROTENOID CLEAVAGE DIOXYGENASE8 (SlCCD8*) is regulating rhizosphere signaling, plant architecture and reproductive development through strigolactone biosynthesis

Wouter Kohlen[*], Juan A. López-Ráez[*], Tobia Pollina, Michiel Lammers, Peter Tóth, Tatsiana Charnikhova, Juan M. García, Ruud A. de Maagd, María J. Pozo , Harro J. Bouwmeester and Carolien Ruyter-Spira

* contributed equally to this work

Adapted version submitted to The Plant Journal (2011)

Abstract

The strigolactones are a new class of phytohormones that inhibit lateral branching of plants while they were initially identified as germination stimulants for seeds of root parasitic plants of the Orobanchaceae and the pre-symbiotic signal inducing hyphal branching in arbuscular mycorrhizal (AM) fungi. In the present work a tomato *CAROTENOID CLEAVAGE DIOXYGENASE 8* (*SlCCD8*) was cloned and its role in strigolactone biosynthesis and plant architecture assessed by making transgenic tomato plants containing a *SlCCD8* RNAi construct. Here, we demonstrate that a mild reduction in strigolactone biosynthesis and concomitant secretion into the rhizosphere is sufficient to reduce root parasitism by *Phelipanche ramosa* by about 90% without compromising apical dominance or AM symbiosis establishment too much. However, lines exhibiting a stronger reduction in *SlCCD8* expression displayed excessive lateral shoot branching, reduced plant height and increased numbers of nodes. The severity of these phenotypes correlated with the levels of orobanchol present in tomato xylem sap. Additional phenotypes in the tomato reproductive development - such as smaller flowers, fruits and seeds which are normally associated with reduced auxin levels - were also found in these strigolactone-deficient transgenic lines. This could be a secondary effect of the excessive branching observed in these lines. However, the fact that free auxin levels in these organs were changed, might indicate that these phenotypes are the consequence of the strigolactone crosstalk with auxin.

Keywords: tomato, strigolactones, shoot branching, arbuscular mycorrhizal fungi, Orobanchaceae, reproductive development

Introduction

Strigolactones are carotenoid derived signaling molecules (Matusova et al., 2005) which were initially identified as the germination stimulants for root parasitic plants of the Orobanchaceae (Cook et al., 1966; Bouwmeester et al., 2003) and the pre-symbiotic signal that induces hyphal branching in arbuscular mycorrhizal (AM) fungi (Akiyama et al., 2005). They have been detected in the root extracts and exudates of monocot as well as dicot plant species (Yoneyama et al., 2007; Goldwasser et al., 2008; Gomez-Roldan et al., 2008; López-Ráez et al., 2008; Umehara et al., 2008; Kohlen et al., 2011). Recently, strigolactones were identified as the elusive branching inhibiting signal (Sorefan et al., 2003; Bainbridge et al., 2005; Gomez-Roldan et al., 2008; Umehara et al., 2008). This signal is graft transmissible and originates, at least in part, from the roots (Beveridge et al., 1994; Napoli, 1996; Turnbull et al., 2002). However, the exact tissue origin of the strigolactones that are supposed to inhibit axillary bud outgrowth in the shoot remains unknown (Foo et al., 2001). Nevertheless, it is likely that they are transported acropetally to the aerial parts of the plant where they exert their inhibiting effect on shoot branching (Bennett et al., 2006). Supporting this hypothesis, it was recently demonstrated that in *Arabidopsis thaliana* and tomato (*Solanum lycopersicum*) at least one strigolactone (orobanchol) is transported through the xylem (Kohlen et al., 2011).
Several new strigolactone functions have been identified in addition to their role in regulating shoot architecture. Recently, a small-molecule screen identified several putative functions for strigolactones in Arabidopsis development, from seed germination to hypocotyl elongation (Tsuchiya et al., 2010). Moreover, strigolactones have been recently shown to be involved in root system architecture (RSA) (Kapulnik et al., 2011; Ruyter-Spira et al., 2011).

Four enzymes involved in strigolactone biosynthesis have so far been identified. CAROTENOID CLEAVAGE DIOXYGENASE7 (CCD7) and CAROTENOID CLEAVAGE DIOXYGENASE8 (CCD8) sequentially (Sorefan et al., 2003; Booker et al., 2004; Gomez-Roldan et al., 2008; Umehara et al., 2008) cleave an unknown carotenoid substrate to an unknown apocarotenoid which is then likely modified by DWARF27 (Lin et al., 2009), MORE AXILLARY GROWTH1 (MAX1) (Stirnberg et al., 2002; Booker et al., 2005; Crawford et al., 2010; Kohlen et al., 2011) and possibly other enzymes to likely form 5-deoxystrigol as the first real strigolactone (Matusova et al., 2005; Rani et al., 2008). In addition, two proteins, MAX2 (Stirnberg et al., 2002; Stirnberg et al., 2007) and D14 (Arite et al., 2009), were identified to act in strigolactone downstream signaling. Mutations in any of these enzymes/proteins result in highly branched phenotypes.
Tomato is an important model in strigolactone research and its strigolactone composition (solanacol, orobanchol and didehydro-orobanchol isomers 1 and 2) has been elucidated (López-Ráez et al., 2008). In tomato, just as in other plant species, the biosynthesis and secretion of the strigolactones into the rhizosphere is up-regulated under phosphate-limiting conditions (López-Ráez et al., 2008), a response which is believed to stimulate AM symbiosis (Akiyama et al., 2005). However, it was recently demonstrated in rice and Arabidopsis that elevated strigolactone levels under phosphate-limiting concentrations is likely also functioning as a signal to reduce shoot branching under these growth-limiting conditions, where plants need to invest in root rather than in shoot branching. This could represent a second evolutionary advantage which would be an additional driving force for the conservation/development of low-phosphate-induced strigolactone biosynthesis (Umehara et al., 2010; Kohlen et al., 2011).
Also in tomato, a correlation between strigolactones and abscisic acid (ABA) in three different ABA-deficient mutants (*notabilis, flacca* and *sitiens*) was reported, suggesting a possible involvement of

this phytohormone in strigolactone biosynthesis (López-Ráez et al., 2010). Furthermore, it was demonstrated that carotenoid accumulation in the *high pigment-2*^{darkgreen} (*hp-2*^{dg}) mutant reduced strigolactone biosynthesis and secretion into the rhizosphere, leading to a reduced infection by the root parasitic *Phelipanche ramosa* (López-Ráez et al., 2008). This is one of the first reports showing that controlling strigolactone biosynthesis might be a good strategy to reduce the root parasitic weed problem (López-Ráez et al., 2009). The first tomato strigolactone biosynthetic gene, *SlCCD7*, was recently cloned and characterized, proving that strigolactones function in the control of lateral outgrowth of tomato as well (Vogel et al., 2010). In addition, a previously identified *Orobanche* resistant and AM deficient tomato mutant, *slort1,* was reported to produce only minor amounts of strigolactones through reduced biosynthesis in this mildly branched mutant (Koltai et al., 2010). However, the gene underlying *slort1* and its function in regulating strigolactone biosynthesis remains unknown.

Having full insight into the strigolactone biosynthetic pathway in tomato is vital, as this would make it an excellent model for combining analytical and molecular tools for strigolactone research. In the present study the tomato *SlCCD8* gene was cloned and its role in strigolactone biosynthesis assessed. The effect of reduced *CCD8* expression on tomato shoot architecture was investigated as well as its effect on rhizosphere signaling. In addition to this, we provide evidences for the role of the tomato *SlCCD8* in tomato reproductive development by analyzing flowers, fruit set and seed development.

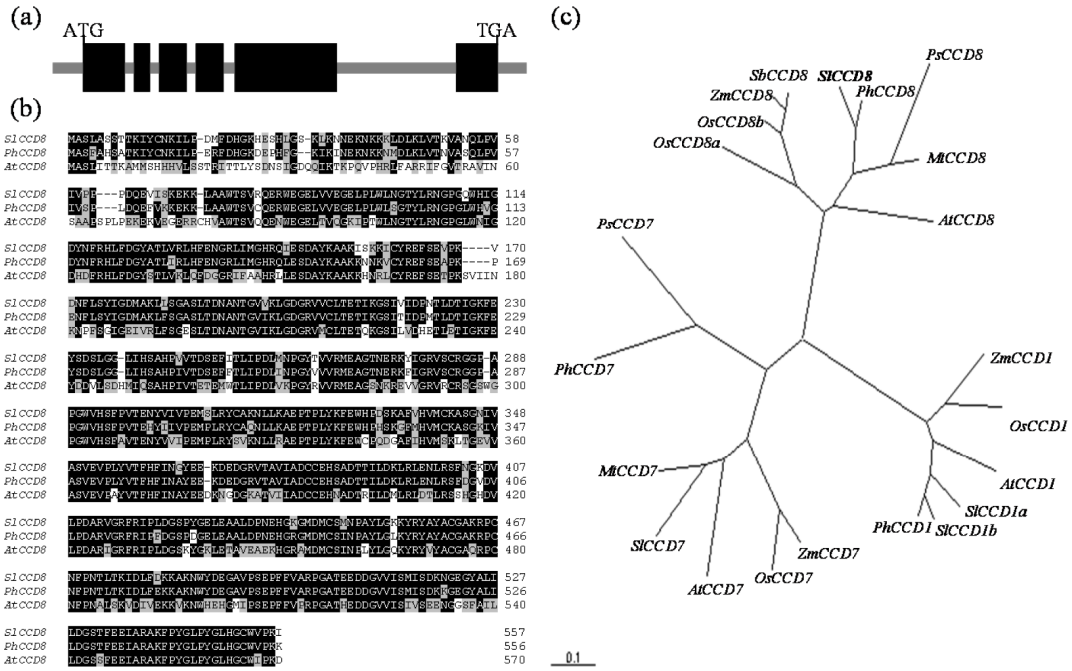

Figure 1. The tomato *CCD8* (*SlCCD8*) gene, **(a)** The postulated intron/exon structure for the complete *SlCCD8* gene (4100 nt), **(b)** Alignment of the putative SlCCD8 amino acid sequence with those from known CCD8 proteins; Sl, *Solanum lycopersicum*; Ph, *Petunia hybrida*; At, *Arabidopsis thaliana*. Identical and similar amino acids are shaded in black and grey, respectively, **(c)** Phylogenetic tree of known *CCD1*, *CCD7* and *CCD8* nucleotide sequences; Ps, *Pisum sativum*; Os, *Oryza sativa*; Zm, *Zea mays*; Mt, *Medicago truncatula*; Sb, *Sorghum bicolor* (*AtCCD1* (AT3G63520), *OsCCD1* (Os12g0640600), *PhCCD1* (AY576003), *SlCCD1a* (AY576001), *SlCCD1b* (AY576002), *ZmCCD1* (GRMZM2G057243), *AtCCD7* (AT2G44990), *MtCCD7* (Medtr7g040830), *OsCCD7* (Os04g0550600), *PsCCD7* (DQ403160), *PhCCD7* (FJ790878), *SlCCD7* (GQ468556), *ZmCCD7* (GRMZM2G158657), *AtCCD8* (AT4G32810), *MtCCD8* (Medtr3g127920), *OsCCD8a* (Os01g0566500), *OsCCD8b* (Os01t0746400), *PsCCD8* (AY557342), *PhCCD8* (AY743219), *SbCCD8* (Sb03g034400), *ZmCCD8* (GRMZM2G446858).

Results

SlCCD8 cloning and characterization

A search of the available tomato EST libraries failed to identify sequences with homology to any published *CCD8* sequences. Therefore, a PCR-based approach using primers designed against highly conserved regions in known plant *CCD8s* in combination with RACE was used to isolate the full-length coding sequence of the putative tomato *CCD8*/*MAX4*, hereafter designated as *SlCCD8*. *SlCCD8* has an open reading frame (ORF) of 1674 bp (Supplemental Table S3.1). *SlCCD8* was BLASTed against the tomato genome (Bombarely et al., 2011) and aligned with a 4100 bp region located on chromosome 8. *SlCCD8* is predicted to contain six exons (Figure 1a). The ORF encodes a 557 amino acid protein (Supplemental Table S3.2) with a 89% and 66% homology to *Petunia hybrida* CCD8/DAD1 (PhCCD8/DAD1) and Arabidopsis CCD8/MAX4 (AtCCD8/MAX4) proteins, respectively (Figure 1b). In a phylogenetic alignment *SlCCD8* clustered closely together with *PhCCD8/DAD1* in what seems to constitute a sub-clade of dicot *CCD8s* (Figure 1c). Monocot *CCD8s* of maize, rice and sorghum clustered separately from the dicot ones.

SlCCD8 was primarily expressed in the roots and stems of tomato, with the highest expression in the roots (Figure 2a). *SlCCD8* expression could also be detected in other plant tissues such as leaves, flowers and green fruits, although in low levels only (Figure 2a).

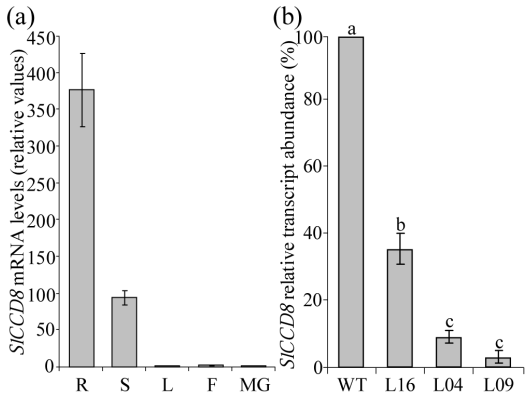

Figure 2: SlCCD8 transcript accumulation, **(a)** Expression of SlCCD8 in tomato Craigella (wild-type) in different plant tissues: root (R), stem (S), leaf (L), flower (F) and mature green fruit (MG) (n=3), **(b)** Expression of SlCCD8 in the roots of Craigella and three independent SlCCD8 RNAi lines (L16, L04, and L09) The expression in wild-type tomato is set at 100%. Bars represent means of 3 replicates ± s.e. Bars with different letters differ significantly at P<0.05.

In order to address the biological function of *SlCCD8*, an RNAi construct was created and transformed into the tomato cultivar Craigella. Three independent *SlCCD8* antisense lines (L16, L04 and L09) displaying a 64%, 91% and 97% reduction in *SlCCD8* RNA levels in the roots, respectively (Figure 2b) were selected and propagated to the T_3 generation. Transcript levels of the homologous *SlCCD7* was not reduced in any of the transgenic lines (data not shown), confirming the construct specificity for *SlCCD8*.

The role of *SlCCD8* in rhizosphere signaling

To assess the effect of the reduction in *SlCCD8* expression in the transgenic lines on strigolactone exudation and rhizosphere signaling, root exudates from tomato plants were collected and their strigolactone levels analyzed by liquid chromatography-tandem mass spectrometry (MRM-LC-MS/MS). The levels of all four strigolactones that could be detected in tomato root exudates were reduced in all three transgenic lines compared with the wild-type. In L16 the exuded strigolactone levels were reduced by 52%, whereas in L04 and L09 a 95% reduction was observed in both lines (Figure 3a). AM colonization by *Glomus intraradices* in L16, L04 and L09 was reduced by 27%, 44% and 65% compared with the wild-type, respectively (Figure 3b). This reduction in AM symbiosis correlated to some extent with the decrease in strigolactone exudation (Figure 3a). In addition, a 90% reduction in the emergence of shoots of *P. ramosa* was observed for all three lines compared

with the wild-type (Figure 3c). *P. ramosa* seed germination in 4000-fold diluted root exudates was significantly lower for the transgenic lines (Figure 3d) and this decrease correlated well with the reduction in strigolactone levels detected by MRM-LC-MS/MS (Figure 3a).

Effect of decreased *SlCCD8* expression on shoot architecture

To assess the consequence of the reduced strigolactone levels on shoot architecture, L16, L04 and L09 were grown in pots for 8 weeks. All three knock-down lines were significantly more branched compared with the wild-type, displaying a 1.7, 4.4 and 7.3-fold increase in lateral shoot branches, respectively (Figure 4a, b). The increase in lateral branching was inversely correlated to the levels of *SlCCD8* transcript (Figure 2b). To get a more detailed insight in the effect of the reduction in *SlCCD8* expression on lateral branching, the distribution of first and second order branches was assessed. In wild-type plants approximately 50% of the primary stem nodes were carrying a visible lateral branch, most of which were shorter than 5 cm (Figure 4c). Compared with the wild-type, the *SlCCD8* knock-down lines showed a significant (*P<0.05*) increase in the number of branches of the first order (Supplemental Figure S3.1). Moreover, the distribution of their length was shifted towards the longer categories. No branches of the second order were observed in any of the wild-type plants at this stage of development (Figure 4c), whereas all knock-down lines displayed multiple lateral branches of the second order (Figure 4d, Supplemental Figure S3.1). Again, the increase in secondary lateral branches correlated inversely with the reduction in *SlCCD8* transcript (Figure 1b). The three *SlCCD8* knock-down lines L16, L04 and L09 displayed a reduction in the primary stem height compared with wild-type plants of 19%, 52% and 60%, respectively (Figure 4e), while the total number of nodes increased slightly, but significantly (*P<0.05*) (Figure 4f). When the transgenic lines were grown hydroponically and lateral branches were frequently removed, the reduction in plant height could be partially rescued (Supplemental Figure S3.2; compare with Figure 4e). Finally, a striking phenotype of the transgenic *SlCCD8* knock-down lines was that they formed massive amounts of root primordia and adventitious roots on the stems (Supplemental Figure S3.3). This phenotype was less severe in L16 compared with L04 and L09 (Supplemental Figure S3.3) which correlates with the stronger reduction in strigolactone exudation in the latter two lines (Figure 3a).

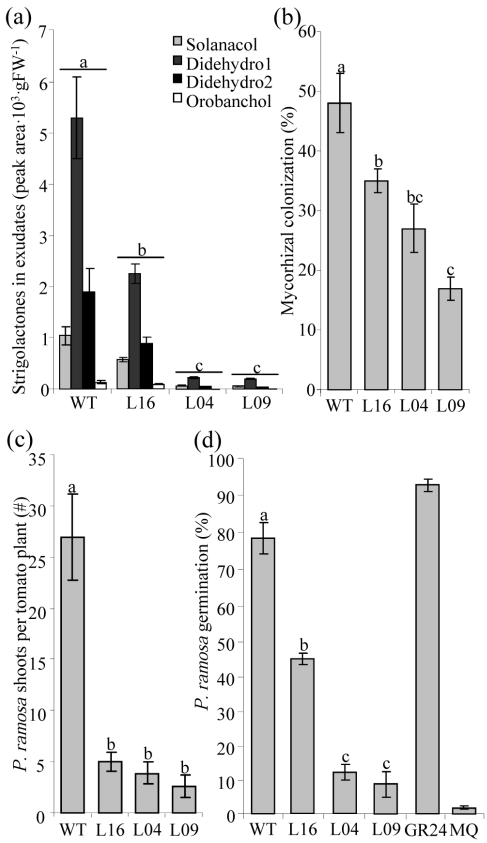

Figure 3: Strigolactone content and rhizosphere interaction analysis of tomato Craigella (wild-type) and three independent SlCCD8 RNAi lines (L16, L04, and L09), (a) MRM-LC-MS/MS quantification of the major tomato strigolactones (solanacol, didehydro-orobanchol isomer 1, didehydro-orobanchol isomer 2 and orobanchol) in root exudates according to the peak area (n=3), (b) Total root colonization by arbuscular mycorrhizal fungi (%) (n=6), (c) P. ramosa infestation counted as emerged shoots per tomato plant (n=6), (d) P. ramosa seed germination induced by 4000-fold diluted root exudates. GR24 (10-9 M) and demineralised water (MQ) are positive and negative control, respectively) (n=3) Bars represent means ± s.e. Bars with a different letter differ significantly; P<0.05.

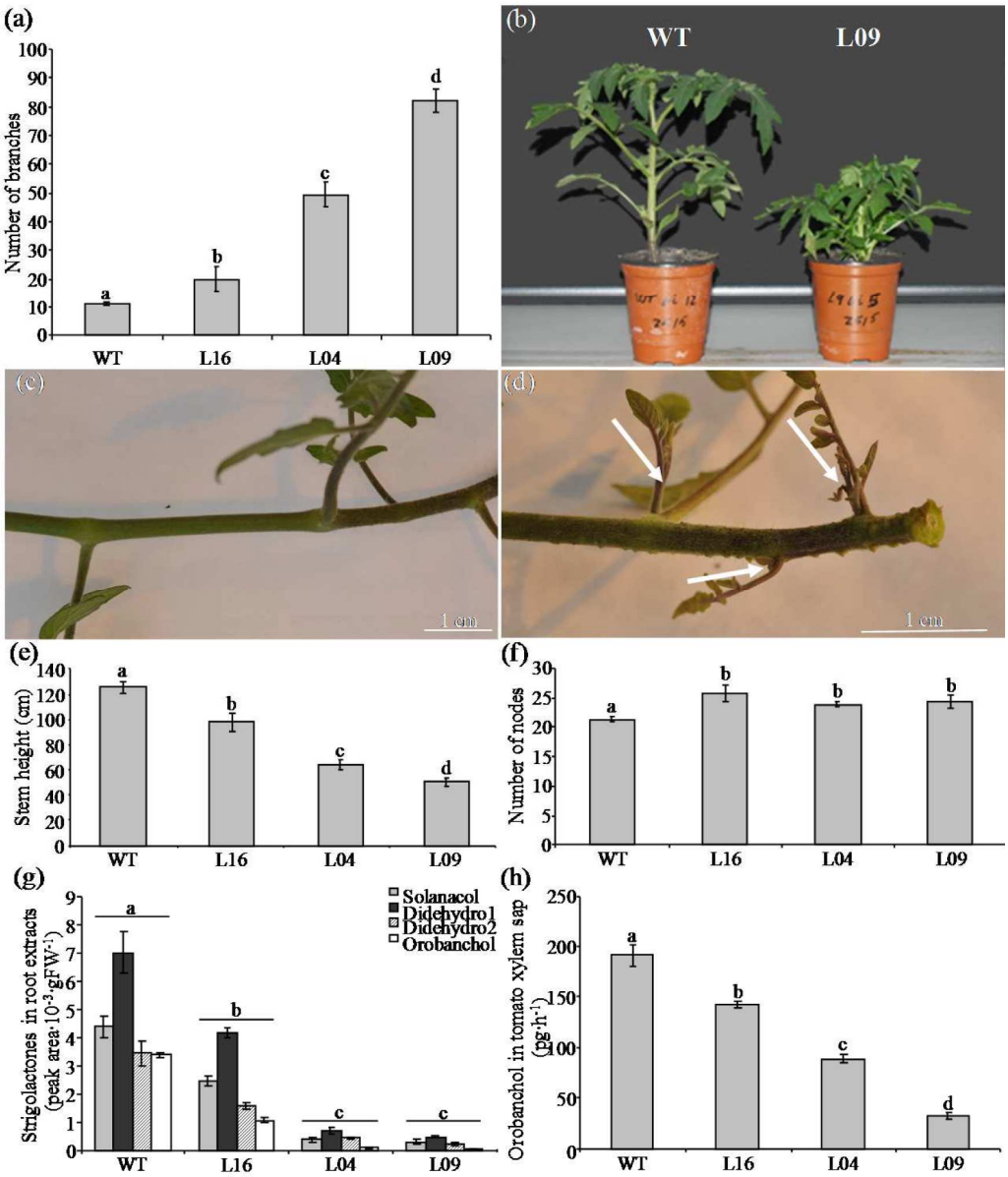

Figure 4: Analysis of shoot architecture (a-f, 8 week-old plants) and strigolactone (g-h, 5 week-old plants) content of tomato Craigella (wild-type) and three independent SlCCD8 RNAi lines (L16, L04, and L09), **(a)** Average number of branches (n=5), **(b)** Photo of wild-type and transgenic SlCCD8 knock-down L09 plants, **(c)** Close-up of wild-type secondary branches, **(d)** Close-up of L09 secondary branches (arrows indicate secondary branches), **(e)** Average main stem height (n=5), **(f)** Average number of nodes per main stem (n=5), **(g)** Strigolactone levels in root extracts (n=3), **(h)** Orobanchol levels in tomato xylem sap (n=5), Bars represent means ± s.e. Bars with different letters differ significantly; P<0.05

Effect of decreased *SlCCD8* expression on strigolactone levels *in planta*

Since the involvement of strigolactones in the inhibition of shoot branching most likely concerns strigolactones that are transported to the shoot rather than exuded into the rhizosphere, strigolactone levels in root extracts of L16, L04 and L09 were analyzed. As in exudates, a clear reduction in the content of all four strigolactones was found in all three lines compared with the wild-type (Figure 4g). On average, the strigolactone concentration in root extracts of L16, which showed the mildest reduction in *SlCCD8* expression, was reduced by 53%, whereas strigolactone levels in L04 and L09 were reduced by 92 and 94%, respectively (Figure 4g), which is almost identical

to the reduction in the exudate (52% for L16 and 95% for L04 and L09).
We previously described that in Arabidopsis and tomato strigolactone formation is induced under phosphate-limiting conditions (López-Ráez et al., 2008; Kohlen et al., 2011). In addition, we recently discovered that in these plants orobanchol is transported through the xylem, and that in Arabidopsis the concentration in the xylem sap is elevated under phosphate deficiency (Kohlen et al., 2011). In the present study, a 5-fold increase in orobanchol level was measured in the xylem sap of phosphate-starved tomato plants (Supplemental Figure S3.4). The three knock-down lines L16, L04 and L09 showed a clear reduction in xylem sap orobanchol levels of 26%, 55% and 84%, respectively, compared with the wild-type (Figure 4h). In addition to orobanchol, orobanchyl acetate was identified in the tomato xylem sap of Craigella (Supplemental Figure S3.5). However, in the experiments to assess the effect of phosphate starvation and *SlCCD8* transcript reduction on xylem sap strigolactones the concentration of orobanchyl acetate was too low for accurate quantification. Interestingly, neither solanacol nor the didehydro-orobanchol isomers were detected in the xylem sap.

The effect of *SlCCD8* knock-down on tomato reproductive development

An additional phenotype of the *SlCCD8* knock-down lines was that the flowers were smaller than in the wild-type (Figure 5a). In order to quantify this effect and elucidate a putative role of strigolactones in flower development, the length of sepals, petals and anthers was measured at anthesis. The average length of all these organs was slightly, but significantly (P<0.05) reduced in all three transgenic lines (Figure 5b). In addition to this, the average diameter of the ovaries was significantly reduced (Figure 5c). It has been postulated that the effect of strigolactones on the inhibition of shoot branching is mediated through the control of auxin fluxes in the plant (Prusinkiewicz et al., 2009). To assess whether the effect of *SlCCD8* knock-down on flower size could also be mediated through auxin, the level of free indole-3-acetic acid (IAA) was determined in flowers collected at anthesis. A reduction of 18%, 34% and 46% in IAA was observed in L16, L04 and L09, respectively (Figure 5d).To gain further insight into the effect of *SlCCD8* silencing on reproductive development, the diameter of tomato ovaries was measured at the beginning of phase III (cell expansion) (Gillaspy et al., 1993) of fruit development. Comparable with un-pollinated ovaries, the diameter of the developing fruits at this stage of development of all *SlCCD8* knock-down lines was smaller than in the wild-type (Figure 6a). No differences in free IAA levels were detected between fruits of the transgenic lines and the wild-type (Figure 6b). However, when the pericarp was separated from the rest of the ovary, a 5-fold higher IAA

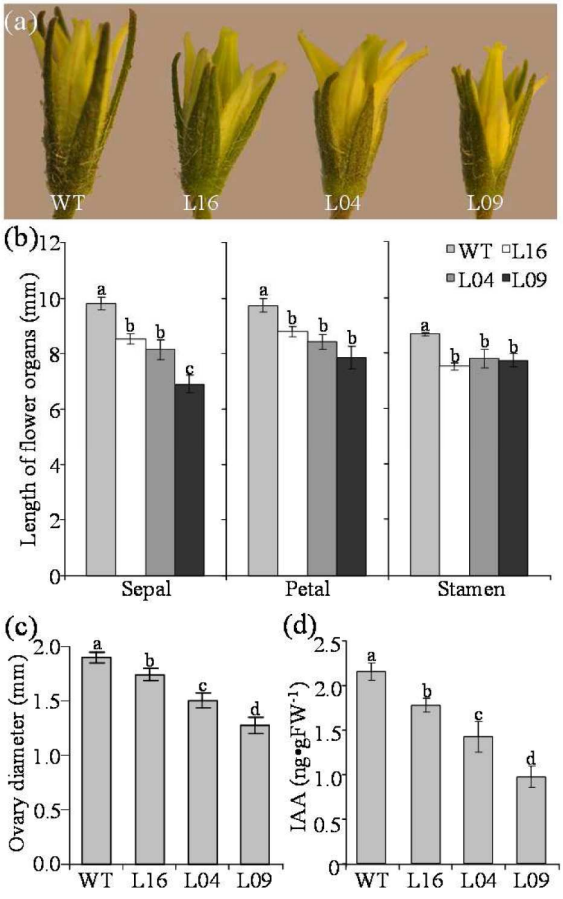

Figure 5: Analysis of flowers of tomato Craigella (wild-type) and three independent SlCCD8 RNAi lines (L16, L04, and L09) at anthesis, **(a)** Flowers at anthesis, **(b)** Average length of flower organs (n=5), **(c)** Average ovary diameter (n=5), **(d)** Free auxin concentration in complete flowers (n=3), Bars represent means ± s.e. Bars with a different letter differ significantly; P<0.05

concentration was detected in wild-type pericarp compared with the remaining tissue, whereas in the two knock-down lines that were tested, L04 and L09, there was no difference in the auxin concentration between pericarp and the rest of the ovary (Figure 6c).

The effect of *SlCCD8* knock-down on fruit size remained during the entire fruit development, leading to significantly smaller mature green (40 days after pollination, DAP) tomato fruits in all knock-down lines (Figure 6d, e). Interestingly, when lateral branches were frequently removed to mimic a relatively normal growth, this effect remained, although it was smaller (Supplemental Figure S3.6). As fruit growth usually correlates with seed quantity, the effect of *SlCCD8* knock-down on seed set was also investigated. Indeed, a significant reduction in both seed quantity and size was found for all three knock-down lines (Figure 7a, b). Overall, these results show that strigolactones play a role in reproductive development in tomato.

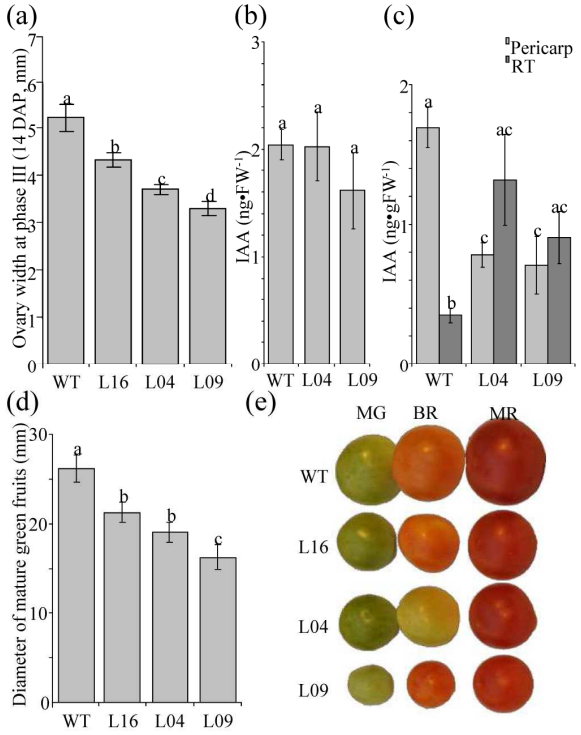

Figure 6: Analysis of fruits of tomato Craigella (wild-type) and three independent SlCCD8 RNAi lines (L16, L04, and L09), **(a)** Average fruit diameter at 14 DAP (days after pollination) (n=10), **(b)** Concentration of free auxin in whole fruits at 14 DAP (n=3), **(c)** Concentration of free auxin in pericarp and remainder of the ovary at 14 DAP (n=3), **(d)** Fruit diameter mature green at 40 DAP (n=10), **(e)** Fruits; mature green (MG), breaker (BR) and mature red (MR), Bars represent means ± s.e. Bars with a different letter differ significantly; P<0.05

orobanchol levels and increased lateral shoot outgrowth was found in these transgenic lines. Furthermore, *P. ramosa* infection was strongly reduced in *SlCCD8* knock-down lines, whereas AM interaction was only mildly affected. In addition, a novel function for strigolactones in reproductive development was identified as flower, fruit and seed development were affected in *SlCCD8* knock-down lines.

SlCCD8 showed highest homology to the petunia *PhDAD1/CCD8* (Figure 1b; Supplemental Table S3) and belongs to a dicot sub-clade within the *CCD8* cluster. Interestingly, petunia strigolactone levels in root extracts are approximately 100-fold lower than in tomato (Kohlen, unpublished

Discussion

In addition to the recently characterized *SlCCD7* (Vogel et al., 2010) we here identified and characterized a second gene encoding a strigolactone biosynthetic enzyme in tomato, *SlCCD8*. We cloned *SlCCD8* and demonstrate that it is involved in the regulation of tomato plant architecture through strigolactone biosynthesis, using *SlCCD8* knock-down lines. A direct negative correlation between xylem sap

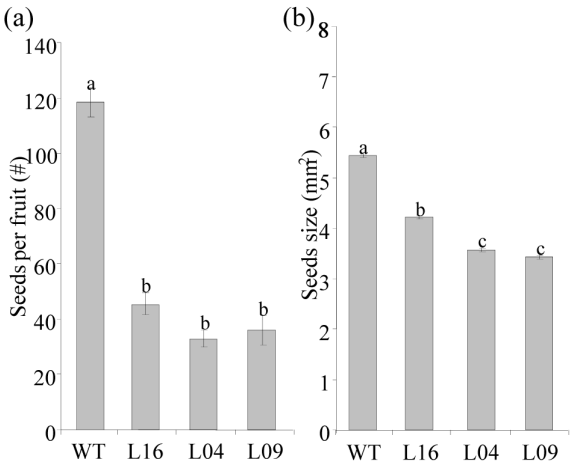

Figure 7: Analysis of seeds of tomato Craigella (wild-type) and three independent SlCCD8 RNAi lines (L16, L04, and L09), **(a)** Average number of seeds per fruit (n=10), **(b)** Average seed size (n>100), Bars represent means ± s.e. Bars with a different letter differ significantly; P<0.05

results). Petunia – as an ornamental plant – was domesticated for abundant branching, whereas in tomato a strong apical dominance is favorable as it results in higher quality fruits. It is not unlikely that the differences in strigolactone concentration are the consequence of this different selection criteria. *SlCCD8* is expressed in all tissues examined, although its transcription is predominantly located in the root and stem tissues (Figure 2a). This is in agreement with the results of *CCD8* expression studies in other plant species (Napoli, 1996; Sorefan et al., 2003; Bainbridge et al., 2005), indicating a conserved function in the plant kingdom.

***SlCCD8* knock-down reduces parasitic plant infestation to a higher extent than AM symbiosis**

The strigolactones were initially identified as germination stimulants for root parasitic plants (Bouwmeester *et al.*, 2003; Cook *et al.*, 1966) and hyphal branching stimulants for AM fungi (Akiyama *et al.*, 2005). Interestingly, the reduction in AM root colonization was not as severe as expected considering the reduction in strigolactone levels in the mutant lines (figure 3a,b). Mycorrhizal colonization was most severely reduced in L09 (a 60% reduction compared to the wild type), whereas strigolactone secretion was reduced by 95%. It has been proposed that the role of strigolactones as branching stimulants is mostly required for hyphae from germinating spores. Thus, AM colonization is less affected by reduced strigolactone levels when using whole inoculum (see experimental procedures) than when using only spores (Koltai *et al.*, 2010). In the present experiment, whole inoculum was used, which could explain the non-linear correlation between AM colonization and the reduction in strigolactone levels.

In contrast, the infection of *SlCCD8* knock-down tomato lines by *P. ramosa* was found to be reduced by 90% in all three transgenic lines (Figure 3c). The observed reduction in emerging parasite shoots found in the antisense L16 cannot be exclusively contributed to the inability of its root exudate to induce *P. ramosa* germination, as germination was only reduced by approximately 50% in this line (Figure 3d). Possibly, the increased lateral shoot branching of the host and the associated resource requirement, inhibits *P. ramosa* development. However, it could also be that strigolactones produced by the host are required in later phases of the *P. ramosa* lifecycle in addition to seed germination. Overall, these results indicate that a small reduction in strigolactone levels could be sufficient to significantly reduce parasitic plant infection in the field, without severely compromising apical dominance (Figure 4) or establishment of AM symbiosis (Figure 3b). This would make strigolactone biosynthesis an excellent target for controlling root parasitism, as was previously postulated (López-Ráez et al., 2009). However, more research will be needed to further assess the consequence of this mild reduction in strigolactone production on crop yield and parasitic weed resistance under field conditions.

***SlCCD8* expression controls shoot architecture through strigolactone levels**

All *SlCCD8* knock-down lines displayed an increase in the total number of lateral branches (Figure 4a) and strigolactone levels in root extracts were reduced similarly as in root exudates. This indicates that – as expected - strigolactone biosynthesis and not secretion is compromised in these transgenic lines. Moreover, the increase in lateral branching is inversely correlated - to some extent - to both the reduction in *SlCCD8* expression (Figure 2b) and the strigolactone levels found in root exudates and extracts (Figure 3a, 4g). Interestingly, in roots of L04 the reduction in *SlCCD8* expression and strigolactone level are more severe than expected considering the only moderate increase in lateral shoot growth when compared with L09. However, when orobanchol levels in the xylem sap were analyzed, a better, linear inverse correlation between the orobanchol concentration in the xylem sap (Figure 4h) and lateral shoot branching (Figure 4a) was found across the knock-down lines. These results show that the level of orobanchol in the xylem sap is less affected than in the exudate,

suggesting preferential orobanchol loading into the xylem.

In addition, a reduction in main stem height was observed for all the lines, again correlating with xylem sap orobanchol levels. The reduction in plant height also inversely correlated to the increased number of shoot branches. However, this could also indicate that the observed dwarfism is a secondary effect of the increased lateral shoot growth. In experiments, in which plants were grown hydroponically under continuously sufficient nutrient conditions and in which lateral branches were frequently removed the phenotype could only be partially rescued, suggesting that the increase in the number of lateral branches cannot be exclusively responsible for the reduction in plant height. However, it is not unlikely that the removal of visible branches is not sufficient to restore the source sink balance of these plants. Finally, the total number of internodes was slightly increased in the transgenic lines, indicating that the observed reduction in plant height is due to shorter, not less internodes. Interestingly, a quantitative trait locus (QTL) controlling the number of tomato internodes is located in the vicinity of the putative *SlCCD8* position on chromosome 8 (Paran et al., 1997). The increase in the number of internodes suggests that strigolactones might not only be involved in the outgrowth of lateral buds, but also in the timing of organ development in tomato. Additional research will be needed to elucidate this in more detail.

Differences in strigolactone composition between roots and xylem sap

When strigolactone biosynthesis was assessed under limiting phosphate conditions, a strong increase in solanacol, orobanchol and the didehydro-orobanchol isomers was detected in root exudates and extracts (data not shown) which is in line with previous findings (López-Ráez et al., 2008). In the present study it was demonstrated that these stress conditions also induced a 5-fold increase in orobanchol levels in the tomato xylem sap. It has been recently demonstrated that in Arabidopsis the amount of orobanchol in the xylem sap is increased by 25% under phosphate-limiting conditions (Kohlen et al., 2011). The present results with tomato suggest that the up-regulation of orobanchol (strigolactones) in xylem sap under phosphate deficiency is a conserved trade in all dicots and possibly in the whole plant kingdom. Interestingly, our results show that only a small fraction of the orobanchol produced in roots is secreted into the rhizosphere (<5%) (Figure 4g, 3a). Besides orobanchol, one of its derivatives - orobanchyl acetate (Xie et al., 2010) - was detected in xylem sap of wild-type phosphate-starved tomato plants (Supplemental Figure S3.5). This strigolactone was not detected in the xylem sap of plants grown under phosphate-sufficient conditions or any of the *SlCCD8* knock-down lines, confirming its biosynthesis and transport is regulated similar to orobanchol. However, the concentration of this compound remained below the level needed for accurate quantification (data not shown).

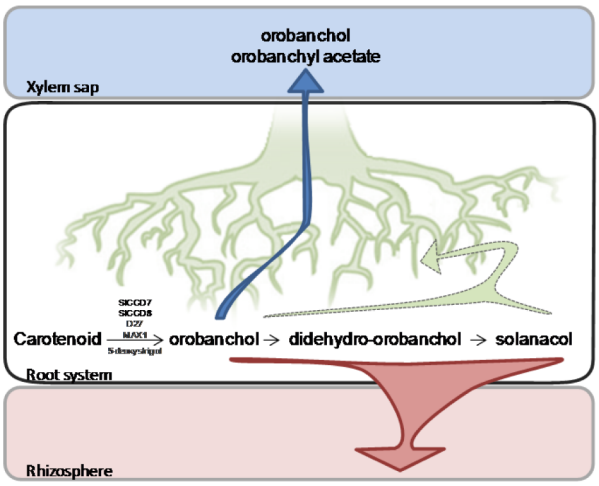

Figure 8: Proposed model for strigolactone movement in and outside the plant

Interestingly, neither solanacol nor any of the didehydro-orobanchol isomers were detected in the tomato xylem sap, whereas these strigolactones were abundantly present in root extracts (Figure 3g, 4a). This suggests that a selective mechanism of localized strigolactone biosynthesis and/or transport ensures that only orobanchol and orobanchyl acetate are transported through

the xylem to the shoot. Orobanchol and orobanchyl acetate (or a derivative of these) would then be involved in the regulation of shoot branching, whereas solanacol and the didehydro-orobanchol isomers would mainly function as signaling molecules in the rhizosphere. As strigolactones were also found to regulate RSA (Kapulnik et al., 2011; Ruyter-Spira et al., 2011) it is possible that solanacol and the didehydro-orobanchol isomers are involved in this function (Figure 8). It was previously proposed that solanacol is derived from orobanchol through didehydro-orobanchol (Xie et al., 2010). Thus, orobanchol may play a double role as the signal that is transmissible and regulates root and shoot architecture, and as the precursor of the signaling molecules that are responsible for communication in the rhizosphere.

Do strigolactones control reproductive development in tomato?

It has been proposed that strigolactones function in more aspects of plant development than just controlling lateral shoot outgrowth (Tsuchiya et al., 2010; Kapulnik et al., 2011; Ruyter-Spira et al., 2011). A putative function for strigolactones in fruit development was postulated since *SlCCD7* is highly expressed in mature green and turning fruits (Vogel et al., 2010) and both *AcCCD7* and *AcCCD8* expression in kiwifruit (*Actinidia chinensis*) is relatively high in young fruits and seeds (Ledger et al., 2010). It has also been described that the petunia *dad1* mutant produces smaller flowers (Snowden et al., 2005). In the tomato *SlCCD8* knock-down lines sepals, petals and anthers of the flowers were smaller than in wild-type. It is possible that these observed phenotypes are a secondary effect of the excessive branching observed in these lines. However, the altered auxin levels in whole flowers suggest that their might be a more direct role of strigolactones in reproductive development. The role of auxin in flower development has been shown as several double and triple mutants in the YUC auxin biosynthesis pathway produce abnormal flowers (Zhao, 2010). For example, the *yuc2yuc6* double mutant has flowers with shorter stamens that were male sterile (Cheng et al., 2006; Gallavotti et al., 2008). Furthermore, the auxin distribution pattern in developing flowers as visualized by DR5::GUS and immune-localization suggest a change from conjugated to free IAA during flower development (Aloni et al., 2006). Strigolactones are believed to regulate shoot branching in crosstalk with auxin, by controlling the auxin transport capacity in plants (Prusinkiewicz et al., 2009; Crawford et al., 2010). In agreement with this, reduced auxin levels were observed in flowers collected from the *SlCCD8* knock-down lines (Figure 5d). This suggests that the effect of strigolactones on flower development is also mediated through auxin. We postulate that the reduction in auxin is the consequence of a higher auxin transport capacity from these organs. This could explain why the observed phenotype is less severe than in the auxin biosynthesis mutants as the organs of the *SlCCD8* antisense lines are still able to produce auxin. The reduction in free auxin correlated with the reduction of orobanchol in the xylem sap. It is therefore possible that the strigolactones involved in the regulation of auxin levels in the reproductive organs are coming from the roots and/or stems. However, the involvement of local strigolactone biosynthesis in the flower cannot be excluded. Also, the auxin measurements were performed on entire flowers.Analysis of auxin levels in individual flower organs might provide more detailed insight into possible changes in the auxin distribution in *SlCCD8* knock-down flowers. More research is needed to further investigate the possible role of strigolactones in flower development.

In the *SlCCD8* knock-down lines fruit size was smaller than in the wild-type. The relative reduction in fruit size in the transgenic lines was identical to the relative reduction in the diameter of un-pollinated ovaries (Figure 5c, 6a, d). Additional experiments in which plants were grown under high nutrient conditions and frequently pruned partially rescue this phenotype, indicating the reduction in fruit size might be caused by competition for resources by the strong lateral shoot growth of these lines. IAA analyses of whole fruits at 14 DAP showed no differences in free auxin levels. However,

when auxin levels in the pericarp and remaining fruit were measured separately, a strong auxin gradient was found in wild-type fruits (Figure 6c). This gradient was absent in fruits from any of the tested *SlCCD8* knock-down lines, suggesting a role for strigolactones in regulating this gradient. It was recently demonstrated that the auxin efflux carriers *SlPIN1*, *SlPIN2* and *SlPIN3* are highly expressed in all tomato flower organs except stamens, which coincided with a high auxin response in stamens, as visualized by DR5::GUS. The expression of *SlPIN1* and *SlPIN2* was dynamic in early tomato fruit development, as both genes were expressed at anthesis, highly induced after pollination and virtually not expressed two weeks later (Nishio et al., 2010). This suggests that precise auxin distribution is very important in the development of the reproductive organs and fruit set. It is plausible that the strigolactone-deficient lines are not able to display these dynamics in expression levels correctly and this might be the reason for the observed phenotypes.

Furthermore, the number of seeds produced by the *SlCCD8* knock-down lines was found to be reduced by approximately 60% (Figure 7a). We can only speculate on how strigolactones control seed set in tomato. However as both male and female sterility have been described in auxin biosynthesis mutants (Cheng et al., 2006; Gallavotti et al., 2008) it is plausible that this is also to some extent the case in the *SlCCD8* knock-down lines, again linking strigolactone function to auxin. Possibly, the reduction in seed number finally caused the observed reduction in fruit size, as auxin produced in developing seeds is reported to stimulate fruit growth (Mapelli et al., 1978). However, as this auxin is produced by the developing seeds this cannot explain the observed reduction in ovary size before pollination (Figure 5c).

In addition to reduced number, seeds of the *SlCCD8* knock-down lines were also smaller than of the wild-type (Figure 7b). It has been reported that auxin is required for the accumulation of storage proteins in maturing seeds (Walz et al., 2002). Possibly, strigolactones alter auxin or auxin gradients in developing seeds and the reduction in strigolactone concentration in the transgenic lines may hence have caused the reduction in size. However, despite their reduced number and size, the quality of the seeds appeared to be unaffected as no differences in germination rate were observed in any of these lines (data not shown).

In contrast to *SlCCD7* expression (Vogel et al., 2010), only minor expression of *SlCCD8* was found in mature green fruits. This could indicate that both enzymes SlCCD7 and SlCCD8 contribute equally to strigolactone biosynthesis in roots and stems, but that in tomato fruits SlCCD8 is the rate limiting enzyme for strigolactone biosynthesis. However, it is also possible that strigolactones required for fruit development are produced in other parts of the plants and transported to the fruit likely through the xylem sap. In that case, SlCCD7 may have an additional function besides strigolactone biosynthesis, as was suggested by Floss and Walter (Floss and Walter, 2009).

All observed additional phenotypes could be related to the excessive branching of the transgenic knock down plants but it is also possible that there is an additional role for strigolactones in the reproductive development of tomato. It seems plausible that this putative novel strigolactone function depends on crosstalk with auxin and it is perhaps based on the same mechanism that underlies the regulation of shoot branching: the regulation of auxin transport, and consequently auxin concentration, by strigolactones. As mentioned above, additional research will be needed to further substantiate this novel function for the strigolactones.

Materials and methods

Plant material, growth conditions and chemicals

Seeds of tomato (*Solanum lycopersicum*) cultivar Craigella (LA3247) and the independent transgenic *SlCCD8* knock-down lines L16, L04, and L09 were sterilized in 4% sodium hypochlorite containing 0.02% (v/v) Tween 20, rinsed thoroughly with sterile water, and germinated for 48 h on moistened filter paper at 25ºC in darkness. For strigolactone analysis germinated seeds were pre-grown on perlite for 7 d. Then, all perlite was removed from the roots and ten seedlings were transferred to an X-stream 20 aeroponics system (Nutriculture, UK) operating with 5 L of modified half-strength Hoagland solution (López-Ráez et al., 2008) and grown for an additional 3 weeks. To up-regulate strigolactone production a 7 d phosphate starvation stress was applied to the plants by replacing the nutrient solution by modified half-strength Hoagland solution without phosphate (López-Ráez et al., 2008). Twenty four hours prior to exudate collection the nutrient solution was refreshed in order to remove all accumulated strigolactones. The exudates were collected 24 h later and were purified and concentrated within 2 h. The roots were frozen in liquid nitrogen and stored at -80°C for further analysis. For phenotypical analysis, plants were grown in pots with soil for 8 weeks and weekly irrigated with full strength Hoagland nutrient solution. All plants were grown under controlled conditions in a greenhouse at 16h light/8h dark, 23°C/20°C, and 60% relative humidity. Additional light was provided when needed to achieve a minimum light intensity of 250 $\mu mol \cdot m^{-2} \cdot s^{-2}$

Cloning of the full-length *SlCCD8*

A 1233 bp partial coding sequence of *SlCCD8* was amplified from tomato (cultivar Moneymaker) by reverse-transcriptase polymerase chain reaction (RT-PCR) using specific primers (forward, 5'-GCTGAGTGGCACGTACCTAA-3'; reverse, 5'-TCATCTTCTTCGGTTGCAC-3') specifically designed on a in plants highly conserved region of *CCD8*. The *SlCCD8* 5'- and 3'-cDNA ends were obtained using the SMART RACE cDNA Amplification Kit (Clontech) (5'-RACE, 5'-GCGTCCGATTCGATTTC-3' and 3' RACE, 5'-TCCTGCTTATTTAGGCAAG-3') The complete *SlCCD8* coding sequence (1674 bp) was PCR amplified from root cDNA (forward, 5'-ATGGCTTCTTTTGCTCATTCAG-3'; reverse, 5'-CTATTTCTTTGGAACCCAGC-3'). Finally, the amplified cDNA fragment was modified using the A-tailing procedure and cloned into pGEM-T Easy vector (Promega) according to the manufacturer instructions, and sequenced.

RNAi-mediated silencing of *SlCCD8* and tomato transformation

The silencing of *SlCCD8* in tomato plants was carried out by means of a 349 bp fragment plus the gateway CACC directional cloning sequence that was PCR amplified using specific primers (forward, 5'-CACCCAGGACAATGGCACATAGGT-3'; reverse, 5'- TCTAGGGTGTTCGGATCAA-3'). The PCR fragment was cloned into the pENTR/D vector (Gateway Technology, Invitrogen) and then introduced into the binary destination vector pHellsgate8 (Helliwell et al., 2002) by recombination using LR clonase II (Invitrogen). The pHellsgate8::CCD8 RNAi construct was transferred to *Agrobacterium tumefaciens* strain LB4404 and used to transform tomato (Craigella) plants as previously described (van Roekel et al., 1993).

RNA isolation and gene expression analysis by real time quantitative RT-PCR (qPCR)

Total RNA was extracted using Tri-Reagent (Sigma-Aldrich) according to the manufacturer's instructions. The RNA was treated with RQ1 DNase (Promega), purified through a silica column using the NucleoSpin RNA Clean-up kit (Macherey-Nagel) and stored at -80ºC until use. For gene expression analysis by real time quantitative RT-PCR (qPCR) the iCycler iQ5 system (Bio-Rad) was used (Spinsanti et al., 2008) using specific primers. For the tomato elongation factor-1α (household

gene) *SlEF*: 5'- GATTGGTGGTATTGGAACTGTC-3' and 5'-AGCTTCGTGGTGCATCTC-3'; for *SlCCD7*: 5'-AGCCAAGAATTCGAGATCCC-3' and 5'-GGAGAAAGCCCACATACTGC-3'; for *SlCCD8*: 5'-CCAATTGCCTGTAATAGTTCC-3' and 5'-GCCTTCAACGACGAGTTCTC-3'. The first-strand cDNA was synthesized with 1 µg of purified total RNA using the iScript cDNA Synthesis kit (Bio-Rad) according to manufacturer's instructions. Three independent biological replicates were used and each PCR reaction was done in triplicate. Relative quantification of mRNA was performed using the comparative C_t method (Livak and Schmittgen, 2001). Values were normalized using the C_t value for the tomato household gene *SlEF* (Rotenberg et al., 2006). All the values were used to determine the change in gene expression according to the following calculation: fold-change = $2^{-\Delta(\Delta Ct)}$, where $\Delta C_t = C_t$ (target) - C_t (household) and $\Delta(\Delta C_t) = \Delta C_t$ (treatment) - ΔC_t (control).

Strigolactone and auxin analysis by multiple reaction monitoring liquid chromatography-tandem mass spectrometry (UPLC-MS/MS)

Root exudates were purified and concentrated as previously described by López Ráez *et al.* (2010) with some modifications. Five liters of root exudate was loaded onto a pre-equilibrated C18 column (GracePure C18-Fast 5000 mg / 20 ml). Subsequently, columns were washed with 50 ml of demineralised water and 50 ml of 30% acetone/water. Strigolactones were eluted with 50 ml of 60% acetone/water. All exudates were collected within two hours and stored at -20°C. Strigolactones were extracted from root material as previously described (López-Ráez et al., 2010). Xylem sap was collected and purified as was previously described (Kohlen et al., 2011). Strigolactone analysis was performed using UPLC-MS/MS, as previously described by (Kohlen et al., 2011). IAA was extracted from plant tissues and analyzed as previously described by Ruyter-Spira *et al*. (2011).

***P. ramosa* germination assay and infection study**

Germination assays with *P. ramosa* seeds were conducted as reported by Matusova *et al*. (2005). The synthetic strigolactone analogue GR24 (10^{-9} M) and demineralised water were included as positive and negative controls, respectively. To perform the *P. ramosa* infection assay, 3 L pots were filled with a soil-sand mixture (3:1) and seeds were added following the procedure previously described (Kroschel, 2001). *P. ramosa* seeds were sown in a layer of approximately 3-10 cm below the surface at a density of 15 mg·pot^{-1}. In order to keep a moist environment, the pots were watered with 60 ml of tap water daily for 12 d. Then, 5-day-old tomato seedlings were introduced into the pots and watered for 5 d as described before. Subsequently, pots were irrigated with 300 ml of tap water twice a week and once with 300 ml of full strength Hoagland solution. Emerged *P. ramosa* shoots were counted 10 weeks after tomato planting.

Analysis of AM colonization of *SlCCD8* knock-down lines

The AM fungus *G*. *intraradices* (BEG 121) was maintained as a soil-sand based inoculum containing a mix of diverse fungal propagules (spores, hyphae and chopped mycorrhizal roots). Tomato seeds of the knock-down lines L04, L09 and L16, and corresponding wild-type (Craigella) were surfaced-sterilized and germinated for 3 d on a container with sterile vermiculite at 25°C in darkness. Subsequently, individual seedlings were transferred to 0.25 L pots with a sterile sand:soil (4:1) mixture. Pots were inoculated by adding 10% (v:v) *G*. *intraradices* inoculum. The same amount of soil:sand mix but free from AM was added to control plants. For each treatment five replicate plants were used. Plants were randomly distributed and grown in a greenhouse at 24/16°C with 16/8 hr photoperiod and 70% humidity and watered three times a week with Long Ashton nutrient solution (Hewitt, 1966) containing 25% of the standard phosphorous concentration. Plants were harvested

after 8 weeks of growth. Hereto, roots were stained with trypan blue (Phillips and Hayman, 1970) and examined using a Nikon Eclipse 50i microscope under bright-field conditions. The percentage of root length colonized by the AM fungus was determined by the gridline intersection method (Giovannetti and Mosse, 1980).

Statistical analysis

Data for strigolactone and auxin content were subjected to one-way analysis of variance (ANOVA) using GenStat for Windows (9th edition). To analyze the results of germination bioassays, ANOVA after arcsine[square root(X)] transformation was used. When appropriate, data were subjected to the Student's t-test.

Acknowledgment

We acknowledge Ralph Bours, Ronny Joosen and Francel Verstappen for their technical support. The synthetic strigolactone analogue GR24 was kindly provided by Binne Zwanenburg (Department of Organic Chemistry, Radboud University, Nijmegen, The Netherlands). The strigolactone standards used in this study were kindly provided by Koichi Yoneyama (Weed Science Center, Utsunomiya University, Japan). *P. ramosa* seeds were kindly provided by Maurizio Vurro (Instituto di Scienze delle Produzioni Alimentari, Bari, Italy). We acknowledge funding by the Netherlands Organization for Scientific Research (NWO; VICI grant, 865.06.002 and Equipment grant, 834.08.001 to HJB) and the European Commission (Intra-European Marie Curie postdoctoral fellowship FP6-MEIF-CT-2005-024345 to JAL-R, FP7-PIEF-GA-2008-220177 to PT and Reintegration Grant PERG-02-2007-224751 to JAL-R). JAL-R was also supported by a postdoctoral contract (JAE-Doc) from the Spanish Research Council (CSIC). This project was co-financed by the Centre for BioSystems Genomics (CBSG) which is part of the Netherlands Genomics Initiative/Netherlands Organization for Scientific Research.

References

Akiyama K, Matsuzaki K, Hayashi H (2005) Plant sesquiterpenes induce hyphal branching in arbuscular mycorrhizal fungi. Nature **435:** 824-827

Aloni R, Aloni E, Langhans M, Ullrich C (2006) Role of auxin in regulating *Arabidopsis* flower development. Planta **223:** 315-328

Arite T, Umehara M, Ishikawa S, Hanada A, Maekawa M, Yamaguchi S, Kyozuka J (2009) *d14*, a strigolactone-insensitive mutant of rice, shows an accelerated outgrowth of tillers. Plant and Cell Physiology **50:** 1416-1424

Bainbridge K, Sorefan K, Ward S, Leyser O (2005) Hormonally controlled expression of the Arabidopsis *MAX4* shoot branching regulatory gene. The Plant Journal **44:** 569-580

Bennett T, Sieberer T, Willett B, Booker J, Luschnig C, Leyser O (2006) The Arabidopsis MAX pathway controls shoot branching by regulating auxin transport. Current Biology **16:** 553-563

Beveridge CA, Ross JJ, Murfet IC (1994) Branching mutant *rms-2* in *Pisum sativum* (grafting studies and endogenous indole-3-acetic acid levels). Plant Physiology **104:** 953-959

Bombarely A, Menda N, Tecle IY, Buels RM, Strickler S, Fischer-York T, Pujar A, Leto J, Gosselin J, Mueller LA (2011) The Sol Genomics Network (solgenomics.net): growing tomatoes using Perl. Nucleic Acids Research **39:** D1149-D1155

Booker J, Auldridge M, Wills S, McCarty D, Klee H, Leyser O (2004) MAX3/CCD7 is a carotenoid cleavage dioxygenase required for the synthesis of a novel plant signaling molecule. Current Biology **14:** 1232-1238

Booker J, Sieberer T, Wright W, Williamson L, Willett B, Stirnberg P, Turnbull C, Srinivasan M, Goddard P, Leyser O (2005) MAX1 encodes a cytochrome P450 family member that acts downstream of MAX3/4 to produce a carotenoid-derived branch-inhibiting hormone. Developmental Cell **8:** 443-449

Bouwmeester HJ, Matusova R, Zhongkui S, Beale MH (2003) Secondary metabolite signalling in host-parasitic plant interactions. Current Opinion in Plant Biology **6:** 358-364

Cheng YF, Dai XH, Zhao YD (2006) Auxin biosynthesis by the YUCCA flavin monooxygenases controls the formation of floral organs and vascular tissues in Arabidopsis. Genes & Development **20:** 1790-1799

Cook CE, Whichard LP, Turner B, Wall ME, Egley GH (1966) Germination of witchweed (*Striga lutea Lour.*): isolation and properties of a potent stimulant. Science **154:** 1189-1190

Crawford S, Shinohara N, Sieberer T, Williamson L, George G, Hepworth J, Müller D, Domagalska MA, Leyser O (2010) Strigolactones enhance competition between shoot branches by dampening auxin transport. Development **137:** 2905-2913

Floss DS, Walter MH (2009) Role of carotenoid cleavage dioxygenase 1 (CCD1) in apocarotenoid biogenesis revisited. Plant Signalling and Behavior **4:** 4

Foo E, Turnbull CGN, Beveridge CA (2001) Long-distance signaling and the control of branching in the *rms1* mutant of pea. Plant Physiology **126:** 203-209

Gallavotti A, Barazesh S, Malcomber S, Hall D, Jackson D, Schmidt RJ, McSteen P (2008) sparse inflorescence1 encodes a monocot-specific YUCCA-like gene required for vegetative and reproductive development in maize. Proceedings of the National Academy of Sciences of the United States of America **105:** 15196-15201

Gillaspy G, Ben-David H, Gruissem W (1993) Fruits: A developmental perspective. Plant Cell **5:** 1439-1451

Giovannetti M, Mosse B (1980) An evaluation of techniques for measuring vesicular arbuscular mycorrhizal infection in roots. New Phytologist **84:** 489-500

Goldwasser Y, Yoneyama K, Xie X, Yoneyama K (2008) Production of strigolactones by *Arabidopsis thaliana* responsible for *Orobanche aegyptiaca* seed germination. Plant Growth Regulation **55:** 21-28

Gomez-Roldan V, Fermas S, Brewer PB, Puech-Pages V, Dun EA, Pillot J-P, Letisse F, Matusova R, Danoun S, Portais J-C, Bouwmeester H, Becard G, Beveridge CA, Rameau C, Rochange SF (2008) Strigolactone inhibition of shoot branching. Nature **455:** 189-194

Helliwell CA, Wesley SV, Wielopolska AJ, Waterhouse PM (2002) High-throughput vectors for efficient gene silencing in plants. Functional Plant Biology **29:** 1217-1225

Hewitt EJ (1966) Sand and water culture methods used in the study of plant nutrition / by E.J. Hewitt. Commonwealth Agricultural Bureaux, Farnham Royal, England :

Kapulnik Y, Delaux P-M, Resnick N, Mayzlish-Gati E, Wininger S, Bhattacharya C, Séjalon-Delmas N, Combier J-P, Bécard G, Belausov E, Beeckman T, Dor E, Hershenhorn J, Koltai H (2011) Strigolactones affect lateral root formation and root-hair elongation in Arabidopsis. Planta **233:** 209-216

Kohlen W, Charnikhova T, Liu Q, Bours R, Domagalska MA, Beguerie S, Verstappen F, Leyser O, Bouwmeester H, Ruyter-Spira C (2011) Strigolactones are transported through the xylem and play a key role in shoot architectural response to phosphate deficiency in nonarbuscular mycorrhizal host Arabidopsis. Plant Physiology **155:** 974-987

Koltai H, LekKala SP, Bhattacharya C, Mayzlish-Gati E, Resnick N, Wininger S, Dor E, Yoneyama K, Yoneyama K, Hershenhorn J, Joel DM, Kapulnik Y (2010) A tomato strigolactone-impaired mutant displays aberrant shoot morphology and plant interactions. Journal of Experimental Botany **61:** 1739-1749

Kroschel J (2001) A Technical Manual for Parasitic Weed Research and Extension. Kluwer Academic Publishers, Dordrecht, The Netherlands

Ledger SE, Janssen BJ, Karunairetnam S, Wang T, Snowden KC (2010) Modified CAROTENOID CLEAVAGE DIOXYGENASE8 expression correlates with altered branching in kiwifruit (*Actinidia chinensis*). New Phytologist **188:** 803-813

Lin H, Wang R, Qian Q, Yan M, Meng X, Fu Z, Yan C, Jiang B, Su Z, Li J, Wang Y (2009) DWARF27, an iron-containing protein required for the biosynthesis of strigolactones, regulates rice tiller bud outgrowth. Plant Cell **21:** 1512-1525

Livak KJ, Schmittgen TD (2001) Analysis of relative gene expression data using real-time quantitative PCR and the 2(T)(-Delta Delta C) method. Methods **25:** 402-408

López-Ráez JA, Charnikhova T, Gómez-Roldán V, Matusova R, Kohlen W, Vos RD, Verstappen F, Puech-Pages V, Bécard G, Mulder P, Bouwmeester H (2008) Tomato strigolactones are derived from carotenoids and their biosynthesis is promoted by phosphate starvation. New Phytologist **178:** 863-874

López-Ráez JA, Charnikhova T, Mulder P, Kohlen W, Bino R, Levin I, Bouwmeester H (2008) Susceptibility of the tomato mutant high pigment-2dg (hp-2dg) to *Orobanche spp*. infection. Journal of Agricultural and Food Chemistry **56:** 6326-6332

López-Ráez JA, Kohlen W, Charnikhova T, Mulder P, Undas AK, Sergeant MJ, Verstappen F, Bugg TDH, Thompson AJ, Ruyter-Spira C, Bouwmeester H (2010) Does abscisic acid affect strigolactone biosynthesis? New Phytologist **187:** 343-354

López-Ráez JA, Matusova R, Cardoso C, Jamil M, Charnikhova T, Kohlen W, Ruyter-Spira C, Verstappen F, Bouwmeester H (2009) Strigolactones: ecological significance and use as a target for parasitic plant control. Pest Management Science **65:** 471-477

Mapelli S, Frova C, Torti G, Soressi GP (1978) Relationship between set, development and activities of growth regulators in tomato fruits. Plant and Cell Physiology **19:** 1281-1288

Matusova R, Rani K, Verstappen FWA, Franssen MCR, Beale MH, Bouwmeester HJ (2005) The strigolactone germination stimulants of the plant-parasitic *Striga* and *Orobanche spp*. are derived from the carotenoid pathway. Plant Physiology **139:** 920-934

Napoli C (1996) Highly branched phenotype of the petunia *dad1-1* mutant is reversed by grafting. Plant Physiology **111:** 27-37

Nishio S, Moriguchi R, Ikeda H, Takahashi H, Takahashi H, Fujii N, Guilfoyle T, Kanahama K, Kanayama Y (2010) Expression analysis of the auxin efflux carrier family in tomato fruit development. Planta **232:** 755-764

Paran I, Goldman I, Zamir D (1997) QTL analysis of morphological traits in a tomato recombinant inbred line population. Genome **40:** 242-

248

Phillips JM, Hayman DS (1970) Improved procedures for clearing roots and staining parasitic and vesicular-arbuscular mycorrhizal fungi for rapid assessment of infection. Transactions of the British Mycological Society **55:** 158-161, IN116-IN118

Prusinkiewicz P, Crawford S, Smith RS, Ljung K, Bennett T, Ongaro V, Leyser O (2009) Control of bud activation by an auxin transport switch. Proceedings of the National Academy of Sciences **106:** 17431-17436

Rani K, Zwanenburg B, Sugimoto Y, Yoneyama K, Bouwmeester HJ (2008) Biosynthetic considerations could assist the structure elucidation of host plant produced rhizosphere signalling compounds (strigolactones) for arbuscular mycorrhizal fungi and parasitic plants. Plant Physiology and Biochemistry **46:** 617-626

Rotenberg D, Thompson TS, German TL, Willis DK (2006) Methods for effective real-time RT-PCR analysis of virus-induced gene silencing. Journal of Virological Methods **138:** 49-59

Ruyter-Spira C, Kohlen W, Charnikhova T, van Zeijl A, van Bezouwen L, de Ruijter N, Cardoso C, López-Ráez JA, Matusova R, Bours R, Verstappen F, Bouwmeester H (2011) Physiological effects of the synthetic strigolactone analog GR24 on root system architecture in Arabidopsis: Another belowground role for strigolactones? Plant Physiology **155:** 721-734

Snowden KC, Simkin AJ, Janssen BJ, Templeton KR, Loucas HM, Simons JL, Karunairetnam S, Gleave AP, Clark DG, Klee HJ (2005) The *Decreased apical dominance 1/petunia hybrida carotenoid cleavage dioxygenase8* gene affects branch production and plays a role in leaf senescence, root growth, and flower development. Plant Cell **17:** 746-759

Sorefan K, Booker J, Haurogné K, Goussot M, Bainbridge K, Foo E, Chatfield S, Ward S, Beveridge C, Rameau C, Leyser O (2003) *MAX4* and *RMS1* are orthologous dioxygenase-like genes that regulate shoot branching in Arabidopsis and pea. Genes & Development **17:** 1469-1474

Spinsanti G, Panti C, Marsili L, Casini S, Fossi MC (2008) Selection of reference genes for quantitative RT-PCR studies in striped dolphin (*Stenella coeruleoalba*) skin biopsies. Marine Environmental Research **66:** 141-141

Stirnberg P, Furner IJ, Leyser HMO (2007) MAX2 participates in an SCF complex which acts locally at the node to suppress shoot branching. The Plant Journal **50:** 80-94

Stirnberg P, van de Sande K, Leyser HMO (2002) MAX1 and MAX2 control shoot lateral branching in Arabidopsis. Development **129:** 1131-1141

Tsuchiya Y, Vidaurre D, Toh S, Hanada A, Nambara E, Kamiya Y, Yamaguchi S, McCourt P (2010) A small-molecule screen identifies new functions for the plant hormone strigolactone. Nature Chemical Biology **6:** 741-749

Turnbull CGN, Booker JP, Leyser HMO (2002) Micrografting techniques for testing long-distance signalling in Arabidopsis. The Plant Journal **32:** 255-262

Umehara M, Hanada A, Magome H, Takeda-Kamiya N, Yamaguchi S (2010) Contribution of strigolactones to the inhibition of tiller bud outgrowth under phosphate deficiency in rice. Plant and Cell Physiology**:** 1118-1126

Umehara M, Hanada A, Yoshida S, Akiyama K, Arite T, Takeda-Kamiya N, Magome H, Kamiya Y, Shirasu K, Yoneyama K, Kyozuka J, Yamaguchi S (2008) Inhibition of shoot branching by new terpenoid plant hormones. Nature **455:** 195-200

van Roekel J, Damm B, Melchers L, Hoekema A (1993) Factors influencing transformation frequency of tomato (*Lycopersicon esculentum*). Plant Cell Reports **12:** 644-647

Vogel JT, Walter MH, Giavalisco P, Lytovchenko A, Kohlen W, Charnikhova T, Simkin AJ, Goulet C, Strack D, Bouwmeester HJ, Fernie AR, Klee HJ (2010) SlCCD7 controls strigolactone biosynthesis, shoot branching and mycorrhiza-induced apocarotenoid formation in tomato. The Plant Journal **61:** 300-311

Walz A, Park S, Slovin JP, Ludwig-Muller J, Momonoki YS, Cohen JD (2002) A gene encoding a protein modified by the phytohormone indoleacetic acid. Proceedings of the National Academy of Sciences of the United States of America **99:** 1718-1723

Xie X, Yoneyama K, Yoneyama K (2010) The strigolactone story. Annual Review of Phytopathology **48:** 93-117

Yoneyama K, Yoneyama K, Takeuchi Y, Sekimoto H (2007) Phosphorus deficiency in red clover promotes exudation of orobanchol, the signal for mycorrhizal symbionts and germination stimulant for root parasites. Planta **225:** 1031-1038

Zhao Y (2010) Auxin biosynthesis and its role in plant development. Annual Review of Plant Biology **61:** 49-64

Chapter 4

Does abscisic acid affect strigolactone biosynthesis?

Juan Antonio López-Ráez*, Wouter Kohlen*, Tatsiana Charnikhova, Patrick Mulder, Anna Undas, Martin Sergeant, Francel Verstappen, Timothy Bugg, Andrew Thompson, Carolien Ruyter-Spira, Harro Bouwmeester

* contributed equally to this work

Adapted version published as López-Ráez et al., (2010) New Phytologist 187: 343-354.

Abstract

Strigolactones are considered a novel class of plant hormones that - in addition to their endogenous signaling function - are also exuded into the rhizosphere acting as a signal to stimulate hyphal branching of arbuscular mycorrhizal (AM) fungi and germination of root parasitic plant seeds. Considering the importance of the strigolactones and their biosynthetic origin from the carotenoids, we investigated the relationship with the plant hormone abscisic acid (ABA). For this, strigolactone production and ABA content in the presence of specific inhibitors of oxidative carotenoid cleavage enzymes and in several tomato ABA-deficient mutants were analyzed by MRM-LC-MS/MS. In addition, the expression of two genes involved in strigolactone biosynthesis was studied. The carotenoid cleavage dioxygenase (CCD) inhibitor D2 reduced strigolactone but not ABA content of roots. However, in abamineSG treated plants, an inhibitor of 9-*cis*-epoxycarotenoid dioxygenase (NCED), and the ABA mutants *notabilis*, *sitiens* and *flacca*, ABA and strigolactones were greatly reduced. The reduction in strigolactone production correlated with the down-regulation of *LeCCD7* and *LeCCD8* genes in all three mutants. Our results show a correlation between ABA levels and strigolactone production, and suggest a role for ABA in the regulation of strigolactone biosynthesis.

Key Words: Strigolactones, abscisic acid, hormone regulation, tomato, mutants, inhibitors.

Introduction

Strigolactones are important signaling molecules that were first described as germination stimulants for the seeds of parasitic plants of the genera *Striga* and *Orobanche* (Cook et al., 1966; Bouwmeester et al., 2003). Later, they were also described as hyphal branching factors for germinating spores of the symbiotic arbuscular mycorrhizal (AM) fungi (Akiyama et al., 2005). Therefore, strigolactones play a dual and important role in the rhizosphere as host detection signals for AM fungi and root parasitic plants (Akiyama et al., 2005; Harrison, 2005; Paszkowski, 2006; Bouwmeester et al., 2007). In addition to their important role as rhizosphere signaling molecules, it has recently been demonstrated that strigolactones also act as a new hormone class that inhibits shoot branching in plants and hence regulates above-ground plant architecture (Gomez-Roldan et al., 2008; Umehara et al., 2008).

Strigolactones have been detected in the root exudates of a wide range of mono- and dicotyledonous plant species. The strigolactones discovered so far all have a similar chemical structure suggesting that they are all derived from the same biosynthetic pathway (Bouwmeester et al., 2007; Yoneyama et al., 2008). Indeed, we have previously demonstrated that the ABC-part of the strigolactones (Figure 1) is derived from carotenoids through oxidative cleavage by carotenoid cleavage dioxygenases, hence classifying the strigolactones as apocarotenoids (Matusova et al., 2005; López-Ráez et al., 2008; Rani et al., 2008). In addition, we have postulated how, after carotenoid cleavage, further enzymatic conversions are likely to lead to the production of all the strigolactones known to date (Matusova et al., 2005; Rani et al., 2008). Indeed, it was recently demonstrated that two carotenoid cleavage dioxygenases (CCDs), CCD7 and CCD8 - which were already proposed to be responsible for the biosynthesis of the elusive shoot branching inhibiting signal (Sorefan et al., 2003; Booker et al., 2004) - are directly involved in the biosynthesis of strigolactones (Gomez-Roldan et al., 2008; Umehara et al., 2008). The latter papers showed that mutants of pea *ramosus5* (*rms5*) and *ramosus1* (*rms1*) and rice *high-tillering dwarf1* or *dwarf17* (*htd1* or *d17*) and *dwarf 10* (*d10*) for CCD7 and CCD8, respectively, produce significantly less strigolactones than the corresponding wild-types. In pea, the *rms1* mutation reduced mycorrhizal symbiosis which could be restored by exogenously applied synthetic strigolactone (Gomez-Roldan et al., 2008). Moreover, root exudates of *rms5* and *rms1* induced less AM fungal hyphae branching and less germination of *Orobanche* seeds (Gomez-Roldan et al., 2008). Similarly in rice, the orthologous mutants were less infected by *Striga hermonthica* (Umehara et al., 2008).

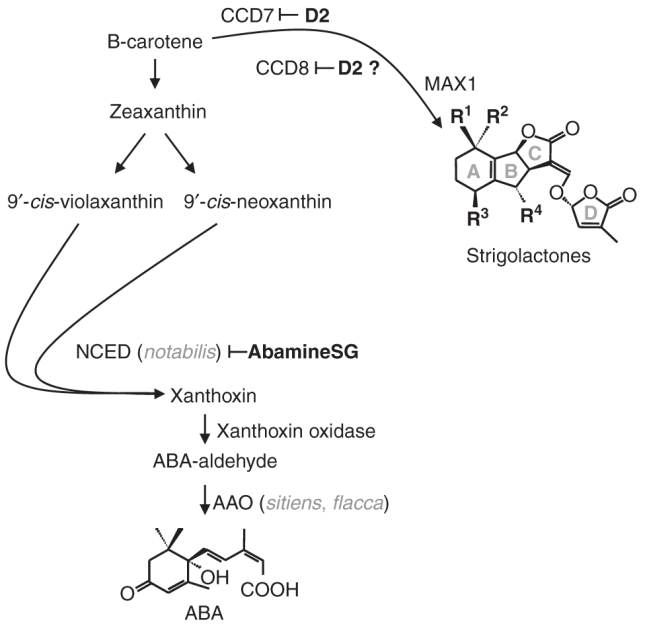

Figure 1: Abscisic acid (ABA) and strigolactone biosynthetic pathways. Mutants and inhibitors used or discussed in this study are shown in italics and bold text, respectively. NCED, 9-cis-epoxycarotenoid dioxygenase; AAO, aldehyde oxidase; CCD7 and CCD8, carotenoid cleavage dioxygenase 7 and 8, respectively; MAX1, corresponds to the cytochrome p450 shown to be involved in the biosynthesis of the branching inhibiting signal

In addition to the reduced production of strigolactones by the *ccd7* and *ccd8* mutants, it was

previously shown that exudates of the mutants *viviparous14* (*vp14*) in maize and *notabilis* in tomato, with a null mutation in the genes *ZmNCED* and *LeNCED1* and encoding for 9-*cis*-epoxycarotenoid dioxygenases, also induced less germination of *S. hermonthica* and *Orobanche ramosa* seeds, respectively (Matusova et al., 2005; López-Ráez et al., 2008). Moreover, by MRM-LC-MS/MS analysis it was demonstrated that in the case of the tomato mutant this reduction in germination stimulatory activity correlates closely with a reduction in the production of strigolactones, suggesting that NCED enzymes are involved, either directly or indirectly, in the biosynthesis of these signaling molecules (López-Ráez et al., 2008). NCEDs belong to the family of carotenoid cleavage dioxygenase enzymes - to which also CCD7 and CCD8 belong - that form a small family composed of nine different members in Arabidopsis and twelve in rice of which five and six, respectively, belong to the NCED subgroup (Auldridge et al., 2006; Bouwmeester et al., 2007; Tan et al., 2007). NCEDs catalyze a critical step in the regulation of the biosynthesis of the phytohormone abscisic acid (ABA) in higher plants. 9'-*Cis*-neoxanthin and 9-*cis*-violaxanthin have been proposed to be the precursors for ABA biosynthesis (Li and Walton, 1990; Rock and Zeevaart, 1991; Parry et al., 1992). Cleavage of these molecules by NCED enzymes leads to the formation of xanthoxin that is converted to ABA-aldehyde by a short-chain alcohol dehydrogenase ABA2. Finally, an aldehyde oxidase (AAO) transforms ABA-aldehyde into the bioactive ABA (Figure 1) (Schwartz et al., 1997; Taylor et al., 2005). In addition to *notabilis*, in tomato two more ABA-deficient mutants - *sitiens* and *flacca* - have been characterized. *Sitiens* has been shown to be mutated in the enzyme AAO and *flacca* has a mutation in a molybdenum cofactor (MoCo) which is required for the activity of the enzyme AAO (Figure 1) (Cornish and Zeevaart, 1988; Taylor et al., 1988; Sagi et al., 2002).

ABA plays a regulatory role in many physiological processes in all higher and lower plants (Zeevaart and Creelman, 1988). It mediates plant responses to different kinds of abiotic stress such as drought stress and is involved in long distance signaling in plants. ABA is the key signal regulating stomatal aperture (Davies et al., 2005; Jiang and Hartung, 2008). In seeds, ABA promotes seed development, embryo maturation, synthesis of storage products (proteins and lipids), desiccation tolerance, and is involved in apoptosis and maintenance of dormancy (inhibition of germination) (Zeevaart and Creelman, 1988; Bethke et al., 1999). In concert with other plant signalling molecules, ABA is also implicated in mediating responses to pathogens and wounding (Adie et al., 2007). Moreover, ABA also affects plant architecture, including root growth and morphology, and root-to-shoot ratios (De Smet et al., 2006). In line with its important role as a phytohormone, ABA concentrations in the plant are controlled by a tightly regulated balance between biosynthesis, inactivation and degradation (Zeevaart and Creelman, 1988, 1988).

In the present study, the production of strigolactones in tomato mutants affected in ABA biosynthesis at different steps of the pathway such as *notabilis*, *flacca* and *sitiens* was assessed. Moreover, the effect of specific inhibitors of different oxidative carotenoid cleavage enzymes such as abamineSG (NCED specific) and D2 (CCD7 specific) was also analyzed. The role of the phytohormone ABA in regulating the production of strigolactones in plants is discussed.

Results

Germination stimulatory activity of *notabilis*, *sitiens* and *flacca* root exudates

We previously demonstrated that ABA-deficient maize (*vp14*) and tomato (*notabilis*) mutants with a mutation in NCED exhibit a decreased strigolactone production by the roots(Matusova et al., 2005; Matusova et al., 2005; López-Ráez et al., 2008; López-Ráez et al., 2008) (Matusova et al., 2005;

López-Ráez et al., 2008). It has been suggested that NCEDs are the key enzymes in the ABA biosynthetic pathway (Figure 1). To assess whether the reduction in strigolactone biosynthesis in the NCED mutants is caused directly by reduced NCED action or indirectly because of its effect on the ABA content of these mutants, in addition to *notabilis*, the tomato ABA-deficient mutants *sitiens* and *flacca* and their parental isogenic lines were studied. *Sitiens* and *flacca* are blocked in the final step of the ABA biosynthetic pathway, where the enzyme AAO catalyzes the oxidation of abscisic aldehyde to ABA (Figure 1) (Taylor et al., 1988; Schwartz et al., 2003). *Sitiens* is known to have a mutation in the AAO enzyme and mutant leaves contain only about 11% of the wild-type ABA levels (Cornish and Zeevaart, 1988; Taylor et al., 1988). The mutant *flacca* has a mutation in a MoCo cofactor required for the activity of AAO and mutant leaves contain about 33% of the wild-type ABA levels (Cornish and Zeevaart, 1988; Sagi et al., 2002).

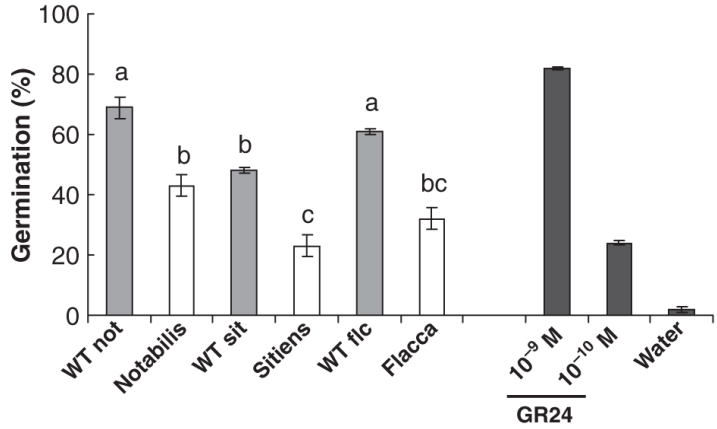

Figure 2: Germination of Orobanche ramosa seeds induced by the root exudates of the tomato mutants *notabilis* (*not*), *sitiens* (*sit*) and *flacca* (*flc*) (open bars) compared with the corresponding wild types (WT) (grey bars). GR24 (10^{-9} and 10^{-10} M) and demineralized water (closed bars) were used as positive and negative controls, respectively. Within each experiment, the concentrations of the root exudates were equalized by dilution to the same ratio of volume of exudate to root fresh weight. Bars represent the average of five independent replicates ± SE. Bars with a different letter differ significantly ($P < 0.05$)

The mutants *notabilis*, *sitiens* and *flacca* showed the characteristic wilty phenotype (Taylor et al., 1988; Thompson et al., 2000). Root exudates of the three mutants and their corresponding wild-types were collected for a germination bioassay with *Phelipanche* (*Orobanche*) *ramosa* (Joel, 2009) seeds. The synthetic germination stimulant GR24, as a positive control, always induced the germination of preconditioned *P. ramosa* seeds (up to about 85%). Water, used as a negative control, only induced 2% germination (Figure 2). As we described before (López-Ráez et al., 2008), root exudates of *notabilis* induced about 40% less germination than the corresponding wild-type (Figure 2). The germination stimulatory activity of *sitiens* and *flacca* exudates was about 52 and 48%, respectively, lower than for those of the corresponding wild-types (Figure 2). In addition to the differences between the mutants and corresponding wild-types, there was some variation between the germination stimulatory activities of the wild-type exudates (Figure 2). For example, the wild-type for *sitiens* (cv. Rheinlands Ruhm) induced lower germination than the wild-type for *flacca* and *notabilis* (cv. Ailsa Craig) (Figure 2).

LC-MS/MS analysis and quantification of strigolactones

To assess whether the lower germination stimulatory activity of the ABA-deficient tomato mutants was due to a decrease in the production of strigolactones, MRM-LC-MS/MS analysis was performed to compare the levels of strigolactones in the root exudates of the mutants and corresponding wild-types. All the three major strigolactones detected - solanacol and the two didehydro-orobanchol isomers - were significantly ($P < 0.05$) reduced in the *notabilis*, *sitiens* and *flacca* root exudates compared with the wild-types (Figure 3a). The other strigolactone present in tomato - orobanchol - was also detected, but its concentration was too low for accurate quantification. The concentration of strigolactones in the root extracts showed a similar trend as for the root exudates (Figure 3b),

indicating that there is a reduction in strigolactone biosynthesis in the mutants rather than just a decrease in the exudation. Interestingly, in the roots the decrease in didehydro-orobanchol 1 in the ABA mutants was larger than the decrease in solanacol and the didehydro-orobanchol 2 isomer, whereas in exudates the decrease in their concentration was similar (Figure 3). Overall, the level of strigolactones in the exudates of *notabilis*, *sitiens* and *flacca* was about 40, 47 and 52%, respectively, lower than the corresponding wild-types, which correlates well with the reduction in the germination stimulatory activity of the mutant exudates (40%, 52% and 48%, respectively). In an attempt to rescue the phenotype of the mutants, ABA (0.5 µM) was exogenously applied by irrigation to all the three mutants. However, no effect on strigolactone biosynthesis was observed in comparison with the untreated plants (data not shown). The same pattern was observed when higher ABA concentrations (1 and 10 µM) were applied to *sitiens* and its corresponding wild-type (Supplemental Figure S4.1). Although no increase in ABA was detected in the roots after exogenous ABA application, expression analysis of the ABA-responsive gene *Le4* (Kahn et al., 1993) and *SlCYP707A1*, an ABA-8'-hydroxylase involved in ABA catabolism (Taylor et al., 2005; Nitsch et al., 2009), showed a 250- and 15-fold increase, respectively upon ABA treatment (Supplemental Figure S4.2), indicating that ABA was effectively taken up by the roots but is also effectively catabolised.

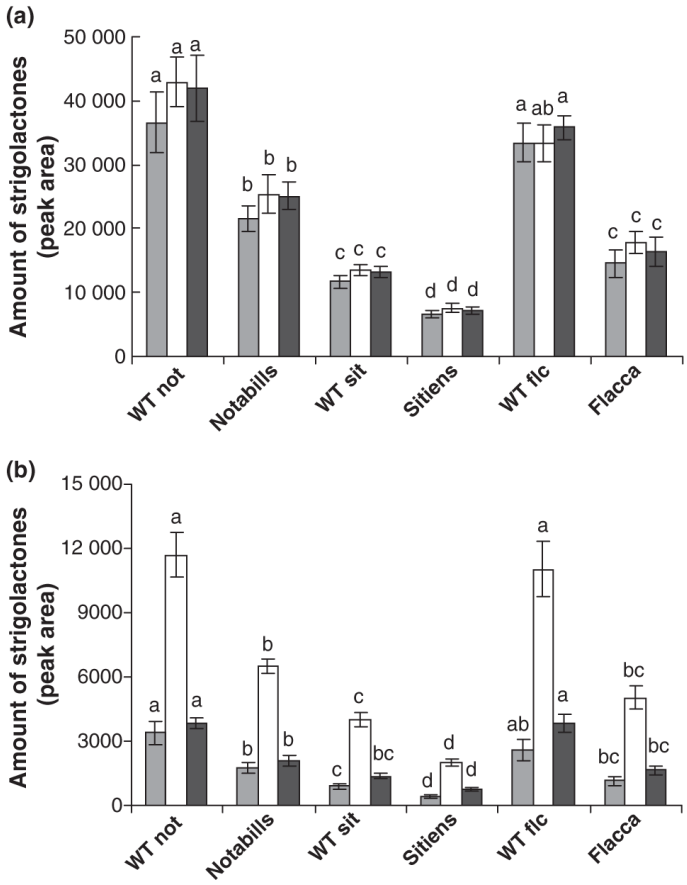

Figure 3: Strigolactone content in tomato root exudates and extracts. The amount (according to the peak area) of the strigolactone solanacol (tinted bars) and the didehydro-orobanchol isomers 1 and 2 (didehydro-1 (open bars) and didehydro-2(closed bars)) of the tomato mutants notabilis, sitiens and flacca, and corresponding wild types (WT) was quantified **(a)** root exudates, **(b)** root extracts. Bars represent the average of five independent replicates ± SE. Bars with a different letter differ significantly ($P < 0.05$)

Corresponding to the differences in germination stimulatory activity (see above), differences in strigolactone concentration between the different wild-types were observed, with the background of *notabilis* and *flacca* (cv. Ailsa Craig) producing more strigolactones than the background of *sitiens* (cv. Rheinlands Ruhm) (Figure 3a).

ABA quantification by MRM-LC-MS/MS

The tomato mutants *notabilis*, *sitiens* and *flacca* have previously been characterized to have a lower ABA content mainly in the leaves (Cornish and Zeevaart, 1988; Thompson et al., 2000). Since in the current work we wished to study the relationship between ABA and the root-produced strigolactones, we have also analyzed the levels of ABA in the roots of these three mutants. The

concentration of ABA detected in the roots of *notabilis*, *sitiens* and *flacca* was about 45, 60 and 65%, respectively, lower than in the corresponding wild-types (Table 1). ABA levels in the aerial part (stems and leaves combined) showed similar reductions as in the roots, although their levels were much higher (about 25-fold) than in the roots (Table 1). Just as for the concentration of the strigolactones and the germination stimulatory activity, significant ($P < 0.05$) differences between the different wild-types in the ABA content were observed (Table 1).

Specific carotenoid cleavage enzyme inhibitors

To further investigate the involvement of NCEDs in strigolactone biosynthesis an experiment with the specific NCED inhibitor abamineSG (Figure 1) was carried out. In parallel, the effect of another inhibitor - D2 - specific for the other class of carotenoid-cleaving enzymes CCD7 and CCD8, which are involved in strigolactone biosynthesis (Figure 1), was also tested. AbamineSG is a tertiary amine derivative acting as a competitive inhibitor of the NCEDs (Kitahata et al., 2006). D2 is a derivative of a hydroxamic acid (aryl-C_2N) and is a potent inhibitor of CCD enzymes cleaving at the 9,10 position of carotenoids (Sergeant et al., 2009), but is considerably less active against NCEDs (11,12 cleavage) *in vitro*. It has been postulated that CCD7 cleaves β-carotene at the 9,10 position to produce the apocarotenoid 10-apo-β-carotene which is then further cleaved by CCD8 in the pathway leading to the strigolactones (Alder et al., 2008; Gomez-Roldan et al., 2008; Umehara et al., 2008).

Tomato plants were treated with the inhibitors abamineSG or D2 by irrigation and the amount of strigolactones produced by the plants was measured by MRM-LC-MS/MS. Phosphate starvation clearly induced the production of the tomato strigolactones solanacol, didehydro-orobanchol 1 and 2 compared with control plants grown under adequate phosphate nutrition in a time-dependent manner (Figure 4). Again, orobanchol was also detected, but its concentration was too low for accurate quantification. In plants treated with the inhibitor abamineSG (ABA inhibitor), the increase in strigolactone production induced by phosphate starvation was significantly ($P < 0.05$) reduced (Figure 4), suggesting again an involvement of NCEDs in strigolactone biosynthesis. This inhibition was more evident after seven days of treatment, when the production and/or exudation of solanacol and the two didehydro-orobanchol isomers was reduced by 58, 77 and 59%, respectively. When plants were treated with D2 (strigolactone inhibitor), similarly as after treatment with abamineSG, a clear reduction in strigolactone production was

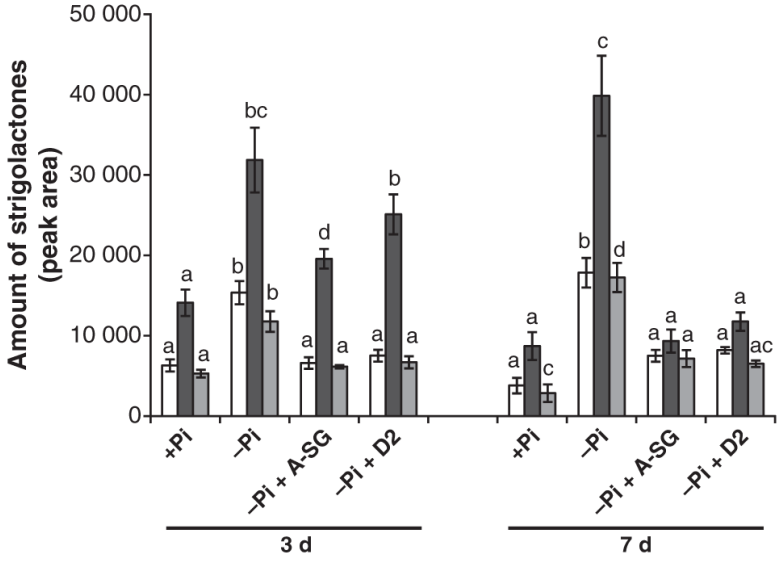

Figure 4: Effect of phosphate (Pi) starvation and treatment with inhibitors on strigolactone production in tomato. The amounts (according to the peak area and corrected to 1 g root fresh weight) of the strigolactones solanacol (open bars), and the didehydro-orobanchol isomers 1 and 2 (didehydro-1 (closed bars) and didehydro-2 (tinted bars)) in the root exudates of tomato (cv MoneyMaker) plants under Pi starvation (−Pi) and under Pi starvation plus treatment with 50 µM of abamineSG (−Pi + A-SG) or D2 (−Pi + D2) for 3 d and 7 d. Bars represent the average of five independent replicates ± SE. Bars with a different letter differ significantly ($P < 0.05$)

observed in a time-dependent manner (Figure 4), In this case, the decrease in the production of solanacol and the two didehydro-orobanchol isomers after seven days was 54, 70 and 62%, respectively.

To check the effect of these two inhibitors on ABA biosynthesis, the ABA content in the roots and shoots after seven days treatment was quantified. Here, a low but significant ($P < 0.05$) reduction of about 27% was only observed in the roots of plants treated with abamineSG, whereas there was no effect on ABA content after treatment with the inhibitor D2 (Table 2). When ABA levels were analyzed in the shoots, no effect of either of the two inhibitors was observed. Phosphate starvation alone did not affect ABA content neither in the roots nor in the shoots (Table 2), which is in line with previous findings in castor bean (*Ricinus communis*) where it was shown that ABA synthesis in roots, ABA xylem transport and ABA catabolism in shoots were induced upon phosphorus stress, while ABA content in both roots and shoots was not affected (Jeschke et al., 1997).

Table 1: Quantification of ABA in roots and shoots of the tomato mutants notabilis, sitiens and flacca, and corresponding wild types (WT)

	[ABA] ng/g FW	
Genotype	**Roots**	**Shoots**
WT *notabilis*	9.51 ± 2.06[a]	203.91 ± 10.19[a]
notabilis	5.22 ± 1.06[b]	112.02 ± 11.42[b]
WT *sitiens*	6.26 ± 0.72[b]	180.92 ± 22.07[a]
sitiens	2.51 ± 0.60[c]	67.91 ± 7.14[c]
WT *flacca*	7.19 ± 0.51[ab]	198.63 ± 15.34[a]
flacca	2.54 ± 0.67[c]	66.60 ± 9.09[c]

Values represent the average of five independent replicates ± SD.
a,b,c Statistically significant differences between means ($P < 0.05$).

Gene expression analysis for ABA and strigolactone biosynthetic genes

Expression analysis by quantitative real time RT-PCR (qPCR) was performed to check expression of tomato genes encoding different carotenoid cleavage enzymes. As the tomato genome is not completely sequenced, only some of the genes coding for enzymes from this family are known. The genes studied in the present work are *LeCCD1*-B, *LeCCD7*, *LeCCD8*, *LeNCED1* and *LeNCED4*. LeCCD1-A and -B are involved in the production of the flavor volatiles β-ionone, pseudo-ionone and geranylacetone (Simkin et al., 2004). CCD7 and CCD8 have been described to be involved in the biosynthesis of strigolactones in pea, rice and Arabidopsis (Gomez-Roldan et al., 2008; Umehara et al., 2008). More recently, CCD7 from tomato was cloned and characterized and shown to be involved in strigolactone biosynthesis, shoot branching and formation of mycorrhiza-induced apocarotenoids (Vogel et al., 2010). In Arabidopsis all NCEDs, except AtNCED4 are known to be involved in ABA production (Auldridge et al., 2006; Bouwmeester et al., 2007).

Table 2: Quantification of ABA in the roots and shoots of tomato plants (cv MoneyMaker) upon phosphate starvation and after treatment with inhibitors for 7 d

	[ABA] ng/g FW	
Treatment	**Roots**	**Shoots**
0h	2.37 ± 0.16[a]	133.75 ± 12.06[a]
+Pi	2.47 ± 0.19[a]	138.37 ± 11.98[a]
-Pi	2.44 ± 0.25[a]	130.40 ± 9.94[a]
-Pi + A-SG	1.79 ± 0.20[b]	126.92 ± 13.92[a]
-Pi + D2	2.37 ± 0.14[a]	131.67 ± 7.30[a]

ABA was analysed in extracts of tomato plants with suficient phosphate (+Pi), under Pi starvation (−Pi) and under Pi starvation plus treatment with 50 µM of abamineSG (−Pi +A-SG) or D2 (−Pi + D2) for 3 and 7 d. Values represent the average of five independent replicates ± SD.a,b Statistically significant differences between means ($P < 0.05$)

Expression of *LeCCD7* and *LeCCD8* was clearly reduced in all three ABA-deficient mutants - *notabilis*, *sitiens* and *flacca* - compared with the corresponding wild-types, whereas the expression of the other carotenoid cleavage genes was not affected (Figure 5a). Moreover, this reduction was more evident

in *sitiens* and *flacca*, which had a lower ABA content than *notabilis* (Table 1). In *notabilis*, with a null mutation in *LeNCED1* caused by a single A/T base pair deletion (Burbidge et al., 1999), the expression of this gene was not significantly reduced, in agreement with previous observations that expression of *LeNCED1* was not regulated by ABA (Thompson et al., 2000). The other NCED gene so far described in tomato - *LeNCED4* - was significantly reduced although to a lesser extent than *LeCCD7* and *LeCCD8* (Figure 5a). When gene expression was assessed in roots upon seven days application of the inhibitors abamineSG and D2, no significant changes were detected in the expression levels of any of the selected genes (Figure 5b). None of the genes was significantly affected by phosphate starvation (data not shown).

Discussion

ABA is an important phytohormone playing many physiological roles in plants (Zeevaart and Creelman, 1988; Davies et al., 2005; De Smet et al., 2006; Adie et al., 2007; Jiang and Hartung, 2008). ABA is an apocarotenoid produced via oxidative cleavage of epoxycarotenoids through action of NCEDs, which catalyze the rate-limiting step in ABA biosynthesis (Parry and Horgan, 1992; Thompson et al., 2000; Taylor et al., 2005) (Figure 1). We have previously demonstrated that in the ABA-deficient mutants *vp14* and *notabilis* in maize and tomato, respectively - having a mutation in an NCED and therefore showing a lower ABA content - the production of strigolactones was decreased by about 40% (Matusova et al., 2005; López-Ráez et al., 2008). From these results it was concluded that the NCEDs either have a direct role in strigolactone biosynthesis or that ABA has a regulatory role in this process (Matusova et al., 2005; López-Ráez et al., 2008). We show here that the corresponding decrease in ABA and strigolactone production also occurs in two other well characterized tomato ABA-deficient mutants *sitiens* and *flacca* that are mutated in the last step of ABA biosynthesis - transformation of ABA aldehyde into ABA by an AAO - (Figure 1) (Taylor et al., 1988; Schwartz et al., 2003). The decrease in ABA content in the roots of these mutants was stronger than for *notabilis*, being 60 and 65% lower than the corresponding wild-types, respectively. This reduction in ABA content in the roots and also in the shoots of *sitiens* and *flacca* is somewhat lower than previously reported, when 89 and 67% reduction, respectively were detected in leaves (Cornish and Zeevaart, 1988). This discrepancy is likely due to differences in the conditions under which the plants were grown and/or the analytical method used. In the present study ABA content as well as strigolactones were measured using the

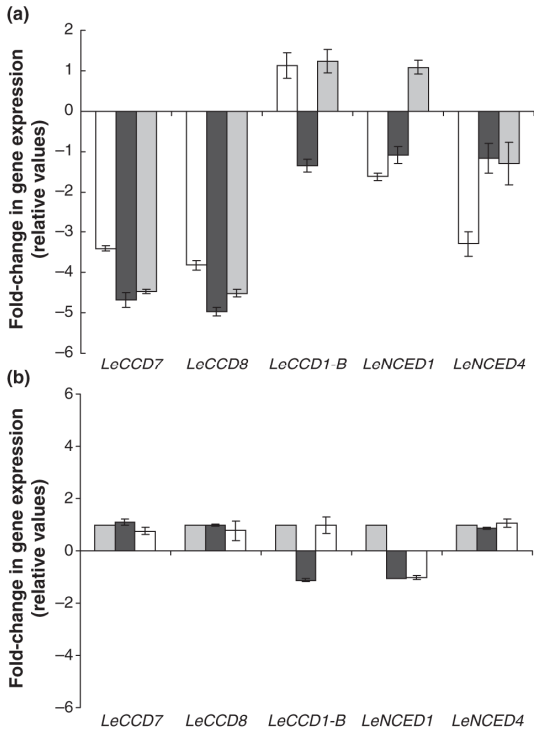

Figure 5: Gene expression analysis by real-time quantitative PCR (qPCR) for the carotenoid cleaving genes LeCCD7, LeCCD8, LeCCD1-B, LeNCED1 and LeNCED4 in tomato roots. **(a)** Gene expression of the tomato mutants notabilis (open bars), sitiens (closed bars) and flacca (tinted bars). **(b)** Gene expression in roots of tomato (cv MoneyMaker) plants grown under phosphate (Pi) starvation (−Pi, grey bars) and under Pi starvation plus treatment with 50 µM of abamineSG (−Pi + A-SG, closed bars) or D2 (−Pi + D2, open bars) for 7 d. The expression for each gene in the different mutants is given relative to the expression of the same gene in the corresponding wild-type. Bars, mean values ± SE of three independent biological replicates.

same methodology – MRM-LC-MS/MS in MRM mode - and using the same plant material. The levels of strigolactones produced by the roots of *sitiens* and *flacca* were also lower than for *notabilis* (Figure 3a). A strong correlation was observed between the reduction of ABA and strigolactone content in the roots when comparing a mutant with its corresponding wild-type, but across cultivars and mutants there was no correlation between ABA and strigolactone levels. Strigolactone-deficient mutants are characterized by a shoot branching phenotype (Gomez-Roldan et al., 2008; Umehara et al., 2008), but this phenotype was not observed for *notabilis*, *sitiens* and *flacca*, even though the strigolactone content of these mutants is reduced. Apparently, the reduced strigolactone level is still high enough to maintain normal shoot architecture. In a recent study on tomato expressing an *SlCCD7* antisense construct it was shown that an 80% reduction in strigolactone level induced only a weak branching phenotype, whereas in two other lines with over 90% reduction in strigolactone level branching was strongly increased (Vogel et al., 2010).

The fact that ABA-deficient mutants with mutations in enzymes of the biosynthetic pathway other than the NCEDs also produce less strigolactones seems to indicate that NCED is not directly involved in strigolactone biosynthesis, but that its biosynthetic product ABA might be involved somehow in regulating strigolactone biosynthesis. ABA has previously been associated to AM symbiosis as well (Herrera-Medina et al., 2007; Aroca et al., 2008). These authors showed that the mutant *sitiens* was less prone to colonization by AM fungi than the wild-type, but that continuous exogenous application of ABA could not significantly compensate this effect in the mutant. Herrera-Medina and co-workers proposed that ABA increases the susceptibility of tomato to AM colonization and that this is necessary for a proper AM establishment. The authors also suggest that ABA may play a role in the development of the arbuscule and in regulating its functionality (Herrera-Medina et al., 2007). We show here that in *sitiens*, as well as in the other two ABA-deficient mutants *notabilis* and *flacca*, the production of strigolactones is significantly reduced compared with the corresponding wild-types (Figures 2 and 3). Therefore, the reduction in AM colonization observed in *sitiens* may also be due to a reduction in the production of strigolactones by this mutant, although an additional role of ABA in the establishment of AM symbiosis cannot be discarded. Indeed, root exudates of the pea strigolactone-deficient mutants *rms1* and *rms5*, with a mutation in the *CCD8* and *CCD7* genes respectively, have been shown to have a significantly reduced activity in promoting AM fungal hyphae branching when compared with wild-type exudates (Gomez-Roldan et al., 2008). Interestingly, when ABA was exogenously applied to *sitiens* no effect on strigolactone production was observed. The failure to complement the strigolactone phenotype of *sitiens* by exogenous ABA application is in line with the above-mentioned failure to complement the AM-colonization phenotype of *sitiens* by exogenous ABA application (Aroca et al., 2008). The same lack of effect was observed when ABA was applied to the other two mutants *notabilis* and *flacca*. These results suggest that endogenous ABA may be required for strigolactone production in specific root cells or tissues and hence for AM colonization and development. Apparently this requirement cannot be replaced by exogenous ABA application. That exogenous ABA application may not be suitable to replace endogenous ABA is also clear from a study on drought-stress induced ABA using luciferase ABA-reporter plants. Exposure of Arabidopsis seedlings to exogenous ABA resulted in a uniform pattern of reporter expression, whereas reporter expression in response to drought stress was predominantly confined to the vasculature and stomata (Christmann et al., 2005). ABA is known to stimulate its own degradation via the ABA hydroxylases in order to control its homeostasis (Cutler et al., 1997). Indeed, we observed induction of the gene encoding ABA hydroxylase upon ABA application.

In addition to the differences between the ABA-deficient mutants and corresponding wild-types, we also observed significant differences in the germination stimulatory capacity for *P. ramosa* seeds of root exudates from the wild-type cultivars Ailsa Craig and Rheinlands Ruhm (Figure 2). MRM-LC-MS/MS analysis confirmed that the activity differences correlate with differences in the level of strigolactones in the root exudates (Figure 3a), and these correlated to the strigolactone levels in root extracts (Figure 3b). The results show that there is genetic variation for the production of strigolactones in different tomato cultivars, as we previously observed for two other tomato cultivars MoneyMaker and Manapal (López-Ráez et al., 2008). The genetic variation in strigolactone production indicates that selection of tomato cultivars producing low levels of germination stimulants - strigolactones - may be a strategy to breed tomato varieties resistant or less susceptible to *Phelipanche (López-Ráez et al., 2009)*. Selection for low germination stimulant germplasm has been successfully used in other crops such as sorghum in order to produce *Striga* resistant varieties (Ejeta, 2007). The selection process in sorghum was based on the use of germination bioassays, but with the advent of extremely sensitive analytical methods such as LC-MS/MS in MRM mode described in the present paper, an analytically-supported selection process seems now feasible.

Besides ABA-deficient mutants, specific inhibitors for different carotenoid cleaving enzymes were used in the present study (Figure 1). The inhibitor abamineSG - a specific inhibitor for NCEDs and therefore for ABA biosynthesis (Kitahata et al., 2006) - reduced the production of the three major strigolactones present in tomato, solanacol and the two didehydro-orobanchol isomers in plants grown under phosphate-limited conditions (Figure 4). After seven days treatment, the reduction in strigolactone production in the abamineSG-treated plants was similar to the reduction observed in the mutants *sitiens* and *flacca*. Moreover, this reduction in strigolactones was accompanied by a minor but significant decrease in ABA content in the roots of the treated-plants, again suggesting a regulatory effect of ABA in strigolactone biosynthesis. The other members of the carotenoid cleavage enzyme family are the CCDs, involved in the formation of apocarotenoid compounds such as flavour volatiles, cyclohexanone and mycorradicin derivatives (the yellow pigment formed in host roots upon arbuscular mycorrhizal colonization) and strigolactones (Simkin et al., 2004; Strack and Fester, 2006; Sun et al., 2008). CCD7 and CCD8 are involved in the control of plant architecture because they are involved in the production of the strigolactones (Sorefan et al., 2003; Booker et al., 2004; Gomez-Roldan et al., 2008; Umehara et al., 2008). It was shown that AtCCD7 can convert C40 carotenoids into C27 apocarotenoids (Schwartz et al., 2004) and that, subsequently, CCD8 can cleave the C27 into a C18 apocarotenoid, the probable precursor of the plant branching inhibitor (Alder et al., 2008). D2 specifically inhibits these CCDs, so also strigolactone biosynthesis and was included to investigate whether low strigolactone levels also affect ABA levels. Recently, it was shown that D2 showed selectivity *in vitro* towards CCDs that cleave at the 9,10 position - such as CCD7 - rather than towards NCEDs that cleave at the 11,12 position of C40 *cis*-carotenoids (Sergeant et al., 2009). In the present study, D2 indeed caused a reduction in strigolactone production suggesting that this inhibitor did indeed inhibit either CCD7 or CCD8 or both (Figure 4). However, no effect on ABA content was observed in the roots of D2-treated plants, confirming that NCEDs are not significantly inhibited *in vivo*, thus supporting the observed *in vitro* selectivity of the inhibitor (Sergeant et al., 2009). These results also show that a short-term reduction in strigolactone levels does not lead to a reduction in ABA. The results are also in agreement with those observed previously where continuous application of D2 increased the number of side branches from the rosette nodes of Arabidopsis, mimicking the Arabidopsis *max3* (*ccd7*) bushy phenotype, presumably by inhibiting one or more of the CCDs involved in strigolactone biosynthesis (Sergeant et al., 2009). However, in that study it was not analytically assessed whether that phenotype was caused by an inhibition of strigolactone

biosynthesis. Here we show that application of D2 indeed inhibits strigolactone production, and thus it is a useful and selective inhibitor for use in *in vivo* studies on strigolactones.

When the expression of *LeCCD7* and *LeCCD8* was checked by real time qPCR, a clear decrease in expression for both genes was observed in all three mutants *notabilis*, *sitiens* and *flacca* (Figure 5a). This reduction was most clear in *sitiens* and *flacca*, the mutants with the strongest reduction in ABA content (Table 1). No differences were observed in the expression of the other carotenoid-cleaving enzymes known in tomato (Figure 5a). Although a reduction in gene expression levels does not necessarily imply a reduction in the enzyme activity (Fraser et al., 2007; Carbone et al., 2009), the results shown here confirm the involvement of CCD7 and CCD8 in strigolactone biosynthesis in tomato (Vogel et al., 2010). In contrast, the reduction in strigolactone level by abamineSG treatment did not correlate with a down-regulation of *LeCCD7* and *LeCCD8* (Figure 5b). This suggests that these genes are not transcriptionally regulated by ABA in the short-term. Post-transcriptional regulation of CCD8 by auxin was postulated to occur in Arabidopsis (Bainbridge et al., 2005). In *sitiens* the levels of IAA in the roots have been reported to be lower than in the corresponding wild-type (Dunlap and Binzel, 1996). Therefore, the decrease in strigolactone production in the tomato ABA-mutants may be mediated by a decrease in auxin levels in the roots which negatively affects *LeCCD7* and *LeCCD8* expression and hence, the production of strigolactones in these mutants. A short-term decrease in ABA through abamineSG application does not lead to a similar reduction in *LeCCD7* and *LeCCD8* expression, even though strigolactone production is decreased, suggesting that a short-term response of strigolactone production to ABA is not mediated through a decrease in auxin levels and its negative effect on *LeCCD7* and *LeCCD8* expression.

It has been shown that phosphate starvation promotes strigolactone biosynthesis (Yoneyama et al., 2007; López-Ráez et al., 2008; Umehara et al., 2008). Despite the fact that the strigolactones are carotenoid derived, the amount of carotenoids is not increased in roots under phosphate starvation (López-Ráez et al., 2008) and no changes in the expression of genes encoding enzymes involved in carotenoid biosynthesis were observed under phosphate deprivation using microarray studies (Wasaki et al., 2003; Misson et al., 2005; Hernandez et al., 2007; López-Ráez and Bouwmeester, 2008). Here we observed that phosphate starvation, like ABA application, does also not affect the expression of the strigolactone biosynthetic genes *LeCCD7* and *LeCCD8*. This suggests that the effect of phosphorous deficiency on strigolactone production might be at the post-transcriptional level or on an as yet unknown step in the strigolactone biosynthetic pathway. Our results suggest that ABA could be involved in this regulation.

This is the first report in which a correlation is demonstrated between the levels of the phytohormone ABA and the new class of phytohormones strigolactones. Our results obtained with tomato ABA-deficient mutants blocked at different steps in the ABA biosynthetic pathway and the application of specific inhibitors for NCEDs and CCDs suggest that ABA is one of the regulators of strigolactone biosynthesis through an as yet unknown mechanism. Further research is required to elucidate the mechanism by which strigolactone biosynthesis is fine-tuning regulated and the hormone network behind this regulation.

Materials and methods

Plant material and chemicals

Seeds of tomato (*Solanum lycopersicum*) *sitiens* (LA0574) and its parental isogenic cv. Rheinlands Ruhm, and *flacca* (LA3613) and corresponding parental isogenic cv. Ailsa Craig, were obtained from the Tomato Genetics Resource Center (TGRC) at the University of California, Davis, CA, USA. Seeds of cv. Ailsa Craig and *notabilis* (LA3614) were kindly provided by Wim Vriezen (Department of Plant Cell Biology, Radboud University, Nijmegen, The Netherlands). Seeds of tomato cv. MoneyMaker were purchased at a local garden centre. *P. ramosa* seeds were kindly provided by Maurizio Vurro (Instituto di Scienze delle Produzioni Alimentari, Bari, Italy). The synthetic strigolactone analogue GR24 was kindly provided by Binne Zwanenburg (Department of Organic Chemistry, Radboud University, Nijmegen, The Netherlands). The strigolactone standards orobanchol and solanacol were kindly provided by Koichi Yoneyama (Weed Science Center, Utsunomiya University, Japan). The inhibitor abamineSG was kindly provided by Tadao Asami (RIKEN, Saitama, Japan). [$^2H_6$]-*cis*, *trans*-ABA was purchased at Olchemlm Ltd (Czech Republic).

Growth conditions and experiments

Tomato seeds were sterilized in 4% (v/v) sodium hypochlorite containing 0.02% (v/v) Tween 20, rinsed thoroughly with sterile water, and then germinated for 48 h on moistened filter paper at 25ºC in darkness. Subsequently, tomato seedlings were grown in a greenhouse as described before (López-Ráez et al., 2008). Phosphate (Pi) starvation promotes the production of strigolactones (Yoneyama et al., 2007; López-Ráez et al., 2008). Therefore, one week before root exudate collection the substrate (sand:vermiculite; 1:1, v/v) in the pots was rinsed with 1.5 l (2 times the pot volume) of modified half-strength Hoagland solution without phosphate to remove the strigolactones accumulated. Then plants were watered (twice a week) with modified half-strength Hoagland nutrient solution without Pi. For root exudate collection, the substrate in the pots was first rinsed as describe above to remove the strigolactones accumulated. After another 5h, 0.7 l of modified half-strength Hoagland solution without phosphate was applied to the pots and the root exudate collected. Roots from each pot were then collected separately and frozen in liquid nitrogen and stored at -80°C until use. Purification of the root exudates and the germination bioassay were carried out as described before (López-Ráez et al., 2008).

Treatment with inhibitors and ABA

Half-strength Hoagland solution without phosphate and with or without 50 µM of the inhibitors abamineSG or D2 were applied to four-weeks-old tomato plants which were then grown for an additional three or seven days. To maintain the effect of the inhibitors, after three days plants for the seven days treatment were watered with fresh nutrient solution containing the inhibitors. Root exudates and roots were collected on day three and day seven as described above. In an attempt to rescue the strigolactone exudation phenotype of the ABA mutants, mutants were grown as described above. Half-strength Hoagland solution without phosphate and with or without 0.5 µM ABA was applied to four-weeks-old plants and grown for an additional seven days. To maintain the ABA levels, after three days plants were watered with fresh nutrient solution containing ABA. Root exudates and roots were collected after seven days for analyses.

Extraction of ABA and strigolactones from roots and shoots

For ABA and strigolactone analysis, 0.5 g of root or shoot tissue was ground in a mortar with liquid nitrogen. The samples were extracted with 2 ml of cold ethyl acetate containing [$^2H_6$]-ABA as internal

standard (0.025 nmol or 0.25 nmol for root or shoot tissue, respectively) in a 10 ml glass vial. The vials were vortexed and sonicated for 10 min in a Branson 3510 ultrasonic bath (Branson Ultrasonics, Danbury, CT, US). Samples were centrifuged for 10 min at 2500 *g* in an MSE Mistral 2000 centrifuge (Mistral Instruments, Leicester, UK) after which the organic phase was carefully transferred to a 4 ml glass vial. The pellets were re-extracted with another 2 ml of ethyl acetate. The combined ethyl acetate fractions were dried under a flow of N_2 and the residue dissolved in 250 µl of acetonitrile:water:formic acid (25:75:0.1, v/v/v). Before analysis, samples were filtered through Minisart SRP4 0.45 µm filters (Sartorius, Germany) and MRM-LC-MS/MS was performed as described below.

Strigolactone and ABA detection and quantification by liquid chromatography-tandem mass spectrometry (LC-MS/MS)

Analysis of strigolactones in tomato exudates and root extracts was conducted by comparing retention times and mass transitions with those of available strigolactone standards as described before (López-Ráez et al., 2008). ABA analysis was performed by MRM-LC-MS/MS using a published protocol with some modifications (Saika et al., 2007). Analyses were carried out on a Waters Micromass Quattro Premier XE tandem mass spectrometer (Waters, Milford, MA, USA) equipped with an ESI source and coupled to an Acquity UPLC system (Waters, USA). Chromatographic separation was achieved using an Acquity UPLC BEH C_{18} column (150 x 2.1 mm, 1.7 µm) (Waters, USA), applying a water/acetonitrile gradient, starting at 0% acetonitrile for 2.0 min, raised to 50% (v/v) acetonitrile in 8.0 min, followed by a 1.0 min gradient to 90% (v/v) acetonitrile which was then maintained for 0.1 min and followed by a 0.2 min gradient back to 0% acetonitrile before the next run. The column was then equilibrated at this solvent composition for 2.8 min. Total run time was 15 min. The column was operated at 50ºC with a flow-rate of 0.4 ml min^{-1} and sample injection volume was 30 µl. The mass spectrometer was operated in positive electrospray ionization (ESI) mode. The nebuliser and desolvation gas flows were 50 and 800 l h^{-1}, respectively. The capillary voltage was set at 2.7 kV, the cone voltage at 10 V, the source temperature at 120ºC and the desolvation gas temperature at 450ºC. Fragmentation was performed by collision induced dissociation with argon at 3.0 x 10^{-3} mbar. Multiple reaction monitoring (MRM) was used for ABA quantification. Parent-daughter transitions were set according to the MS/MS spectra obtained for the standards ABA and [$^2H_6$]-ABA. Transitions were selected based on the most abundant and specific fragment ions for which the collision energy (CE) was optimized. For ABA, the MRM transitions *m/z* 265>229 at a CE of 10 eV and 265>247 at 5 eV; and for [$^2H_6$]-ABA, the transitions *m/z* 271>234 at 10 eV and 271>253 at 5 eV were selected. ABA was quantified using a calibration curve with known amount of standards and based on the ratio of the summed area of the MRM transitions for ABA to those for [$^2H_6$]-ABA. Data acquisition and analysis were performed using MassLynx 4.1 software (Waters, USA). The summed area of all the corresponding MRM transitions was used for statistical analysis.

RNA isolation and first strand cDNA synthesis

Total RNA from tomato roots was extracted using Tri-Pure reagent (Roche, Germany) according to the manufacturer's protocol. The RNA was sequentially treated with DNase I (Invitrogen, The Netherlands) at 37ºC for 15 min in order to remove the remaining genomic DNA. Before cDNA synthesis, the RNA was purified through a silica column using the RNeasy RNA Cleanup kit (Qiagen, Germany). The first strand cDNA was synthesized with 1 µg of purified total RNA using the iScript cDNA Synthesis kit (Bio-Rad, The Netherlands) according to the manufacturer's instructions.

Gene expression analysis by real time quantitative RT-PCR (qPCR)

For gene expression analysis by real time quantitative RT-PCR (qPCR) the iCycler iQ5 system (Bio-Rad, The Netherlands) was used (Spinsanti et al., 2006) using specific primers. *LeActin*: 5'-TCCCAGGTATTGCTGATAGAA-3' and 5'-TGAGGGAAGCCAAGATAGAG-3'; *LeNCED1*: 5'-ACCCACGAGTCCAGATTTC-3' and 5'-GGTTCAAAAAGAGGGTTAGC-3'; *LeNCED4*: 5'-ACAACATCGAAAATGAAGCCG-3' and 5'-GGCGAAAAGTTTACCTCCA-3'; *LeCCD1-B*: 5'-AGAACAGCGTGACGGTTTCACA-3' and 5'-AGTGTAGTTCTCGTTGATCCGTG-3'; *LeCCD7*: 5'-AGCCAAGAATTCGAGATCCC-3' and 5'-GGAGAAAGCCCACATACTGC-3'; *LeCCD8*: 5'-CAGGACAATGGCACATAGGT-3' and 5'-GCGTCCGATTCGATTTG-3'; *SlCYP7070A1:* 5'-TGTCCAGGGAATGAACTTGC-3' and 5'-CAATGGGACTGGGAATGGTC-3'; *Le4*: 5'-ACTCAAGGCATGGGTACTGG-3' and 5'-CCTTCTTTCTCCTCCCACCT-3'. Three independent biological replicates were used and each PCR reaction was done in triplicate. Relative quantification of mRNA amount was performed using the comparative C_t method (Livak and Schmittgen, 2001). These values were then normalized using the C_t value for the tomato household gene *LeActin*. All the values were used to determine the change in gene expression according to the following calculation: fold-change = $2^{-\Delta(\Delta Ct)}$, where $\Delta C_t = C_t$ (target) - C_t (household) and $\Delta(\Delta C_t) = \Delta C_t$ (treatment) - ΔC_t (control). Down-regulation of expression is shown as negative values.

Statistical analysis

Data for ABA and strigolactone content of tomato roots and strigolactone content in tomato root exudates were subjected to one-way analysis of variance (ANOVA) using GenStat for Windows (9th edition). To analyze the results of germination bioassays, ANOVA after arcsine[squareroot(X)] transformation was used. When appropriate, data were subjected to the Duncan's honestly significant difference test.

Acknowledgements

We acknowledge funding by the European Commission (Intra-European Marie Curie postdoctoral fellowship FP6-MEIF-CT-2005-024345 and Reintegration Grant PERG-02-2007-224751 to Juan A. López-Ráez), The Netherlands Organisation for Scientific Research (NWO; VICI-grant to HB), and the UK BBSRC (Grant BB/D005787/1 to AJT and TDHB). This project was co-financed by the Centre for BioSystems Genomics (CBSG) which is part of the Netherlands Genomics Initiative/Netherlands Organisation for Scientific Research. We thank Binne Zwanenburg for supplying GR24, Koichi Yoneyama for advice and strigolactone standards, Tadao Asami for supplying abamineSG and Maurizio Vurro for supplying *P. ramosa* seeds, Wim Vriezen for supplying Ailsa Craig and *notabilis* seeds, and Harry Klee and Jonathan Vogel for *LeCCD7* sequence information.

References

Adie BAT, Perez-Perez J, Perez-Perez MM, Godoy M, Sanchez-Serrano JJ, Schmelz EA, Solano R (2007) ABA is an essential signal for plant resistance to pathogens affecting JA biosynthesis and the activation of defenses in Arabidopsis. Plant Cell **19:** 1665-1681

Akiyama K, Matsuzaki K, Hayashi H (2005) Plant sesquiterpenes induce hyphal branching in arbuscular mycorrhizal fungi. Nature **435:** 824-827

Alder A, Holdermann I, Beyer P, Al-Babili S (2008) Carotenoid oxygenases involved in plant branching catalyse a highly specific conserved apocarotenoid cleavage reaction. Biochemical Journal **416:** 289-296

Aroca R, Alguacil MD, Vernieri P, Ruiz-Lozano JM (2008) Plant responses to drought stress and exogenous ABA application are modulated differently by mycorrhization in tomato and an ABA-deficient mutant (*sitiens*). Microbial Ecology **56:** 704-719

Auldridge ME, Block A, Vogel JT, Dabney-Smith C, Mila I, Bouzayen M, Magallanes-Lundback M, DellaPenna D, McCarty DR, Klee HJ (2006) Characterization of three members of the Arabidopsis carotenoid cleavage dioxygenase family demonstrates the divergent roles of this multifunctional enzyme family. The Plant Journal **45:** 982-993

Bainbridge K, Sorefan K, Ward S, Leyser O (2005) Hormonally controlled expression of the Arabidopsis *MAX4* shoot branching regulatory gene. The Plant Journal **44:** 569-580

Bethke PC, Lonsdale JE, Fath A, Jones RL (1999) Hormonally regulated programmed cell death in barley aleurone cells. Plant Cell **11:** 1033-1045

Booker J, Auldridge M, Wills S, McCarty D, Klee H, Leyser O (2004) MAX3/CCD7 is a carotenoid cleavage dioxygenase required for the synthesis of a novel plant signaling molecule. Current Biology **14:** 1232-1238

Bouwmeester HJ, Matusova R, Zhongkui S, Beale MH (2003) Secondary metabolite signalling in host-parasitic plant interactions. Current Opinion in Plant Biology **6:** 358-364

Bouwmeester HJ, Roux C, López-Ráez JA, Bécard G (2007) Rhizosphere communication of plants, parasitic plants and AM fungi. Trends in Plant Science **12:** 224-230

Burbidge A, Grieve TM, Jackson A, Thompson A, McCarty DR, Taylor IB (1999) Characterization of the ABA-deficient tomato mutantnotabilisand its relationship with maizeVp14. The Plant Journal **17:** 427-431

Carbone F, Preuss A, De Vos RCH, D'Amico E, Perrotta G, Bovy AG, Martens S, Rosati C (2009) Developmental, genetic and environmental factors affect the expression of flavonoid genes, enzymes and metabolites in strawberry fruits*. Plant Cell and Environment **32:** 1117-1131

Christmann A, Hoffmann T, Teplova I, Grill E, Muller A (2005) Generation of active pools of abscisic acid revealed by in vivo Imaging of water-stressed Arabidopsis. Plant Physiology **137:** 209-219

Cook CE, Whichard LP, Turner B, Wall ME, Egley GH (1966) Germination of witchweed (*Striga lutea Lour.*): isolation and properties of a potent stimulant. Science **154:** 1189-1190

Cornish K, Zeevaart JAD (1988) Phenotypic expression of wild-type tomato and three wilty mutants in relation to abscisic acid accumulation in roots and leaflets of reciprocal grafts. Plant Physiology **87:** 190-194

Cutler AJ, Squires TM, Loewen MK, Balsevich JJ (1997) Induction of (+)-abscisic acid 8' hydroxylase by (+)-abscisic acid in cultured maize cells. Journal of Experimental Botany **48:** 1787-1795

Davies WJ, Kudoyarova G, Hartung W (2005) Long-distance ABA signaling and its relation to other signaling pathways in the detection of soil drying and the mediation of the plant's response to drought. Journal of Plant Growth Regulation **24:** 285-295

De Smet I, Zhang HM, Inze D, Beeckman T (2006) A novel role for abscisic acid emerges from underground. Trends in Plant Science **11:** 434-439

Dunlap JR, Binzel ML (1996) NaCl reduces indole-3-acetic acid levels in the roots of tomato plants independent of stress-induced abscisic acid. Plant Physiology **112:** 379-384

Ejeta G (2007) Breeding for Striga resistance in sorghum: Exploitation of an intricate host-parasite biology. Crop Science **47:** S216-S227

Fraser PD, Enfissi EMA, Halket JM, Truesdale MR, Yu DM, Gerrish C, Bramley PM (2007) Manipulation of phytoene levels in tomato fruit: Effects on isoprenoids, plastids, and intermediary metabolism. Plant Cell **19:** 3194-3211

Gomez-Roldan V, Fermas S, Brewer PB, Puech-Pages V, Dun EA, Pillot J-P, Letisse F, Matusova R, Danoun S, Portais J-C, Bouwmeester H, Becard G, Beveridge CA, Rameau C, Rochange SF (2008) Strigolactone inhibition of shoot branching. Nature **455:** 189-194

Harrison MJ (2005) Signaling in the arbuscular mycorrhizal symbiosis. Annual Review of Microbiology **59:** 19-42

Hernandez G, Ramirez M, Valdes-Lopez O, Tesfaye M, Graham MA, Czechowski T, Schlereth A, Wandrey M, Erban A, Cheung F, Wu HC, Lara M, Town CD, Kopka J, Udvardi MK, Vance CP (2007) Phosphorus stress in common bean: Root transcript and metabolic responses. Plant Physiology **144:** 752-767

Herrera-Medina MJ, Steinkellner S, Vierheilig H, Bote JAO, Garrido JMG (2007) Abscisic acid determines arbuscule development and functionality in the tomato arbuscular mycorrhiza. New Phytologist **175:** 554-564

Jeschke WD, Peuke AD, Pate JS, Hartung W (1997) Transport, synthesis and catabolism of abscisic acid (ABA) in intact plants of castor bean (*Ricinus communis L*.) under phosphate deficiency and moderate salinity. Journal of Experimental Botany **48:** 1737-1747

Jiang F, Hartung W (2008) Long-distance signalling of abscisic acid (ABA): the factors regulating the intensity of the ABA signal. Journal of Experimental Botany **59:** 37-43

Joel DM (2009) The new nomenclature of *Orobanche* and *Phelipanche*. Weed Research **49:** 6-7

Kahn TL, Fender SE, Bray EA, Oconnell MA (1993) Characterization of expression of drought- and abscisic acid-regulated tomato genes in the drought-resistant species *Lycopersicon pennellii*. Plant Physiology **103:** 597-605

Kitahata N, Han SY, Noji N, Saito T, Kobayashi M, Nakano T, Kuchitsu K, Shinozaki K, Yoshida S, Matsumoto S, Tsujimoto M, Asami T (2006) A 9-cis-epoxycarotenoid dioxygenase inhibitor for use in the elucidation of abscisic acid action mechanisms. Bioorganic & Medicinal Chemistry **14:** 5555-5561

Li Y, Walton DC (1990) Violaxanthin is an abscisic acid precursor in water-stressed dark-grown bean leaves. Plant Physiology **92:** 551-559

Livak KJ, Schmittgen TD (2001) Analysis of relative gene expression data using real-time quantitative PCR and the 2(T)(-Delta Delta C) method. Methods **25:** 402-408

López-Ráez JA, Bouwmeester H (2008) Fine-tuning regulation of strigolactone biosynthesis under phosphate starvation. Plant Signaling & Behavior **3**

López-Ráez JA, Charnikhova T, Gómez-Roldán V, Matusova R, Kohlen W, De Vos R, Verstappen F, Puech-Pages V, Bécard G, Mulder P, Bouwmeester H (2008) Tomato strigolactones are derived from carotenoids and their biosynthesis is promoted by phosphate starvation. New Phytologist **178:** 863-874

López-Ráez JA, Charnikhova T, Gómez-Roldán V, Matusova R, Kohlen W, Vos RD, Verstappen F, Puech-Pages V, Bécard G, Mulder P, Bouwmeester H (2008) Tomato strigolactones are derived from carotenoids and their biosynthesis is promoted by phosphate starvation. New Phytologist **178:** 863-874

López-Ráez JA, Charnikhova T, Mulder P, Kohlen W, Bino R, Levin I, Bouwmeester H (2008) Susceptibility of the tomato mutant high pigment-2dg (hp-2dg) to *Orobanche spp*. infection. Journal of Agricultural and Food Chemistry **56:** 6326-6332

López-Ráez JA, Matusova R, Cardoso C, Jamil M, Charnikhova T, Kohlen W, Ruyter-Spira C, Verstappen F, Bouwmeester H (2009) Strigolactones: ecological significance and use as a target for parasitic plant control. Pest Management Science **65:** 471-477

Matusova R, Rani K, Verstappen FWA, Franssen MCR, Beale MH, Bouwmeester HJ (2005) The strigolactone germination stimulants of the plant-parasitic *Striga* and *Orobanche* spp are derived from the carotenoid pathway. Plant Physiology **139:** 920-934

Matusova R, Rani K, Verstappen FWA, Franssen MCR, Beale MH, Bouwmeester HJ (2005) The strigolactone germination stimulants of the plant-parasitic *Striga* and *Orobanche spp*. are derived from the carotenoid pathway. Plant Physiology **139:** 920-934

Misson J, Raghothama KG, Jain A, Jouhet J, Block MA, Bligny R, Ortet P, Creff A, Somerville S, Rolland N, Doumas P, Nacry P, Herrerra-Estrella L, Nussaume L, Thibaud MC (2005) A genome-wide transcriptional analysis using *Arabidopsis thaliana* Affymetrix gene chips determined plant responses to phosphate deprivation. Proceedings of the National Academy of Sciences of the United States of America **102:** 11934-11939

Nitsch LMC, Oplaat C, Feron R, Ma Q, Wolters-Arts M, Hedden P, Mariani C, Vriezen WH (2009) Abscisic acid levels in tomato ovaries are regulated by *LeNCED1* and *SlCYP707A1*. Planta **229:** 1335-1346

Parry AD, Griffiths A, Horgan R (1992) Abscisic acid biosynthesis in roots. 2. The effects of water stress in wild type and abscisic acid deficient mutant (*notabilis*) plants of *Lycopersicon esculentum Mill.* Planta **187:** 192-197

Parry AD, Horgan R (1992) Abscisic acid biosynthesis in roots. 1. The identification of potential abscisic acid precursors, and other carotenoids. Planta **187:** 185-191

Paszkowski U (2006) Mutualism and parasitism: The yin and yang of plant symbioses. Current Opinion in Plant Biology **9:** 364-370

Rani K, Zwanenburg B, Sugimoto Y, Yoneyama K, Bouwmeester HJ (2008) Biosynthetic considerations could assist the structure elucidation of host plant produced rhizosphere signalling compounds (strigolactones) for arbuscular mycorrhizal fungi and parasitic plants. Plant Physiology and Biochemistry **46:** 617-626

Rock CD, Zeevaart JAD (1991) The ABA mutant of Arabidopsis thaliana is impaired in epoxy-carotenoid biosynthesis. Proceedings of the National Academy of Sciences of the United States of America **88:** 7496-7499

Sagi M, Scazzocchio C, Fluhr R (2002) The absence of molybdenum cofactor sulfuration is the primary cause of the flacca phenotype in tomato plants. The Plant Journal **31:** 305-317

Saika H, Okamoto M, Miyoshi K, Kushiro T, Shinoda S, Jikumaru Y, Fujimoto M, Arikawa T, Takahashi H, Ando M, Arimura S, Miyao A, Hirochika H, Kamiya Y, Tsutsumi N, Nambara E, Nakazono M (2007) Ethylene promotes submergence-induced expression of OsABA8ox1, a gene that encodes ABA 8 '-hydroxylase in rice. Plant and Cell Physiology **48:** 287-298

Schwartz SH, Qin XQ, Loewen MC (2004) The biochemical characterization of two carotenoid cleavage enzymes from Arabidopsis indicates that a carotenoid-derived compound inhibits lateral branching. Journal of Biological Chemistry **279:** 46940-46945

Schwartz SH, Qin XQ, Zeevaart JAD (2003) Elucidation of the indirect pathway of abscisic acid biosynthesis by mutants, genes, and enzymes. Plant Physiology **131:** 1591-1601

Schwartz SH, Tan BC, Gage DA, Zeevaart JAD, McCarty DR (1997) Specific oxidative cleavage of carotenoids by VP14 of maize. Science **276:** 1872-1874

Sergeant MJ, Li JJ, Fox C, Brookbank N, Rea D, Bugg TDH, Thompson AJ (2009) Selective inhibition of carotenoid cleavage dioxygenases: Phenotypic effects on shoot branching. Journal of Biological Chemistry **284:** 5257-5264

Simkin AJ, Schwartz SH, Auldridge M, Taylor MG, Klee HJ (2004) The tomato *carotenoid cleavage dioxygenase 1* genes contribute to the formation of the flavor volatiles beta-ionone, pseudoionone, and geranylacetone. The Plant Journal **40:** 882-892

Sorefan K, Booker J, Haurogné K, Goussot M, Bainbridge K, Foo E, Chatfield S, Ward S, Beveridge C, Rameau C, Leyser O (2003) *MAX4* and *RMS1* are orthologous dioxygenase-like genes that regulate shoot branching in Arabidopsis and pea. Genes & Development **17:** 1469-1474

Spinsanti G, Panti C, Lazzeri E, Marsili L, Casini S, Frati F, Fossi CM (2006) Selection of reference genes for quantitative RT-PCR studies in striped dolphin (*Stenella coeruleoalba*) skin biopsies. Bmc Molecular Biology **7**

Strack D, Fester T (2006) Isoprenoid metabolism and plastid reorganization in arbuscular mycorrhizal roots. New Phytologist **172:** 22-34

Sun Z, Hans J, Walter MH, Matusova R, Beekwilder J, Verstappen FWA, Ming Z, van Echtelt E, Strack D, Bisseling T, Bouwmeester HJ (2008) Cloning and characterisation of a maize carotenoid cleavage dioxygenase (ZmCCD1) and its involvement in the biosynthesis of apocarotenoids with various roles in mutualistic and parasitic interactions. Planta **228:** 789-801

Tan X, Calderon-Villalobos LIA, Sharon M, Zheng C, Robinson CV, Estelle M, Zheng N (2007) Mechanism of auxin perception by the TIR1

ubiquitin ligase. Nature **446:** 640-645

Taylor IB, Linforth RST, Al-Naieb RJ, Bowman WR, Marples BA (1988) The wilty tomato mutants *flacca* and *sitiens* are impaired in the oxidation of ABA-aldehyde to ABA. Plant, Cell & Environment **11:** 739-745

Taylor IB, Sonneveld T, Bugg TDH, Thompson AJ (2005) Regulation and manipulation of the biosynthesis of abscisic acid, including the supply of xanthophyll precursors. Journal of Plant Growth Regulation **24:** 253-273

Thompson AJ, Jackson AC, Parker RA, Morpeth DR, Burbidge A, Taylor IB (2000) Abscisic acid biosynthesis in tomato: Regulation of zeaxanthin epoxidase and 9-cis-epoxycarotenoid dioxygenase mRNAs by light/dark cycles, water stress and abscisic acid. Plant Molecular Biology **42:** 833-845

Thompson AJ, Jackson AC, Symonds RC, Mulholland BJ, Dadswell AR, Blake PS, Burbidge A, Taylor IB (2000) Ectopic expression of a tomato 9-cis-epoxycarotenoid dioxygenase gene causes over-production of abscisic acid. The Plant Journal **23:** 363-374

Umehara M, Hanada A, Yoshida S, Akiyama K, Arite T, Takeda-Kamiya N, Magome H, Kamiya Y, Shirasu K, Yoneyama K, Kyozuka J, Yamaguchi S (2008) Inhibition of shoot branching by new terpenoid plant hormones. Nature **455:** 195-200

Vogel JT, Walter MH, Giavalisco P, Lytovchenko A, Kohlen W, Charnikhova T, Simkin AJ, Goulet C, Strack D, Bouwmeester HJ, Fernie AR, Klee HJ (2010) SlCCD7 controls strigolactone biosynthesis, shoot branching and mycorrhiza-induced apocarotenoid formation in tomato. The Plant Journal **61:** 300-311

Wasaki J, Yonetani R, Kuroda S, Shinano T, Yazaki J, Fujii F, Shimbo K, Yamamoto K, Sakata K, Sasaki T, Kishimoto N, Kikuchi S, Yamagishi M, Osaki M (2003) Transcriptomic analysis of metabolic changes by phosphorus stress in rice plant roots. Plant Cell and Environment **26:** 1515-1523

Yoneyama K, Xie X, Sekimoto H, Takeuchi Y, Ogasawara S, Akiyama K, Hayashi H (2008) Strigolactones, host recognition signals for root parasitic plants and arbuscular mycorrhizal fungi, from Fabaceae plants. New Phytologist **179:** 484-494

Yoneyama K, Yoneyama K, Takeuchi Y, Sekimoto H (2007) Phosphorus deficiency in red clover promotes exudation of orobanchol, the signal for mycorrhizal symbionts and germination stimulant for root parasites. Planta **225:** 1031-1038

Zeevaart JAD, Creelman RA (1988) Metabolism and Physiology of Abscisic-Acid. Annual Review of Plant Physiology and Plant Molecular Biology **39:** 439-473

Zeevaart JAD, Creelman RA (1988) Metabolism and physiology of abscisic acid. Annual Review of Plant Physiology and Plant Molecular Biology **39:** 439-473

Chapter 5

Strigolactone biosynthesis requires the symbiotic GRAS-type transcription factors NSP1 and NSP2

Wei Liu, Wouter Kohlen, Alessandra Lillo, Rik op den Camp, Sergey Ivanov, Marijke Hartog, Erik Limpens, Muhammad Jamil, Cezary Smaczniak, Kerstin Kaufmann, Wei-Cai Yang, Guido Hooiveld, Tatsiana Charnikhova, Harro Bouwmeester, Ton Bisseling and René Geurts.

Adapted version accepted by the Plant Cell (2011)

Abstract

Legume GRAS-type transcription factors NSP1 and NSP2 are essential for rhizobium Nod factorinduced nodulation. Both proteins are considered to be Nod factor response factors regulating gene expression upon symbiotic signaling. However, legume NSP1 and NSP2 can be functionally replaced by non-legume orthologs; including rice (*Oryza sativa*) OsNSP1 and OsNSP2. This shows that both proteins are functionally conserved in higher plants, suggesting an ancient function that is maintained during evolution. Here we show that NSP1 and NSP2 are indispensable for strigolactone biosynthesis in the legume *Medicago truncatula* as well as rice. Mutant *nsp1* plants don't produce strigolactones, whereas in *M. truncatula* MtNSP2 is essential for conversion of orobanchol into didehydro-orobanchol; the main strigolactone produced by this species. The disturbed strigolactone biosynthesis in *nsp1-nsp2* mutant backgrounds correlates with reduced *DWARF27* expression; a gene essential for strigolactone biosynthesis. *In vitro* binding studies indicate that *M. truncatula DWARF27* is a primary target of MtNSP1. Rice and Medicago represent distinct phylogenetic lineages that split ~150 million years ago. Therefore we conclude that regulation of strigolactone biosynthesis by NSP1 and NSP2 is an ancestral function conserved in higher plants. As NSP1 and NSP2 are single copy genes in legumes, it implies that both proteins fulfill dual regulatory functions of different downstream targets; symbiotic and non-symbiotic, respectively.

Keywords: Strigolactones, *Medicago truncatula,* Transcription factor*,* NSP1*,* NSP2*,* DWARF27

Introduction

Strigolactones exuded by plant roots into the rhizosphere are well known *ex planta* stimuli for symbiotic arbuscular mycorrhizal fungi of the order Glomeromycota that are co-opted by root parasitic plants of the *Orobanchaceae* family (Cook et al., 1966; Akiyama et al., 2005; Bouwmeester et al., 2007). Recently, it was found that Strigolactones, or their derivatives, also function as endogenous plant hormones controlling outgrowth of axillary shoot buds as well as affect root architecture (Gomez-Roldan et al., 2008; Umehara et al., 2008; Koltai et al., 2010; Kapulnik et al., 2011; Ruyter-Spira et al., 2011). They do so in cross-talk with auxin, the most prominent plant hormone (Dun et al., 2009; Ferguson and Beveridge, 2009; Crawford et al., 2010; Stirnberg et al., 2010; Xie et al., 2010). Biosynthesis and subsequent secretion of Strigolactones is highly adaptive upon availability of nutrients; mainly phosphate (Yoneyama et al., 2007; López-Ráez et al., 2008; Umehara et al., 2008; Kohlen et al., 2011). To understand this adaptive regulation of these novel hormones it is important to unravel the molecular mechanisms of strigolactone biosynthesis, transport and signaling. Here we show that the GRAS-type transcription factors NODULATION SIGNALING PATHWAY1 (NSP1) and NSP2, which in legumes (*Fabaceae*) are essential for rhizobium root nodule formation, are indispensable for strigolactone biosynthesis under nonsymbiotic conditions.

Legumes can establish an endosymbiosis with nitrogen fixing rhizobium bacteria. To host rhizobium, a novel lateral root organ, the root nodule, is formed in response to specific lipo-chito oligosaccharides secreted by the bacterium. These signals, named nodulation (Nod) factors, trigger cell divisions in the root cortex resulting in the formation of a nodule primordium. Furthermore, Nod factors are essential for intracellular infection by rhizobium. The Nod factor signaling cascade has been genetically dissected (Kouchi et al., 2010). Nod factor signaling activates several transcription factors among which are the GRAS-type proteins NSP1 and NSP2 (Kaló et al., 2005; Smit et al., 2005; Heckmann et al., 2006; Murakami et al., 2007). Both transcription factors are essential for nearly all rhizobium induced symbiotic responses, including Nod factor induced early nodulin gene expression (Mitra et al., 2004). Biochemical studies indicate that NSP1 and NSP2 form a protein complex that binds to a specific DNA element present in the promoter of some early nodulin genes, e.g. Mt*ENOD11* (Hirsch *et al.*, 2009). This suggests that NSP1 and NSP2 function as Nod factor responsive transcription factors upon heterodimerization (Smit et al., 2005; Hirsch et al., 2009).

Legumes have recruited several components of the Nod factor signaling pathway from the network that is essential for the more ancient endomycorrhizal symbiosis. Genes that are essential for mycorrhizal as well as rhizobium Nod factor induced signaling form the so-called common symbiotic signaling pathway and comprise a plasma membrane receptor kinase (MtDMI2 in *Medicago truncatula* (Medicago) and LjSYMRK in *Lotus japonicus*), several components in the nuclear envelope including a cation ion channel (MtDMI1, LjCASTOR and LjPOLLUX), subunits of nuclear pores (LjNUP85 and LjNUP133), and a nuclear localized Calcium Calmodulin dependent Kinase (CCaMK; MtDMI3 and LjCCaMK) (Kouchi et al., 2010). Mycorrhizae and rhizobium induced signaling starts to bifurcate downstream of CCaMK, possibly due to a different nature of the calcium signal (Kosuta et al., 2008). NSP1 and NSP2, which are essential for rhizobium Nod factor induced signaling, are positioned downstream of CCaMK. Although both transcription factors are not essential for mycorrhizal symbiosis, it was recently found that NSP2 promotes mycorrhizal colonization (Maillet et al., 2011). This suggests that NSP2 does not function exclusively in rhizobium Nod factor signaling; a hypothesis which is supported by the presence of orthologous *NSP* genes in non-legume plant species (Kaló et al., 2005; Smit et al., 2005; Heckmann et al., 2006; Murakami et al., 2007). Here we

aim to characterize this novel function at a molecular level, as it will provide insight how these GRAS-type transcription factors have been recruited during nodule evolution.

GRAS-type transcription factors can be grouped in at least eight different classes that are largely conserved in higher plants (Tian et al., 2004; Lee et al., 2008). For example, potential orthologs of *NSP1* (class III) and *NSP2* (class VII) can be found in many higher plant species, including *Oryza sativa* (rice) (Os03g29480/OsNSP1 & Os03g15680/OsNSP2) and *Arabidopsis thaliana* (Arabidopsis) (At3g13840 & At4g08250) (Kaló et al., 2005; Smit et al., 2005; Heckmann et al., 2006; Murakami et al., 2007). As Arabidopsis is unable to establish mycorrhizal symbiosis, it suggests a more generic function for both transcription factors. Notably, NSP1 and NSP2 are functionally conserved in higher plants as demonstrated in trans-complementation studies of legume *nsp1* and *nsp2* knockout mutants with non-legume *NSP1* and *NSP2* homologs (Heckmann *et al.*, 2006; Yokota *et al.*, 2010). All together this supports the idea that *NSP1* and *NSP2* fulfill a conserved function in non-symbiotic plant growth and development.

We studied the genetic network controlled by NSP1 and NSP2 under non-symbiotic conditions and provide evidence that both transcription factors are indispensable for strigolactone biosynthesis in legumes as well as non-legumes. A Medicago Mt*nsp1* mutant or M*tnsp1*Mt*nsp2* double knockout mutant as well as a rice Os*nsp1*Os*nsp2* double knockdown line hardly produce Strigolactones. By analyzing the root transcriptome in Medicago we found that the effect on strigolactone production correlates with a strongly reduced Mt*DWARF27* (Mt*D27*) expression. Likewise, rice Os*nsp1*Os*nsp2* double RNAi knockdown lines have reduced Os*DWARF27* (Os*D27*) expression. This underlines a conserved function of NSP1 and NSP2 in regulating strigolactone biosynthesis.

Results

MtNSP1 and MtNSP2 control genes in the carotenoid biosynthetic pathway

To identify the non-symbiotic genes that are directly or indirectly activated by NSP1 and NSP2, we analyzed the transcriptome of Medicago Mt*nsp1* and Mt*nsp2* knockout mutants. Mt*NSP1* and Mt*NSP2* are expressed mainly in root and nodules (Benedito et al., 2008). Therefore we conducted microarray studies on 7-day-old roots and compared the Mt*nsp1-1* and Mt*nsp2-2* mutants to wild-type Medicago (Jemalong A17) grown on minimal medium without nitrogen (1.7 mM phosphate). Expression values were obtained of three independent biological replicates (GSE26548). As MtNSP1 and MtNSP2 can act as heterodimer (Hirsch *et al.*, 2009), we searched for genes with at least 2-fold decreased expression in both mutants. In total 42 probe sets, representing 39 genes, fulfill this criterion (Table S1). The expression of these genes was subsequently studied by qRT-PCR in an independent experiment that now also included the Medicago *Mtnsp1Mtnsp2* double mutant. Reduced expression in roots of both *nsp* mutants could be confirmed for 16 genes. These genes were also down-regulated in the double mutant (Table 1).

Table 1: Genes down-regulated in root tissue of 7-day-old Medicago Mtnsp1 and Mtnsp2 mutants and the Mtnsp1Mtnsp2 double mutant. Plants were grown in absence of a nitrogen source. Gene expression was analyzed using microarray analysis and qRT-PCR. Accession numbers: MtD27 (accession number), MtMAX1 (accession number) and MtCRTISO (accession number).

	FC microarray		FC qRT-PCR		
	Mt*nsp1*	Mt*nsp2*	Mt*nsp1*	Mt*nsp2*	Mt*nsp1*Mt*nsp2*
DWARF27	-3.2	-3.4	-6.1	-8.0	-7.4
Carotenoid isomerase	-2.1	-2.2	-2.2	-2.5	-3.5
MAX1	-2.5	-2.3	-1.9	-2.0	-1.6
Nine-cis-epoxycarotenoid dioxygenase 4	-2.0	-3.0	-2.6	-2.4	-3.2
1-cys peroxiredoxin	-3.6	-3.7	-2.3	-1.9	-9.2
Abnormal gametophytes (AGM)	-3.4	-2.8	-3.2	-2.5	-2.5
Alanine--tRNA ligase	-3.3	-3.4	-1.9	-1.7	-4.4
Allyl alcohol dehydrogenase	-2.1	-2.0	-18.2	-14.9	-23.8
C2H2 type Zinc finger protein 6	-7.8	-10.1	-5.0	-5.4	-29.4
Cytokinin-specific binding protein	-2.4	-2.5	-1.9	-1.7	-2.1
Dirigent-like protein	-6.1	-5.4	-4.4	-3.5	-5.3
Mannose-6-phosphate isomerase	-2.5	-2.3	-1,7	-1.8	-1.6
Nudix hydrolase	-3.5	-4.5	-1.5	-3.4	-15.6
Seed maturation protein LEA 4	-3.2	-3.0	-1.2	-1.2	-11.1
Legume specific protein	-7.7	-7.7	-1.9	-1.8	-10.5
Legume specific protein	-4.6	-7.8	-1.5	-3.0	-2.5

To obtain insight in the biological function of the down-regulated genes, extended sequences were retrieved from the Medicago genome data, and compared to homologous genes in other plant species. Two genes appeared to be legume specific, whereas the remaining 14 genes have clear homologs in non-legume species (Table 1). Four of these genes encode a protein that catalyses a conversion in the carotenoid biosynthetic pathway (a carotenoid isomerase homolog) or pathways leading from carotenoids to the plant hormones strigolactones and ABA (a MAX1 homolog, a 9-cis-epoxycarotenoid dioxygenase homologous to Arabidopsis AtNCED4 and an iron-containing protein highly homologous to rice OsDWARF27 (OsD27)) (Xie et al., 2010; Cardoso et al., 2011). Especially the expression of the *DWARF27* homologous gene was strongly affected (~90% reduced expression) in roots of both Mt*nsp1* and Mt*nsp2* mutants as well as the double mutant (Figure 1a). Subsequent searches in the Medicago genome and EST resources revealed that Medicago has only a single *DWARF27* homologous gene that was covered by two probes on the Medicago GeneChip. The encoded protein, MtDWARF27 (MtD27), displays 54% identity with the rice ortholog OsD27 (Figure 1b-c, Supplemental Table S1).

To confirm that down regulation of Mt*D27* was the result of the knockout of *NSP* genes and not a result of a background mutation present in both mutants, we complemented the Medicago Mt*nsp1-1* mutant with a Mt*NSP1:*Mt*NSP1* construct and subsequently determined the Mt*D27* expression in transgenic roots. This revealed that the expression of Mt*D27* did indeed depend on the presence of a functional MtNSP1 protein (Figure 1d).

Next we determined whether expression of Mt*D27* under non-symbiotic conditions depends on components of the common symbiotic signaling pathway that is essential for rhizobium Nod factor signaling as well as mycorrhizal signaling. Mt*D27* transcript levels were quantified in roots of Medicago Mt*dmi1*, Mt*dmi2* and Mt*dmi3* mutants. Mt*D27* expression showed not to be reduced in these mutants (Figure 1e). Therefore we conclude that the regulation of Mt*D27* expression under

nonsymbiotic conditions is independent of the common symbiotic signaling pathway, but does depend on MtNSP1 and MtNSP2.

Strigolactone biosynthesis in Medicago requires MtNSP1 and MtNSP2

In rice, Os*D27* is essential for strigolactone biosynthesis (Lin *et al.*, 2009). Since the expression of Mt*D27* is nearly undetectable in roots of Mt*nsp1,* Mt*nsp2* and Mt*nsp1*Mt*nsp2* mutants, we determined whether strigolactone biosynthesis is affected in these mutants. First we characterized the major strigolactone s produced by Medicago. Since it is reported that the amount of strigolactones in root exudate strongly increases upon phosphate starvation (Yoneyama et al., 2007; López-Ráez et al., 2008; Umehara et al., 2008; Lin et al., 2009), we grew 4 week old Medicago plants for 7 days under limited or phosphate-sufficient conditions. First, we determined the expression levels of Mt*NSP1*, Mt*NSP2* and Mt*D27* in root systems grown under these conditions. Expression levels of Mt*NSP1* and Mt*NSP2* were not affected. In contrast, Mt*D27* displayed a strong (>30-fold) up-regulation already upon 1-day of phosphate starvation (Figure 2a). Next, root exudates from low and high phosphate-grown plants were collected and purified using C18 column chromatography. In both root exudates two peaks were detected that corresponded to known strigolactones. The major peak had a retention time and transitions corresponding to didehydro-orobanchol (Supplemental Figure S5.1a). The nature of this strigolactone was confirmed by co-injection (data not shown) and comparing the MS/MS spectrum to the MS/MS spectrum obtained from one of the didehydro-orobanchol isomeres found in tomato (*Solanum lycopersicum*) (López-Ráez *et al.*, 2008) (Supplemental Figure S5.1b). The minor peak was identified as orobanchol based on the retention time and transitions (Supplemental Figure S5.1c), and this was confirmed by comparing the MS/MS spectrum to that of an orobanchol standard (Supplemental Figure S5.1d). Although didehydro-orobanchol and orobanchol could be detected in the exudate of non-phosphate-starved plants, amounts increased approximately 10-fold upon phosphate starvation (Figure 2b). This indicates that, like in many other species, strigolactones secretion - and likely biosynthesis – by Medicago roots is also induced by phosphate-limiting conditions. This increase in strigolactone secretion correlates with the transcriptional up-regulation of Mt*D27*.

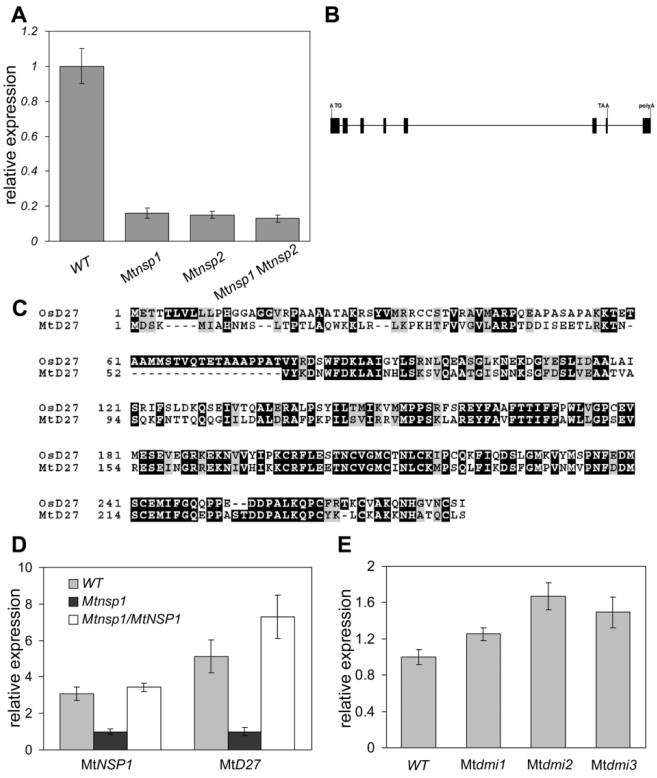

Figure 1: Medicago *MtD27* expression controlled by *MtNSP1* and MtNSP2. **(a)** Relative expression level of *MtD27* in nitrogen-starved roots of Medicago wild type, *Mtnsp1*, *Mtnsp2* and *Mtnsp1Mtnsp2* mutant plants as determined by qRT-PCR. **(b)** Gene structure of *MtD27*. *MtD27* consists of 7,908 bp including 8 exons spanning a coding region of 759 bp (Genbank accession: XXXXXXX). **(c)** Protein alignment of Medicago *MtD27* and rice *OsD27* (70% homology / 54% identity). **(d)** Expression of *MtD27* can be rescued in the roots of Mtnsp1 complemented with *pMtNSP1*:*MtNSP1*. **(e)** Expression of *MtD27* in nitrogen-starved roots of the Medicago common symbiotic signalling pathway mutants *Mtdmi1*, *Mtdmi2* and *Mtdmi3* determined by qRT-PCR.

Subsequently, the Medicago Mt*nsp1*, Mt*nsp2* and Mt*nsp1*Mt*nsp2* mutants were grown under phosphate starvation. Profiling of Mt*D27* expression under these growth conditions revealed that Mt*D27* expression was repressed in all three mutants. In case of Mt*nsp1* as well as Mt*nsp1*Mt*nsp2* mutant plants Mt*D27* expression was nearly absent, whereas in roots of the Mt*nsp2* mutant Mt*D27* expression was repressed to ~20% of wild-type levels (Figure 2a). The finding that Mt*D27* expression in phosphate-starved roots is dependent on MtNSP1 and MtNSP2 is in line with results obtained in nitrogen starved roots, though with this difference that under phosphate limitation transcriptional activation of Mt*D27* can occur partly independent of MtNSP2. Analyzes of root exudates by MRM-LC-MS/MS showed that no strigolactones are secreted by the Mt*nsp1* mutant as well as the Mt*nsp1*Mt*nsp2* double mutant (Figure 2c, d). In contrast, in root exudates of the Mt*nsp2* mutant orobanchol accumulated in 10-fold higher levels than observed in exudate of wild-type plants (Figure 2d). Interestingly, didehydro-orobanchol was absent in root exudate of this mutant suggesting that MtNSP2 controls a specific step in strigolactone biosynthesis. To rule out that Mt*nsp1* and Mt*nsp2* are merely affected in secretion of certain strigolactones, and not in biosynthesis, we investigated the strigolactone content also root extracts. This revealed similar results as observed in root exudates (Supplemental Figure S5.2). Taken together these findings demonstrate that genes controlled by MtNSP1-MtNSP2 are essential early in the strigolactone biosynthetic pathway and include Mt*D27*.

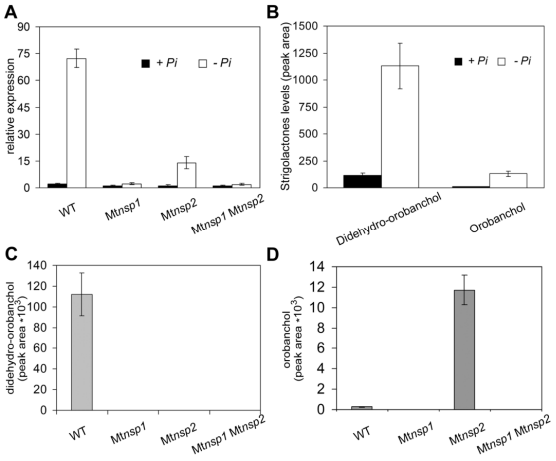

Figure 2: (a) Expression analyses of *MtD27* under low and sufficient phosphate growth conditions in roots of Medicago wild type (A17), *Mtnsp1*, *Mtnsp2*, and *Mtnsp1Mtnsp2* mutant plants. **(b)** The effect of phosphate-starvation on strigolactone levels in Medicago wild type plants (A17). Bar represents average ± s.e. **(c, d)** Analysis of strigolactones, didehydro-orobanchol **(c),** orobanchol **(d),** in root exudates of phosphate-starved Medicago plants; wild type (A17), *Mtnsp1*, *Mtnsp2*, and *Mtnsp1Mtnsp2* mutant (n=3).

MtNSP1 binds to cis regulatory element in MtD27 promoter

As Mt*D27* expression is strongly dependent on MtNSP1 we raised the question whether Mt*D27* could be a direct target of this GRAS-type transcription factor. In a previous study a MtNSP1 *cis* regulatory binding element has been characterized in the promoter region of the early nodulin gene Mt*ENOD11* (Hirsch *et al.*, 2009). The conserved sequence element AATTT that showed to be essential for MtNSP1 binding is abundantly present in ~1,000 bp putative promoter region of Mt*D27*; 7 times in forward and 2 times in reverse orientation, respectively (Supplemental Figure S5.3a). To investigate whether MtNSP1 can bind directly to the Mt*D27* promoter electrophoretic mobility shift assays (EMSA) were conducted. Binding affinity was studied of *in vitro* translated MtNSP1 protein to five Mt*D27* ~100 bp promoter regions containing at least one AATTT sequence element (putative binding element (PBE) 1 to 5) (Supplemental Figure S5.3b). As control two Mt*ENOD11* ~100 bp promoter regions (Supplemental

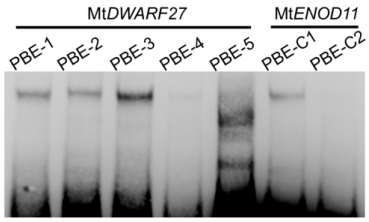

Figure 3: MtNSP1 in vitro binding ability to *MtD27* promoter elements. Five probes containing NRE-like elements (PBE-1 to PBE-5) originating from the *MtD27* promoter region were used in an EMSA assay. MtNSP1 binds to PBE-1, PBE-2 and PBE-3. Two promoter regions of MtENOD11 where used as control (PBE-C1 and PBE-C2). PBE-C1 contains a NRE element and acts as positive control.

Figure S5.3b) containing at least one AATTT sequence element were used (PBE-C1 and C2), of which one (PBE-C1) contains a nodulation responsive element (NRE) (Hirsch *et al.*, 2009). This revealed that MtNSP1 has a binding affinity for 3 of the tested elements of the Mt*D27* promoter (PBE-1, 2 & 3) as well as for the NRE element in the Mt*ENOD11* promoter (PBE-C1) that we used as positive control (Figure 3). This suggests that Mt*D27* is indeed a direct target of MtNSP1, similar as reported for Mt*ENOD11* (Hirsch *et al.*, 2009).

OsNSP1/OsNSP2 control Strigolactone biosynthesis in rice

As *NSP1* and *NSP2* orthologous genes are present in non-legume species we investigated whether the control of strigolactone biosynthesis is a conserved function of these proteins. The role of *DWARF27* in strigolactone biosynthesis is well characterized in rice (Lin *et al.*, 2009; Wang and Li, 2010), and rice, as a monocot, is phylogenetically really distinct from Medicago. Therefore, we decided to focus on this species. qRT-PCR analysis on root RNA showed that transcripts of both *NSP* genes are present, though the level of Os*NSP2* expression was close to the detection limit (Figure 4a). This is in line with a previous study that reported that the expression level of Os*NSP1* as well as Os*NSP2* is extremely low (Yokota *et al.*, 2010). To study whether OsNSP1 and OsNSP2 are essential for strigolactone biosynthesis in rice, double RNAi knockdown lines where created by *Agrobacterium tumefaciens* mediated transformation. In total 14 lines were obtained, and 2 of these showed severe knockdown (>90%) of Os*NSP1* in roots (Figure 4b). Since Os*NSP2* only is expressed at a very low level, the knock down level of this gene could not be determined reliably. The expression of Os*D27* in these knockdown lines is reduced >90% when compared to wild-type (Figure 4c), showing that also in rice the expression of *D27* is NSP1/NSP2 dependent.

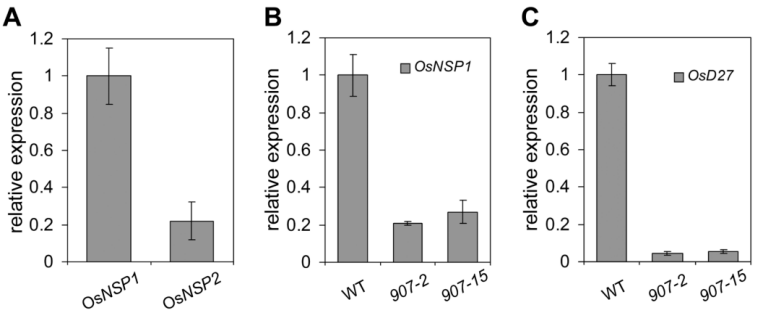

Figure 4: Expression analysis of *OsNSP1*, *OsNSP2* and *OsD27* in rice determined by qRT-PCR. **(a)** *OsNSP1* and *OsNSP2* expression in roots of wild type rice (ZH11). **(b)** Expression of *OsNSP1* in roots of the *Osnsp1Osnsp2* double knockdown lines 907-2 and 907-15. **(c)** Expression of *OsD27* in roots of the *Osnsp1Osnsp2* double knockdown lines 907-2 and 907-15.

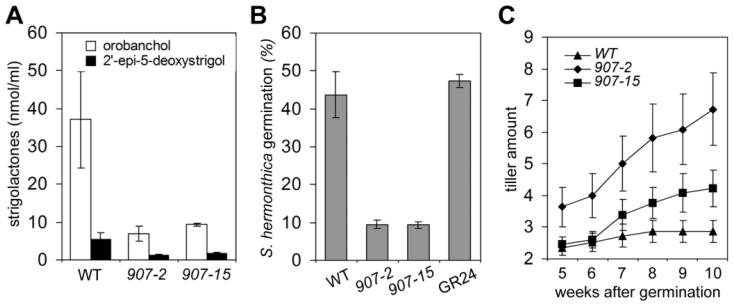

Figure 5: Tillering phenotype and strigolactone biosynthesis in root exudates of wild type rice (ZH11) and two independent *Osnsp1Osnsp2* double knockdown lines. **(a)** Analysis of 2'-epi-5-deoxystrigol and orobanchol content in root exudates of phosphate-starved wild type rice (ZH11) and *Osnsp1Osnsp2* double knockdown lines 907-2 and 907-15 (n=3). **(b)** Germination of Striga hermonthica seeds induced by root exudates of wild type (ZH11) and *Osnsp1Osnsp2* double knockdown lines 907-2 and 907-15 (n=3). Data are means ± s.e. **(c)** Quantification of tillering in rice. Tillers of wild type rice (ZH11) and *Osnsp1Osnsp2* double knockdown lines (907-2 and 907-15) were quantified 5 to 10 weeks post planting (n=15). Data are means ± s.e.

To determine whether down-regulation of Os*D27* expression correlates with reduced strigolactone biosynthesis, root exudates of Os*nsp1*Os*nsp2* RNAi lines were analyzed using MRM-LC-MS/MS analysis. In rice, 2'-epi-5-deoxystrigol and orobanchol are the major strigolactones (Umehara

et al., 2008), and both could be detected in root exudates of wild-type rice plants (Figure 5a). In the Os*nsp1*Os*nsp2* RNAi lines the amounts of 2'-epi-5-deoxystrigol and orobanchol in the root exudates were ~5- and ~8-fold lower, respectively, than in wild-type plants (Figure 5a). This reduction was also visualized in a *Striga hermonthica* seed germination bio-assay. Seeds of the parasitic plant *S. hermonthica* are known to respond in a semi-quantitative way to strigolactones (Cook *et al.*, 1966; Matusova *et al.*, 2005). The germination inducing activity of the Os*nsp1*Os*nsp2* RNAi plant root exudates was 4 to 5-fold reduced compared with exudates from wild-type plants (Figure 5b). Therefore we conclude that also in rice OsNSP1 and OsNSP2 are essential for strigolactone biosynthesis.

NSP1/NSP2 control lateral shoot growth in rice, but not in Medicago

In rice, an Os*d27* knockout mutation causes increased tillering in combination with reduced plant height (Lin *et al.*, 2009). In rice, Os*D27* is highly expressed in the bases of shoots, culms, panicles and axillary buds (Lin *et al.*, 2009). In contrast, in Medicago we noted that Mt*D27* is expressed mainly in root tissue (Supplemental Figure S5.4) (Benedito et al., 2008). Since absence of *NSP1-NSP2* expression in rice and Medicago resulted in a markedly reduced strigolactone biosynthesis in root tissue we tested whether these plant mutants also display a more branched shoot phenotype. In rice the amount of tillers was quantified at different time points from 5 to 10 weeks after germination. The Os*nsp1*Os*nsp2* RNAi lines had an increased number of tillers when compared to wild-type rice (Figure 5c). However, these knockdown lines did not display obvious differences in plant height, as reported for the Os*d27* knockout mutant (Lin *et al.*, 2009). So, whereas the increased tillering is in line with the phenotype of the rice Os*d27* knockout mutant, plant height seems less critical as residual levels Os*D27* expression and strigolactone biosynthesis seems to be sufficient to support normal shoot growth. Next we studied shoot branching in the Medicago Mt*nsp1*Mt*nsp2* double mutant and compared it to wild-type. Wild-type Medicago formed 3-4 branches at the first 4 knots and well-developed secondary branches, during 10 weeks of plant growth. We did not find an increased amount of branches in the Mt*nsp1*Mt*nsp2* double mutant. Therefore we conclude that severe reduction in strigolactone concentration in the Mt*nsp1*Mt*nsp2* does not affect shoot architecture. This is possibly due because Medicago does not display a strong apical dominance and this is consistent with a lack of Mt*D27* expression in shoot tissues.

Discussion

Here we show that the non-symbiotic function of the GRAS-type transcriptional regulators NSP1 and NSP2 is the control of strigolactone biosynthesis in Medicago as well as rice. Both species represent distinct phylogenetic lineages that have split ~150 million years ago (Moore et al., 2007; Smith et al., 2010). Therefore we conclude that the regulation of strigolactone biosynthesis by NSP1 and NSP2 is an ancestral function conserved in higher plants. During evolution these two transcriptional regulators have been recruited to play an essential role in legume root nodule symbiosis. As NSP1 and NSP2 are single copy genes in legumes, it implies that in these species single proteins fullfill both functions.

The absence of strigolactone biosynthesis in *nsp1-nsp2* mutant backgrounds correlate with a reduced expression of several genes that encode enzymes of the carotenoid and strigolactone biosynthetic pathways; including *D27*. The precise biochemical function of the plastid localized, iron-containing protein D27 remains to be elucidated, but it was shown to be essential for strigolactone

biosynthesis in rice (Lin *et al.*, 2009). Our study in Medicago revealed that the transcriptional regulation of the strigolactone biosynthetic enzyme Mt*D27* is tightly regulated by nutrient status of the plant. Especially phosphate starvation triggers a dramatic up-regulation of Mt*D27* transcription. As MtNSP1 and MtNSP2 expression is not, or only very mildly affected by the nutrient status of the plant (Barbulova et al., 2007), we conclude that the activity of both transcription factors is controlled at the protein level, similar as hypothesize for their symbiotic functioning in rhizobium Nod factor induced signaling in legumes (Geurts *et al.*, 2005).
We found that *in vitro* MtNSP1 binds to Mt*D27* promoter elements that show resemblance to the NRE *cis* regulatory elements in the promoter of the early nodulin gene Mt*ENOD11*. Although we did not investigate this binding in case of Os*D27* of rice, similar NRE-like *cis* regulatory elements are present also in the rice Os*D27* promoter (Supplemental Figure S5.3c). This suggests a conserved regulatory mechanism for this gene. Interestingly, *in vivo* binding of MtNSP1 to NRE elements in the Mt*ENOD11* promoter requires MtNSP2, suggesting that both proteins function in a heterodimeric complex (Hirsch *et al.*, 2009). In line with this, we hypothesize that also in case of Mt*D27* regulation MtNSP1 functions in a heterodimeric complex. As under phosphate starvation MtNSP2 is partly redundant resulting in a mild Mt*D27* up-regulation , it suggests that MtNSP1 can interact also with another protein that is possibly homologous to MtNSP2.

We showed that Medicago produces two types of strigolactones; orobanchol and didehydro-orobanchol, similar as its close relative red clover (*Trifolium pratense*) (Yokota et al., 1998; Matusova et al., 2005; Xie et al., 2010). The differential regulation of strigolactone biosynthesis by MtNSP1 and MtNSP2 in Medicago is intriguing; whereas in Mt*nsp1* mutant background no detectable amounts of strigolactones are present in root exudates, the Mt*nsp2* mutant specifically secretes high amounts of orobanchol (Figure 6). This shows that the limited expression of Mt*D27* in an Mt*nsp2* mutant background is sufficient to control orobanchol biosynthesis. As the precise biochemical pathway of different strigolactones has not yet been elucidated, the finding that the Medicago Mt*nsp2* mutant accumulates orobanchol, rather than didehydro-orobanchol as found in wild-type Medicago plants, may provide a tool to identify key enzymes in biosynthesis of different strigolactones. It is assumed that didehydro-orobanchol is derived from orobanchol in a three-step process; a homoallylic hydroxylation of orobanchol to hydroxyl-orobanchol, an oxidation or dehydration to oxo-orobanchol, and a migration of the methyl group leading to didehydro-orobanchol (Rani *et al.*, 2008; Xie *et al.*, 2010). The enzymes involved in these steps might be under transcriptional regulation of MtNSP2 (Figure 6). A preliminary analysis of genes that are differentially down regulated in Mt*nsp2* mutant roots, but not in wild-type and the Mt*nsp1* mutant revealed a subset of such genes (Supplemental Table S5.2), among which are several candidates encoding enzymes that could be involved in this process. Functional analysis of these genes could provide access to key enzymes in strigolactone biosynthesis.

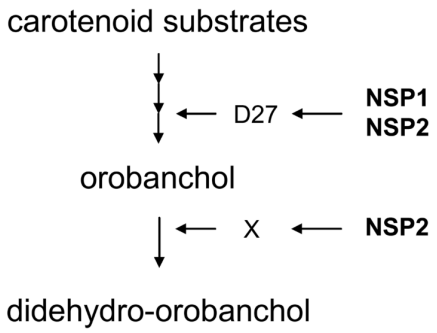

Figure 6: Schematic representation of the SL biosynthesis pathway in Medicago controlled by the GRAS-type transcription factors MtNSP1 and MtNSP2. Orobanchol is synthesized in a multi-step process from carotenoid substrates and requires MtD27, which is under transcriptional control of MtNSP1-MtNSP2. In this step MtNSP2 is partly redundant. The conversion of orobanchol in didehydro-orobanchol requires unknown enzyme X that is under direct or indirect control of MtNSP2.

In legumes, NSP1 and NSP2 are key components in the rhizobium Nod factor induced signaling pathway, and a knockout mutation in either of these genes impairs gene induction by Nod factors; including Mt*ENOD11* (Catoira et al., 2000; Oldroyd and Long, 2003; Mitra et al., 2004). This Nod factor induced transcription requires the common symbiotic signaling pathway, including the nuclear localized kinase CCaMK. So, there is a puzzling difference between the symbiotic and non-symbiotic activity of these GRAS-type transcription factors. Under symbiotic conditions MtNSP1 needs to be activated by the Nod factor induced signaling pathway, whereas none of the components of this pathway, even the kinase MtCCaMK directly active upstream of MtNSP1 and MtNSP2, are required for non-symbiotic activity leading to Mt*D27* expression. The finding that both NSPs can function independent of CCaMK is in line with the fact that some plant species that cannot establish a mycorrhizal symbiosis, e.g. Arabidopsis, have lost many of the components in the common symbiotic signaling pathway, including CCaMK, but maintained NSP1 and NSP2 orthologous genes (Kaló *et al.*, 2005; Smit *et al.*, 2005; Zhu *et al.*, 2006). The recruitment of a conserved transcription factor into the signaling pathway triggered by rhizobium Nod factors, as occurred in legumes, is therefore intriguing. It suggests that in case of Nod factor signaling the NSP controlled transcriptional regulation is activated in a different manner. It remains to be elucidated how at a molecular level this difference is created. We hypothesize that this is achieved by modification of the NSP1 and NSP2 protein complexes upon CCaMK activity. This might be a direct modification, or involves a different component that affects the binding affinity of the transcription factor complex. However, the occurrence of NSP1 binding sites in the promoter of *D27*, that are identical to the motifs found in the Mt*ENOD11* promoter, suggests that both mechanisms have parts in common.

Since NSP1 and NSP2 control biosynthesis of strigolactones, which are important *ex planta* stimuli for branching of mycorrhizal hyphae, it seems probable that these GRAS-type transcription factors also have a function in the interaction of plants with arbuscular mycorrhizae. A recent study in Medicago indeed revealed that specifically the Mt*nsp2* mutant displays a reduced level of mycorrhizal colonization, whereas the Mt*nsp1* can be mycorrhized effectively (Maillet et al., 2011). As we now have demonstrated that MtNSP1 is indispensable for strigolactone biosynthesis, whereas this mutant affectively can be mycorrhized (Catoira *et al.*, 2000; Maillet *et al.*, 2011), it strongly suggests that strigolactones are not essential for mycorrhizal infection and arbuscle formation in Medicago roots. Furthermore, it suggests that reduced mycorrhizal colonization as observed in a Mt*nsp2* mutant background (Maillet et al., 2011) is either the result of accumulation of orobanchol in this mutant, or caused by differentially regulated genes that are under specific control of MtNSP2, but are unrelated to strigolactone biosynthesis. During the past decade, genes encoding enzymes essential for strigolactone biosynthesis have been elucidated. Here we identified the first two transcription factors, NSP1 and NSP2, that are key regulators of strigolactone biosynthesis. Strigolactone biosynthesis is highly regulated among others by environmental conditions. Therefore NSP1 and NSP2 will be important tools in future studies on the molecular mechanisms by which environmental sensing is translated into regulation of strigolactone biosynthesis.

Materials and Methods

Plant materials, growth conditions and transformation

Medicago was grown in a growth chamber at 20°C and 16/8 h day/night regime. Jemalong A17, Mt*nsp1-1* (B85) (Catoira *et al.*, 2000; Smit *et al.*, 2005) and Mt*nsp2-2* (0-4) (Oldroyd and Long, 2003; Kaló et al., 2005) were used as wild-type, Mt*nsp1* and Mt*nsp2*, respectively. The Mt*nsp1*Mt*nsp2* double mutant was obtained by pollinating Mt*nsp1-1* plants with Mt*nsp2-2* pollen. Mt*nsp1*Mt*nsp2* homozygote plants were selected by PCR-based genotyping of F2 individuals.

Medicago plants used for gene expression analysis were grown vertically on Fårhaeus medium plates without nitrate (Fähraeus, 1957). RNA was isolated from the Nod factor susceptible zone of 7-day-old roots samples snap-frozen in liquid N2. Total RNA was extracted using the E.Z.N.A. Plant RNA Kit, combined with Qiagen RNase-Free DNase Set for on-column DNase treatment.

Agrobacterium rhizogenes based root transformation of Medicago was conducted according to Limpens *et al.* (Limpens *et al.*, 2004). Plants with transgenic roots were selected based on DsRED1 fluorescence.

Oryza sativa ssp. japonica cv. Zhonghua 11 (ZH11) was used as wild-type rice. Rice plants were grown in a greenhouse at 28°C in 16/8 h day/night regime. For tillering assays, rice plants were grown on half-strength full nutrient Hoagland's solution (Hoagland and Arnon, 1950) and watered once a week. Rice transformations were conducted using *Agrobacterium tumefaciens* strain *AGL1* according to Toki *et al.* (Toki et al., 2006) and subsequent Hygromycin B selection.

Constructs and plasmids

For complementation of the Medicago Mt*nsp1* mutant we used the MtNSP1p::MtNSP1 construct as generated by Smit e*t al.* (Smit et al., 2005).

Based on the principle that the RNA interference (RNAi) functions through ~20 nucleotides fragment, a chimaeric RNAi construct was made by fusing two fragments from Os*NSP1* (295 bp) and Os*NSP2* (488 bp) in a single hair-pin. First, fragments of Os*NSP1* and Os*NSP2* were PCR amplified from rice genomic DNA with primer pair OsNSP1-F/OsNSP-mr and OsNSP-mf/OsNSP2-R, respectively (Supplemental Table S5.3). Subsequently, both fragments were fused by overlap PCR with primer pair OsNSP1-F and OsNSP2-R (Supplemental Table S5.3). This chimaeric fragment then was subcloned into pENTR1,2 resulting pENTR1,2_OsNSP1-2i. Following, this construct was recombined into pHGWIWG2(II)-RR-R1R2 to get the binary construct pHGWIWG2(II)-RR-OsNSP1+2i.

Affymetrix GeneChip oligoarray hybridization, scanning, and quality control

Total RNA (5 μg) was labeled using the Affymetrix One-Cycle Target Labeling Assay kit (Affymetrix, Santa Clara, CA). Labeled RNA samples were hybridized on Affymetrix Medicago Genome arrays, washed, stained, and scanned on an Affymetrix GeneChip 3000 7G scanner. Detailed protocols for array handling can be found in the Genechip Expression Analysis Technical Manual, section 2, chapter 2 (Affymetrix; P/N 701028, revision 5) and are available on request. Packages from the Bioconductor project (Gentleman et al., 2004) were used to analyze the array data. Various advanced quality metrics, diagnostic plots, pseudoimages, and classification methods were used to determine the quality of the arrays prior statistical analysis (Heber and Sick, 2006). An extensive description of the applied criteria is available on request. Array data have been submitted to the Gene Expression Omnibus under accession number GSE26548.

Expression estimates were obtained by GC-robust multiarray (GCRMA) analysis, using the empirical Bayes approach to adjust for background (Wu et al., 2004). Differentially expressed probe sets were identified using linear models, applying moderated t-statistics that implemented empirical Bayes regularization of standard errors (Smyth, 2004). To adjust for both the degree of independence of variances relative to the degree of identity and the relationship between variance and signal intensity, the moderated t-statistic was extended by a Bayesian hierarchical model to define a intensity-based moderated T-statistic (IBMT) (Sartor et al., 2006). P-values were corrected for multiple testing using a false discovery rate (FDR) method (Storey and Tibshirani, 2003). Probe sets that satisfied the criterion of FDR < 5% (q-value < 0.05) were considered to be significantly regulated.

qRT-PCR analysis

Total RNA (1 µg) was reverse transcripted into cDNA by using iScript cDNA synthesis kit (Bio-Rad) following the supplier's manual. Real-time PCR was set up in 20 µl reaction system by using Eurogentec qPCR Core kit and iQ5 Real-time PCR detecting system according to the manuals supplied by the manufacturers. Gene specific primers were designed with Primer-3-Plus software (Untergasser et al., 2007) (Supplemental Table S5.3). For Medicago Mt*UBQ* and Mt*PTB* where used as internal control, whereas for rice Os*UBQ* was used (Lin *et al.*, 2009).

Characterization and Quantification of strigolactones

For strigolactone analysis 15 one-week-old, Medicago plants were transplanted (16 h light, 23°C, 60% relative humidity) into a X-stream 20 aeroponic system (Nutriculture, UK) operating with 5 L of modified half-strength Hoagland's solution (Hoagland and Arnon, 1950). Four weeks after transplanting, phosphate starvation was introduced by replacing the nutrient solution by half-strength Hoagland's solution without phosphate. Twenty-four hours prior to exudate collection the nutrient solution was refreshed in order to remove all accumulated strigolactones. For strigolactone analysis in rice, plants were grown as previously described by Jamil *et al.* (Jamil *et al.*, 2010).

Medicago exudates were purified and concentrated as previously described by López-Ráez et al., (López-Ráez *et al.*, 2010) with some modifications. Five liters of root exudate was loaded onto a pre-equilibrated C18 column (Grace Pure C18-Fast 5000 mg / 20 ml) per sample. Subsequently, columns were washed with 50 ml of demineralised water and 50 ml of 30% acetone/water. strigolactones were eluted with 50 ml of 60% acetone/water. Rice exudates were purified and concentrated as previously described by Jamil et al., (Jamil *et al.*, 2010). All exudates were collected within three hours and stored at -20°C before further use. strigolactones were extracted from medicago root material as previously described for tomato by López-Ráez *et al.* (López-Ráez *et al.*, 2010).

Analysis of strigolactones was performed by comparing retention times and mass transitions with those of available strigolactone standards (sorgolactone, strigol, 2'-epistrigol, orobanchol, 2'-epiorobanchol, 5-deoxystrigol, 2'-epi-5-deoxystrigol, solanacol, and orobanchyl acetate, sorgomol, 7-oxoorobanchol, 7-oxoorobanchyl acetate) using ultra performance liquid chromatography coupled to tandem mass spectrometry (UPLC-MS/MS), as previously described by Kohlen *et al.* (Kohlen *et al.*, 2011). Didehydro-orobanchol MS/MS fragmentation spectra of medicago and tomato root exudates were obtained as previously described López-Ráez *et al*. (López-Ráez *et al.*, 2008).

Root exudates obtained from different rice lines were assessed for germination stimulatory activity by germination bioassays with *Striga hermonthica* as previously described by Jamil *et al.* (Jamil *et al.*, 2010).

Electrophoretic Mobility Shift Assays

EMSA experiments were performed mainly as described previously (Kaufmann et al., 2005). The coding sequence of MtNSP1 was PCR-amplified from a pool of cDNA using following primers with NcoI (fwd) and ClaI (rev) restriction sites (Supplemental Table S5.3). The amplified fragment was cloned into the pSPUTK, an *in vitro* transcription/translation vector (Strategene). The protein was produced by *in vitro* transcription/translation with the TNT SP6 High-Yield Wheat Germ Protein Expression System following the manufacturer's instructions (Promega). Promoter fragments of Mt*D27* and Mt*ENOD11* were PCR-amplified from Medicago genomic DNA and cloned via TA-cloning into the pGEM-T vector (Supplemental Table S5.3). Biotin-labelled pGEM-T specific primers, directly flanking the cloning site, were used for generation of the DNA probes by PCR. The MtNSP1 Protein (2 µl of the *in vitro* reaction reaction) was incubated with 40 fmol of biotin-labelled DNA probes in binding solution (1 mM EDTA pH 8.0, 0.25 mg/ml BSA, 7 mM HEPES pH 7.3, 0.7 mM DTT, 60 µg/ml salmon sperm DNA, 1.3 mM spermidine, 2.5% CHAPS, 8% glycerol) for 1 h on ice. DNA-protein complexes were analysed on a 5% native PAGE (37.5:1 acrylamide:bisacrylamide). After electrophoresis, the gel was blotted to Amersham Hybond-N+ membrane and signal was detected by using the chemiluminescent nucleic acid detection module (Pierce) in a Genius:BOX gel documentation system (Westburg).

Acknowledgement

This research was funded by the Royal Netherlands Academy of Arts and Sciences KNAW and Chinese Academy of Sciences (KNAW-CAS sandwich program: 06PhD12 to WL, WCY, TB and RG), the Dutch Science Organization NWO (VIDI 864.06.007 to RG, Dutch Russian Research Cooperation 047.018.001 to SI, EL, RG and TB, VICI 865.06.002 to HJB and Equipment 834.08.001 to HJB), EC Marie Curie Research Training Network Programme MRTN-CT-2006-035546 NODPERCEPTION (to AL & RG), HEC (to MJ). HJB is co-financed by the Centre for BioSystems Genomics (CBSG) which is part of the Netherlands Genomics Initiative / Netherlands Organisation for Scientific Research.

References

Akiyama K, Matsuzaki K, Hayashi H (2005) Plant sesquiterpenes induce hyphal branching in arbuscular mycorrhizal fungi. Nature **435:** 824-827

Barbulova A, Rogato A, D'Apuzzo E, Omrane S, Chiurazzi M (2007) Differential effects of combined N sources on early steps of the Nod factor-dependent transduction pathway in Lotus japonicus. Molecular plant-microbe interactions **20:** 994-1003

Benedito VA, Torres-Jerez I, Murray JD, Andriankaja A, Allen S, Kakar K, Wandrey M, Verdier J, Zuber H, Ott T, Moreau S, Niebel A, Frickey T, Weiller G, He J, Dai XB, Zhao PX, Tang YH, Udvardi MK (2008) A gene expression atlas of the model legume Medicago truncatula. Plant Journal **55:** 504-513

Bouwmeester HJ, Roux C, López-Ráez JA, Bécard G (2007) Rhizosphere communication of plants, parasitic plants and AM fungi. Trends in Plant Science **12:** 224-230

Cardoso C, Ruyter-Spira C, Bouwmeester HJ (2011) Strigolactones and root infestation by plant-parasitic Striga, Orobanche and Phelipanche spp. Plant Science **180:** 414-420

Catoira R, Galera C, de Billy F, Penmetsa RV, Journet EP, Maillet F, Rosenberg C, Cook D, Gough C, Denarie J (2000) Four genes of *Medicago truncatula* controlling components of a nod factor transduction pathway. Plant Cell **12:** 1647-1665

Cook CE, Whichard LP, Turner B, Wall ME, Egley GH (1966) Germination of witchweed (*Striga lutea Lour.*): isolation and properties of a potent stimulant. Science **154:** 1189-1190

Crawford S, Shinohara N, Sieberer T, Williamson L, George G, Hepworth J, Müller D, Domagalska MA, Leyser O (2010) Strigolactones enhance competition between shoot branches by dampening auxin transport. Development **137:** 2905-2913

Dun EA, Brewer PB, Beveridge CA (2009) Strigolactones: discovery of the elusive shoot branching hormone. Trends in Plant Science **14:** 364-372

Fähraeus G (1957) The infection of clover root hairs by nodule bacteria studied by a simple glass technique. Journal of General

Microbiology **16:** 374-381

Ferguson BJ, Beveridge CA (2009) Roles for auxin, cytokinin, and strigolactone in regulating shoot branching. Plant Physiology **149:** 1929-1944

Gentleman RC, Carey VJ, Bates DM, Bolstad B, Dettling M, Dudoit S, Ellis B, Gautier L, Ge YC, Gentry J, Hornik K, Hothorn T, Huber W, Iacus S, Irizarry R, Leisch F, Li C, Maechler M, Rossini AJ, Sawitzki G, Smith C, Smyth G, Tierney L, Yang JYH, Zhang JH (2004) Bioconductor: open software development for computational biology and bioinformatics. Genome Biology **5:** r80

Geurts R, Fedorova E, Bisseling T (2005) Nod factor signaling genes and their function in the early stages of *Rhizobium* infection. Current Opinion in Plant Biology **8:** 346-352

Gomez-Roldan V, Fermas S, Brewer PB, Puech-Pages V, Dun EA, Pillot J-P, Letisse F, Matusova R, Danoun S, Portais J-C, Bouwmeester H, Becard G, Beveridge CA, Rameau C, Rochange SF (2008) Strigolactone inhibition of shoot branching. Nature **455:** 189-194

Heber S, Sick B (2006) Quality assessment of affymetrix GeneChip data. Omics-a Journal of Integrative Biology **10:** 358-368

Heckmann AB, Lombardo F, Miwa H, Perry JA, Bunnewell S, Parniske M, Wang TL, Downie JA (2006) Lotus japonicus nodulation requires two GRAS domain regulators, one of which is functionally conserved in a non-legume. Plant Physiology **142:** 1739-1750

Hirsch S, Kim J, Munoz A, Heckmann AB, Downie JA, Oldroyd GED (2009) GRAS proteins form a DNA binding complex to induce gene expression during nodulation signaling in *Medicago truncatula*. Plant Cell **21:** 545-557

Hoagland DR, Arnon DI (1950) The water-culture method for growing plants without soil. Circular. California Agricultural Experiment Station **347:** 1-32

Jamil M, Charnikhova T, Verstappen F, Bouwmeester H (2010) Carotenoid inhibitors reduce strigolactone production and *Striga hermonthica* infection in rice. Archives of Biochemistry and Biophysics **504:** 123-131

Kaló P, Gleason C, Edwards A, Marsh J, Mitra RM, Hirsch S, Jakab J, Sims S, Long SR, Rogers J, Kiss GB, Downie JA, Oldroyd GED (2005) Nodulation signaling in legumes requires NSP2, a member of the GRAS family of transcriptional regulators. Science **308:** 1786-1789

Kapulnik Y, Delaux P-M, Resnick N, Mayzlish-Gati E, Wininger S, Bhattacharya C, Séjalon-Delmas N, Combier J-P, Bécard G, Belausov E, Beeckman T, Dor E, Hershenhorn J, Koltai H (2011) Strigolactones affect lateral root formation and root-hair elongation in Arabidopsis. Planta **233:** 209-216

Kaufmann K, Anfang N, Saedler H, Theissen G (2005) Mutant analysis, protein–protein interactions and subcellular localization of the Arabidopsis B sister (ABS) protein. Molecular Genetics and Genomics **274:** 103-118

Kohlen W, Charnikhova T, Liu Q, Bours R, Domagalska MA, Beguerie S, Verstappen F, Leyser O, Bouwmeester H, Ruyter-Spira C (2011) Strigolactones are transported through the xylem and play a key role in shoot architectural response to phosphate deficiency in nonarbuscular mycorrhizal host Arabidopsis. Plant Physiology **155:** 974-987

Koltai H, Dor E, Hershenhorn J, Joel D, Weininger S, Lekalla S, Shealtiel H, Bhattacharya C, Eliahu E, Resnick N, Barg R, Kapulnik Y (2010) Strigolactones' effect on root growth and root-hair elongation may be mediated by auxin-efflux carriers. Journal of Plant Growth Regulation **29:** 129-136

Kosuta S, Hazledine S, Sun J, Miwa H, Morris RJ, Downie JA, Oldroyd GED (2008) Differential and chaotic calcium signatures in the symbiosis signaling pathway of legumes. Proceedings of the National Academy of Sciences of the United States of America **105:** 9823-9828

Kouchi H, Imaizumi-Anraku H, Hayashi M, Hakoyama T, Nakagawa T, Umehara Y, Suganuma N, Kawaguchi M (2010) How many peas in a pod? Legume genes responsible for mutualistic symbioses underground. Plant and Cell Physiology **51:** 1381-1397

Lee MH, Kim B, Song SK, Heo JO, Yu NI, Lee SA, Kim M, Kim DG, Sohn SO, Lim CE (2008) Large-scale analysis of the GRAS gene family in *Arabidopsis thaliana*. Plant Molecular Biology **67:** 659-670

Limpens E, Ramos J, Franken C, Raz V, Compaan B, Franssen H, Bisseling T, Geurts R (2004) RNA interference in *Agrobacterium rhizogenes* transformed roots of Arabidopsis and *Medicago truncatula*. Journal of Experimental Botany **55:** 983-992

Lin H, Wang R, Qian Q, Yan M, Meng X, Fu Z, Yan C, Jiang B, Su Z, Li J, Wang Y (2009) DWARF27, an iron-containing protein required for the biosynthesis of strigolactones, regulates rice tiller bud outgrowth. Plant Cell **21:** 1512-1525

López-Ráez JA, Charnikhova T, Gómez-Roldán V, Matusova R, Kohlen W, Vos RD, Verstappen F, Puech-Pages V, Bécard G, Mulder P, Bouwmeester H (2008) Tomato strigolactones are derived from carotenoids and their biosynthesis is promoted by phosphate starvation. New Phytologist **178:** 863-874

López-Ráez JA, Kohlen W, Charnikhova T, Mulder P, Undas AK, Sergeant MJ, Verstappen F, Bugg TDH, Thompson AJ, Ruyter-Spira C, Bouwmeester H (2010) Does abscisic acid affect strigolactone biosynthesis? New Phytologist **187:** 343-354

Maillet F, Poinsot V, André O, Puech-Pagès V, Haouy A, Gueunier M, Cromer L, Giraudet D, Formey D, Niebel A (2011) Fungal lipochitooligosaccharide symbiotic signals in arbuscular mycorrhiza. Nature **469:** 58-63

Matusova R, Rani K, Verstappen FWA, Franssen MCR, Beale MH, Bouwmeester HJ (2005) The strigolactone germination stimulants of the plant-parasitic *Striga* and *Orobanche spp*. are derived from the carotenoid pathway. Plant Physiology **139:** 920-934

Mitra RM, Shaw SL, Long SR (2004) Six nonnodulating plant mutants defective for Nod factor-induced transcriptional changes associated with the legume-rhizobia symbiosis. Proceedings of the National Academy of Sciences of the United States of America **101:** 10217-10222

Moore MJ, Bell CD, Soltis PS, Soltis DE (2007) Using plastid genome-scale data to resolve enigmatic relationships among basal angiosperms. Proceedings of the National Academy of Sciences **104:** 19363-19368

Murakami Y, Miwa H, Imaizumi-Anraku H, Kouchi H, Downie JA, Kawaguchi M, Kawasaki S (2007) Positional cloning identifies Lotus japonicus NSP2, a putative transcription factor of the GRAS family, required for *NIN* and *ENOD40* gene expression in nodule initiation. DNA research **13:** 255-265

Oldroyd GED, Long SR (2003) Identification and characterization of *nodulation-signaling pathway 2*, a gene of *Medicago truncatula* involved in Nod factor signaling. Plant Physiology **131:** 1027-1032

Rani K, Zwanenburg B, Sugimoto Y, Yoneyama K, Bouwmeester HJ (2008) Biosynthetic considerations could assist the structure elucidation of host plant produced rhizosphere signalling compounds (strigolactones) for arbuscular mycorrhizal fungi and parasitic plants. Plant Physiology and Biochemistry **46:** 617-626

Ruyter-Spira C, Kohlen W, Charnikhova T, van Zeijl A, van Bezouwen L, de Ruijter N, Cardoso C, López-Ráez JA, Matusova R, Bours R, Verstappen F, Bouwmeester H (2011) Physiological effects of the synthetic strigolactone analog GR24 on root system architecture in Arabidopsis: Another belowground role for strigolactones? Plant Physiology **155:** 721-734

Sartor MA, Tomlinson CR, Wesselkamper SC, Sivaganesan S, Leikauf GD, Medvedovic M (2006) Intensity-based hierarchical Bayes method improves testing for differentially expressed genes in microarray experiments. BMC bioinformatics **7:** 538

Smit P, Raedts J, Portyanko V, Debellé F, Gough C, Bisseling T, Geurts R (2005) NSP1 of the GRAS protein family is essential for rhizobial Nod factor-induced transcription. Science **308:** 1789-1791

Smith SA, Beaulieu JM, Donoghue MJ (2010) An uncorrelated relaxed-clock analysis suggests an earlier origin for flowering plants. Proceedings of the National Academy of Sciences **107:** 5897-5902

Smyth GK (2004) Linear models and empirical Bayes methods for assessing differential expression in microarray experiments. Statistical applications in genetics and molecular biology **3:** 3

Stirnberg P, Ward S, Leyser O (2010) Auxin and strigolactones in shoot branching: Intimately connected? Biochemical Society Transactions**:** 717-722

Storey JD, Tibshirani R (2003) Statistical significance for genomewide studies. Proceedings of the National Academy of Sciences of the United States of America **100:** 9440-9945

Tian C, Wan P, Sun S, Li J, Chen M (2004) Genome-wide analysis of the GRAS gene family in rice and Arabidopsis. Plant Molecular Biology **54:** 519-532

Toki S, Hara N, Ono K, Onodera H, Tagiri A, Oka S, Tanaka H (2006) Early infection of scutellum tissue with Agrobacterium allows high speed transformation of rice. The Plant Journal **47:** 969-976

Umehara M, Hanada A, Yoshida S, Akiyama K, Arite T, Takeda-Kamiya N, Magome H, Kamiya Y, Shirasu K, Yoneyama K, Kyozuka J, Yamaguchi S (2008) Inhibition of shoot branching by new terpenoid plant hormones. Nature **455:** 195-200

Untergasser A, Nijveen H, Rao X, Bisseling T, Geurts R, Leunissen JAM (2007) Primer3Plus, an enhanced web interface to Primer3. Nucleic Acids Research **35:** W71-W74

Wang Y, Li J (2010) Branching in rice. Current Opinion in Plant Biology**:** 94-99

Wu ZJ, Irizarry RA, Gentleman R, Martinez-Murillo F, Spencer F (2004) A model-based background adjustment for oligonucleotide expression arrays. Journal of the American Statistical Association **99:** 909-917

Xie X, Yoneyama K, Yoneyama K (2010) The strigolactone story. Annual Review of Phytopathology **48:** 93-117

Yokota K, Soyano T, Kouchi H, Hayashi M (2010) Function of GRAS proteins in root nodule symbiosis is retained in homologs of a non-legume, rice. Plant and Cell Physiology **51:** 1436-1442

Yokota T, Sakai H, Okuno K, Yoneyama K, Takeuchi Y (1998) Alectrol and orobanchol, germination stimulants for *Orobanche* minor, from its host red clover. Phytochemistry **49:** 1967-1973

Yoneyama K, Yoneyama K, Takeuchi Y, Sekimoto H (2007) Phosphorus deficiency in red clover promotes exudation of orobanchol, the signal for mycorrhizal symbionts and germination stimulant for root parasites. Planta **225:** 1031-1038

Zhu H, Riely BK, Burns NJ, Ane J-M (2006) Tracing nonlegume orthologs of legume genes required for nodulation and arbuscular mycorrhizal symbioses. Genetics **172:** 2491-2499

Chapter 6

Strigolactones are transported through the xylem and play a key role in shoot architectural response to phosphate deficiency in non-arbuscular mycorrhizal host Arabidopsis

Wouter Kohlen*, Tatsiana Charnikhova*, Qing Liu, Ralph Bours, Malgorzata A. Domagalska, Sebastien Beguerie, Francel Verstappen, Ottoline Leyser, Harro Bouwmeester and Carolien Ruyter-Spira.

* contributed equally to this work

Adapted version published as Kohlen et al., (2011) Plant Physiology, 155, 974–987

Abstract

The biosynthesis of the recently identified novel class of plant hormones, strigolactones, is up-regulated upon phosphate deficiency in many plant species. It is generally accepted that the evolutionary origin of strigolactone up-regulation is their function as a rhizosphere signal that stimulates hyphal branching of arbuscular mycorrhizal fungi. In this work, we demonstrate that this induction is conserved in Arabidopsis (*Arabidopsis thaliana*), although Arabidopsis is not a host for arbuscular mycorrhizal fungi. We demonstrate that the increase in strigolactone production contributes to the changes in shoot architecture observed in response to phosphate deficiency. Using high-performance liquid chromatography, column chromatography, and multiple reaction monitoring-liquid chromatography-tandem mass spectrometry analysis, we identified two strigolactones (orobanchol and orobanchyl acetate) in Arabidopsis and have evidence of the presence of a third (5-deoxystrigol). We show that at least one of them (orobanchol) is strongly reduced in the putative strigolactone biosynthetic mutants *more axillary growth1* (*max1*) and *max4* but not in the signal transduction mutant *max2*. Orobanchol was also detected in xylem sap and up-regulated under phosphate deficiency, which is consistent with the idea that root-derived strigolactones are transported to the shoot, where they regulate branching. Moreover, two additional putative strigolactone-like compounds were detected in xylem sap, one of which was not detected in root exudates. Together, these results show that xylem transported strigolactones contribute to the regulation of shoot architectural response to phosphate-limiting conditions.

Keywords: Strigolactones, xylem transport, Arabidopsis*, max* mutants, phosphate, shoot branching

Introduction

For many years, strigolactones have been known as rhizosphere signaling molecules. They were first described as germination stimulants for the seeds of parasitic plant species of the genera Striga, Orobanche, and Phelipanche (Cook et al., 1966; Bouwmeester et al., 2003). A relationship between phosphorus starvation and root parasitism became apparent when it was shown that red clover (Trifolium pratense) exudates, collected from phosphate-starved plants, induced higher germination of Orobanche minor seeds (Yoneyama et al., 2001) and that the increase in germination was due to increased secretion of orobanchol (Yoneyama et al., 2007). Recently, it was proven that phosphate starvation increased not only the secretion but also the production of orobanchol, solanacol, and the didehydro-orobanchol isomers 1 and 2 in the roots of tomato (Solanum lycopersicum; (López-Ráez et al., 2008) and orobanchol and 5-deoxystrigol in rice (Oryza sativa; (Umehara et al., 2008; Jamil et al., 2011).

Low-phosphate conditions have also been shown to improve the colonization rate by arbuscular mycorrhizal (AM) fungi in carrot (*Daucus carota*) and tomato (Nagahashi and Douds, 2000) through the stimulation of hyphal branching of the symbiotic AM fungi (Akiyama et al., 2005). This led to the hypothesis that the production and secretion of strigolactones in soils with a limited availability of free phosphate functions to improve the establishment of AM symbiosis (Bouwmeester et al., 2007). Hence, this shows that the strigolactones have a dual role in the rhizosphere, as host detection signals for both AM fungi and root parasitic plants (Akiyama et al., 2005; Harrison, 2005; Paszkowski, 2006; Bouwmeester et al., 2007; Yoneyama et al., 2008). Several strigolactones have been identified in the root exudates and extracts of a wide range of monocotyledonous and dicotyledonous plant species, including the non-AM fungi host Arabidopsis (*Arabidopsis thaliana*; (Goldwasser et al., 2008). It has been postulated that all strigolactones are derived from a single carotenoid substrate through oxidative cleavage performed by a carotenoid cleavage dioxygenase (CCD), the product of which is subsequently oxidized by cytochrome P450s (Matusova et al., 2005). Indeed, the involvement of CCD enzymes in strigolactone biosynthesis was recently confirmed. The *ramosus5* (*rms5*) and *rms1* mutants in pea (*Pisum sativum*) and high tillering *dwarf1* (*htd1*) or *dwarf17* (*d17*) and *d10* mutants in rice, which are compromised in CCD7 and CCD8 activity, respectively, produce no strigolactones, whereas their corresponding wild types do (Gomez-Roldan et al., 2008; Umehara et al., 2008). Earlier, CCD7 and CCD8 were also reported to be responsible for the biosynthesis of the elusive shoot-branchinginhibiting signal (Sorefan et al., 2003; Booker et al., 2004). Application of the synthetic strigolactone analog GR24 indeed rescued the bushy phenotype of these mutants and their Arabidopsis orthologous *more axillary growth* (*max*) mutants *max3* and *max4* but not in the putative signaling mutants *max2* (Stirnberg et al., 2002; Stirnberg et al., 2007), *rms4* in pea, and *d3* in rice, providing evidence that strigolactones, or strigolactone derivatives, are responsible for branching inhibition (Gomez-Roldan et al., 2008; Umehara et al., 2008). A third putative strigolactone biosynthetic mutant in Arabidopsis, *max1* (with a mutation in the cytochrome P450-encoding AtCyp711A; (Stirnberg et al., 2002; Booker et al., 2005), shows the same branching phenotype as the other max mutants, and also in this mutant, GR24 application reduced branching to wild-type levels (Gomez-Roldan et al., 2008; Crawford et al., 2010). MAX1 is believed to act downstream of CCD7 and CCD8 in the biosynthesis of the branch inhibiting signal (Booker et al., 2005). However, proof of the involvement of MAX1 in strigolactone biosynthesis through analytical means is lacking, as an orthologous mutant is described neither in pea nor rice.

Interestingly, phosphate starvation in plants leads to a reduced number of shoot branches (Troughton, 1977; Cline, 1997) and changes in the root system (López-Bucio et al., 2002; Al-Ghazi et al., 2003; Ma et al., 2003; Nacry et al., 2005; Sánchez-Calderón et al., 2005). In Arabidopsis, it has been demonstrated that upon phosphate starvation, auxin activity in the root system is altered, leading to a drastic modification of the root morphology (Williamson et al., 2001; López-Bucio et al., 2002; Nacry et al., 2005; Sánchez-Calderón et al., 2005{Ma, 2003 #24). The growth of the primary root is reduced and the outgrowth of the lateral roots near the soil surface is stimulated such that phosphate-rich areas that are usually found in the top layers of the soil can be explored (Al-Ghazi et al., 2003). In addition to these changes in root system architecture, resources are redirected from the shoot to the root (López-Bucio et al., 2002), contributing to the change in the root-to-shoot ratio, enabling the plant to better cope with its environment (Bonser et al., 1996).

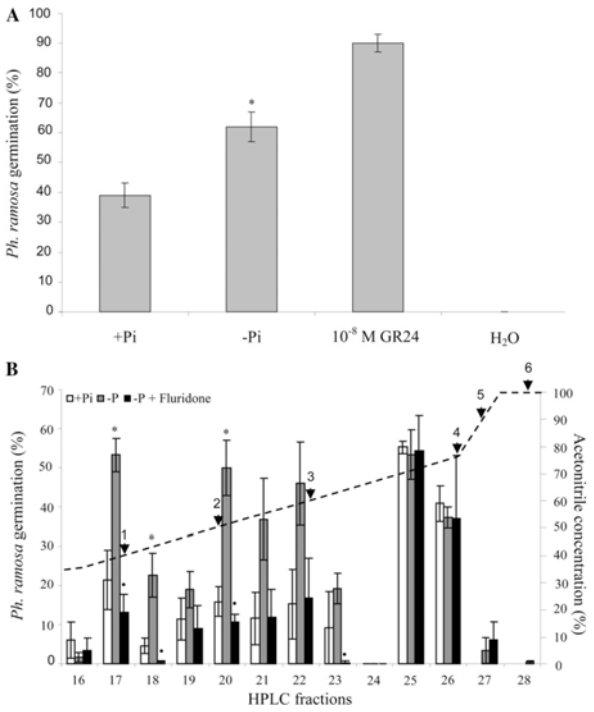

Figure 1: Germination of P. ramosa seeds induced by root exudates of Arabidopsis (Col-0). **(a),** Effect of phosphate starvation on the germination stimulatory capacity of 20-fold-concentrated Arabidopsis root exudates. Bars represent the average of three independent biological replicates ± SE. * Significant difference between limiting phosphate (–Pi) and sufficient phosphate (+Pi) treatment ($P < 0.05$). **(b),** Effect of treatments, sufficient phosphate (+Pi), limiting phosphate (–Pi), and limiting phosphate plus fluridone (–Pi + fluridone), on the germination stimulatory capacity of HPLC fractions of Arabidopsis root exudates. Bars represent the average of five independent biological replicates ± SE. * Significant difference between –Pi and +Pi treatment; • significant difference between –Pi + fluridone treatment and –Pi treatment ($P < 0.05$). The dashed line indicates the HPLC gradient of acetonitrile concentration, and arrowheads point to fractions in which strigolactone standards elute: 1, solanacol and 7-hydroxyorobanchyl acetate; 2, 2'-epiorobanchol, orobanchol, strigol, and sorgomol; 3, GR24; 4, orobanchyl acetate; 5, sorgolactone; 6, 5-deoxystrigol.

Grafting studies performed in several species showed that a wild-type rootstock grafted to either a *ccd7* or *ccd8* mutant scion was able to restore wild-type branching patterns, indicating that a transmissible signal (as we now know likely strigolactone or strigolactone derived) is produced in the roots (Beveridge et al., 1994; Napoli, 1996; Turnbull et al., 2002). However, wild-type shoots on mutant roots also have near wild-type branching patterns (Beveridge et al., 1994; Napoli, 1996; Beveridge et al., 1997; Beveridge et al., 1997; Sorefan et al., 2003). In addition, wild-type epicotyl interstock grafts into *rms1* and hypocotyl grafts into Arabidopsis *max3* are also able to reduce branching (Foo et al., 2001), indicating that biosynthesis is not limited to the root system. At present, therefore, the exact origin of strigolactones in the shoot is unknown. Nevertheless, it is likely that they must be transported to the shoot, where they exert their shoot-branching-inhibiting effect (Bennett, 2006). It has been shown that other phytohormones that are also produced in the roots, such as abscisic acid and cytokinins, are transported through the xylem (Hartung et al., 2002; Sakakibara, 2006), making the xylem a good candidate for strigolactone transport.

In this study, strigolactones in Arabidopsis were analyzed using multiple reaction monitoring-liquid chromatography-tandem mass spectrometry (MRMLC-MS/MS) and germination bioassays with seeds of *Phelipanche* (*Orobanche*) *ramosa* (Joel, 2009). The regulation of strigolactone levels by phosphate starvation was investigated, and the involvement of MAX1 and MAX4 in strigolactone biosynthesis was examined. Furthermore, the role of strigolactones or strigolactone-like compounds in phosphate starvation-induced shoot architectural changes was investigated using strigolactone biosynthesis and signal transduction mutants *max1*, *max2*, and *max4*. Finally, the involvement of the xylem in the transport of strigolactones and or strigolactone-like compounds from the root to the shoot was explored.

Results

Germination stimulatory activity of Arabidopsis root exudates

To assess if the induction by Arabidopsis root exudates of germination of *P. ramosa* seed is increased by phosphate deficiency, four-week-old Arabidopsis plants were subjected to phosphate starvation for two weeks, in parallel with fully fertilized plants. Ten-fold concentrated Arabidopsis root exudates were applied to *P. ramosa* seeds, and germination was scored after six days. The exudates of fully fertilized plants induced 38% germination, whereas exudates of phosphate starved plants induced 63% germination of *P. ramosa* seeds. The synthetic strigolactone GR24 (10^{-8} µM) was used as a positive control and induced 90% germination, whereas water (negative control) induced no germination (Figure 1a). When these exudates were tested for strigolactone content using MRM-LC-MS/MS, no strigolactones were detectable.

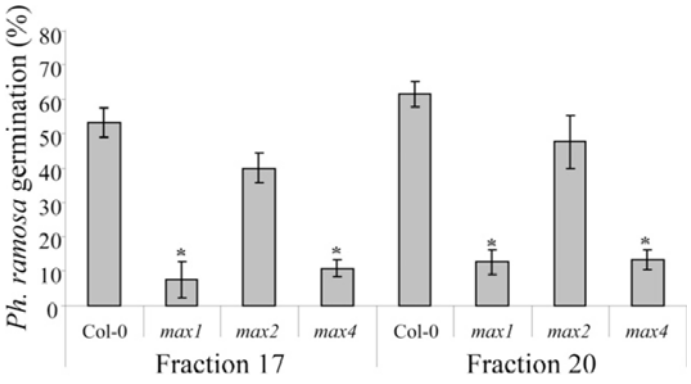

Figure 2: Germination of P. ramosa seeds induced by HPLC fractions 17 and 20 of Arabidopsis (Col-0, max1-1, max2-1, and max4-1) root exudates. Bars represent the average of three independent biological replicates ± SE. * Significant difference from Col-0 ($P < 0.05$).

HPLC Fractionation for Germination Stimulant Profiling To investigate whether strigolactones are responsible for the increase in germination stimulatory activity under phosphate starvation, HPLC purification was used to fractionate Arabidopsis root exudates. To identify the strigolactone-containing fractions, a mix of strigolactone standards was also fractioned using the same protocol and analyzed using MRM-LC-MS/MS. The first strigolactone from the standard mix to elute from the column was detected in fractions 11 and 12, which both contained 7-hydroxyorobanchol. 7-Oxoorobanchol eluted in fraction 15, solanacol and 7-hydroxyorobanchyl acetate in fraction 17, and 7-oxoorobanchyl acetate in fraction 19. Orobanchol, strigol, and sorgomol co-eluted in fraction 20, and orobanchyl acetate, sorgolactone, and 5-deoxystrigol eluted in fractions 26, 27, and 28, respectively (Figure 1b; Supplemental Table S6.1). Exudates of Arabidopsis plants grown on sufficient phosphate, without phosphate (for 2 weeks), and without phosphate + 0.01 µM fluridone, an inhibitor of carotenoid biosynthesis that also blocks strigolactone biosynthesis, were fractioned and assayed for their germination stimulatory activity on *P. ramosa* seeds (Figure 1b). No germination was induced by HPLC fractions eluting before fraction 15 in any of the treatments (data not shown). Fraction 16 induced a small percentage of germination in all treatments. Fractions 17, 20, 21, and 22 from plants grown on sufficient phosphate induced some germination (22%, 16%, 12%, and 14%,

respectively), while phosphate starvation strongly increased germination stimulatory activity of these fractions (2.5-, 3.1-, 3.2-, and 3.3-fold, respectively). When plants were grown in the presence of fluridone, the germination induced by these fractions was reduced by 71%, 78%, 70%, and 65%, respectively. High germination was also observed in fractions 25 (54%) and 26 (40%) of plants grown under sufficient phosphate levels, but no effect of phosphate starvation or fluridone was observed in these fractions. Fractions 27 and higher induced only little germination, and this was not affected by phosphate starvation or fluridone (Figure 1b).

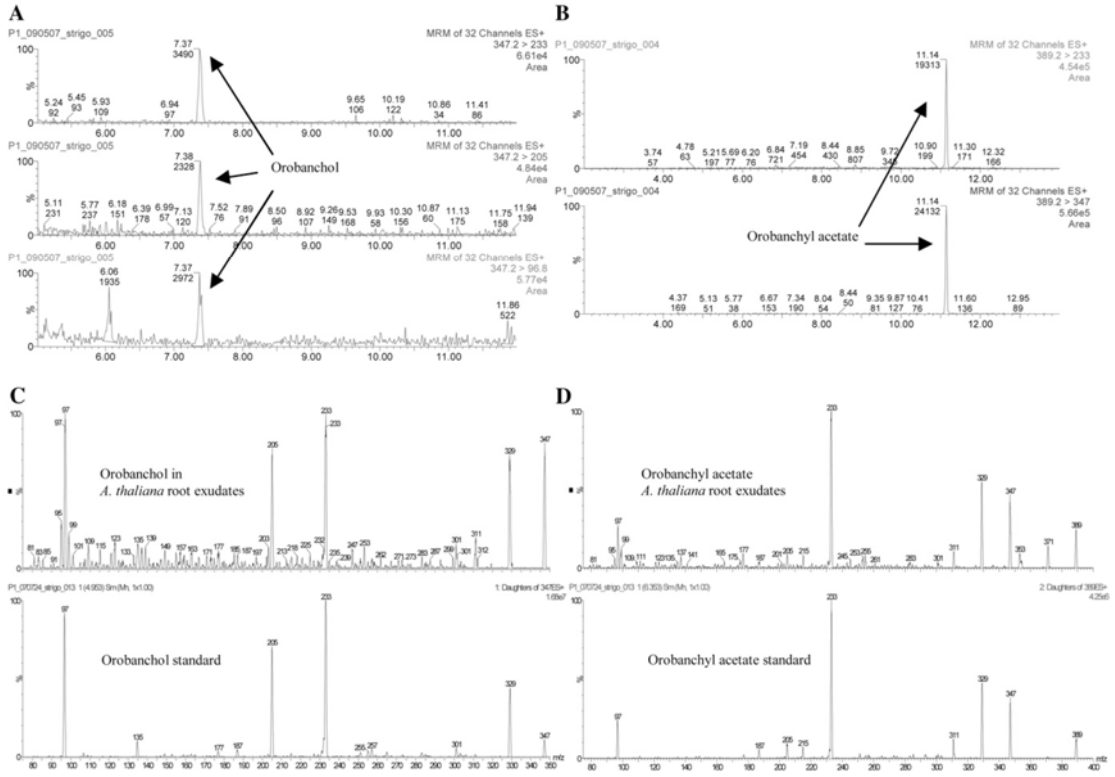

Figure 3: MRM-LC-MS/MS analysis of Arabidopsis root exudates of plants grown under phosphate starvation. **(a)**, Transitions 347 > 233, 347 > 205, and 347 > 96.8 for orobanchol. **(b)**, Transitions 389.2 > 233 and 389.2 > 347 for orobanchyl acetate. **(c)**, Full daughter ion scan MS/MS spectrum of orobanchol in Arabidopsis exudate and orobanchol standard. **(d)**, Full daughter ion scan MS/MS spectrum of orobanchyl acetate in Arabidopsis exudate and orobanchyl acetate standard.

Germination stimulatory activity of HPLC-fractioned root exudates of *max* mutants

Root exudates of phosphate-starved Arabidopsis ecotype Columbia (Col-0), *max1-1*, *max2-1*, and *max4-1* genotypes were HPLC fractioned. Fractions 17 and 20 were analyzed with the *P. ramosa* germination bioassay. As described above, these fractions responded both to phosphate starvation and fluridone treatment, suggesting that they may contain strigolactone(-like) compounds. Moreover, known strigolactones were shown to co-elute with these fractions (Figure 1b). The germination bioassay showed a high percentage of germination in both fractions in the Col-0 wild type (52% and 61%, respectively), and this was strongly reduced in the putative strigolactone biosynthetic mutants *max1-1* and *max4-1* (fraction 17, 85% and 79% lower germination; fraction 20, 81% and 77% lower germination). Fractions of the exudates collected from the putative strigolactone signal transduction mutant *max2-1* did not differ significantly in their bioactivity from the wild type (Figure 2). As described above, neither fraction 25 nor 26 responded to phosphate deficiency or fluridone treatment, even though the HPLC fractionation of strigolactone standards shows that germination in the latter fraction may be (partially) due to orobanchyl acetate. However, when fractions 25 and 26 were analyzed for germination-inducing activity in the *max* mutants, no differences were found.

MRM-LC-MS/MS analysis of strigolactones

For strigolactone analysis in root exudates, approximately 800 Arabidopsis plants were grown for four weeks under phosphate-sufficient conditions. Because our bioassays indicated an up-regulation of strigolactone secretion upon phosphate deficiency, plants were grown under phosphate-limiting conditions for two weeks prior to root exudate collection. The exudates were purified using C18 and silica column chromatography. Orobanchol, orobanchyl acetate, and 5-deoxystrigol were detected in the exudates of phosphate-starved plants (Figure 3, a and b; Supplemental Figure S6.2). To verify the presence of these strigolactones, the MS/MS spectra of the putative orobanchol (Figure 3c) and orobanchyl acetate peaks were compared with the MS/MS spectra of standards (Figure 3d) and the samples were spiked with these standards (data not shown). No MS/MS spectrum could be obtained from 5-deoxystrigol; however, spiking (data not shown) and ratio analysis of the MRM transitions suggested the compound to be 5-deoxystrigol. Orobanchol and orobanchyl acetate were also detected in root extracts of Col-0 (Supplemental Figure S6.3).

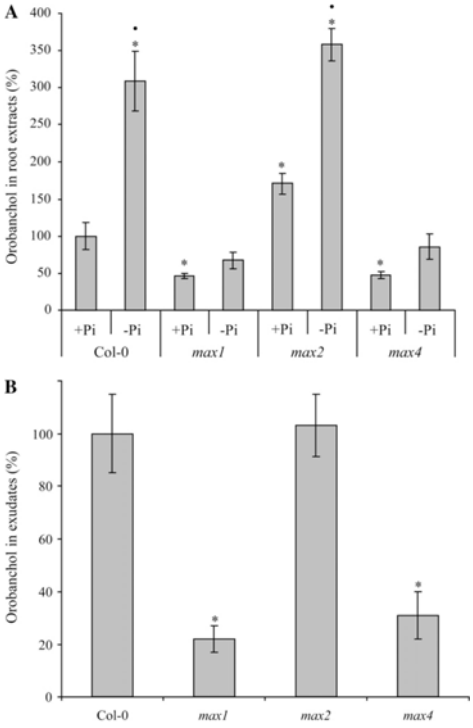

Figure 4: Analysis of orobanchol content in Arabidopsis Col-0, max1-1, max2-1, and max4-1. **(a)**, Effect of treatments with sufficient phosphate (+Pi) and limiting phosphate (–Pi) on root extracts (mean value for orobanchol level in Col-0 +Pi root extract was set to 100%). Bars represent the average of three independent biological replicates. • Significant –Pi up-regulation within genotypes ($P < 0.05$); * significant difference compared with Col-0 +Pi ($P < 0.05$). **(b)**, Root exudate analysis of –Pi (mean value for orobanchol level in Col-0 –Pi [$P < 0.05$] root exudate was set to 100%). Bars represent the average of three independent biological replicates each consisting of about 800 plants ± se. * Significant difference compared with Col-0 ($P < 0.05$).

When root extracts of Col-0, *max1-1*, *max2-1*, and *max4-1* were analyzed, an up-regulation of orobanchol production under phosphate-limiting conditions was observed in Col-0 and *max2* (3.1- and 2.1-fold, respectively) but not in *max1* and *max4* (Figure 4a). Moreover, a strong reduction in orobanchol content was found in *max1-1* and *max4-1* under phosphate-sufficient conditions (54% and 52% lower than the wild type, respectively) as well as under phosphate starvation (78% and 72% lower than the wild type, respectively; Figure 4a). In line with these findings, orobanchol was also reduced in the exudates of both biosynthetic mutants under phosphate starvation (78% and 69% lower than the wild type, respectively; Figure 4b). Interestingly, orobanchol biosynthesis in max2 grown under phosphate-sufficient conditions was 1.7-fold higher than in Col-0 (Figure 4a). In these experiments, the concentration of orobanchyl acetate and 5-deoxystrigol in both Col-0 and the *max* mutants was below the detection level required for accurate quantification.

Effect of phosphate deficiency on shoot architecture

To assess whether strigolactones are involved in the shoot architectural response to phosphate stress, the branching phenotype of max mutants under phosphate starvation was assessed. Arabidopsis Col-0, *max1-1*, *max2-1*, and *max4-1* plants were grown for four weeks under phosphate-sufficient conditions. Phosphate starvation was induced in half of the plants three days prior to bolting by reducing the phosphate concentration in the medium to 10% of the control. After two

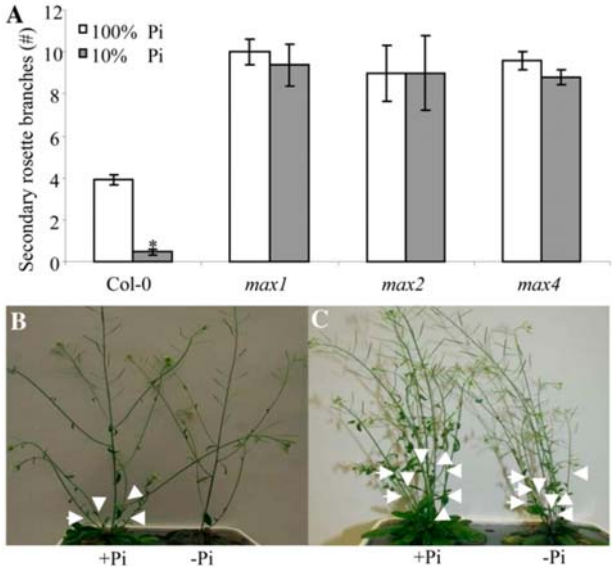

Figure 5: The effect of phosphate levels on Arabidopsis axillary shoot branching. Measurements were done 2 weeks after initiation of the treatments in 7-week-old plants grown under long-day conditions. Bars indicate average of 10 independent replicates ± se. **(a),** Effect of phosphate starvation on the number of secondary rosette branches. * Significant difference of low-phosphate (10% Pi) from high-phosphate (100% Pi) treatment ($P < 0.05$). **(b),** Col-0 grown under phosphate-sufficient conditions (left) and under low phosphate (right). **(c),** max4-1 grown under phosphate-sufficient conditions (left) and under low phosphate (right). Arrowheads point to secondary rosette branches.

weeks, plants were analyzed and the number of secondary rosette branches was assessed. Under phosphate-sufficient conditions, Col-0 had on average four secondary rosette branches per plant (Figure 5, a and b). All three max mutants (*max1-1*, *max2-1*, and *max4-1*) had a higher number of secondary rosette branches (10, 9, and 9.5, respectively; Figure 5, a and c). Under phosphate deficiency, the number of secondary rosette branches in Col-0 was strongly reduced ($P < 0.05$; Figure 5, a and b), but the max mutants showed no significant reduction (Figure 5, a and c).

Germination stimulatory activity of Arabidopsis xylem sap

To investigate whether a signal responsible for the change in branching phenotype under phosphate starvation is transported from the root to the shoot through the vascular tissue, xylem sap was collected from Col-0 plants. The strigolactone-like nature of putative compounds in the xylem sap was assessed using the *P. ramosa* germination assay. Twenty-fold diluted xylem sap from plants grown under phosphate-sufficient conditions induced about 13% germination, whereas phosphate-starved plants induced much higher germination (58%; Figure 6a). Upon 40-fold and 80-fold dilution, xylem sap from phosphate-starved plants still induced 40% and 19% germination, respectively, whereas xylem sap collected from control plants did not induce any germination at these dilutions (Figure 6a). Subsequently, xylem sap was fractioned on HPLC using the same gradient as used for the exudates, and the fractions were analyzed for their induction of *P. ramosa* germination. Fraction 11 of xylem sap collected from plants grown under phosphate-sufficient conditions induced germination (32%), whereas above it was shown that fraction 11 of the root exudates was inactive. Upon phosphate starvation, germination stimulated by this fraction increased 1.8-fold (Figure 6b). Fractions 17 and 20 induced 11% and 18% germination, respectively. Upon phosphate starvation, germination induced by fraction 17 increased 2.2-fold compared with the control. This increase was not observed in fraction 20 (Figure 6b). For both these xylem sap fractions in max4-1 plants, there was a 90% reduction ($P < 0.05$) in germination stimulation (Figure 6c). No germination was detected in response to fractions higher than fraction 20. Xylem sap fractions 11 of *max1-1* and *max4-1* induced much lower germination (90% and 91% lower than the wild type, respectively; Figure 6d). Xylem sap fraction 11 of *max2-1* showed no significant change in germination stimulation compared with wild-type plants (Figure 6D).

Strigolactone detection in xylem sap

Xylem sap from Col-0 was collected from ten phosphate-starved plants, divided over two experiments. These samples were individually purified and analyzed by MRM-LC-MS/MS. A clear peak of orobanchol (Figure 7a) was detected in all samples, although the concentration was below the level required for MS/MS analysis. The concentration of orobanchol in xylem sap of plants grown

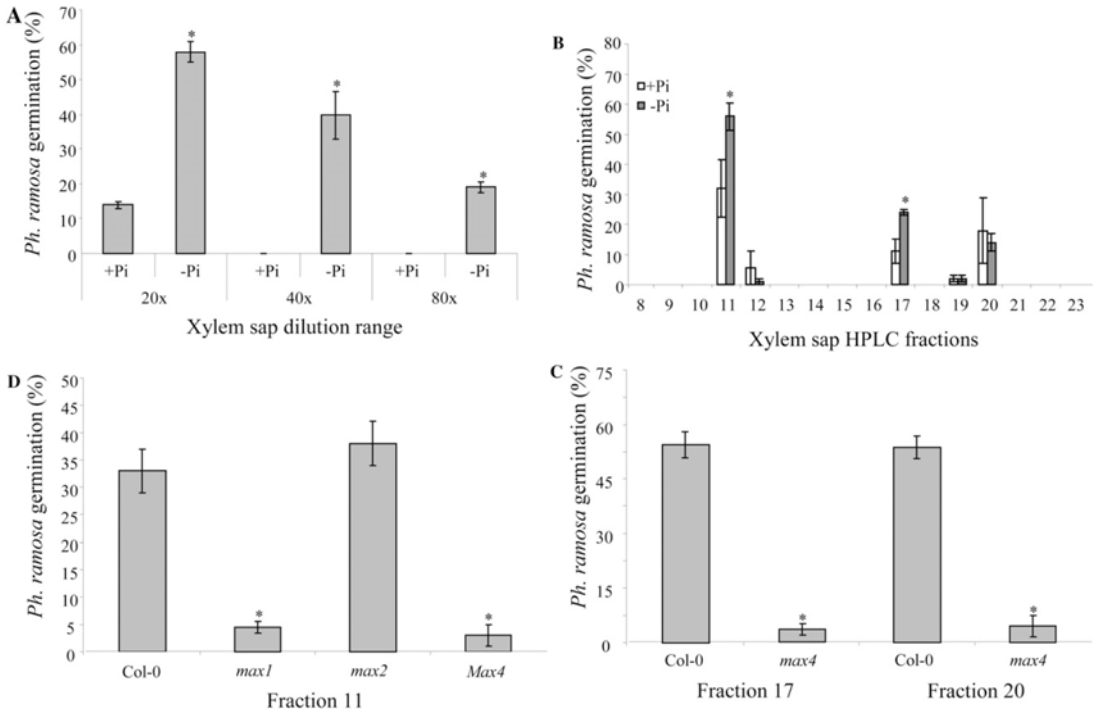

Figure 6: Germination of *P. ramosa* seeds induced by xylem sap collected from Arabidopsis. **(a)**, Effect of several concentrations of xylem sap of Col-0, grown under sufficient phosphate (+Pi) and limiting phosphate (–Pi) levels, on germination of *P. ramosa*. Bars represent the average of three independent biological replicates ± se. * Significant difference of low-phosphate from high-phosphate treatment ($P < 0.05$). **(b)**, Effect of treatments with sufficient phosphate and limiting phosphate on germination stimulatory capacity of HPLC-fractioned xylem sap. Bars represent the average of three independent biological replicates ± se. * Significant difference of low-phosphate from high-phosphate treatment ($P < 0.05$). **(c)**, Germination induced by HPLC fractions 17 and 20 of Arabidopsis (Col-0 and max4-1) xylem sap. Bars represent the average of three independent biological replicates ± se. * Significant difference compared with Col-0 ($P < 0.05$). **(d)**, Germination induced by HPLC fraction 11 of Arabidopsis (Col-0, max1-1, max2-1, and max4-1) xylem sap. Bars represent the average of three independent biological replicates ± se. * Significant difference compared with Col-0 ($P < 0.05$).

under limited phosphate was 27% higher than in plants grown under sufficient phosphate (Figure 8). To confirm these findings, tomato xylem sap was analyzed for the presence of strigolactones. Also, tomato xylem sap contained orobanchol, which could be unambiguously confirmed by MS/MS analysis and comparison with an authentic standard (Figure 7, b and c). To investigate further whether strigolactones can be transported from the root to the shoot, the synthetic strigolactone analog GR24 was applied to the roots of hydroponically grown Arabidopsis. Extracts from the aerial parts were made, and GR24 was detected using MRM-LC-MS/MS in tissues that had not been in contact with the medium (Supplemental Figure S6.4).

Discussion

Arabidopsis produces strigolactones

In the work reported here, two (orobanchol and orobanchyl acetate) and possibly three (5-deoxystrigol) strigolactones were identified in Arabidopsis exudates using MRM-LC-MS/MS. It was shown that strigolactone production in Arabidopsis is up-regulated by phosphate deficiency and that MAX1 and MAX4 activity is required for the biosynthesis of orobanchol and the germination stimulatory compounds eluting in HPLC fractions 11 and 17. Furthermore, it was demonstrated that strigolactone (-like) compounds are involved in the regulation of shoot branching under phosphate starvation and that they are transported from the root to the shoot through the xylem.

The increase in *P. ramosa* germination induced by Arabidopsis root exudates of plants grown under phosphate starvation shows that phosphate limitation increases the secretion of germination stimulatory compounds by this non-AM host (Figure 1a). HPLC fractionation of Arabidopsis root exudates resulted in a number of bioactive fractions, which are only partially explained by our MRM-LC-MS/MS data (Figure 1b). The germination stimulatory activity in fractions 17 and 20 was shown to be carotenoid derived (inhibited by fluridone; Figure 1b) and dependent on MAX1 and MAX4 (Figure 2) and hence is very likely strigolactone like in nature, whereas fractions 25 and 26 were not (Figure 1b). MRM-LC-MS/MS analysis of HPLC-fractioned strigolactone standards showed that the strigolactones 7-hydroxyorobanchyl acetate and solanacol elute in fraction 17 and orobanchol elutes in fraction 20 (Figure 1b; Supplemental Table S6.1), with traces of these strigolactone standards also present in the next fractions (18 and 21, respectively), which probably explains the residual germination observed in these fractions (Figure 1b). When fractions 17 and 20 were analyzed in three of the *max* mutants (*max1*, *max2*, and *max4*), there was a significant reduction in germination-inducing activity for these fractions in the putative strigolactone biosynthetic mutants *max1-1* and *max4-1* but not in the putative signaling mutant *max2-1* (Figure 2). Together, these results indicate that the active compounds responsible for the induction of *P. ramosa* seed germination in these two fractions are strigolactone like.

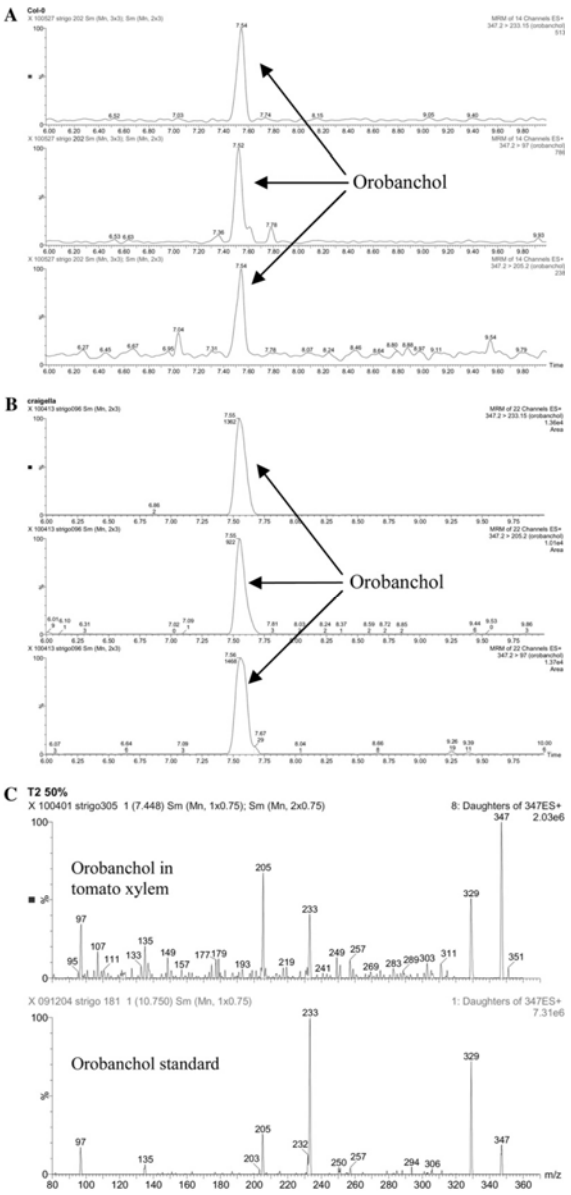

Figure 7: (a), MRM-LC-MS/MS analysis of Arabidopsis xylem sap (Col-0) showing transitions 347 > 233, 347 > 205, and 347 > 96.8 for orobanchol. **(b)**, MRM-LC-MS/MS analysis of tomato xylem sap (cv Craigella) showing transitions 347 > 233, 347 > 205, and 347 > 96.8 for orobanchol. **(c)**, Full daughter ion scan MS/MS spectrum of orobanchol in tomato xylem sap and orobanchyl acetate standard.

No known strigolactone from the standard mix eluted in fraction 22, which could indicate the presence of a so far unidentified strigolactone in Arabidopsis. No effect of fluridone, phosphate starvation (Figure 1b), or max mutation (Supplemental Figure S6.1) was observed on the germination-inducing activity of fractions 25 and 26, indicating that the activity in these fractions is not carotenoid derived and thus not strigolactone like. It has been reported that the germination of several *Orobanche* and *Phelipanche* species is induced by compounds other than strigolactones. For example, the germination of *Orobanche foetida* is induced by polyphenolic compounds isolated from pea (Evidente et al., 2010). It is possible that Arabidopsis root exudates contain similar non-strigolactone-like germination stimulants. The secretion of these unknown stimulants under all conditions (Figure 1b) indicates that they could be

responsible for the relatively high germination-inducing activity of crude root exudates of plants grown under phosphate-sufficient conditions (Figure 1a). In addition, these compounds could be masking the germination stimulatory activity of orobanchyl acetate, which we detected in purified crude exudates and the standard of which elutes in fraction 26 (Figure 1b). Additional purification or a different HPLC gradient could possibly resolve this.

Detection of strigolactones in Arabidopsis root exudates and extracts

Analysis of an orobanchol standard in an Arabidopsis root exudate matrix using MRM-LC-MS/MS resulted in an 80% reduction in the recovery of orobanchol (data not shown). This suggests that insource ion suppression is interfering with strigolactone (orobanchol) detection in Arabidopsis samples. Ion suppression occurs when easily ionizable molecules co-elute from the liquid chromatograph and are therefore co-injected into the ionization chamber, preventing optimal ionization and thus detection of the target compound. Purification and concentration of crude Arabidopsis root exudates using silica column chromatography resulted in a much better recovery of strigolactones and allowed us to identify two known strigolactones, orobanchol and orobanchyl acetate, and to have evidence of the presence of a third one, 5-deoxystrigol, under phosphate starvation. The fact that orobanchol could now be detected suggests that the additional purification eliminated interfering molecules and effectively reduced ion suppression. Orobanchol standard addition to the purified sample confirmed this (data not shown). MS/MS spectra (Figure 3, c and d) and spiking (data not shown) with standards of the first two compounds proved that they were indeed orobanchol and orobanchyl acetate. The concentration of 5-deoxystrigol proved to be insufficient for MS/MS analysis (Supplemental Figure S6.2). However, spiking of the sample with a 5-deoxystrigol standard (data not shown) and comparison of the ratio between MRM transitions of the sample and that of the 5-deoxystrigol standard indicate that 5-deoxystrigol is likely present in Arabidopsis. The germination bioassay on fraction 28, where a 5-deoxystrigol standard elutes, only revealed a low percentage of germination (less than 1%), an indication that the concentration of 5-deoxystrigol in Arabidopsis root exudates is very low. No strigolactones were detected in exudates of plants grown under phosphate-sufficient conditions, again confirming their induction upon phosphate deficiency. Orobanchol has been reported in Arabidopsis before, although no MS/MS spectrum was obtained (Goldwasser et al., 2008). Based on germination assays using HPLC-fractioned Arabidopsis root exudates, Goldwasser et al. (2008) postulated that orobanchyl acetate may also be present in Arabidopsis exudate. However, it was not detected by LC-MS/MS analysis at that time, nor was 5-deoxystrigol (Goldwasser et al., 2008), but in our work here, the presence of both in Arabidopsis was analytically confirmed. The detection of orobanchol by MRM-LC-MS/MS makes it likely that this strigolactone is responsible for the germination-inducing activity of fraction 20. Interestingly, all three strigolactones detected in this study were postulated to be biosynthetically linked to each other (Supplemental Figure S6.5; Rani et

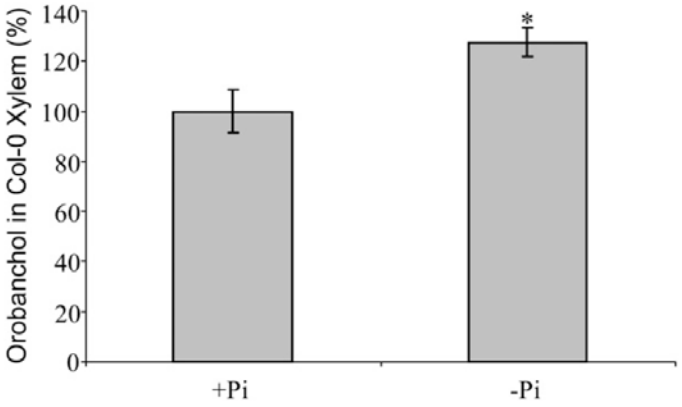

Figure 8: Analysis of orobanchol content of Arabidopsis Col-0 xylem sap. * Significant difference compared with sufficient phosphate conditions (+Pi; $P < 0.05$).

al., 2008). In the biosynthetic scheme proposed by Rani et al. (2008), 5-deoxystrigol is the first real strigolactone in the pathway and serves as the common substrate for all known strigolactones, which could be an explanation for the low 5-deoxystrigol concentration. In one branch of the proposed pathway, 5-deoxystrigol is hydroxylated at position 4 to form orobanchol (Supplemental Figure S6.5). Acetylation, a common reaction in the strigolactone pathway (Rani et al., 2008), of orobanchol would then yield orobanchyl acetate. In line with this, a reasonable hypothesis is that the activity detected in fraction 17, which shows the typical strigolactone-like pattern (Figures 1b and 2), is due to another related strigolactone, the recently discovered 7-hydroxyorobanchyl acetate (Koichi Yoneyama, personal communication; Supplemental Table S6.1), which is proposed to be two putative biosynthetic steps away from orobanchol (Xie et al., 2010). However, 7-hydroxyorobanchyl acetate was not detected by MRM-LCMS/MS analysis in any of the Arabidopsis samples.

Strigolactones reduced in *max* mutants

MRM-LC-MS/MS analysis revealed a strong reduction in orobanchol in root extracts and exudates of both putative biosynthetic *max* mutants, *max1-1* and *max4-1*, but not in the signal transduction mutant, *max2-1* (Figure 4, a and b), providing evidence for a role in strigolactone biosynthesis for both MAX1 and MAX4 and hence analytically confirming the complementation studies with GR24 carried out with these mutants (Gomez-Roldan et al., 2008; Umehara et al., 2008; Crawford et al., 2010). Similar to the rice strigolactone response mutant *d3* (Umehara et al., 2008), extracts of *max2* grown under phosphate-sufficient conditions displayed an elevated orobanchol concentration compared with Col-0. This could be explained by impaired feedback regulation on strigolactone biosynthesis in this mutant (Mashiguchi et al., 2009). Our germination bioassays show that MAX1 and MAX4 activity is needed for the formation of the *P. ramosa* germination-inducing compound eluting in fraction 20 (probably orobanchol), which further confirms our analytical data.

It was previously postulated that one or more cytochrome P450 enzymes must be involved in strigolactone biosynthesis (Matusova et al., 2005; Humphrey et al., 2006; Rani et al., 2008). The reduction of orobanchol in *max1-1* (Figure 4) indicates that, indeed, MAX1, which was shown to encode a cytochrome P450 (Booker et al., 2005), is essential for the biosynthesis of this strigolactone. The biosynthesis of the unknown, putative strigolactones eluting in exudate fraction 17 and xylem sap fraction 11 also requires MAX1 (Figures 2 and 6d). We cannot conclude whether MAX1 catalyzes an early step in strigolactone biosynthesis or whether it is involved in the conversion of one strigolactone or group of strigolactones into another. However, the facts that all strigolactone-like activities require MAX1 and that the predicted catalytic activity of MAX1 is that of intramolecular rearrangement (Booker et al., 2005) make it likely that MAX1 involvement in strigolactone biosynthesis is located upstream of 5-deoxystrigol. In the comparison of root exudates and root extracts of the max mutants with Col-0, 5-deoxystrigol was below the detection level, making it impossible to confirm MAX1 involvement in its biosynthesis.

The fact that the *max* biosynthetic mutants *max1-1* and *max4-1* still produce some orobanchol (Figure 4) indicates that either both mutants are leaky or that there is a second, less active, pathway leading to strigolactone biosynthesis, separate from the MAX1/3/4 pathway. It has been reported that the bushy phenotype of *max4-5* is more severe than that of *max1-1* or *max4-1* (Bennett, 2006), suggesting that the mutants used in this study retain some catalytic activity. The possibility of alternative biosynthetic pathways is also plausible. An alternative low-level pathway would explain why overexpression of MAX2 in *max* biosynthetic mutant backgrounds can partially suppress their increased branching phenotypes (Stirnberg et al., 2007). Multiple biosynthetic pathways have been described for auxin (Zhao, 2010) and cytokinins (Sakakibara, 2006). In addition, two so-called

bypasses in the conversion of xanthoxin to abscisic acid have been postulated for abscisic acid biosynthesis (Cutler and Krochko, 1999; Seo and Koshiba, 2002)

Strigolactone-mediated regulation of shoot branching under low-phosphorus conditions

When plants were grown under phosphate deficiency, the outgrowth of secondary rosette branches in Col-0 was strongly suppressed, but no such suppression was observed in the *max* mutants (*max1-1*, *max2-1*, and *max4-1*; Figure 5a). This confirms results with rice, where inhibition of tiller outgrowth under phosphate starvation was observed in wild-type rice but not in the strigolactone mutants *d3* and *d10* (Umehara et al., 2010). However, here, we show that this effect is also present in Arabidopsis, a plant species that is not an AM host. The fact that the reduction in secondary rosette branches was not observed in any of the analyzed max mutants (*max1-1*, *max2-1*, and *max4-1*) indicates that the architectural response to low phosphate levels in Arabidopsis is likely mediated by strigolactones and transduced through MAX2. Interestingly, strigolactone secretion was reported to be unaffected by phosphate deficiency in another non-AM host, *Lupinus albus* (Yoneyama et al., 2008), indicating that the response to phosphate deficiency is not conserved in the whole plant kingdom. However, *L. albus* has a different strategy to ensure phosphate uptake by forming cluster roots (Lambers et al., 2006). Therefore, it is possible that strigolactone biosynthesis in that species is up-regulated without increased exudation. Unfortunately, analysis of root extracts in *L. albus* to investigate the effect on strigolactone biosynthesis was not performed.

Strigolactones are transported through the xylem

In xylem sap, three germination-stimulating fractions (fractions 11, 17, and 20) were identified. When tested in *max4-1*, fractions 17 and 20 showed a 90% reduction in germination compared with the wild type (Figure 6c). A similar reduction in fractions 17 and 20 was observed in root exudates of *max1-1* and *max4-1* (Figure 2). This suggests that the compounds responsible for germination in both fractions are the same for root exudates and xylem sap. Interestingly, no activity was detected in fraction 11 of root exudates in any of the experiments, whereas the germination activity in xylem sap fraction 11 was up-regulated upon phosphate deficiency, reduced in *max1-1* and *max4-1*, and present in *max2-1* xylem sap (Figure 6d). This suggests that this xylem sap fraction contains a strigolactonelike compound. However, it is much more polar than any of the known Arabidopsis strigolactones. It is possible that this shift in polarity is caused by minor modifications such as hydroxylation. In line with the hypothesis about fraction 17 (possibly 7-hydroxyorobanchyl acetate), the compound in fraction 11 could be 7-hydroxyorobanchol (Supplemental Table S6.1). The fact that germination activity was detected in xylem sap fraction 11 but not in the same fraction of root exudates suggests that the compound responsible for the *P. ramosa* germination in this fraction is either not synthesized in the root (but, for example, in the hypocotyl) or is produced in the root and by selective mechanisms of strigolactone secretion and/or transport is only secreted into the xylem. More research is needed to identify the active compound present in fraction 11 and to study its biological function.

When xylem sap collected from Col-0 was purified by silica column chromatography and analyzed by MRM-LC-MS/MS, orobanchol was detected (Figure 7a), providing, to our knowledge for the first time, evidence that this strigolactone is transported through the xylem. The transport rate of orobanchol in xylem sap was estimated to be 50 $pg \cdot plant^{-1} \cdot h^{-1}$. The orobanchol concentration in Arabidopsis xylem sap samples proved to be insufficient for MS/MS analysis. To confirm the presence of strigolactones in xylem sap, xylem sap of tomato, a relatively high strigolactone producer, was analyzed. Again, a clear peak was detected (Figure 7b), and MS/MS analysis identified the compound

as orobanchol (Figure 7c). Finally, GR24 applied to the root system of Arabidopsis was detected in the hypocotyl and stem (Supplemental Figure S6.4), indicating also that this synthetic strigolactone is transported. Taken together, these findings provide compelling evidence that strigolactones themselves are transported through the xylem.

When germination-inducing activity of these three xylem sap fractions (11, 17, and 20) was analyzed under phosphate limitation, a clear increase in germination was detected in fractions 11 and 17 but not in fraction 20. This suggests that only the active compounds in the first two fractions, assuming that they are strigolactone(-like), would be involved in the regulation of shoot branching under phosphate deficiency. However, fraction 20 induced only minor germination, and a large variation was observed within the replicates. When concentrated Col-0 xylem sap was analyzed by MRM-LC-MS/MS (n = 5), a significant 27% increase ($P > 0.05$) of orobanchol was detected under phosphate depletion compared with plants grown under phosphate-sufficient levels (Figure 8), indicating that orobanchol, likely fraction 20, is also involved in the regulation of the shoot architectural response to phosphate starvation.

Are Arabidopsis strigolactones involved in rhizosphere signaling?

It has been postulated that the evolution of plant-AM fungal symbiosis was a key step in the evolution of plants, enabling them to leave the oceans and colonize the land (Pirozynski and Malloch, 1975; Bonfante and Genre, 2008). In addition, it is believed that the main selective driving force for the up-regulation of strigolactone secretion upon phosphate deficiency in plants is to function as a signal in the rhizosphere to stimulate hyphal branching of AM fungi (Bouwmeester et al., 2007). However, Arabidopsis does not engage in symbiosis with AM fungi and seems to have no need for strigolactone secretion into the rhizosphere. Given that most land plants are mycorrhizal, this is almost certainly the ancestral condition; hence, lack of AM symbiosis in Arabidopsis could be a derived trait. It is possible, therefore, that strigolactone exudation from roots is a relic of this ancestral trait, which was lost by Arabidopsis, for example, because orthologs of genes such as *DMI3* (Zhu et al., 2006) and *DXS-2* (Walter et al., 2007) were lost. However, in this study, we demonstrate that up-regulation of strigolactone biosynthesis during phosphate starvation likely plays a role in the regulation of processes resulting in a reduced shoot-branching phenotype. This response allows the plant to ensure production of some high quality seed as well as to invest energy in enhanced lateral root formation, a process shown to occur under phosphate-limiting conditions ((Bates and Lynch, 1996; Williamson et al., 2001; López-Bucio et al., 2002; Sánchez-Calderón et al., 2005). This enables the plant to focus and intensify root growth in topsoil, where phosphorus is usually at higher concentrations. We assume that these responses also represent an evolutionary advantage, which would be the driving force for the preservation of low-phosphate-induced strigolactone biosynthesis in Arabidopsis.

Materials and methods

Plant material and chemicals

Arabidopsis (Arabidopsis thaliana) Col-0, *max1-1* introduced into the Col-0 genetic background by seven backcrosses (Stirnberg et al., 2002), *max2-1*, and *max4-1* plants were used for all experiments. The carotenoid pathway inhibitor fluridone was obtained from Duchefa Biochemie. The synthetic germination stimulant, strigolactone analog GR24, was kindly provided by Binne Zwanenburg (Department of Organic Chemistry, Radboud University). The natural germination stimulants 5-deoxystrigol, 7-hydroxyorobanchol, 7-hydroxyorobanchyl acetate, 7-oxoorobanchol, 7-

oxoorobanchyl acetate, orobanchol, orobanchyl acetate, sorgolactone, solanacol, sorgomol, and strigol were kindly provided by Koichi Yoneyama (Weed Science Center, Utsunomiya University).

Growth conditions and experimental setup

Arabidopsis seeds were sterilized in 4% sodium hypochlorite containing 0.02% (v/v) Tween 20, rinsed thoroughly with sterile water, and stratified for 48 h on moistened filter paper at 4°C in darkness. For hydroponics, seeds were sown on Rockwool filled Eppendorf vials of which the bottom was removed to enable the root to access the liquid medium. Plants were grown under controlled conditions in a climate chamber at 16h of light/8h of dark, 20°C/18°C, 60% relative humidity, and a light intensity of 150 $\mu mol \cdot m^{-2} \cdot s^{-2}$ using either one-third-strength Hoagland solution or Tocquin Arabidopsis medium (Tocquin et al., 2003). Phosphate starvation was induced by reducing the level of$NH_4H_2PO_4$ to 10% (0.013mM) of the control nutrient solution. Root exudates were collected for 24 h in 50-mL tubes. For LC-MS/MS analysis of strigolactones, Arabidopsis was grown in pots filled with 500 mL of a sand:vermiculite mixture (1:1). Seeds were sown on a small block of washed Rockwool. Each pot contained 24 plants, and each sample consisted of 40 pots. The plants were grown in a greenhouse from March until May at 16h of light/8h of dark, 20°C/18°C, and 60% relative humidity. Extra light was provided to achieve a relatively high light intensity of 300 $\mu mol \cdot m^{-2} \cdot s^{-2}$. Plants were watered using one-third-strength Hoagland solution. Two weeks before root exudate collection, pots were rinsed with 1.5 L (three times the pot volume) of tap water to remove phosphate. Plants were then watered (three times per week) with 50 mL per pot of one-third-strength Hoagland nutrient solution without phosphate. For root exudate collection, 1 L of tap water was added to the pots and the flow-through was collected. Root material was collected, quick frozen using liquid nitrogen, and stored at -80°C until further use.

HPLC fractionation

Fifty milliliters of root exudate was loaded onto the preequilibrated column (Grace Pure C18-Fast 500 mg/3 mL SPE). Subsequently, the columns were washed with 5 mL of demineralized water and eluted with 5 mL of acetone. Five hundred microliters of C18 purified sample was concentrated to 100 µL and injected into an XBridge C18 column (4.6 X 150 mm;Waters) using the following gradient: 1 min of 100% water, 2 min of 27% (v/v) acetonitrile in water, 15 min of 45% (v/v) acetonitrile, 24 min of 80% (v/v) acetonitrile, and 24.2 min of 100% acetonitrile, which was maintained for 4 min to clean the column. The flow rate was 1 mL min 21, and the column temperature was set at 25°C. One-minute fractions were collected using a Biofrac fraction collector (Bio-Rad).

Germination bioassay

Germination assays with *Phelipanche ramosa* seeds were conducted as reported previously (Matusova et al., 2005). Seeds of *P. ramosa* were cleaned using a sucrose gradient (Hartman and Tanimonure, 1991) and preconditioned ("warm stratification") for ten to twelve days at 21°C. Aliquots (50 mL) of root exudates or xylem sap (without organic solvent) were added to triplicate 1 cm discs containing approximately 50 preconditioned seeds each. The synthetic germination stimulant GR24 at 3.3 3 10^{-9} M (inducing about 50% germination) and demineralized water were included as positive and negative controls, respectively, in each bioassay. After six days, the germinated and non-germinated seeds were counted using a stereomicroscope. Seeds were considered germinated when the radicle had protruded through the seed coat. Root exudates were concentrated 10-fold before germination assays, and xylem sap was diluted 20-fold.

Xylem extraction

Xylem sap was collected from Arabidopsis plants by the syringe-suction method as described by Beveridge et al. (Beveridge et al., 1997) with minor modifications. Plants were decapitated above the hypocotyl. A flexible silicon tube (length, 30 mm; internal diameter, 1 mm) attached to a 5 mL syringe was placed about 5 to 10 mm over the stump and tied tightly in place. The plunger of the syringe was pulled and held at that position to create a vacuum within the syringe. About 100 µL of xylem sap was collected per plant. For tomato (*Solanum lycopersicum*) xylem sap collection, tomato plants were grown in a hydroponic system on one-half-strength Hoagland solution. Four-week-old plants were decapitated above the hypocotyl, and a plastic ring was placed around the stem. The accumulating xylem sap was collected every 30 min.

All xylem sap was collected for 90 min after decapitation, and the first and last plant were decapitated within 30 min of each other. In order to remove any debris, xylem sap was centrifuged at 13,500 rpm (germination assay) or hand filtered (MRM-LC-MS/MS analysis) with a Minisart SRP4 0.45-mm filter (Sartorius Stedim Biotech), after which the xylem sap was frozen in liquid nitrogen and stored at -80°C before further use.

Silica column chromatography

To further purify strigolactones, silica column chromatography was performed. Silica columns were custom made using 200 mg of silica gel 60 (Merck), particle size 0.063 to 0.200mm (70–230 mesh ASTM), for each 1 mg of residue. The residue was dissolved in chloroform, after which 100 mg of silica was added. The solvent was evaporated, and the silica-bound sample was added to the silica column. A mixture of n-hexane and an increasing percentage of ethyl acetate was used to elute compounds. In total, 10 silica fractions were collected from 0% to 100% in 10% increments of ethyl acetate. Solvents of these fractions were evaporated under vacuum, and the residue was dissolved in 1 mL of acetone and stored at -20°C until further use. Before MRM-LC-MS/MS measurement, silica fractions were concentrated 4-fold.

Strigolactone purification from root exudates

For MRM-LC-MS/MS analysis, 5 L of root exudates was loaded onto a preequilibrated column (Grace Pure C18-Fast 5000 mg/20 mL SPE). Subsequently, the columns were washed with 50 mL of 30% acetone in water and strigolactones were eluted with 50 mL of 60% acetone in water, creating a C18 fraction in which all known strigolactones elute. Samples were evaporated to dryness, and the residue was dissolved in chloroform and purified by silica column chromatography, as described above.

Strigolactone extraction from roots

For strigolactone analysis, 0.5 g of roots was ground with a mortar and pestle in liquid nitrogen. The samples were extracted with 2 mL of cold ethyl acetate containing [$^{13}C_3$]strigol as an internal standard in a 10 mL glass vial. The vials were vortexed and sonicated for 10 min in a Branson 3510 ultrasonic bath (Branson Ultrasonics). Samples were centrifuged for 10 min at 2,000 rpm in an MSE Mistral 2000 centrifuge (Mistral Instruments), after which the organic phase was transferred to a 4 mL glass vial. The pellets were re-extracted with another 2 mL of ethyl acetate. The combined ethyl acetate supernatants were dried under a flow of nitrogen gas, and the residue was purified by silica column chromatography as described above.

Strigolactone extraction from xylem sap

For Arabidopsis, 450 µL xylem sap from three individual plants was pooled (n = 5) and loaded onto the pre-equilibrated column (Grace Pure C18-Fast 50 mg/1.5 mL SPE). Subsequently, the columns were washed with 0.5 mL of demineralized water and eluted with 0.5 mL of acetone. Samples were evaporated to dryness, and the residue was purified by silica column chromatography as described above. For tomato strigolactone analysis, 1 mL of xylem sap pooled from three individual plants was used (n = 5).

GR24 Feeding Experiment

For GR24 uptake and transport analysis, Arabidopsis plants were hydroponically grown on one-half-strength Hoagland solution. Six-week-old flowering Arabidopsis plants were transferred to individual 50-mL tubes and provided with nutrient solution containing either 2.5 µM or 0 µM GR24 (n = 3). Root, hypocotyl, rosette stem, lower stem, and higher stem (Supplemental Figure S6.4) were individually sampled, extracted, and analyzed for GR24 content using MRM transitions 299 > 97, 299 > 157, and 299 > 185.

Strigolactone detection and quantification by LC-MS/MS

Analysis of strigolactones in Arabidopsis root exudates was performed by comparing retention times and mass transitions with those of available strigolactone standards (sorgolactone, strigol, 2'-epistrigol, orobanchol, 2'-epiorobanchol, 5-deoxystrigol, 2'-epi-5-deoxystrigol, solanacol, orobanchyl acetate, sorgomol, 7-oxoorobanchol, and 7-oxoorobanchyl acetate) using ultra performance liquid chromatography (UPLC) coupled to MS/MS essentially as described by López-Ráez et al. (López-Ráez et al., 2008) with some modifications. Analyses were performed using a Waters Micromass Quattro Premier XE tandem mass spectrometer and Waters Xevo tandem quadruple mass spectrometer equipped with an electrospray ionization source and coupled to an Acquity UPLC system (Waters). Chromatographic separation was obtained on an Acquity UPLC BEH C18 column (150 X 2.1 mm, 1.7 mm; Waters) by applying a water/acetonitrile gradient to the column, starting from 5% acetonitrile for 2.0 min and rising to 50% (v/v) acetonitrile in 8.0 min, followed by a 1.0 min gradient to 90% (v/v) acetonitrile, which was maintained for 0.1 min before going back to 5% acetonitrile using a 0.2 min gradient, prior to the next run. Finally, the column was equilibrated for 2.8 min using this solvent composition. Operation temperature and flow rate of the column were 50°C and 0.4 mL min^{-1}, respectively. Sample injection volume was 15 µL. The mass spectrometer was operated in positive electrospray ionization mode. Cone and desolvation gas flows were set to 50 and 1,000 L h^{-1}, respectively. The capillary voltage was set at 3.0 kV, the source temperature at 150°C, and the desolvation temperature at 650°C. The cone voltage was optimized for each standard compound using the Waters IntelliStart MS Console. Argon was used for fragmentation by collision-induced dissociation in the ScanWave collision cell. MRM was used for identification of strigolactones in root exudates and extracts by comparing retention times and MRM mass transitions with those of the strigolactone standards. MRM transitions were optimized for each standard compound using the Waters IntelliStart MS Console. Data acquisition and analysis were performed using MassLynx 4.1 (TargetLynx) software (Waters).

Statistical analysis

Student's t-tests were performed when appropriate.

Acknowledgements

We thank Binne Zwanenburg for supplying GR24, Thierry Levgeux for provided *P. ramosa* seeds, Koichi Yoneyama for advice and strigolactone standards, Juan Antonio López-Raéz, Peter Toth, James H. Westwood, and Wim Vriezen for their intellectual input, and Padraic Flood for critical reading of the manuscript. This work was funded by the Netherlands Organization for Scientific Research (NWO; VICI-grant to HB) and Marie Curie Intra European Fellowship within the 7th European Community Framework Program (grant to MAD). This project was co-financed by the Centre for BioSystems Genomics (CBSG) which is part of the Netherlands Genomics Initiative/Netherlands Organisation for Scientific Research.

References

Akiyama K, Matsuzaki K, Hayashi H (2005) Plant sesquiterpenes induce hyphal branching in arbuscular mycorrhizal fungi. Nature **435:** 824-827

Al-Ghazi Y, Muller B, Pinloche S, Tranbarger TJ, Nacry P, Rossignol M, Tardieu F, Doumas P (2003) Temporal responses of *Arabidopsis* root architecture to phosphate starvation: evidence for the involvement of auxin signalling. Plant, Cell & Environment **26:** 1053-1066

Bates TR, Lynch JP (1996) Stimulation of root hair elongation in *Arabidopsis thaliana* by low phosphorus availability. Plant, Cell & Environment **19:** 529-538

Bennett T (2006) The regulation of shoot branching in *Arabidopsis thaliana*. PhD thesis **University of York, York**

Beveridge CA, G.M. S, I.C. M, JJ. R, C aR (1997) The *rms1* mutant of pea has elevated indole-3-acetic acid levels and reduced root-sap zeatin riboside content but increased branching controlled by graft-transmissible signal(s). Plant Physiology **115: :** 1251-1258.

Beveridge CA, Murfet IC, Kerhoas L, Sotta B, Miginiac E, Rameau C (1997) The shoot controls zeatin riboside export from pea roots. Evidence from the branching mutant *rms4*. The Plant Journal **11:** 339-345

Beveridge CA, Ross JJ, Murfet IC (1994) Branching mutant *rms-2* in *Pisum sativum* (grafting studies and endogenous indole-3-acetic acid levels). Plant Physiology **104:** 953-959

Bonfante P, Genre A (2008) Plants and arbuscular mycorrhizal fungi: an evolutionary-developmental perspective. Trends in Plant Science **13:** 492-498

Bonser AM, Lynch J, Snapp S (1996) Effect of phosphorus deficiency on growth angle of basal roots in *Phaseolus vulgaris*. New Phytologist **132:** 281-288

Booker J, Auldridge M, Wills S, McCarty D, Klee H, Leyser O (2004) MAX3/CCD7 is a carotenoid cleavage dioxygenase required for the synthesis of a novel plant signaling molecule. Current Biology **14:** 1232-1238

Booker J, Sieberer T, Wright W, Williamson L, Willett B, Stirnberg P, Turnbull C, Srinivasan M, Goddard P, Leyser O (2005) MAX1 encodes a cytochrome P450 family member that acts downstream of MAX3/4 to produce a carotenoid-derived branch-inhibiting hormone. Developmental Cell **8:** 443-449

Bouwmeester HJ, Matusova R, Zhongkui S, Beale MH (2003) Secondary metabolite signalling in host-parasitic plant interactions. Current Opinion in Plant Biology **6:** 358-364

Bouwmeester HJ, Roux C, López-Ráez JA, Bécard G (2007) Rhizosphere communication of plants, parasitic plants and AM fungi. Trends in Plant Science **12:** 224-230

Cline M (1997) Concepts and terminology of apical dominance. American Journal of Botany **84:** 1064-1069

Cook CE, Whichard LP, Turner B, Wall ME, Egley GH (1966) Germination of witchweed (*Striga lutea Lour.*): isolation and properties of a potent stimulant. Science **154:** 1189-1190

Crawford S, Shinohara N, Sieberer T, Williamson L, George G, Hepworth J, Müller D, Domagalska MA, Leyser O (2010) Strigolactones enhance competition between shoot branches by dampening auxin transport. Development **137:** 2905-2913

Cutler AJ, Krochko JE (1999) Formation and breakdown of ABA. Trends in Plant Science **4:** 472-478

Evidente A, Cimmino A, Fernández-Aparicio M, Andolfi A, Rubiales D, Motta A (2010) Polyphenols, including the new peapolyphenols A-C, from pea root exudates stimulate *Orobanche foetida* seed germination. Journal of Agricultural and Food Chemistry **58:** 2902-2907

Foo E, Turnbull CGN, Beveridge CA (2001) Long-distance signaling and the control of branching in the *rms1* mutant of pea. Plant Physiology **126:** 203-209

Goldwasser Y, Yoneyama K, Xie X, Yoneyama K (2008) Production of strigolactones by *Arabidopsis thaliana* responsible for *Orobanche aegyptiaca* seed germination. Plant Growth Regulation **55:** 21-28

Gomez-Roldan V, Fermas S, Brewer PB, Puech-Pages V, Dun EA, Pillot J-P, Letisse F, Matusova R, Danoun S, Portais J-C, Bouwmeester H, Becard G, Beveridge CA, Rameau C, Rochange SF (2008) Strigolactone inhibition of shoot branching. Nature **455:** 189-194

Harrison MJ (2005) Signaling in the arbuscular mycorrhizal symbiosis. Annual Review of Microbiology **59:** 19-42

Hartman GL, Tanimonure OA (1991) Seed populations of Striga species in Nigeria. Plant Disease **75:** 494-496

Hartung W, Sauter A, Hose E (2002) Abscisic acid in the xylem: where does it come from, where does it go to? Journal of Experimental Botany **53:** 27-32

Humphrey AJ, Galster AM, Beale MH (2006) Strigolactones in chemical ecology: waste products or vital allelochemicals? Natural Product Reports **23:** 592-614

Jamil M, Charnikhova T, Cardoso C, Jamil T, Ueno K, Verstappen F, Asami T, Bouwmeester HJ (2011) Quantification of the relationship between strigolactones and *Striga hermonthica* infection in rice under varying levels of nitrogen and phosphorus. Weed Research**:** no-no

Joel DM (2009) The new nomenclature of *Orobanche* and *Phelipanche*. Weed Research **49:** 6-7

Lambers H, Shane MW, Cramer MD, Pearse SJ, Veneklaas EJ (2006) Root structure and functioning for efficient acquisition of phosphorus: Matching morphological and physiological traits. Annals of Botany **98:** 693-713

López-Bucio J, Hernandez-Abreu E, Sanchez-Calderon L, Nieto-Jacobo MF, Simpson J, Herrera-Estrella L (2002) Phosphate availability alters architecture and causes changes in hormone sensitivity in the Arabidopsis root system. Plant Physiology **129:** 244-256

López-Ráez JA, Charnikhova T, Gómez-Roldán V, Matusova R, Kohlen W, Vos RD, Verstappen F, Puech-Pages V, Bécard G, Mulder P, Bouwmeester H (2008) Tomato strigolactones are derived from carotenoids and their biosynthesis is promoted by phosphate starvation. New Phytologist **178:** 863-874

López-Ráez JA, Charnikhova T, Mulder P, Kohlen W, Bino R, Levin I, Bouwmeester H (2008) Susceptibility of the tomato mutant high pigment-2dg (hp-2dg) to *Orobanche spp*. infection. Journal of Agricultural and Food Chemistry **56:** 6326-6332

Ma Z, Baskin TI, Brown KM, Lynch JP (2003) Regulation of root elongation under phosphorus stress involves changes in ethylene responsiveness. Plant Physiology **131:** 1381-1390

Mashiguchi K, Sasaki E, Shimada Y, Nagae M, Ueno K, Nakano T, Yoneyama K, Suzuki Y, Asami T (2009) Feedback-regulation of strigolactone biosynthetic genes and strigolactone-regulated genes in Arabidopsis. Bioscience, Biotechnology, and Biochemistry **73:** 2460-2465

Matusova R, Rani K, Verstappen FWA, Franssen MCR, Beale MH, Bouwmeester HJ (2005) The strigolactone germination stimulants of the plant-parasitic *Striga* and *Orobanche spp*. are derived from the carotenoid pathway. Plant Physiology **139:** 920-934

Nacry P, Canivenc G, Muller B, Azmi A, Van Onckelen H, Rossignol M, Doumas P (2005) A role for auxin redistribution in the responses of the root system architecture to phosphate starvation in Arabidopsis. Plant Physiology **138:** 2061-2074

Nagahashi G, Douds DD (2000) Partial separation of root exudate components and their effects upon the growth of germinated spores of AM fungi. Mycological Research **104:** 1453-1464

Napoli C (1996) Highly branched phenotype of the petunia *dad1-1* mutant is reversed by grafting. Plant Physiology **111:** 27-37

Paszkowski U (2006) Mutualism and parasitism: The yin and yang of plant symbioses. Current Opinion in Plant Biology **9:** 364-370

Pirozynski KA, Malloch DW (1975) The origin of land plants: A matter of mycotrophism. Biosystems **6:** 153-164

Rani K, Zwanenburg B, Sugimoto Y, Yoneyama K, Bouwmeester HJ (2008) Biosynthetic considerations could assist the structure elucidation of host plant produced rhizosphere signalling compounds (strigolactones) for arbuscular mycorrhizal fungi and parasitic plants. Plant Physiology and Biochemistry **46:** 617-626

Sakakibara H (2006) CYTOKININS: Activity, biosynthesis, and translocation. Annual Review of Plant Biology **57:** 431-449

Sánchez-Calderón L, Lopez-Bucio J, Chacon-Lopez A, Cruz-Ramirez A, Nieto-Jacobo F, Dubrovsky JG, Herrera-Estrella L (2005) Phosphate starvation induces a determinate developmental program in the roots of *Arabidopsis thaliana*. Plant Cell Physiology **46:** 174-184

Seo M, Koshiba T (2002) Complex regulation of ABA biosynthesis in plants. Trends in Plant Science **7:** 41-48

Sorefan K, Booker J, Haurogné K, Goussot M, Bainbridge K, Foo E, Chatfield S, Ward S, Beveridge C, Rameau C, Leyser O (2003) *MAX4* and *RMS1* are orthologous dioxygenase-like genes that regulate shoot branching in Arabidopsis and pea. Genes & Development **17:** 1469-1474

Stirnberg P, Furner IJ, Leyser HMO (2007) MAX2 participates in an SCF complex which acts locally at the node to suppress shoot branching. The Plant Journal **50:** 80-94

Stirnberg P, van de Sande K, Leyser HMO (2002) MAX1 and MAX2 control shoot lateral branching in Arabidopsis. Development **129:** 1131-1141

Tocquin P, Corbesier L, Havelange A, Pieltain A, Kurtem E, Bernier G, Perilleux C (2003) A novel high efficiency, low maintenance, hydroponic system for synchronous growth and flowering of *Arabidopsis thaliana*. BMC Plant Biology **3:** 2

Troughton A (1977) The effect of phosphorus nutrition upon the growth and morphology of young plants of *Lolium perenne L*. Annals of Botany **41:** 85-92

Turnbull CGN, Booker JP, Leyser HMO (2002) Micrografting techniques for testing long-distance signalling in Arabidopsis. The Plant Journal **32:** 255-262

Umehara M, Hanada A, Magome H, Takeda-Kamiya N, Yamaguchi S (2010) Contribution of strigolactones to the inhibition of tiller bud outgrowth under phosphate deficiency in rice. Plant and Cell Physiology**:** 1118-1126

Umehara M, Hanada A, Yoshida S, Akiyama K, Arite T, Takeda-Kamiya N, Magome H, Kamiya Y, Shirasu K, Yoneyama K, Kyozuka J, Yamaguchi S (2008) Inhibition of shoot branching by new terpenoid plant hormones. Nature **455:** 195-200

Walter MH, Floß DS, Hans J, Fester T, Strack D (2007) Apocarotenoid biosynthesis in arbuscular mycorrhizal roots: Contributions from

methylerythritol phosphate pathway isogenes and tools for its manipulation. Phytochemistry **68:** 130-138

Williamson LC, Ribrioux SPCP, Fitter AH, Leyser HMO (2001) Phosphate availability regulates root system architecture in Arabidopsis. Plant Physiology **126:** 875-882

Xie X, Yoneyama K, Yoneyama K (2010) The strigolactone story. Annual Review of Phytopathology **48:** 93-117

Yoneyama K, Takeuchi Y, Yokota T (2001) Production of clover broomrape seed germination stimulants by red clover root requires nitrate but is inhibited by phosphate and ammonium. Physiologia Plantarum **112:** 25-30

Yoneyama K, Xie X, Sekimoto H, Takeuchi Y, Ogasawara S, Akiyama K, Hayashi H (2008) Strigolactones, host recognition signals for root parasitic plants and arbuscular mycorrhizal fungi, from Fabaceae plants. New Phytologist **179:** 484-494

Yoneyama K, Yoneyama K, Takeuchi Y, Sekimoto H (2007) Phosphorus deficiency in red clover promotes exudation of orobanchol, the signal for mycorrhizal symbionts and germination stimulant for root parasites. Planta **225:** 1031-1038

Zhao Y (2010) Auxin biosynthesis and its role in plant development. Annual Review of Plant Biology **61:** 49-64

Zhu H, Riely BK, Burns NJ, Ane J-M (2006) Tracing nonlegume orthologs of legume genes required for nodulation and arbuscular mycorrhizal symbioses. Genetics **172:** 2491-2499

Chapter 7

Physiological effects of the synthetic strigolactone analog GR24 on root system architecture in Arabidopsis: another belowground role for strigolactones?

Carolien Ruyter-Spira*, Wouter Kohlen*, Tatsiana Charnikhova, Arjan van Zeijl, Laura van Bezouwen, Norbert de Ruijter, Catarina Cardoso, Juan Antonio López-Ráez, Radoslava Matusova, Ralph Bours, Francel Verstappen and Harro Bouwmeester

* contributed equally to this work

Adapted version published as Ruyter-Spira et al., (2011) Plant Physiology, 155, 721-734

Abstract

In this study, the role of the recently identified class of phytohormones, strigolactones, in shaping root architecture was addressed. Primary root lengths of strigolactone-deficient and -insensitive Arabidopsis (*Arabidopsis thaliana*) plants were shorter than those of wild-type plants. This was accompanied by a reduction in meristem cell number, which could be rescued by application of the synthetic strigolactone analog GR24 in all genotypes except in the strigolactone-insensitive mutant. Upon GR24 treatment, cells in the transition zone showed a gradual increase in cell length, resulting in a vague transition point and an increase in transition zone size. PIN1/3/7-green fluorescent protein intensities in pro-vascular tissue of the primary root tip were decreased, whereas PIN3-green fluorescent protein intensity in the columella was not affected. During phosphate-sufficient conditions, GR24 application to the roots suppressed lateral root primordial development and lateral root forming potential, leading to a reduction in lateral root density. Moreover, auxin levels in leaf tissue were reduced. When auxin levels were increased by exogenous application of naphthylacetic acid, GR24 application had a stimulatory effect on lateral root development instead. Similarly, under phosphate-limiting conditions, endogenous strigolactones present in wild-type plants stimulated a more rapid outgrowth of lateral root primordia when compared with strigolactone-deficient mutants. These results suggest that strigolactones are able to modulate local auxin levels and that the net result of strigolactone action is dependent on the auxin status of the plant. We postulate that the tightly balanced auxin-strigolactone interaction is the basis for the mechanism of the regulation of the plants' root-to-shoot ratio.

Keywords: Arabidopsis, root system architecture, strigolactones, GR24, PIN

Introduction

Strigolactones, exuded from plants, have been known for a long time to act as germination stimulants for seeds of root parasitic plants such as Orobanche and Striga spp. (Cook et al., 1966; Bouwmeester et al., 2007). As root parasitic plants consume a large proportion of the host plants' solutes, they cause wilting and early plant death. Initially, the discovery that strigolactones are also involved in the symbiotic interaction with arbuscular mycorrhizal fungi (Akiyama et al., 2005) was believed to provide an explanation for why the host plants' capacity to produce strigolactones was not lost during evolution. Because arbuscular mycorrhizal fungi are potent providers of nutrients such as phosphate and nitrogen to their host, the observation that phosphate starvation induced strigolactone biosynthesis in host plants' roots was not surprising (Yoneyama et al., 2007; López-Ráez et al., 2008; Umehara et al., 2008). The recent discovery that strigolactones, or closely related compounds, also act as phytohormones inside the host plants and are involved in the inhibition of axillary bud outgrowth (Gomez-Roldan et al., 2008; Umehara et al., 2008) is an additional explanation why plants continue to produce these fatal germination stimulants: plants use the strigolactones to adjust their shoot architecture to the ever-changing environmental conditions. Indeed, phosphate starvation was shown to reduce the number of shoot branches (Cline, 1997), which was recently proven to be related to increased strigolactone production observed under these conditions (Umehara et al., 2010; Kohlen et al., 2011).

The discovery that strigolactones are the same as, or are at least closely related to this branching inhibiting signal (BIS), which is a major player in the process of apical dominance, unexpectedly merged two worlds of research and provides new mutual tools and insights. Early studies on BIS revealed that it concerns a mobile, long-distance signal, which moves acropetally (Turnbull et al., 2002; Sorefan et al., 2003; Booker et al., 2005). In Arabidopsis (*Arabidopsis thaliana*), the carotenoid dioxygenases MORE AXILLARY GROWTH3 (MAX3; AtCCD7), MAX4 (AtCCD8), and the cytochrome P450 MAX1 (AtCyp711A1) are involved in the biosynthesis of BIS (Turnbull et al., 2002; Sorefan et al., 2003; Booker et al., 2005; Auldridge et al., 2006), whereas the F-box and Leu-rich repeats containing MAX2 protein probably acts either in signal perception or transduction (Stirnberg et al., 2002; Booker et al., 2005; Stirnberg et al., 2007). Plants mutated in any of the MAX genes all display increased numbers of shoot branches. This mutant phenotype can be rescued by the application of the synthetic strigolactone analog GR24 (Gomez-Roldan et al., 2008; Umehara et al., 2008) in a MAX2-dependent manner.

Besides strigolactones, auxin is another phytohormone that is essential during the process of shoot branching control in apical dominance. In contrast with strigolactones, auxin moves basipetally in the main stem and indirectly controls axillary bud outgrowth (Booker et al., 2003). In a recent study by Hayward (Hayward et al., 2009), it was shown that auxin positively regulates the expression of the strigolactone biosynthetic genes *MAX3* and *MAX4*. Reduced local endogenous auxin levels, in naphthylphthalamic acid (NPA)-treated or decapitated plants, resulted in a reduction of the expression levels of these genes. In addition, Bainbridge (Bainbridge et al., 2005) showed that auxin can locally induce *MAX4* expression in the root tip. Strigolactone-deficient *max* mutant plants carrying the auxin reporter gene DR5-GUS were shown to have relatively high GUS intensities in vascular tissue of the lower stem (Bennett et al., 2006), suggesting elevated auxin levels. Recently, Prusinkiewicz (Prusinkiewicz et al., 2009) indeed demonstrated the presence of increased auxin levels in the polar transport stream of *max4*. Furthermore, an increase in polar auxin transport capacity, elevated mRNA levels of the polar auxin efflux carrier PIN1, and higher pPIN1-GUS activity in *max* mutants have been reported by Bennett (Bennett et al., 2006). Finally, Crawford (Crawford et

al., 2010) demonstrate that polar auxin transport can be reduced by exogenous application of GR24 and induced endogenous strigolactone production in a *max1* mutant background. The combination of these results suggests that strigolactones and auxin tightly interact and modulate each other's levels and distribution through a feedback mechanism (Hayward et al., 2009).

Also, root growth and root branching are tightly regulated processes coordinately controlled by several plant hormones, of which auxin is playing a key role. Shoot-derived auxin is delivered to the root tip through the polar transport stream that is facilitated by proteins of the PIN family. In the columella root cap, auxin is redistributed laterally toward the epidermal and cortical cell layers where acropetal auxin transport toward the elongation zone establishes a local auxin gradient regulating cell division and elongation. Finally, auxin is returned to the polar transport stream again (Blilou et al., 2005; Leyser, 2009). During this process of PIN activity–dependent auxin recirculation inside the root tip, lateral root (LR) initiation is triggered by the local accumulation of auxin in root pericycle cells adjacent to the xylem vessels (Casimiro et al., 2001; De Smet et al., 2006; De Smet et al., 2007; Dubrovsky et al., 2008; Lucas et al., 2008). Subsequent tightly regulated cell division will then lead to LR primordial development and finally to emergence of a young LR from the parent root.

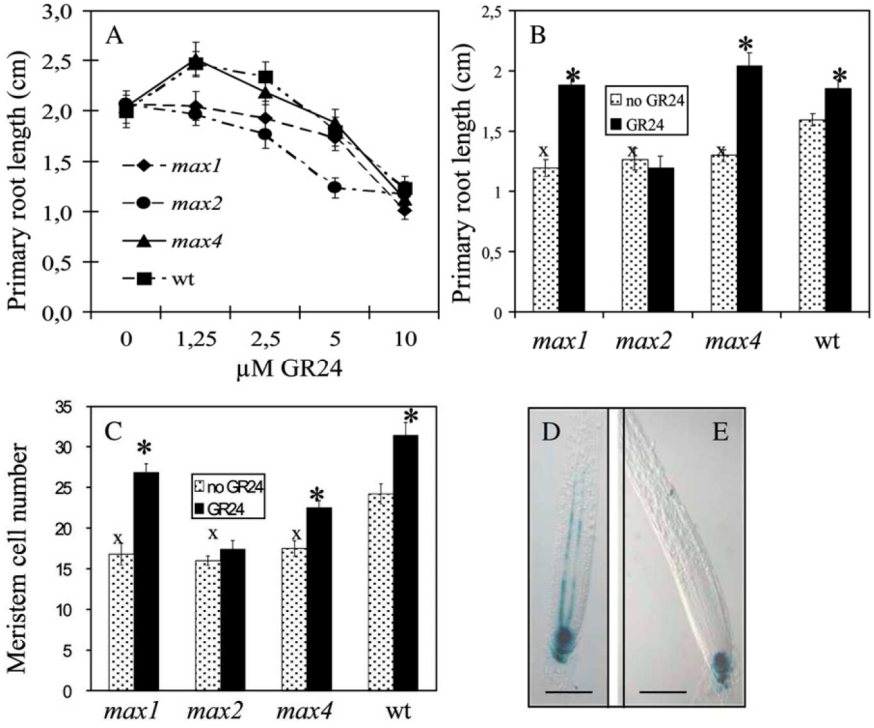

Figure 1: GR24 affects primary root length in a concentration-dependent way. **(a)**, Primary root lengths of 8-d-old max1-1, max2-1, max4-1, and wild-type (wt) Arabidopsis plants grown on vertical MS plates containing 0.5% Suc and different levels of GR24. **(b)**, Primary root length of 12-d-old plants grown on vertical MS plates containing no Suc and 0 or 2.5 µm GR24. Data are means ± se (n = 16–20). **(c),** Cortical meristem cell number, expressed as the number of cells in one cell file extending from the quiescent center to the first elongated cell, of 7-d-old Arabidopsis plants grown on vertical MS plates containing 0.5% Suc and 0 or 2.5 µm GR24. Data are means ± se (n = 5). Marks indicate a statistically significant difference compared with untreated (asterisk) or wild-type plants (x) as determined by Student's t test ($P < 0.05$). **(d-e),** Nomarski images of GUS-stained primary roots of max4 **(d)** and wild-type **(e)** plants containing the DR5-GUS reporter construct. Bars = 0.1 mm.

In contrast with LR initiation, LR development is supported by auxin coming directly from the aerial part of the plant (Bhalerao et al., 2002). To allow and sustain lateral auxin influx from the polar auxin transport stream into the developing LR, PIN1 polarity is rearranged. This dynamic repolarization is mediated by endocytic recycling of the PIN1 protein (Jaillais et al., 2007). The subsequent establishment of a proper auxin gradient inside the developing LR primordia, which is also mediated by members of the PIN protein family, is crucial for correct LR development (Benková et al., 2003). Finally, at the stage when an autonomous meristem is formed, the LR primordium is able to produce its own auxin and becomes independent of auxin from the shoot (Casimiro et al., 2003).

Because auxin and auxin transport play such crucial roles in defining root system architecture (RSA) and strigolactones have been suggested to play a role in regulating auxin fluxes, we investigated the contribution of this new plant hormone to root developmental processes. In this study, we describe the effect of application of the synthetic strigolactone GR24 on primary root and LR development in relation to auxin in both strigolactone-deficient and -insensitive Arabidopsis mutants carrying the auxin reporter construct DR5-GUS. We report that GR24 application has a dual effect on primary root length, LR development, and LR initiation, of which the net result is dependent on the auxin status of the plant. Our results suggest that these effects are mediated through the modulation of local auxin levels in the root tip and developing lateral root primordia (LRP) and a reduction in free auxin levels in the aerial parts of the plant. Finally, we hypothesize that strigolactones are responsible for the changes in RSA of Arabidopsis plants growing under phosphate-limiting conditions.

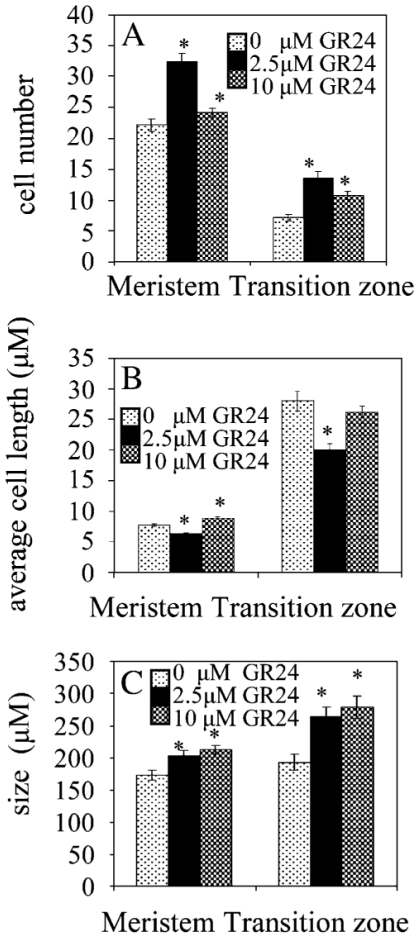

Figure 2: Application of GR24 affects cortical root cell number and length of the meristem and transition zone in a concentration-dependent way. **(a),** Average cortical cell number present in a cell file starting from the quiescent center throughout the meristem and transition zone. **(b),** Average length of cortical cells in meristem and transition zone. **(c),** Meristem and transition zone size. Measurements were performed using 7-d-old wild-type plants grown in the presence of different concentrations of GR24. Data are means ± se (n = 12–16). Asterisks indicate a statistically significant difference between treated and untreated plants ($P < 0.05$).

Results

Application of the strigolactone analog GR24 leads to a MAX2-dependent increase in primary root length

Growth and development of roots of 8-, 11-, and 14-dold Arabidopsis seedlings of the strigolactone biosynthesis mutants *max1-1* and *max4-1*, the strigolactone signaling mutant *max2-1*, and their corresponding wild-type (Columbia-0) was examined. Plants were grown in the presence of different concentrations, ranging from 1.25 to 10 µM, of the synthetic strigolactone analog GR24. This concentration range was based on the level of GR24 required for a complete rescue of the branched phenotype of the *max1*, *3*, and *4* mutant plants (data not shown). Application of 1.25 µM GR24 resulted in increased primary root lengths in eight-day-old wild-type plants and *max4* but not in *max1* and *max2* (Figure 1a). GR24 concentrations above 2.5 to 5 µM inhibited primary

root elongation in a MAX2-independent manner. In 11- and 14-d-old plants, the increase in root length was not observed anymore (data not shown). To explore the possibility that under optimal growing conditions a general high rate of primary root growth could obscure the specific root growth stimulating effect of GR24, plants were subsequently grown under less favorable conditions. Because carbohydrate starvation leads to a decrease in primary root length that is not mediated through reduced meristem activity (Jain et al., 2007), Sucrose was omitted from the medium. Under these conditions, all genotypes, including *max1*, but not *max2*, showed a clear response to GR24 (2.5 µM) treatment, further confirming that the response to GR24 is mediated through MAX2 (Figure 1b). Moreover, roots of untreated max mutant plants were significantly shorter than those of untreated wild-type plants. This correlated with a lower number of cortical cells in the primary root meristem (Figure 1c) and a higher DR5-GUS intensity in primary root tips of *max* mutant plants containing the auxin reporter construct DR5-GUS (Figure 1d-e). Finally, GR24 application at 2.5 µM resulted in an increase in meristem cortical cell number in all genotypes except *max2* (Figure 1c).

GR24-mediated increase in primary root length is accompanied by an increase in meristem and transition zone sizes

To further investigate the effect of GR24 on meristem cells as well as on cells present in the transition zone (the region between meristem and elongation zone), the number and length of all root cortical cells in one cell file extending from the 10th cell above the quiescent center until the elongation zone were determined in wild-type plants. By plotting the cell number of individual plants against their cumulative cell length, an impression of root cell dynamics in response to different concentrations of GR24 is obtained (Supplemental Figure S7.1a–c). Application of 2.5 µM GR24 resulted in a tremendous increase in the number of cells in this region (Figure 2a). When 10 µM GR24 was applied, the meristem and transition zones only showed a minor increase in cell number when compared with untreated plants (Figure 2a). For both GR24 concentrations, cells in the transition zone showed a strikingly slow and irregular increase in cell length before they reached their final stabilized elongated state (Supplemental Figure S7.1b–d). Cells in the meristem zone of plants treated with 2.5 µM GR24 were shorter than in untreated plants, whereas 10 µM GR24 treatment resulted in a small increase in meristem cell length (Figure 2b). Both GR24 concentrations resulted in decreased cell lengths in the transition zone. Despite these reduced cell sizes, the increased cell numbers of the transition zone finally gave rise to an increase in transition zone size (Figure 2c). Also, meristem size was increased by both GR24 treatments. With the higher doses of GR24 (5–10 µM), root curvature was induced in some plants (Supplemental Figure S7.1e). When primary root tips of these plants were studied using confocal microscopy, a distortion of the columella

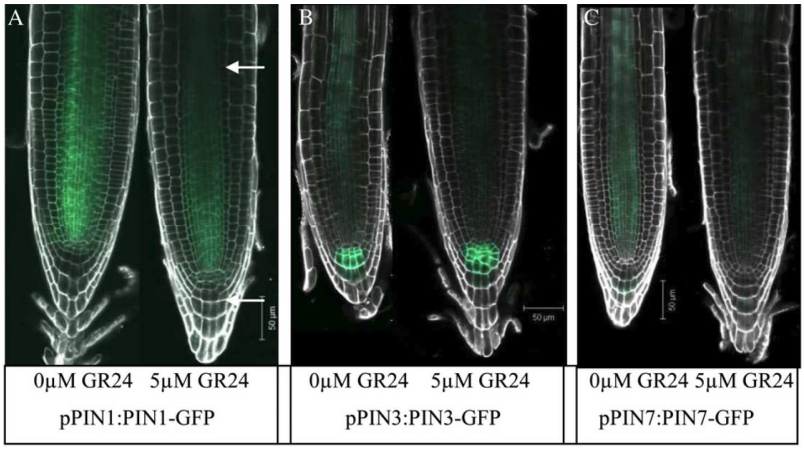

Figure 3: PIN-GFP protein levels and localization in roots of GR24-treated and untreated Arabidopsis plants. **(a-c),** Confocal midplane sections of roots of untreated and 5 µm GR24-treated 6-d-old plants carrying the pPIN1:PIN1-GFP **(a),** pPIN3:PIN3-GFP **(b),** and pPIN7:PIN7-GFP **(c)** transgenes. The upper arrow indicates the provascular region, and the lower arrow indicates the localization of the columella. PI-stained cell walls are represented in white. The intensity of the GFP signal was quantified by converting RGB pixels to brightness values using the program ImageJ (Abramoff et al., 2004).

and quiescent center was observed (Supplemental Figure S7.1f).

The localization of the transition point, as well as the size of the meristem and transition zone, is largely controlled by the local establishment of an auxin gradient. High auxin levels stimulate cell proliferation, whereas low auxin levels favor cell elongation. The establishment of the auxin concentration gradient in the cortical meristem and transition zone is regulated by auxin efflux facilitating proteins of the PIN family. These proteins jointly control the recirculation of auxin in the root tip (Blilou et al., 2005).

To explore a potential effect of GR24 on the levels and distribution of the PIN1, PIN2, PIN3, and PIN7 proteins, which are involved in this auxin circulation process, we examined six-day-old wild-type plants carrying constructs encoding the respective PINpromoter-PINprotein-GFP fusion proteins. In the provascular region, application of 2.5, 5 (Figure 3), and 10 µM GR24 resulted in a significant ($P < 0.05$) reduction in GFP intensity in the PIN1 (38% reduction), PIN3 (50% reduction), and PIN7 (73% reduction) reporter lines. There was no significant effect on PIN2-GFP levels (data not shown). In the columella, treatment with 2.5 µM GR24 resulted in a minor reduction in PIN7-GFP intensity, while the level of PIN3-GFP was not significantly affected. Interestingly, upon GR24 treatment, PIN3-GFP signal was observed in a larger number of columella cells that also displayed irregular shapes (Figure 3b). Although the latter was also occasionally observed in GR24-treated nontransformed plants, the incidence was higher in transgenic plants carrying the pPIN3:PIN3-GFP construct. Finally, root curvature was found to be associated with this distortion of columella cells.

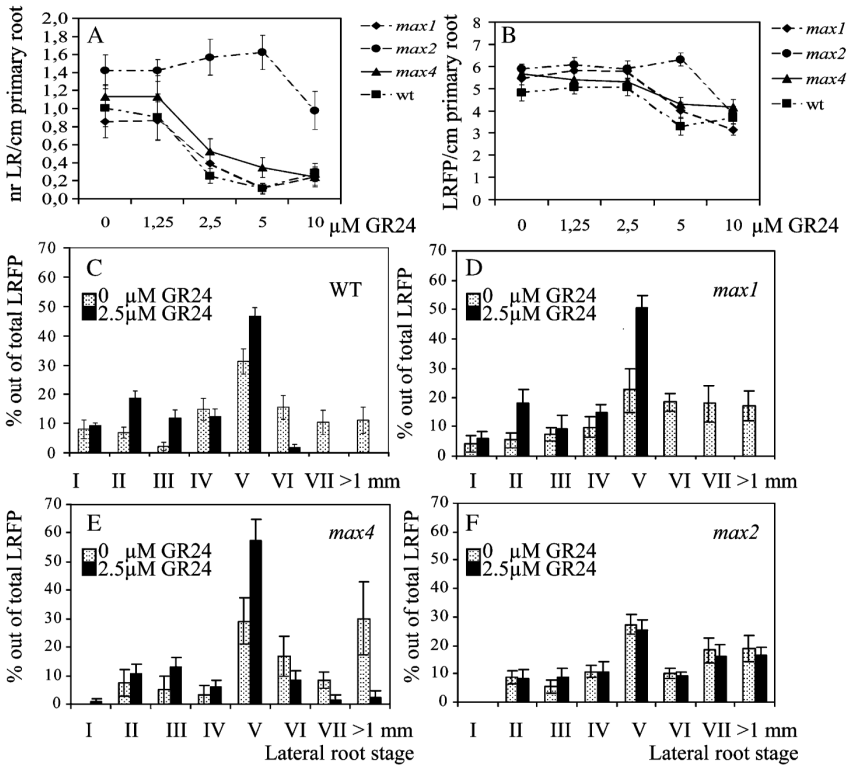

Figure 4: GR24 treatment decreases LRD **(a)** and total LRFP **(b)** and delays LR development **(c–f).** LRFP is defined as the sum of all LRs plus LRP. max1-1, max2-1, max4-1, and wild-type (wt) plants were grown either on a range of GR24 levels **(a-b)** or on a fixed concentration of 2.5 µm GR24 **(c–f)** on vertical MS plates with **(a-b)** or without **(c–f)** 0.5% Suc and were evaluated at 14 **(a-b)** or 12 **(c–f)** d after germination. Data are means ± se (n = 20–25). LR developmental stages were characterized according to the scheme of Malamy and Benfey (1997).

GR24 decreases LR density through a suppression of LR outgrowth and a reduction in LR-forming potential

GR24 also affected lateral root density (LRD) and total lateral root-forming potential (LRFP). The latter is defined as the sum of emerged LRs plus LRP. At concentrations of 2.5 and 5 µM GR24, the

biosynthetic *max* mutants (*max1* and *max4*) and wild-type Arabidopsis showed a significant reduction in LRD but not *max2* (Figure 4a). A MAX2-independent decrease in LRD was observed at the highest concentration of 10 µM GR24. LRFP was not affected at the lower concentrations of 1.25 and 2.5 µM GR24.However, at 5 µM GR24, a clear MAX2-dependent decrease was observed (Figure 4b). Finally, like LRD, LRFP also was negatively affected in the *max2* mutant line when 10 µM GR24 was applied.

Because at 2.5 µM GR24 LRD was decreased while LRFP was not affected, it seems likely that at this concentration the reduction in LRD is caused by a reduction in LRP outgrowth. To explore this assumption and assess whether LR outgrowth was affected randomly or if it concerned the suppression of a specific LRP developmental stage, all LRP in the primary roots of all genotypes under investigation were classified and counted according to the histological scale of Malamy and Benfey (Malamy and Benfey, 1997). For each stage, the number of LRP was expressed as a percentage of the total LRFP. GR24 treatment resulted in a significantly higher accumulation of LRP stage V in all genotypes except *max2* (Figure 4c–f). Also, 2.5 µM GR24 almost completely suppressed the developmental transition of LRP stage V into stage VI and abolished LR formation in both the wild-type and *max1*, but much less so in *max4*, and it did not affect *max2*.

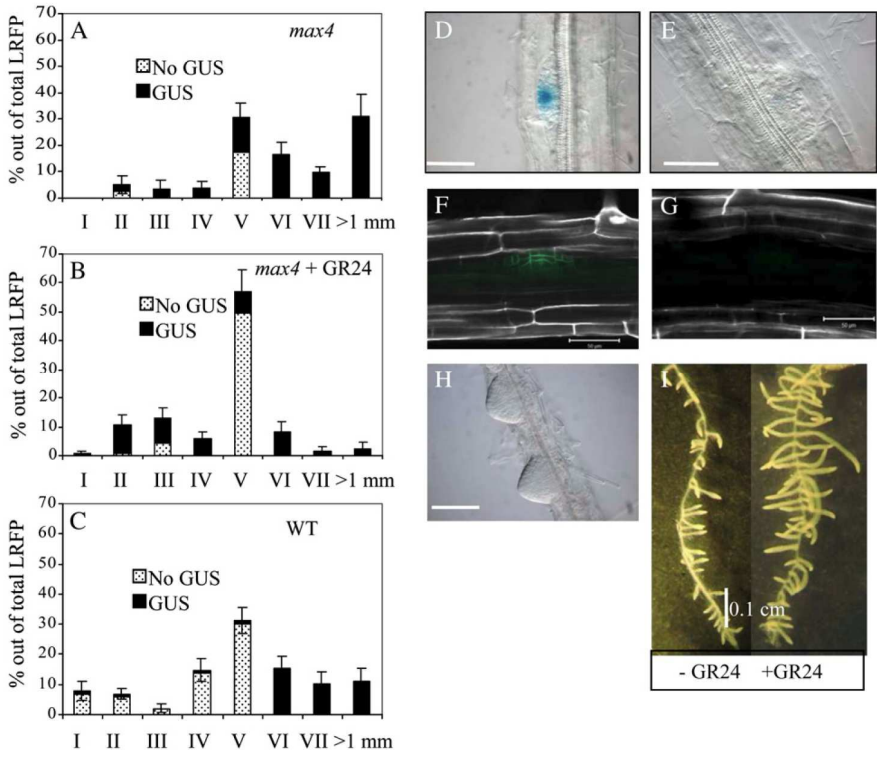

Figure 5: The GR24-induced accumulation and developmental arrest of stage V LRP is mediated through an increase in the percentage of stage V LRP associated with low or no intensities of DR5-GUS. Untreated max4-1 **(a)** and wild type (WT; **c**) and treated (2.5 µm GR24) max4-1 plants **(b)** carrying the DR5-GUS transgene were grown on vertical MS plates and GUS stained when plants were 12 d old. LRP were characterized according to Malamy and Benfey (1997). For each developmental stage, DR5-GUS intensities were scored and the percentage out of the total LRFP was calculated. Data are means ± se (n = 15–20). **(d-e),** Nomarski microscopy images of a GUS-stained stage V LRP showing DR5-GUS intensities and distribution patterns representative for the majority of nonarrested stage V LRP **(d)** and arrested stage V LRP **(e).** Scale bars represent 50 µm. **(f-g),** Confocal microscopy images of untreated **(f)** and GR24-treated (2.5 µm; **g**) wild-type plants carrying the pPIN1:PIN1-GFP transgene. Scale bars represent 50 µm. When plants are grown in the presence of high exogenous auxin levels, the suppressive effect of GR24 on LRP development is lost while LR outgrowth is enhanced. **(h),** Wild-type plants, pregrown for 5 d on standard vertical MS plates, were transferred to MS plates containing 10 µm IAA in combination with 10 µm GR24. The Nomarski image was taken 72 h after the start of the treatment. Scale bar represents 100 µm. I, Image taken 8 d after start of the treatment, showing LR elongation and increased LR density of the GR24-treated plants.

LR development is primarily determined by auxin signaling (for review, see Woodward and Bartel, 2005). To explore if the suppressive effect of GR24 on LRP outgrowth is mediated through the modulation of auxin levels and/or auxin distribution patterns in LRP, the percentage of LRP associated with GUS staining of the auxin reporter gene construct DR5-GUS present in

GR24-treated and untreated *max4* plants was determined. Although LRP with low (or absent) DR5-GUS levels were observed in untreated *max4* plants (Figure 5a), GR24 treatment resulted in a strong increase in the percentage of non-DR5-GUS-stained stage V LRP in *max4* (Figure 5b). Wild-type plants (producing endogenous strigolactones) also exhibited more non-GUS-stained stage V LRP than *max4* (Figure 5c-e), suggesting that the effect of GR24/endogenous strigolactones on LR outgrowth is mediated through a reduction in free auxin levels, thereby leading to an arrest in LRP development. Arrested stage V LRP (Figure 5e) were not able to form the polarized central cell files that are characteristic of stage VI LRP. Because PIN1 activity contributes to the formation of an auxin gradient that is directing cellular organization in developing LRP (Benková et al., 2003), we studied PIN1-GFP abundance in GR24-treated and untreated wild-type stage V LRP expressing *pPIN1*:*PIN1-GFP*. Figure 5f-g, shows that GR24 treatment resulted in decreased PIN1-GFP intensities.

The effect of GR24 on LRP development and outgrowth is dependent on the auxin status of the plant

To investigate the auxin-mediated nature of strigolactone action, the effect of GR24 in the presence of high exogenous levels of auxin was investigated. Wild-type plants were grown for 5 d on vertical plates and subsequently transferred to plates containing 10 μM of the naturally occurring auxin indole-3-acetic acid (IAA) or 2.5 μM of the synthetic auxin naphthylacetic acid (NAA), either supplemented with or without 5 or 10 μM GR24. Roots were evaluated after 12, 24, and 72 h and after 8 d. NAA and IAA treatment strongly stimulated the initiation of LRP. GR24 treatment did not affect the timing of LRP initiation. All LRP in all treatments readily developed into LRs without showing any sign of deviating cellular organization (Figure 5h), indicating that the previously observed inhibitory effect of GR24 on LR development is absent if enough auxin is supplied to the developing LRP. Treatment with 5 μM GR24 did not reduce PIN1-GFP intensities in developing LRP of NAA-treated (2.5 μM) plants (data not shown), suggesting that the previously observed reduction in PIN1-GFP intensity is a secondary effect caused by reduced auxin levels. Only when 10 μM GR24 was applied, a minor decrease in pPIN1:PIN1-GFP intensity was observed. Still, a physiological effect of 5 μM GR24 on LRP development was observed. In contrast with the previous observations showing an inhibitory effect of GR24 application on LRP development, simultaneous application of 2.5 μM NAA and 5 μM GR24 resulted in a stimulation of LRP development. Moreover, after 8 d of treatment, GR24 application resulted in significantly longer roots (0.5 instead of 0.4 mm; $P < 0.02$) in both NAA- and IAA-treated plants (Figure 5i). Surprisingly, LRD also increased from 41 to 64 LR/cm ($P < 0.0005$) as a result of GR24 application.

These results suggest that the physiological response upon GR24 treatment is mediated through a modulation of local auxin levels and is therefore dependent on the auxin status and/or sensitivity of the plant. To test this hypothesis, the effect of GR24 on LR development was investigated in *max* mutant and wild-type plants grown under phosphate starvation. Pérez-Torres (Pérez-Torres et al., 2008) showed that the increase in LR formation in Pi-starved Arabidopsis seedlings is, at least in part, mediated by an increase in auxin sensitivity of root cells. Plants were grown for 5 d under Pi-sufficient conditions and then transferred to plates containing a limiting (20 μM) phosphate concentration supplemented with or without 2.5 μM GR24. The distribution of the different LRP stages was determined 12 d after germination. In wild-type plants, GR24 application resulted in a reduction in the proportion of emerged LRs (Supplemental Figure S7.2a). However, GR24 failed to reduce this proportion in the *max* mutants (Supplemental Figure S7.2b-c). This is also reflected by the absence of a clear effect of GR24 on the accumulation of stage V LRP in these latter genotypes, which did occur in the wild-type. Apparently, the combination of higher initial DR5-GUS intensities as

observed in *max* mutant roots, either suggesting elevated auxin levels or increased auxin sensitivity, and the increased auxin sensitivity induced by phosphate deprivation (López-Bucio et al., 2002; Pérez-Torres et al., 2008) together lead to a loss of the inhibitory effect of GR24 on LR development.

GR24-induced suppression of LRP outgrowth is partially mediated through decreased shoot-derived auxin levels

LRP development is stimulated by shoot-derived auxin. To explore whether the GR24-mediated reduction in DR5-GUS levels in LRP, leading to the suppression of LRP development, could have been mediated through reduced auxin levels in the aerial parts of the plants, DR5-GUS intensities in the rosette leaves and cotyledons of transgenic DR5-GUS *max* and wild-type plants were studied. Plants were grown for 12 d on Murashige and Skoog (MS) agar plates containing 0, 1.25, 2.5, 5, or 10 μM GR24. All GR24 concentrations tested decreased DR5-GUS intensities in the leaf margins and the tissue surrounding the hydathodes (Figure 6a-b), which are the primary sites of auxin production in young Arabidopsis plants (Aloni et al., 2003). The observed reduction was dependent on the presence of MAX2 (Figure 6c). Besides decreased DR5-GUS levels around the auxin biosynthesis sites, vascularization between hydathodes and leaf veins was also negatively affected (Figure 6a-b). Quantification of auxin in leaf material from *max2* and *max4* mutant lines using liquid chromatography-tandem mass spectrometry showed a 79% reduction in auxin levels of *max4* (14.44–2.98 pg/mg fresh weight, Student's *t* test, $P = 0.013$) upon GR24 treatment, while no significant reduction was observed when *max2* was treated with GR24. Finally, the leaf surface area was decreased by application of 2.5 μM GR24 in a MAX2-dependent way (Supplemental Figure S7.3).

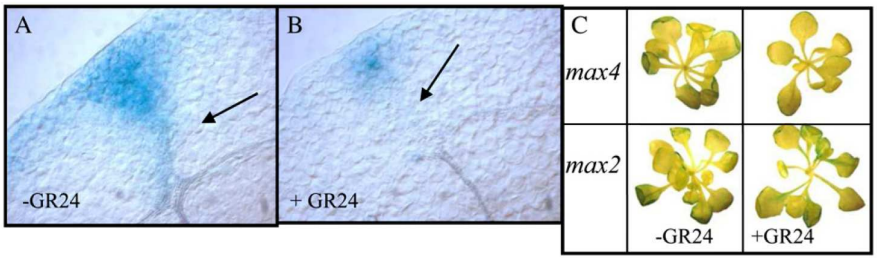

Figure 6: GR24 treatment results in decreased intensities of the auxin reporter DR5-GUS in aerial parts of the plant. **(a-b)**, Close-up of a leaf of an untreated **(a)** and GR24-treated **(b)** max4-1 plant. Arrows point at the locations where developing vasculature is either present (a) or absent (b). **(c)**, GUS staining of the leaves of 12-d-old max4-1 and max2-1 plants carrying the DR5-GUS transgene grown in the presence or absence of 2.5 µm GR24 showing that the decrease in GUS intensities is dependent on MAX2.

Endogenous strigolactones stimulate LR outgrowth during phosphate-Limiting conditions

Because the high levels and potential ectopic localization of GR24 may obscure the true effects that endogenous strigolactones have on root system architecture, the relevance of endogenous strigolactones in determining RSA was investigated.

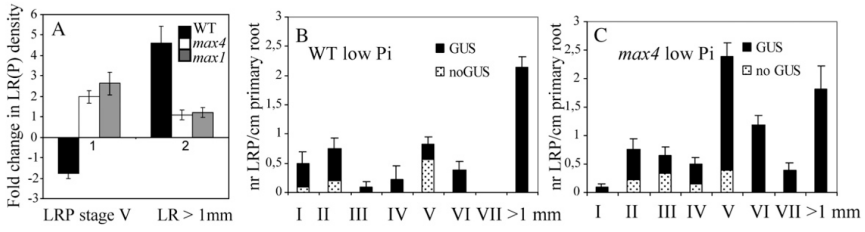

Figure 7: Endogenous strigolactones in wild-type (WT) plants allow a more rapid development of LRP into LRs during phosphate-limiting conditions. (a), Graph showing fold change in LRP V and LRD of 12-d-old wild-type, max4-1, and max1-1 plants as a response to Pi-limiting conditions relative to sufficient Pi conditions. Plants were pregrown for 5 d on vertical MS plates containing sufficient Pi levels (1.5 mm), after which all plants were transferred to either Pi-deficient (20 µm Pi) or Pi-sufficient MS plates. (b-c), DR5-GUS distribution in LRP of wild-type (a) and max4-1 (c) plants carrying the DR5-GUS transgene grown under Pi-limiting conditions showing that the majority of the highly accumulated max4-1 stage V LRP is associated with extremely high GUS intensities. Data are means ± se (n = 15–20).

Therefore, LR development in 12-d-old *max1*, *max4*, and wild-type plants grown under Pi-sufficient and Pi-limiting conditions was studied. Under Pi-sufficient conditions, LRFP was equal for all genotypes (data not shown). However, *max4* plants showed a significantly ($P < 0.05$) higher LRD than wild-type plants, implying that during Pi-sufficient conditions, the endogenous strigolactones of wild-type plants had a suppressive effect on LR development (Supplemental Figure S7.4a).
However, phosphate limitation in the wild-type resulted in an almost 2-fold decrease in LRP of stage V and a more than 4-fold increase in LRD (Supplemental Figure S7.4b). In the *max* mutants, phosphate limitation induced accumulation of stage V LRP instead. DR5-GUS-mediated visualization of the auxin status of all stages of LRP in wild-type and *max4* plants grown under Pi-limiting conditions revealed that the majority of the accumulated stage V LRP of *max4* plants consisted of intensely stained cells (Figure 7b-c).

Discussion

In this study, a novel role for strigolactones in determining root architecture through an effect on primary root growth and LR development is described. Evidence for this role is provided by experiments studying the application of the synthetic strigolactone analog GR24 (discussed in the first half of the discussion). Differences in root architecture between wild-type and strigolactone-deficient plants provide evidence for the role of endogenous strigolactones in this trait. This, together with a broader view on strigolactone action at the whole-plant level, is discussed in the second half of the "Discussion."

GR24 affects primary root growth in a concentration-dependent manner
Arabidopsis plants, grown in the presence of different concentrations of GR24, showed an increase in primary root length at lower levels of GR24 (1.25 and 2.5 μM) and a decrease at higher levels of GR24 (Figure 1a). This decrease was also observed in *max2*. Because a high dose of GR24 also affects the entire plant's appearance and fitness, this is likely to be the result of general toxicity. Still, a high dose of GR24 did not disturb the GR24-specific elongating effect on meristem and transition zone size (Figure 2) and could explain why the primary root length in *max2* shows a stronger decrease at 5 μM GR24 when compared to the other genotypes.
Unexpectedly, *max1* did not show the initial increase in primary root length upon 1.25 μM GR24 application as was observed in *max4* and wild-type plants (Figure 1a). This may be due to a so far unexplained reduced sensitivity to GR24, which was also observed when a concentration range of GR24 was used to rescue the branching phenotype of the *max1*, *max3*, and *max4* mutants (data not shown). Because root length was significantly reduced in all genotypes at 5 and 10 μM GR24, indicating a general *MAX2*-independent response, a putative *MAX2*-dependent increase in *max1* root lengths at higher GR24 levels could have been masked. Although Kohlen (Kohlen et al., 2011) show that the Arabidopsis *max1* mutant is compromised in strigolactone levels, it could be that MAX1 is also involved in more downstream hydroxylation steps and is able to modify the synthetic strigolactone GR24 increasing its biological activity.

GR24-mediated changes in root meristem patterning are indicative of altered local auxin concentrations
The effect of GR24 on primary root growth is accompanied by a GR24 concentration-dependent change in both cell number and cell length of cells located in the root meristem and transition zones (Figure 2). Since high auxin levels are known to stimulate cell division whereas low auxin levels favor

cell elongation, it can be concluded that lower levels (2.5 μM) of GR24 induce an increase in auxin levels in the primary root meristem, while higher doses tend to reduce these levels. These responses reflect the auxin-mediated nature of strigolactone action. Local auxin concentrations are established by the combined action of five auxin efflux proteins of the PIN family, jointly regulating auxin fluxes circulating in the primary root tip (Blilou et al., 2005). Therefore, auxin transport is a major contributor to root meristem patterning (Sabatini et al., 1999; Friml et al., 2003) . Prusinkiewicz (Prusinkiewicz et al., 2009) suggested that strigolactones act by modulating PIN protein cycling between the plasma membrane and endomembrane system, hereby regulating the allocation of PINs to the plasma membrane. A GR24-mediated reduction in PIN protein cycling would then result in a decrease in auxin transport capacity in vascular tissue of both root and shoot, as these are the main sites of *MAX2* expression (Stirnberg et al., 2007). Indeed, it was recently demonstrated that both endogenous strigolactones and GR24 are able to reduce basipetal auxin transport (Crawford et al., 2010). This could finally explain the changes in root meristem patterning we observed in this study. In an in silica study in which reduced auxin transport was enforced by simulating a reduction in vascular *PIN* expression, increased auxin levels were also observed in the border cells (defined as the layer of cells between the vascular and epidermal region) of the primary root tip (Grieneisen et al., 2007). Although the underlying cause for reduced auxin transport in that study may differ from this study, it illustrates that a GR24-mediated reduction in auxin transport is likely to be involved. Interestingly, in the same modeling work, Grieneisen (Grieneisen et al., 2007) also show that the absence of lateral epidermal PINs, responsible for the auxin reflux to the main polar transport stream, results in a more spread out and uneven auxin distribution. This is provoking the loss of a clear transition point separating the meristem zone from the elongation zone, which was also observed in this study. The latter may thus be the consequence of a negative effect of GR24 on the efficiency of these lateral epidermal PINs.

Biological relevance of the GR24-mediated changes in root meristem patterning

The contribution of the GR24-mediated increase in transition zone size to the total increase in primary root length is relatively high (Figure 2c). Expansion of the transition zone is also observed in radicle growth during seed germination (Sliwinska et al., 2009). Interestingly, in Arabidopsis, the strigolactone biosynthetic gene *CCD8* is specifically expressed in the root cortical and epidermal cells of the transition-elongation zone upon auxin treatment (Bainbridge et al., 2005). Moreover, *MAX2* expression also is elevated in this part of the root (Brady et al., 2007). Therefore, strigolactone-mediated modulation of the lateral auxin reflux, which occurs in this particular region, could be responsible for the increase in transition zone size during radicle growth. It is not unlikely that this process is at the basis of the germination of seeds of most plant species, including parasitic plants. Still, the underlying mechanism for exogenous strigolactone dependency of parasitic plant germination remains an intriguing issue.

Interesting is the GR24-induced lateral expansion of PIN3 protein localization to adjacent cells in the root cap. The disturbed cellular organization in this region furthermore suggests irregular cell divisions (Figure 3b). If strigolactones are involved in PIN protein cycling as suggested by Prusinkiewicz (Prusinkiewicz et al., 2009), a GR24-mediated distortion of PIN3 polarization could have resulted in non-regular auxin fluxes and ectopic PIN3 distribution. Asymmetric lateral distribution of the PIN3 protein, leading to auxin asymmetry in the elongation zone, is also characteristic for the induction of root curvature during gravitropism (Friml et al., 2002; Ottenschläger et al., 2003) and may explain the observed induction of root curvature in this study when using higher levels of GR24 (Supplemental Figure S7.1E). In tomato (*Solanum lycopersicum*), Koltai (Koltai et al., 2010) also

observed asymmetric root growth with high levels of GR24 (27 μM). In our study, root curvature was found to be associated with a distortion of the columella and quiescent center (Supplemental Figure S7.1F). Interestingly, especially in the view of the effect of GR24 on auxin levels in the leaves, a similar collapse of this structure was observed in primary root tips that were depleted of auxin (Friml et al., 2004).

It would be of interest to explore whether strigolactones are involved in stimulating directional growth of the parasitic plants' radicle toward the host root. Asymmetric perception of exuded strigolactones by the parasitic plants' radicle might lead to a single-sided reduction in PIN cycling efficiency and subsequent auxin accumulation. As in gravitropism, this would result in the redirection of radicle growth, in this case toward the strigolactone source, the host root.

GR24 application leads to a reduction of auxin levels in leaf tissue

GR24 reduces the intensity of the auxin reporter DR5-GUS and auxin levels in young expanding rosette leaves in a MAX2-dependent way. This is accompanied by a decrease in the number of vascular connections between the auxin production sites surrounding the hydathodes and the major leaf veins. Also, a reduction in leaf size was observed that is a known consequence of a reduction in auxin content (Ljung et al., 2001). Because *MAX2* is expressed in vascular tissue throughout the entire plant, it is likely that the putative GR24-mediated reduction in PIN1 cycling as suggested by Prusinkiewicz (Prusinkiewicz et al., 2009) also occurs in vascular tissue of the leaf and stem resulting in a decrease in auxin transport capacity. Besides this effect, a GR24-induced reduction in PIN1 cycling could also be responsible for a reduction in the auxin-induced, PIN polarization-dependent canalization properties responsible for the formation of new vascular tissue (Sachs, 2000; Sauer et al., 2006; Prusinkiewicz et al., 2009). These effects would lead to a local and temporal accumulation of auxin, finally provoking a negative feedback on free auxin levels, explaining the observed reduction in DR5-GUS intensities and auxin levels in leaf tissue of GR24-treated plants. In a study applying the auxin transport inhibitor NPA to young Arabidopsis plants, Ljung (Ljung et al., 2001) also observed a feedback inhibition of auxin biosynthesis in expanding leaves and cotyledons. In our study, a reduction in both auxin biosynthesis and auxin transport capacity would subsequently lead to a reduction in the auxin supply to the root system, influence primary root growth and meristem patterning, and reduce LRP initiation and development.

Combining the results of Brewer (Brewer et al., 2009), showing that strigolactones act downstream of auxin, and the results of this study in which we show that strigolactones in their turn are able to modulate auxin levels, we postulate that strigolactones and auxin operate in a tightly regulated feedback circuit.

GR24 application Influences LRP Development

GR24 significantly reduced LRD, which is the combined result of suppressed LRP development and reduced total LRFP (Figure 4). These processes are dependent on different auxin fluxes (Lucas et al., 2008). LR initiation is stimulated by auxin circulating in the root tip (Casimiro et al., 2003), being the net result of auxin influx from aerial parts of the plant and the dynamics of auxin (re)fluxes and production in the root tip itself. By contrast, LRP development is solely dependent on auxin sources directly derived from aerial parts of the plant. Auxin is delivered to the LRP through polar auxin transport (Bhalerao et al., 2002) and is subsequently imported into the developing LRP through repolarization of the PIN1 protein allowing lateral auxin influx. Interestingly, the results of this study indicate that GR24/strigolactones are able to modulate all these processes mentioned above. Since it

was observed that GR24 reduces auxin levels in aerial parts of the plant, it is likely that the amount of auxin reaching the majority of the LRP is not sufficient to sustain subsequent LRP development beyond stage V (Figure 8, left part of graph).

The GR24-mediated reduction of PIN-GFP levels in LRP is a secondary effect

When similar levels of GR24, which were previously found to reduce PIN1-GFP intensities in the LRP, were applied in the presence of exogenous auxin, PIN1-GFP intensities were not affected. This suggests that GR24 is not directly affecting *PIN* expression but that the decrease in PIN-GFP levels is a consequence of reduced auxin levels. Indeed, *PIN* gene expression is known to be auxin inducible (Vieten et al., 2005).

Although no changes in PIN1-GFP levels were observed, simultaneous application of GR24 and auxin still affected LRP development. Interestingly, however, under these conditions, GR24 had a stimulatory effect on LRP development instead. Because it is hypothesized that a reduction in PIN cycling is the direct effect resulting from strigolactone action (Prusinkiewicz et al., 2009), it is likely that the lateral auxin influx into the LRP, which is facilitated by repolarization of PIN1 proteins located in vascular tissue of the root, is disturbed by GR24 treatment. This would lead to a reduction in the supra-optimal auxin levels inside the NAA-treated LRP, provoking a shift toward the auxin optimum that is stimulating maximum LRP development (Figure 8, right part of graph). Apparently, this auxin reduction was too low to be reflected by decreased PIN1-GFP intensities. Another observation that is in line with this one is the reduction (in the wild-type) or loss (in *max* mutants) of the suppressive effect of GR24 on LR development when plants were grown under phosphate deficiency, a condition known to enhance auxin sensitivity ((López-Bucio et al., 2002; Pérez-Torres et al., 2008) Supplemental Figure S7.2). These results once more demonstrate that strigolactones act through the modulation of auxin levels and that the net result of strigolactone action is dependent on the auxin status of the plant.

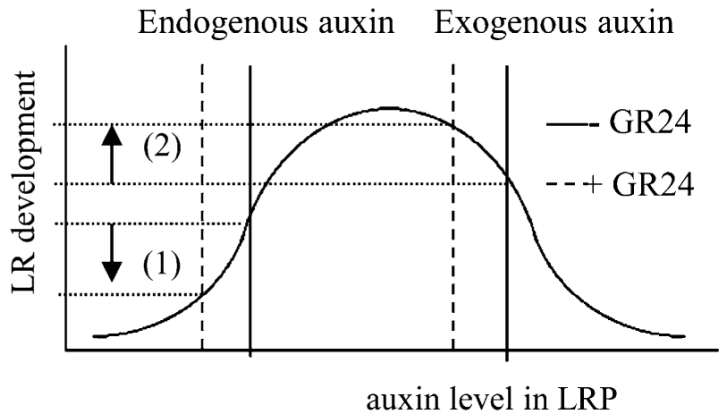

Figure 8: Schematic representation of the putative mechanism of GR24 action in root system architecture. Bell-shaped auxin response model for the auxin-mediated effect of the synthetic strigolactone GR24 on LR development. **(1)** Under sufficient Pi conditions, GR24 application has an inhibitory effect on LR development mediated through a reduction in auxin levels in the polar auxin transport stream coming from the shoot. **(2)** In the presence of exogenous auxin, LR development is increased instead. Under these conditions, a GR24-mediated reduction of auxin levels reaching LRP, through reduced auxin import into the developing LRP, results in an auxin concentration closer to the auxin optimum, thereby increasing the LR developmental

GR24 has a dual effect on LR initiation depending on the auxin status of the plant

LR initiation starts with the auxin-induced division of pericycle founder cells. Auxin reaches these cells through the PIN protein-mediated lateral auxin reflux at the level of the transition zone in the root tip (Casimiro et al., 2001; De Smet et al., 2007). Within the founder cells, a fraction of the auxin reflux accumulates until a LR initiation threshold is reached (Lucas et al., 2008). GR24 has a dual effect on LR initiation depending on the auxin status of the plant. During normal physiological conditions, low levels of GR24 application do not affect LR initiation. As already described, under

these conditions the GR24-mediated decrease in meristem cell size suggests increased auxin levels in the epidermal/cortical meristem zone. When these locally increased auxin levels are combined with a slight reduction in the rate of lateral auxin reflux, which is transporting auxin from the epidermal/cortical cell layers back to the polar transport stream in provascular tissue, net levels of accumulated auxin in founder cells will remain unchanged. Only higher doses of GR24, further reducing the apical auxin supply, hereby reducing the auxin levels in epidermal/cortical cell layers, will lead to a reduction in LR initiation. These results agree with the root branching model, as proposed by Lucas (Lucas et al., 2008), which explains differences in root branching by local changes in auxin transport. When plants are grown in the presence of NAA, LR initiation is significantly enhanced by GR24 application. A constant high exogenous auxin supply, combined with a GR24-induced reduction in lateral cellular auxin efflux, will result in an increase in auxin accumulation in pericycle founder cells. Interestingly, increased LR initiation was also observed for the *pin2 pin3 pin7* triple mutant (Laskowski et al., 2008), which may partially mimic the effect of GR24 application under exogenous NAA administration.

Implications for the role of endogenous strigolactones under natural conditions at the whole-plant level

Our results show that exogenous application of the strigolactone analog GR24 affects both primary root and LR growth as well as LRP initiation and development. GR24 is a synthetic strigolactone and, as used in our experiments, a mixture of two stereoisomers (Mangnus et al., 1992) that may have a different effect on root development. Experiments with pure, natural strigolactones are therefore needed to confirm our findings. However, in our study, we also used strigolactone-deficient mutants, which form the best material to study the true action of strigolactones on root architecture. *max* mutants have shorter primary roots containing fewer meristem cells (Figure 1b-c), while they have a higher DR5-GUS intensity in the provascular region (Figure 1d). Interestingly, *max* mutant plants also have smaller leaves (Supplemental Figure S7.3), which probably reflect higher auxin levels (Ljung et al., 2001). Because LRP development is dependent on auxin derived from the shoot (Bhalerao et al., 2002), this could explain why *max* mutants tend to have a higher LRD. Although this was only significant for *max4* and not *max1* and *max2* (Figure 4c-f), the majority of stage V LRP in *max* mutant plants were associated with a clear DR5-GUS signal, showing the presence of a properly formed auxin maximum. It is likely that most of these stage V LRP will develop into LRs. Therefore, the relatively small difference in LRD observed between young wild-type and *max* mutant plants is likely to become larger during later stages of plant development. The difference in LR development between wild-type and strigolactone-deficient plants could be analogous to GR24 application during Pi-sufficient conditions (Figure 8, left part of graph). Interestingly, under Pi-limiting conditions, the opposite is observed (Figure 7a). In this situation, LR development in wild-type plants is enhanced when compared to the *max* mutants. The mechanism leading to this result is likely to be similar to the situation in which GR24 application in the presence of exogenous NAA was shown to enhance LR outgrowth (Figures 5i and 8, right part of graph).

Strigolactones are also known to suppress bud outgrowth (Gomez-Roldan et al., 2008; Umehara et al., 2008). Because strigolactone production is enhanced under phosphate deficiency in tomato (López-Ráez et al., 2008), red clover (*Trifolium pratense*;(Yoneyama et al., 2007)), and Arabidopsis (Kohlen et al., 2011), the desirable response of reduced shoot branching under low phosphate conditions would be achieved. Recent results in our lab using the Arabidopsis *max* mutants demonstrate that low Pi-induced strigolactone biosynthesis is indeed responsible for the reduction in shoot branching under low phosphate conditions (Kohlen et al., 2011). This results in enhanced

carbon allocation to the roots sustaining an increase in root branching to expand the exploratory capacity of the root system (Bates and Lynch, 1996; López-Bucio et al., 2002; Sánchez-Calderón et al., 2005). In this study, we demonstrate that, in addition to controlling shoot architecture, endogenous strigolactones also play an important role in stimulating LR development under Pi-limiting conditions. This is in contrast with Pi-sufficient conditions, during which endogenous strigolactones limit the outgrowth of LRP. Therefore, we postulate that the major role of strigolactones in plant development lies in the coordinated, balanced control of the root-to-shoot branching ratio under continuously changing environmental conditions.

Material and methods

Plant Material and Growth Conditions

Seeds of the max1-*1*, *max2-1* (Stirnberg et al., 2002), *max4-1* (Sorefan et al., 2003), and their parental Columbia-0 wild-type lines either carrying (Bennett et al., 2006) or not carrying the *DR5-GUS* transgene were kindly provided by Prof. O. Leyser (University of York, UK). Seeds of the *pPIN1/2/3/7*::*PIN1/2/3/7*:*GFP* lines (Benková et al., 2003; Friml et al., 2003) were kindly provided by Prof. J. Friml (Ghent University, Belgium). Before sowing on MS plates, seeds were surface sterilized in 10% (w/v) chlorine bleach and then washed with 70% (w/v) ethanol and sterile distilled water. Seeds were imbibed on wet filter paper at 4°C for 2 to 4 d and plated on MS/agar plates (0.5× MS salts supplemented with 1× Gamborg's B5 vitamin mix, 0.8% [w/v] agar [Daichin], without [unless stated otherwise] Suc at pH 5.8). Plants were grown either on horizontal (for leaf surface measurements) or on near vertical plates (for root system architecture analysis) in a climate chamber under a 22°C/18°C 16-h-light/8-h-dark regime (80 µmol m^{-2} s^{-1}).

phosphate starvation experiments were conducted by transferring plants pregrown (5 d) on Pi-sufficient (1.25 mm) MS plates to low phosphate (20 µm) MS plates. LR induction by high levels of NAA (2.5 and 10 µm) or IAA (10 µm) was performed according to Himanen (Himanen et al., 2002) with the exception that during the 5-d period of pregrowing NPA was omitted from the medium. All experiments were repeated at least three times.

GUS staining

Histochemical GUS staining was performed according to Stomp (Stomp, 1992). The GUS activities were visualized by incubating the seedlings with the GUS substrate 5-bromo-4-chloro-3-indolyl-β-glucuronic acid for 13 h at 37°C. After clearing overnight in 70% ethanol, the plants were stored in 4°C prior to imaging.

Root System Architecture Measurements

Pictures of the root systems grown on MS plates were taken with a digital camera (Canon EOS 350 d) and were proportionally enlarged and printed to measure primary root lengths using a curvimeter. Images of NAA/IAA-treated plants were taken with a digital camera connected to a stereomicroscope at 5× magnification. LRP developmental stages were counted and evaluated using a Nikon Optiphot microscope equipped with Nomarski optics at 10× magnification. Roots were cleared for 2 to 16 h in a drop of Hoyer's solution (7.5 g gum arabic, 100 g chloral hydrate, and 5 mL glycerol in 30 mL water) on a microscope slide. LRP developmental stages were classified according to the system of Malamy and Benfey (Malamy and Benfey, 1997). The number of root meristem cells was determined by counting cortical cells in one cell file, starting from the quiescent center until the first cell showing signs of rapid elongation using confocal microscopy.

Confocal Microscopy

Roots of seedlings expressing GFP were incubated for 10 min in 1 µm propidium iodide (PI) in growth medium prior to imaging, washed, and coverslip mounted for imaging on an Axiovert 200M with a Zeiss 510 META confocal laser scanning microscope (Carl Zeiss). Representative root tips closest to the coverslip were selected for imaging with a 10× (numerical aperture of 0.3) or 20× (numerical aperture of 0.4) Fluar objective. Imaging was done in a reproducible manner starting with similar sample preparation, to image acquisition settings and data processing, for all experiments. Samples were excited with 5% of a 488-nm laser (emission from a 30-mW argon tube) for GFP excitation and 80% of a 543-nm laser (emission from a 1-mW helium-neon tube) for PI excitation. Optical sections of roots and subsequent z series were made using DM 488/543, EM 505 to 530 (GFP in green), and EM LP 615 (PI in white). Transmission images were simultaneously collected.
Single midplane optical sections were selected and compared, while LRP could most accurately be counted from z series, flat projected for maximal pixel value. Image analysis was done using Zeiss LSM Image Examiner (version 3.5), ImageJ version 1-32, and Adobe Photoshop CS2 (Adobe Systems).

Stereomicroscopy

Roots were imaged on a Zeiss stereo Discovery (A12) with a Plan S 1.0× FWD 81 mm (1–100×) objective. Images were taken with an AxioCam MRc5 (5 MPix camera; Zeiss) and analyzed using AxioVision 4.6 software.

IAA Extraction of Arabidopsis Leaf Material

For IAA analysis, 200 mg of root or shoot tissue was ground in a mortar with liquid nitrogen. The samples were extracted with 1 mL of cold methanol containing [phenyl 13C6]-IAA (0.1 nmol/mL) as internal standard in a 2-mL Eppendorf tube. The tubes were vortexed and sonicated for 10 min in a Branson 3510 ultrasonic bath (Branson Ultrasonics) and placed overnight in orbital shaker at 4°C. The samples were centrifuged for 10 min at 11,500 rpm in a Heraeus Fresco 17 centrifuge (Thermo Scientific) at 4°C, after which the organic phase was transferred to a 4-mL glass vial. The pellets were reextracted with another 1 mL of methanol. The combined methanol fractions were further purified by anion-exchange column (Grace Pure Amino 500 mg/3 mL SPE) as previously described (Chen et al., 1988), dried in a SpeedVacuum Savant SPD121P (Thermo Scientific), and the residue dissolved in 200 µL of acetonitrile:water:formic acid (25:75:0.1, v/v/v). Before liquid chromatography-tandem mass spectrometry analysis, samples were filtered through Minisart SRP4 0.45-µm filters (Sartorius).

IAA Detection and Quantification by Liquid Chromatography-Tandem Mass Spectrometry

Analysis of IAA in Arabidopsis (*Arabidopsis thaliana*) leaf extracts was performed by comparing retention times and mass transitions with those of IAA standard using a Waters Xevo tandem quadruple mass spectrometer using the settings previously described by Kohlen (Kohlen et al., 2011) and the gradient described for ABA by López-Ráez (López-Ráez et al., 2010). Multiple reaction monitoring (MRM) was used for IAA quantification. Parent-daughter transitions were set according to the tandem mass spectrometry spectra obtained for the standards IAA and [phenyl $^{13}C_6$]-IAA. Transitions were selected based on the most abundant and specific fragment ions for which the collision energy was optimized. For identification, the MRM transitions mass-to-charge ratio 176 > 103 at a collision energy of 30 eV and 176 > 130 at 16 eV; and for [phenyl $^{13}C_6$]-IAA, the transitions mass-to-charge ratio 182 > 109 at 28 eV and 182 > 136 at 16 eV were selected. Cone voltage was set to 18 eV. IAA was quantified using a calibration curve with known amount of standards and based on the ratio of the area of the MRM transition 176 > 130 for IAA to the MRM transition 182 > 136 for [phenyl $^{13}C_6$]-IAA. Data acquisition and analysis were performed using MassLynx 4.1 software

(Waters). The summed area of all the corresponding MRM transitions was used for statistical analysis.

Leaf Surface Quantification

Twenty-five seedlings were grown horizontally for 12 d on 9-cm-wide petri dishes in triplicates. Images were taken using a digital camera (Nikon D80 with Nikkor AF-S 60 mm f/2.8 G Micro ED) connected to a computer using Nikon camera control pro software version 2.0. Image analysis was performed using ImageJ based on segmentation by color-thresholding using visual scripting for ImageJ according to Joosen (Joosen et al., 2010)

Acknowledgments

We thank Jiři Friml for providing the Arabidopsis lines carrying the pPIN1/2/3/7:PIN1/2/3/7-GFP transgenes. We are grateful to Ottoline Leyser who supplied us with seeds of the max1-1, max2-1, and max4-1 Arabidopsis lines carrying the DR5-GUS transgene. We thank Binne Zwanenburg for supplying GR24. This work was funded by the Netherlands Organization for Scientific Research (VICI grant to H.B.) and the European Commission (Intra-European Marie Curie postdoctoral fellowship FP6–MEIF–CT–2005–024345 and Reintegration grant no. PERG–02–2007–224751 to J.A.L.-R.). This project was co-financed by the Centre for BioSystems Genomics (CBSG) which is part of the Netherlands Genomics Initiative/Netherlands Organisation for Scientific Research.

References

Akiyama K, Matsuzaki K, Hayashi H (2005) Plant sesquiterpenes induce hyphal branching in arbuscular mycorrhizal fungi. Nature **435:** 824-827

Aloni R, Schwalm K, Langhans M, Ullrich CI (2003) Gradual shifts in sites of free-auxin production during leaf-primordium development and their role in vascular differentiation and leaf morphogenesis in Arabidopsis. Planta **216:** 841-853

Auldridge ME, Block A, Vogel JT, Dabney-Smith C, Mila I, Bouzayen M, Magallanes-Lundback M, DellaPenna D, McCarty DR, Klee HJ (2006) Characterization of three members of the Arabidopsis carotenoid cleavage dioxygenase family demonstrates the divergent roles of this multifunctional enzyme family. The Plant Journal **45:** 982-993

Bainbridge K, Sorefan K, Ward S, Leyser O (2005) Hormonally controlled expression of the Arabidopsis *MAX4* shoot branching regulatory gene. The Plant Journal **44:** 569-580

Bates TR, Lynch JP (1996) Stimulation of root hair elongation in *Arabidopsis thaliana* by low phosphorus availability. Plant, Cell & Environment **19:** 529-538

Benková E, Michniewicz M, Sauer M, Teichmann T, Seifertová D, Jürgens G, Friml J (2003) Local, efflux-dependent auxin gradients as a common module for plant organ formation. Cell **115:** 591-602

Bennett T, Sieberer T, Willett B, Booker J, Luschnig C, Leyser O (2006) The Arabidopsis MAX pathway controls shoot branching by regulating auxin transport. Current Biology **16:** 553-563

Bhalerao RP, Eklöf J, Ljung K, Marchant A, Bennett M, Sandberg G (2002) Shoot-derived auxin is essential for early lateral root emergence in Arabidopsis seedlings. The Plant Journal **29:** 325-332

Blilou I, Xu J, Wildwater M, Willemsen V, Paponov I, Friml J, Heidstra R, Aida M, Palme K, Scheres B (2005) The PIN auxin efflux facilitator network controls growth and patterning in Arabidopsis roots. Nature **433:** 39-44

Booker J, Chatfield S, Leyser O (2003) Auxin acts in xylem-associated or medullary cells to mediate apical dominance. Plant Cell **15:** 495-507

Booker J, Sieberer T, Wright W, Williamson L, Willett B, Stirnberg P, Turnbull C, Srinivasan M, Goddard P, Leyser O (2005) MAX1 encodes a cytochrome P450 family member that acts downstream of MAX3/4 to produce a carotenoid-derived branch-inhibiting hormone. Developmental Cell **8:** 443-449

Bouwmeester HJ, Roux C, López-Ráez JA, Bécard G (2007) Rhizosphere communication of plants, parasitic plants and AM fungi. Trends in Plant Science **12:** 224-230

Brady SM, Orlando DA, Lee JY, Wang JY, Koch J, Dinneny JR, Mace D, Ohler U, Benfey PN (2007) A high-resolution root spatiotemporal map reveals dominant expression patterns. Science **318:** 801-806

Brewer PB, Dun EA, Ferguson BJ, Rameau C, Beveridge CA (2009) Strigolactone acts downstream of auxin to regulate bud outgrowth in pea and arabidopsis. Plant Physiology **150:** 482-493

Casimiro I, Beeckman T, Graham N, Bhalerao R, Zhang HM, Casero P, Sandberg G, Bennett MJ (2003) Dissecting Arabidopsis lateral root development. Trends in Plant Science **8:** 165-171

Casimiro I, Marchant A, Bhalerao RP, Beeckman T, Dhooge S, Swarup R, Graham N, Inze D, Sandberg G, Casero PJ, Bennett M (2001) Auxin transport promotes Arabidopsis lateral root initiation. Plant Cell **13:** 843-852

Chen KH, Miller AN, Patterson GW, Cohen JD (1988) A rapid and simple procedure for purification of indole-3-acetic acid prior to GC-SIM-MS analysis. Plant Physiology **86:** 822-825

Cline M (1997) Concepts and terminology of apical dominance. American Journal of Botany **84:** 1064-1069

Cook CE, Whichard LP, Turner B, Wall ME, Egley GH (1966) Germination of witchweed (*Striga lutea Lour.*): isolation and properties of a potent stimulant. Science **154:** 1189-1190

Crawford S, Shinohara N, Sieberer T, Williamson L, George G, Hepworth J, Müller D, Domagalska MA, Leyser O (2010) Strigolactones enhance competition between shoot branches by dampening auxin transport. Development **137:** 2905-2913

De Smet I, Tetsumura T, De Rybel B, Frey NFD, Laplaze L, Casimiro I, Swarup R, Naudts M, Vanneste S, Audenaert D, Inze D, Bennett MJ, Beeckman T (2007) Auxin-dependent regulation of lateral root positioning in the basal meristem of Arabidopsis. Development **134:** 681-690

De Smet I, Vanneste S, Inzé D, Beeckman T (2006) Lateral root initiation or the birth of a new meristem. Plant Molecular Biology **60:** 871-887

Dubrovsky JG, Sauer M, Napsucialy-Mendivil S, Ivanchenko MG, Friml J, Shishkova S, Celenza J, Benkova E (2008) Auxin acts as a local morphogenetic trigger to specify lateral root founder cells. Proceedings of the National Academy of Sciences of the United States of America **105:** 8790-8794

Friml J, Vieten A, Sauer M, Weijers D, Schwarz H, Hamann T, Offringa R, Jürgens G (2003) Efflux-dependent auxin gradients establish the apical-basal axis of Arabidopsis. Nature **426:** 147-153

Friml J, Wiśniewska J, Benková E, Mendgen K, Palme K (2002) Lateral relocation of auxin efflux regulator PIN3 mediates tropism in Arabidopsis. Nature **415:** 806-809

Friml J, Yang X, Michniewicz M, Weijers D, Quint A, Tietz O, Benjamins R, Ouwerkerk PBF, Ljung K, Sandberg G, Hooykaas PJJ, Palme K, Offringa R (2004) A PINOID-dependent binary switch in apical-basal PIN polar targeting directs auxin efflux. Science **306:** 862-865

Gomez-Roldan V, Fermas S, Brewer PB, Puech-Pages V, Dun EA, Pillot J-P, Letisse F, Matusova R, Danoun S, Portais J-C, Bouwmeester H, Becard G, Beveridge CA, Rameau C, Rochange SF (2008) Strigolactone inhibition of shoot branching. Nature **455:** 189-194

Grieneisen VA, Xu J, Maree AFM, Hogeweg P, Scheres B (2007) Auxin transport is sufficient to generate a maximum and gradient guiding root growth. Nature **449:** 1008-1013

Hayward A, Stirnberg P, Beveridge C, Leyser O (2009) Interactions between auxin and strigolactone in shoot branching control. Plant Physiology **151:** 400-412

Himanen K, Boucheron E, Vanneste S, Engler JD, Inzé D, Beeckman T (2002) Auxin-mediated cell cycle activation during early lateral root initiation. Plant Cell **14:** 2339-2351

Jaillais Y, Santambrogio M, Rozier F, Fobis-Loisy I, Miege C, Gaude T (2007) The retromer protein VPS29 links cell polarity and organ initiation in plants. Cell **130:** 1057-1070

Jain A, Poling MD, Karthikeyan AS, Blakeslee JJ, Peer WA, Titapiwatanakun B, Murphy AS, Raghothama KG (2007) Differential effects of sucrose and auxin on localized phosphate deficiency-induced modulation of different traits of root system architecture in Arabidopsis. Plant Physiology **144:** 232-247

Joosen RVL, Kodde J, Willems LAJ, Ligterink W, van der Plas LHW, Hilhorst HWM (2010) GERMINATOR: a software package for high-throughput scoring and curve fitting of Arabidopsis seed germination. The Plant Journal **62:** 148-159

Kohlen W, Charnikhova T, Liu Q, Bours R, Domagalska MA, Beguerie S, Verstappen F, Leyser O, Bouwmeester H, Ruyter-Spira C (2011) Strigolactones are transported through the xylem and play a key role in shoot architectural response to phosphate deficiency in nonarbuscular mycorrhizal host Arabidopsis. Plant Physiology **155:** 974-987

Koltai H, Dor E, Hershenhorn J, Joel D, Weininger S, Lekalla S, Shealtiel H, Bhattacharya C, Eliahu E, Resnick N, Barg R, Kapulnik Y (2010) Strigolactones' effect on root growth and root-hair elongation may be mediated by auxin-efflux carriers. Journal of Plant Growth Regulation **29:** 129-136

Laskowski M, Grieneisen VA, Hofhuis H, Hove CAt, Hogeweg P, Marée AFM, Scheres B (2008) Root system architecture from coupling cell shape to auxin transport. PLoS Biol **6:** e307

Leyser O (2009) The control of shoot branching: an example of plant information processing. Plant, Cell & Environment **32:** 694-703

Ljung K, Bhalerao RP, Sandberg G (2001) Sites and homeostatic control of auxin biosynthesis in Arabidopsis during vegetative growth. The Plant Journal **28:** 465-474

López-Bucio J, Hernandez-Abreu E, Sanchez-Calderon L, Nieto-Jacobo MF, Simpson J, Herrera-Estrella L (2002) Phosphate availability alters architecture and causes changes in hormone sensitivity in the Arabidopsis root system. Plant Physiology **129:** 244-256

López-Ráez JA, Charnikhova T, Gómez-Roldán V, Matusova R, Kohlen W, Vos RD, Verstappen F, Puech-Pages V, Bécard G, Mulder P, Bouwmeester H (2008) Tomato strigolactones are derived from carotenoids and their biosynthesis is promoted by phosphate starvation. New Phytologist **178:** 863-874

López-Ráez JA, Kohlen W, Charnikhova T, Mulder P, Undas AK, Sergeant MJ, Verstappen F, Bugg TDH, Thompson AJ, Ruyter-Spira C, Bouwmeester H (2010) Does abscisic acid affect strigolactone biosynthesis? New Phytologist **187:** 343-354

Lucas M, Guédon Y, Jay-Allemand C, Godin C, Laplaze L (2008) An auxin transport-based model of root branching in *Arabidopsis thaliana*. Plos One **3**

Malamy JE, Benfey PN (1997) Organization and cell differentiation in lateral roots of *Arabidopsis thaliana*. Development **124:** 33-44

Mangnus EM, Dommerholt FJ, De Jong RLP, Zwanenburg B (1992) Improved synthesis of strigol analog GR24 and evaluation of the biological activity of its diastereomers. Journal of Agricultural and Food Chemistry **40:** 1230-1235

Ottenschläger I, Wolff P, Wolverton C, Bhalerao RP, Sandberg G, Ishikawa H, Evans M, Palme K (2003) Gravity-regulated differential auxin transport from columella to lateral root cap cells. Proceedings of the National Academy of Sciences of the United States of America **100:** 2987-2991

Pérez-Torres C-A, Lopez-Bucio J, Cruz-Ramirez A, Ibarra-Laclette E, Dharmasiri S, Estelle M, Herrera-Estrella L (2008) Phosphate availability alters lateral root development in Arabidopsis by modulating auxin sensitivity via a mechanism involving the TIR1 auxin receptor. Plant Cell **20:** 3258-3272

Prusinkiewicz P, Crawford S, Smith RS, Ljung K, Bennett T, Ongaro V, Leyser O (2009) Control of bud activation by an auxin transport switch. Proceedings of the National Academy of Sciences **106:** 17431-17436

Sabatini S, Beis D, Wolkenfelt H, Murfett J, Guilfoyle T, Malamy J, Benfey P, Leyser O, Bechtold N, Weisbeek P, Scheres B (1999) An auxin-dependent distal organizer of pattern and polarity in the Arabidopsis root. Cell **99:** 463-472

Sachs T (2000) Integrating cellular and organismic aspects of vascular differentiation. Plant and Cell Physiology **41:** 649-656

Sánchez-Calderón L, Lopez-Bucio J, Chacon-Lopez A, Cruz-Ramirez A, Nieto-Jacobo F, Dubrovsky JG, Herrera-Estrella L (2005) Phosphate starvation induces a determinate developmental program in the roots of *Arabidopsis thaliana*. Plant Cell Physiology **46:** 174-184

Sauer M, Balla J, Luschnig C, Wiśniewska J, Reinöhl V, Friml J, Benková E (2006) Canalization of auxin flow by Aux/IAA-ARF-dependent feedback regulation of PIN polarity. Genes & Development **20:** 2902-2911

Sliwinska E, Bassel GW, Bewley JD (2009) Germination of *Arabidopsis thaliana* seeds is not completed as a result of elongation of the radicle but of the adjacent transition zone and lower hypocotyl. Journal of Experimental Botany **60:** 3587-3594

Sorefan K, Booker J, Haurogné K, Goussot M, Bainbridge K, Foo E, Chatfield S, Ward S, Beveridge C, Rameau C, Leyser O (2003) *MAX4* and *RMS1* are orthologous dioxygenase-like genes that regulate shoot branching in Arabidopsis and pea. Genes & Development **17:** 1469-1474

Stirnberg P, Furner IJ, Leyser HMO (2007) MAX2 participates in an SCF complex which acts locally at the node to suppress shoot branching. The Plant Journal **50:** 80-94

Stirnberg P, van de Sande K, Leyser HMO (2002) MAX1 and MAX2 control shoot lateral branching in Arabidopsis. Development **129:** 1131-1141

Stomp A (1992) Histochemical localization of b-glucuronidase activity. In SR Gallagher, ed, GUS Protocols: Using the GUS gene as a reporter of gene expression. Academic Press, San Diego**:** 103–113

Turnbull CGN, Booker JP, Leyser HMO (2002) Micrografting techniques for testing long-distance signalling in Arabidopsis. The Plant Journal **32:** 255-262

Umehara M, Hanada A, Magome H, Takeda-Kamiya N, Yamaguchi S (2010) Contribution of strigolactones to the inhibition of tiller bud outgrowth under phosphate deficiency in rice. Plant and Cell Physiology**:** 1118-1126

Umehara M, Hanada A, Yoshida S, Akiyama K, Arite T, Takeda-Kamiya N, Magome H, Kamiya Y, Shirasu K, Yoneyama K, Kyozuka J, Yamaguchi S (2008) Inhibition of shoot branching by new terpenoid plant hormones. Nature **455:** 195-200

Vieten A, Vanneste S, Wiśniewska J, Benková E, Benjamins R, Beeckman T, Luschnig C, Friml J (2005) Functional redundancy of PIN proteins is accompanied by auxin-dependent cross-regulation of PIN expression. Development **132:** 4521-4531

Yoneyama K, Yoneyama K, Takeuchi Y, Sekimoto H (2007) Phosphorus deficiency in red clover promotes exudation of orobanchol, the signal for mycorrhizal symbionts and germination stimulant for root parasites. Planta **225:** 1031-1038

Chapter 8

General discussion

Wouter Kohlen

The aim of the research presented in this thesis was to get a fundamental understanding of the biosynthesis and transport of strigolactones and their function in plants. This chapter will briefly summarize what was learned and how this can be integrated into our knowledge of strigolactone functioning. In addition, the new perspectives for the control of root parasitic plants arising from my work will be discussed.

Strigolactone biosynthesis and the role of MAX1

As mentioned before, strigolactones are carotenoid derived molecules (Matusova et al., 2005) that have been known as germination stimulants for root parasitic plants of the Orobanchaceae (i.e. *Orobanche spp*, *Phelipanche spp* and *Striga spp*) since the early sixties of the last century (Cook et al., 1966; Bouwmeester et al., 2003). The evolutionary advantage for the conservation of these seemingly disadvantageous rhizosphere signaling molecules was discovered when strigolactones were identified as the pre-symbiotic branching factor for arbuscular mycorrhizal (AM) fungi (Akiyama et al., 2005; Besserer et al., 2006). AM fungi are fungi that establish symbiosis with vascular plants and are dependent on carbon provided by their host. In return AM fungi help the plant by improving the uptake of inorganic phosphate and other minerals, and hence improve growth conditions in areas with limited mineral nutrition. This discovery suggests that the beneficial role of the strigolactones in attracting AM fungi outweighs the negative consequences of the attraction of the parasitic plants and shows that the strigolactones have a dual role in rhizosphere signaling (Bouwmeester et al., 2007). More recent, an additional dimension was added when strigolactones – or their derivatives – were shown to be a shoot branching inhibiting signal (Gomez-Roldan et al., 2008; Umehara et al., 2008). In 2005 our group postulated that strigolactones are derived from carotenoids through oxidative cleavage followed by additional enzymatic modifications which involve one or more cytochrome P450s (Matusova et al., 2005). This results in the biosynthesis of the first genuine strigolactones, 5-deoxystrigol and/or 2'-epi-5-deoxystrigol. All other strigolactones known to date can be derived from these two through hydroxylation, acetylation and/or oxidation (Matusova et al., 2005; Humphrey et al., 2006; Rani et al., 2008).

Indeed, two CCDs - CCD8 and CCD7 - were recently identified as part of the strigolactone biosynthetic pathway (Gomez-Roldan et al., 2008; Umehara et al., 2008). Plants carrying mutations in these enzymes have a distinctive branching phenotype, which could be complemented by exogenous application of the synthetic strigolactone analogue GR24. We demonstrated that in tomato (chapter 3) and petunia (unpublished results) *SlCCD8* and *PhCCD8(DAD1)* are also required for strigolactone biosynthesis, confirming that strigolactone biosynthesis is highly dependent on CCD8 cleavage. Strangely, in the moss *Physcomitrella patens* two of the six reported strigolactones - strigol and 7-oxoorobanchyl acetate - were unaffected by the reduction in *PpCCD8* expression. Although this contradicts the importance of CCD8, no explanation for these unexpected results was provided by the authors (Proust et al., 2011).

A third highly branched and putative strigolactone biosynthesis mutant in Arabidopsis - *max1* (Stirnberg et al., 2002; Booker et al., 2005) - could also be rescued by GR24 application (Gomez-Roldan et al., 2008). However, additional, analytical, proof for *MAX1* involvement in strigolactone biosynthesis was not provided. In chapter 6 of this thesis analytical proof of *MAX1* involvement in the biosynthesis of orobanchol in *Arabidopsis thaliana* is presented, as the level of this strigolactone is severely reduced in the *max1* mutant compared to wild-type (Kohlen et al., 2011). Interestingly, so far no *MAX1* orthologs have been identified in any other species, whereas orthologs for *MAX3 (CCD7)* and *MAX4 (CCD8)* have been identified in several species (Booker et al., 2004; Snowden et al., 2005; Zou et al., 2006; Arite et al., 2007; Lin et al., 2009; Ledger et al., 2010; Vogel et al., 2010; Proust et al.,

2011). In rice several putative *MAX1* homologs were reported (Nelson et al., 2004; Umehara et al., 2010). Moreover, a *MAX1* homolog was found in the unicellular green algae *Chlamydomonas reinhardtii* (Nelson et al., 2004). However, the *P. patens* genome was reported to have no *MAX1* ortholog. However, several strigolactones were identified in this moss (Proust et al., 2011). This lead the authors to speculate that strigolactone biosynthesis might be MAX1 independent. This assumption however contradicts our findings in Arabidopsis (Kohlen et al., 2011). We believe it is therefore more likely that in *P. patens* a yet unidentified MAX1 ortholog does exist, and that it could not be recognized or that in *P. patens* another cytochrome P450 evolved to carry out the reaction for which MAX1 is needed in higher plants. Additional work, aimed at the identification of the *MAX1* ortholog(s) in rice supports that strigolactone biosynthesis in higher plants is MAX1 dependent (Cardoso et al., unpublished results).

The regulation of strigolactone biosynthesis

In several studies, it was demonstrated that strigolactone biosynthesis and secretion into the rhizosphere are up-regulated under phosphate starvation (Yoneyama et al., 2007; López-Ráez et al., 2008; Umehara et al., 2008; Kohlen et al., 2011). The ecological significance of this is to improve AM symbiosis under these conditions (Akiyama et al., 2005), but unfortunately also to higher levels of root parasitism (Yoneyama et al., 2001; Bouwmeester et al., 2007). As poor soils are almost synonymous to African farm lands, it becomes vitally important to understand the mechanisms which are underlying these responses.

GRAS-type transcription factors regulating strigolactone biosynthesis.
In *Medicago truncatula* strigolactone biosynthesis is not only up-regulated under phosphate limited conditions but also dependent on two GRAS-type transcription factors, NODULATION SIGNALLING PATHWAY1 (NSP1) and NSP2 (chapter 5) (Liu et al., submitted). These GRAS-type transcription factors were already known to be essential for rhizobium Nod factor induced nodulation (Kaló et al., 2005; Smit et al., 2005; Heckmann et al., 2006; Murakami et al., 2007).

We identified a *DWARF27* (*D27)* homolog in *Medicago truncatula* and showed that it is induced under phosphate-limited conditions. *D27* was the fourth gene identified to be required for strigolactone biosynthesis, but the precise function of this iron containing protein remains unknown (Lin et al., 2009). A mutation in *MtNSP1* completely abolished *MtD27* expression as well as strigolactone biosynthesis. Analysis of *nsp1nsp2* double knock-down lines in rice revealed similar results. In addition, we demonstrated that the *MtD27* is a direct target of MtNSP1, indicating that the up-regulation of strigolactone biosynthesis under phosphate starvation in M*edicago truncatula*, and possibly other plants, might be mediated through NSP1 regulation of *D27* expression.

Furthermore, *D27* expression under phosphate starvation in the *nsp2* background was less affected as its expression was reduced by 80% compared to wild-type. Not only was the total strigolactone pool reduced accordingly, the composition of measured strigolactones changed as well. We identified didehydro-orobanchol isomer 6 (Kohlen et al., unpublished results) as the major, and orobanchol as a minor strigolactone in *Medicago truncatula* (cultivar A17). In *nsp2* didehydro-orobanchol biosynthesis was abolished and orobanchol over-accumulated. As mentioned above, it has been postulated that all strigolactones are derived from modifications of (2'-epi-)5-deoxystrigol (Matusova et al., 2005; Humphrey et al., 2006; Rani et al., 2008) and we postulate that didehydro-orobanchol is derived from orobanchol through two modifications (chapter 2). These results indicate that NSP2 might be regulating this conversion. The fact that in the *nsp2* mutant *MtD27* expression is

down regulated could be a secondary effect caused by a negative – orobanchol induced – feedback loop, making the NSP2 regulation of *MtD27* indirect.

Interestingly, a recent study in *M. truncatula* revealed that the *nsp2* mutant displays a reduced level of AM colonization, whereas the *nsp1* does not (Maillet et al., 2011). Combined with our results, this might indicate that the mycorrhizal colonization phenotype observed in the *M. truncatula nsp2* mutant is related to over-accumulation of orobanchol. It was previously demonstrated that orobanchol is one of the more potent strigolactones in AM hyphal branching induction (Akiyama et al., 2010). It is therefore more likely that *NSP2* also has a function later in the establishment or maintenance of AM symbiosis and that the observed phenotype is not related to strigolactone biosynthesis.

To role of abscisic acid (ABA) in the regulation of strigolactone biosynthesis.

It was already known that the ABA deficient maize mutant *vp14* (containing a mutation in a 9-*cis*-epoxycarotenoid dioxygenase, *NCED*) induced less germination of *Striga* compared to wild-type maize (Matusova et al., 2005). In addition, ABA and strigolactones are biosynthetically closely related, as both are derived from the carotenoids. We demonstrated that three ABA deficient mutants of tomato (*notabilis*, *flacca* and *sitiens*) also had lower strigolactone levels, just as maize *vp14* (chapter 4). Moreover, there was a close correlation between the ABA and strigolactone levels, as both were reduced to a similar extent in the three individual mutants (López-Ráez et al., 2010). The *NOTABILIS* gene encodes an NCED belonging to a sub-cluster within the CCD/NCED gene family (Bouwmeester et al., 2007) and is involved in the cleavage of neoxanthin and/or violaxanthin, the first dedicated step in ABA biosynthesis (Burbidge et al., 1999). *FLACCA* and *SITIENS* are encoding two different components of the final enzymatic step leading to ABA, the oxidation of ABA aldehyde (Taylor et al., 1988). As it is highly unlikely that all three genes are directly involved in both ABA and strigolactone biosynthesis, we concluded that not these enzymes but ABA itself is regulating strigolactone levels. However, a final proof of this hypothesis - restoration of the strigolactone biosynthesis phenotype of these mutants by ABA application – failed, likely due to the fact that it is impossible to apply exogenous ABA at the exact location, concentration and timing, where and when it is needed (López-Ráez et al., 2010). The strigolactone phenotype in these ABA mutants was observed under phosphate starvation. As no branching phenotype was ever reported for any of these tomato mutants (which are normally grown under phosphate sufficient conditions), it is plausible that ABA is involved in the up-regulation of strigolactone biosynthesis under phosphate starvation only and is not controlling strigolactone levels when phosphate is not limited (López-Ráez et al., 2010). Interestingly, ABA has also been reported to be required for the establishment of AM symbiosis, which is usually assessed under limited phosphate (Martín Rodriguez et al., 2010). The importance of strigolactones for the activation of AM fungi makes the correlation between ABA and strigolactones even more interesting. So far no additional reports on the interaction between ABA and strigolactones were published, leaving the precise interaction between strigolactones and ABA and their possible role in the establishment of mycorrhizal symbiosis to be clarified.

The role of the xylem in strigolactone transport

The precise tissue localization of strigolactone biosynthesis remains elusive. It is thought that at least part of the total strigolactone pool is synthesized in the roots (Ruyter-Spira et al., 2011). However, biosynthesis of the strigolactones is likely not limited to the root system alone as the strigolactone biosynthesis genes are expressed in many tissues outside the root system (Sorefan et al., 2003; Booker et al., 2004; Booker et al., 2005). Grafting studies indicate that inter stock grafting with only a

small part of the wild-type epicotyl into pea *rms1* and hypocotyl into Arabidopsis *max3* is sufficient to restore branching in these biosynthetic mutants to near wild-type (Foo et al., 2001). All this makes the exact tissue origin of strigolactones acting in the shoot un-resolved. Still, transport through the plant seems to be required and the xylem is likely to be involved as orobanchol has been detected in the xylem sap of both Arabidopsis and tomato (Kohlen et al., 2011).

Interestingly, of the strigolactones identified in tomato root exudate so far (solanacol, didehydro-orobanchol isomers 1,2,3,4,5 and 6, orobanchol, orobanchyl acetate, 7`-hydroxy-orobanchol, 7`-oxo-orobanchol, 7`-hydroxy-orobanchyl acetate, 7`-oxo-orobanchyl acetate) (López-Ráez et al., 2008), Charnikhova, unpublished results), orobanchol and orobanchyl acetate are the only strigolactones that were detected in the xylem sap. This suggests that a selective mechanism of localized strigolactone biosynthesis or – more likely - transport ensures that only orobanchol and orobanchyl acetate are transported through the xylem to the shoot. This could indicate a differentiation of strigolactone functioning where orobanchol and orobanchyl acetate (or a derivative of these) would be involved in the regulation of shoot branching, whereas solanacol and the didehydro-orobanchol isomers would mainly function as signaling molecules in the rhizosphere or be involved in the regulation of root architecture.

Effect of strigolactones on root architecture

Root development is a tightly regulated process coordinated by several plant hormones, of which auxin is the main player. Auxin involved in this process is transported from the shoot to the root tip. In the columella of the root tip, auxin travels in lateral directions towards the root epidermal cells. Here, auxin is transported in a basipetal direction towards the transition zone. Finally, lateral auxin reflux via cortical cells transport auxin back into the PATS (Leyser, 2006). Auxin transport is facilitated by auxin efflux proteins of the PIN family. As a result of this, PIN proteins tightly control and regulate local auxin gradients (Blilou et al., 2005). As such, auxin plays a predominant role in the regulation of primary root growth. The establishment of a precise auxin gradient is sufficient to guide primary root growth (Grieneisen et al., 2007). Furthermore, application of exogenous auxin reduces the length of the primary root by reducing cell elongation (Rahman et al., 2007). In addition, lateral root (LR) initiation is triggered by the local accumulation of auxin in root pericycle cells adjacent to the xylem vessels (Casimiro et al., 2001; De Smet et al., 2006; De Smet et al., 2007; Dubrovsky et al., 2008; Lucas et al., 2008). Subsequent specific cell divisions leads to the establishment of LR primordia and finally to emergence of a LR. In all these developmental stages the role of PIN proteins is crucial, as they are required for the establishment of adequate auxin gradients inside the developing LR primordia which is needed for correct LR development (Benková et al., 2003).
In early work on petunia branching mutants, even before the role of strigolactones in controlling shoot branching was discovered, it was reported that the petunia *ccd8/dad1* mutant has a root phenotype (Snowden et al., 2005).

Strigolactones in primary root growth
As mentioned above auxin gradients are essential for primary root growth. It has been postulated that the effect of strigolactones on root morphology is mediated through auxin (Koltai et al., 2010, Ruyter-Spira et al., 2011). When grown under phosphate-sufficient conditions GR24 application could counteract the inhibiting effect of auxin application on primary root growth in tomato (Koltai et al., 2010). In addition, It was shown that the length of the primary roots in the *max1, 2 and 4* mutants was reduced compared to wild-type (Col-0) plants when grown under low sucrose (Ruyter-Spira et al., 2011). Detailed analysis revealed that this reduction was due to a reduction in the number of cells

in the primary root meristem. Application of the synthetic strigolactone analogue GR24 rescued this phenotype in all mutants except the signal transduction mutant *max2* (Ruyter-Spira et al., 2011). In addition, the effect of GR24 application on the local auxin gradient in root tip caused an increase in both cell number and size of the cortex cells in the meristem and transition zone, leading to an expansion of this area. Combined, this indicates that strigolactones could be involved in defining the meristem boundary of the primary root and that this is regulated through MAX2. Application of a relatively high concentration of GR24 caused the primary root meristem to collapse in a MAX2 independent way (Ruyter-Spira et al., 2011), suggesting that this concentration is supra-optimal in Arabidopsis seedlings.

Effect of strigolactones on lateral root initiation and development works both ways

As mentioned above, lateral root initiation is controlled through the establishment of PIN mediated auxin gradients (Casimiro et al., 2001; Benková et al., 2003; De Smet et al., 2006; De Smet et al., 2007; Dubrovsky et al., 2008; Lucas et al., 2008). The hypothesis is that strigolactones co-regulate this process by modifying these auxin gradients (Kapulnik et al., 2011; Ruyter-Spira et al., 2011). Under phosphate-sufficient conditions GR24 application indeed reduces lateral root density in a dose dependent manor. Interestingly, when GR24 application was combined with exogenous application of NAA, GR24 had a stimulatory effect on lateral root development and outgrowth instead. Similarly, under phosphate-limiting conditions, the combination of elevated auxin sensitivity – and increased endogenous strigolactone levels in wild type Arabidopsis plants - induced more outgrowth of lateral root primordia when compared with strigolactone-deficient mutants. As discussed above, under phosphate-sufficient conditions, GR24 application reduces the auxin concentration in the leaves (Ruyter-Spira et al., 2011). Apparently, the decrease in auxin transport to/concentration in the roots by GR24 under normal phosphate leads to a reduction in lateral root outgrowth, while under low phosphate a decrease in auxin by GR24 stimulates lateral root outgrowth. It has been postulated that the net result of strigolactone action on lateral root development is related to the auxin optimum. Under phosphate-limited conditions the auxin distribution is changed and auxin signaling is elevated (Lopez-Bucio et al., 2002; Al-Ghazi et al. 2003; Nacry et al., 2005; Pérez-Torres et al., 2008). If the response to auxin becomes too high it will surpass its optimum, as a result lateral root development will be reduced. Under these conditions exogenous GR24 application will reduce the level of free auxin, moving again towards the auxin optimum and thus stimulating lateral root development. Whereas, under phosphate-sufficient conditions the auxin optimum will not be reached. Exogenous application of GR24 will have the opposite effect on the auxin status with respect to the optimum. As a result, lateral root development will be further reduced under these conditions (Ruyter-Spira et al., 2011).

Strigolactone mode of action in defining root system architecture

It has been demonstrated that the establishment of a local auxin gradient is important for root system architecture (Grieneisen et al., 2007; Laskowski et al., 2008). Koltai et al (2010) postulated that the primary effect of strigolactones on root development might be related to the strigolactone mediated control of the auxin transport capacity – and therefore auxin gradients - in the roots. Prusinkiewicz (2009) hypothesized that the effect of strigolactones on auxin transport is mediated through a reduction in efficiency of PIN cycling. Although it was demonstrated that exogenous application of the synthetic strigolactone analogue GR24 reduced the level of the auxin efflux carriers PIN1/3/7 in the vascular region of the root tip and lateral root primordia (Ruyter-Spira et al., 2011), this reduction is believed to be the consequence of reduced auxin concentrations as the combined application of the synthetic auxin naphthalene acetic acid (NAA) and GR24 did not reduce the

$pPIN_{1/3/7}$:$PIN_{1/3/7}$-GFP signal in any of these lines (Ruyter-Spira et al., 2011). As mentioned above it was also demonstrated that GR24 application reduces the level of free auxin in the leaves of Arabidopsis seedlings (Ruyter-Spira et al., 2011). A similar feedback inhibition on auxin biosynthesis in expanding leaves and cotyledons was observed by Ljung et al. (2001) after treatment with the auxin transport inhibitor NPA as was mentioned above. As auxin is reported to induce the expression of PIN proteins (Vieten et al., 2005) it is postulated that the observed effect of GR24 on PIN driven GFP signal is a secondary effect mediated by reduced auxin concentrations.

The phosphate starvation response, how do strigolactones fit in?

When plants are exposed to limiting phosphate conditions they respond in a number of different ways all aimed at increasing the exploration of the rhizosphere for phosphate and reducing the investment of resources into the shoot. In the first place this is achieved by reducing the number of shoot branches (Troughton, 1977; Cline, 1997). It was recently demonstrated that the up-regulation of strigolactone biosynthesis under phosphate starvation (Yoneyama et al., 2007; López-Ráez et al., 2008; Umehara et al., 2008; Jamil et al., 2011; Kohlen et al., 2011) is contributing to this response. Both rice and Arabidopsis mutants impaired in strigolactone biosynthesis or signaling are unable to reduce shoot outgrowth under these conditions (Umehara et al., 2010; Kohlen et al., 2011). In addition, the levels of orobanchol in the xylem sap of Arabidopsis increased by approximately 25% under limiting phosphate conditions (Kohlen et al., 2011).

Also the root system architecture is drastically changed under phosphate limiting conditions (López-Bucio et al., 2002; Al-Ghazi et al., 2003; Ma et al., 2003; Nacry et al., 2005; Sánchez-Calderón et al., 2005). In Arabidopsis it was shown that these changes are accompanied by altered distribution and elevated perception of auxin in the roots (López-Bucio et al., 2002; Al-Ghazi et al., 2003; Pérez-Torres et al., 2008). These elevations in auxin functioning lead to a reduction in primary root growth while the outgrowth of lateral roots near the soil surface is stimulated (Al-Ghazi et al., 2003). It is believed that by this response the plant is able to exploit phosphate rich areas that are usually found in the top layers of the soil (Al-Ghazi et al., 2003).

Combined, these changes in plant architecture under limited phosphate conditions lead to an increase in the root to shoot ratio, enabling the plant to better cope with its environment (Bonser et al., 1996), As mentioned above, strigolactone biosynthesis is up-regulated under phosphate-limited conditions and they promote lateral root development under high auxin levels. This makes it likely that they are involved in these adaptations to phosphate starvation. Indeed, it was demonstrated that roots of *max4* showed no increase in lateral root density under limiting phosphate conditions whereas wild- type plants showed a 4-fold increase (Ruyter-Spira et al., 2011). It is likely that a tightly balanced auxin-strigolactone interaction is the basis for the mechanism by which plants regulate the root to shoot ratio under phosphate limited conditions (Ruyter-Spira et al., 2011).

Additional strigolactone related phenotypes

Several additional strigolactone functions have been proposed in addition to their role in rhizosphere signaling and the regulation of shoot and root architecture. It has been demonstrated that the expression of *SlCCD7* (tomato) and *AcCCD7* and *AcCCD8* (kiwi) is relatively high in developing fruits (Ledger et al., 2010; Vogel et al., 2010), leading the authors to hypothesize that strigolactones may have a function in reproductive development of seed plants. Strigolactones have indeed been reported in fruits of cucumber (Xie et al., 2010). In addition, analysis of the fruits produced by several transgenic lines expressing an antisense construct against *SlCCD8*, revealed a strong reduction in fruit

size (chapter 3). As these lines are heavily branched, the reduced fruit sizes could be a secondary effect of constrains on energy distribution. However, our results show altered levels and distribution of auxin in both flowers and fruits. As auxin levels are also reported to be affected in shoot branching this could be directly related to reduced *CCD8* expression. Indicating possibly a more direct role for strigolactones in the reproductive development of tomato.

It is not unlikely that strigolactones function in even more aspects of plant development. Indeed, a small-molecule screen recently identified several putative functions for GR24 in the regulation of Arabidopsis development. From Arabidopsis seed germination to hypocotyl elongation (Tsuchiya et al., 2010). However, the concentrations required to obtain some of these phenotypes far exceeded the concentrations used by Ruyter-Spira (2011) to affect root development and are close to - or even beyond - the upper limit of what might be considered as biologically relevant. However, it was reported that strigolactones negatively regulate mesocotyl elongation in rice during germination and growth in darkness. GR24 concentrations between 0.01 µM and 1 µM were sufficient to complement the phenotype of the strigolactone biosynthesis mutants (*d10*, *d17* and *d27*). GR24 application had no effect on the signaling mutants d3 or d14 (Hu et al., 2010).

Future perspective

In many aspects of plant development more than one, if not all, phytohormones are interacting with each other. This so-called cross-talk has been the subject of many studies (Bauly et al., 2002; Rock and Sun, 2005; Moubayidin et al., 2009). As described above, the first evidence is being discovered that also strigolactones contribute to these hormonal networks that control many of the developmental processes in plants. The role of strigolactones is now no longer limited to rhizosphere signaling and the inhibition of shoot branching but also includes other developmental processes such as root system architecture, hypocotyl elongation, Arabidopsis seed germination and reproductive development. Auxin seems to play a crucial role in many of the strigolactone related processes. However, interactions between strigolactones and other plant hormones such as cytokinins, ABA and ethylene are emerging and without doubt other plant hormones will follow. Combined, these findings will enable the strigolactones to take their rightful place in the orchestra of plant hormones that regulates plant development. The elucidation of the many roles of strigolactones in plant development is only just beginning, giving the prospect of many exciting future discoveries to look forward to.

Also with regard to strigolactone biosynthesis, there is no complete picture yet. It has been reported that structural differences between strigolactones lead to differential activity on AM branching (Akiyama et al., 2010) and similar claims were made for their role in controlling shoot branching (Yamaguchi, 2010 IPGSA conference) and germination (Yoneyama et al., 2009) so the elucidation of the enzymes downstream of 5-deoxystrigol and 2'-epi-5-deoxystrigol is highly relevant for understanding the different aspects of strigolactone functioning and ultimately controlling the parasitic plant problem. The results we obtained using the *mtnsp2* mutants in Medicago gives us the opportunity to hunt for at least one of these genes. I believe it is especially relevant as we demonstrate that in tomato orobanchol is transported through the xylem and is poorly secreted into the rhizosphere, whereas didehydro-orobanchol and solanacol are not found in the xylem sap but abundantly present in the root exudates. Controlling this conversion might prove a successful strategy for the reduction of broomrape infection without compromising apical dominance. In addition, a better understanding of strigolactone biosynthesis, including the exact location, regulation (e.g under phosphate starvation) and transport will without doubt contribute to a solution

to the parasitic plant problem. The work presented in this thesis provides no direct answers to this. However, it provides some of the tools and ideas to move into the right direction.

Acknowledgements

I thank Harro J. Bouwmeester and Carolien Ruyter-Spira for their valuable suggestions that helped to improve this chapter.

References

Akiyama K, Matsuzaki K, Hayashi H (2005) Plant sesquiterpenes induce hyphal branching in arbuscular mycorrhizal fungi. Nature **435:** 824-827

Akiyama K, Ogasawara S, Ito S, Hayashi H (2010) Structural requirements of strigolactones for hyphal branching in AM fungi. Plant and Cell Physiology **51:** 1104-1117

Al-Ghazi Y, Muller B, Pinloche S, Tranbarger TJ, Nacry P, Rossignol M, Tardieu F, Doumas P (2003) Temporal responses of *Arabidopsis* root architecture to phosphate starvation: evidence for the involvement of auxin signalling. Plant, Cell & Environment **26:** 1053-1066

Arite T, Iwata H, Ohshima K, Maekawa M, Nakajima M, Kojima M, Sakakibara H, Kyozuka J (2007) DWARF10, an RMS1/MAX4/DAD1 ortholog, controls lateral bud outgrowth in rice. The Plant Journal **51:** 1019-1029

Bauly J, Roux C, Dargeviciute A, Perrot-Rechenmann C (2002) Identification of a novel marker for auxin and ethylene cross-talk from tobacco seedlings. Plant Physiology and Biochemistry **40:** 803-811

Benková E, Michniewicz M, Sauer M, Teichmann T, Seifertová D, Jürgens G, Friml J (2003) Local, efflux-dependent auxin gradients as a common module for plant organ formation. Cell **115:** 591-602

Besserer A, Puech-Pagès V, Kiefer P, Gomez-Roldan V, Jauneau A, Roy S, Portais J-C, Roux C, Bécard G, Séjalon-Delmas N (2006) Strigolactones stimulate arbuscular mycorrhizal fungi by activating mitochondria. PLoS Biol **4:** e226

Blilou I, Xu J, Wildwater M, Willemsen V, Paponov I, Friml J, Heidstra R, Aida M, Palme K, Scheres B (2005) The PIN auxin efflux facilitator network controls growth and patterning in Arabidopsis roots. Nature **433:** 39-44

Bonser AM, Lynch J, Snapp S (1996) Effect of phosphorus deficiency on growth angle of basal roots in *Phaseolus vulgaris*. New Phytologist **132:** 281-288

Booker J, Auldridge M, Wills S, McCarty D, Klee H, Leyser O (2004) MAX3/CCD7 is a carotenoid cleavage dioxygenase required for the synthesis of a novel plant signaling molecule. Current Biology **14:** 1232-1238

Booker J, Sieberer T, Wright W, Williamson L, Willett B, Stirnberg P, Turnbull C, Srinivasan M, Goddard P, Leyser O (2005) MAX1 encodes a cytochrome P450 family member that acts downstream of MAX3/4 to produce a carotenoid-derived branch-inhibiting hormone. Developmental Cell **8:** 443-449

Bouwmeester HJ, Matusova R, Zhongkui S, Beale MH (2003) Secondary metabolite signalling in host-parasitic plant interactions. Current Opinion in Plant Biology **6:** 358-364

Bouwmeester HJ, Roux C, López-Ráez JA, Bécard G (2007) Rhizosphere communication of plants, parasitic plants and AM fungi. Trends in Plant Science **12:** 224-230

Burbidge A, Grieve TM, Jackson A, Thompson A, McCarty DR, Taylor IB (1999) Characterization of the ABA-deficient tomato mutantnotabilisand its relationship with maizeVp14. The Plant Journal **17:** 427-431

Casimiro I, Marchant A, Bhalerao RP, Beeckman T, Dhooge S, Swarup R, Graham N, Inze D, Sandberg G, Casero PJ, Bennett M (2001) Auxin transport promotes Arabidopsis lateral root initiation. Plant Cell **13:** 843-852

Cline M (1997) Concepts and terminology of apical dominance. American Journal of Botany **84:** 1064-1069

Cook CE, Whichard LP, Turner B, Wall ME, Egley GH (1966) Germination of witchweed (*Striga lutea Lour.*): isolation and properties of a potent stimulant. Science **154:** 1189-1190

De Smet I, Tetsumura T, De Rybel B, Frey NFD, Laplaze L, Casimiro I, Swarup R, Naudts M, Vanneste S, Audenaert D, Inze D, Bennett MJ, Beeckman T (2007) Auxin-dependent regulation of lateral root positioning in the basal meristem of Arabidopsis. Development **134:** 681-690

De Smet I, Vanneste S, Inzé D, Beeckman T (2006) Lateral root initiation or the birth of a new meristem. Plant Molecular Biology **60:** 871-887

Dubrovsky JG, Sauer M, Napsucialy-Mendivil S, Ivanchenko MG, Friml J, Shishkova S, Celenza J, Benkova E (2008) Auxin acts as a local morphogenetic trigger to specify lateral root founder cells. Proceedings of the National Academy of Sciences of the United States of America **105:** 8790-8794

Foo E, Turnbull CGN, Beveridge CA (2001) Long-distance signaling and the control of branching in the *rms1* mutant of pea. Plant Physiology **126:** 203-209

Gomez-Roldan V, Fermas S, Brewer PB, Puech-Pages V, Dun EA, Pillot J-P, Letisse F, Matusova R, Danoun S, Portais J-C, Bouwmeester H, Becard G, Beveridge CA, Rameau C, Rochange SF (2008) Strigolactone inhibition of shoot branching. Nature **455:** 189-194

Grieneisen VA, Xu J, Maree AFM, Hogeweg P, Scheres B (2007) Auxin transport is sufficient to generate a maximum and gradient guiding root growth. Nature **449:** 1008-1013

Heckmann AB, Lombardo F, Miwa H, Perry JA, Bunnewell S, Parniske M, Wang TL, Downie JA (2006) Lotus japonicus nodulation requires two GRAS domain regulators, one of which is functionally conserved in a non-legume. Plant Physiology **142:** 1739-1750

Hu Z, Yan H, Yang J, Yamaguchi S, Maekawa M, Takamure I, Tsutsumi N, Kyozuka J, Nakazono M (2010) Strigolactones negatively regulate mesocotyl elongation in rice during germination and growth in darkness. Plant and Cell Physiology **51:** 1136-1142

Humphrey AJ, Galster AM, Beale MH (2006) Strigolactones in chemical ecology: waste products or vital allelochemicals? Natural Product Reports **23:** 592-614

Jamil M, Charnikhova T, Cardoso C, Jamil T, Ueno K, Verstappen F, Asami T, Bouwmeester HJ (2011) Quantification of the relationship between strigolactones and *Striga hermonthica* infection in rice under varying levels of nitrogen and phosphorus. Weed Research**:** no-no

Kaló P, Gleason C, Edwards A, Marsh J, Mitra RM, Hirsch S, Jakab J, Sims S, Long SR, Rogers J, Kiss GB, Downie JA, Oldroyd GED (2005) Nodulation signaling in legumes requires NSP2, a member of the GRAS family of transcriptional regulators. Science **308:** 1786-1789

Kapulnik Y, Delaux P-M, Resnick N, Mayzlish-Gati E, Wininger S, Bhattacharya C, Séjalon-Delmas N, Combier J-P, Bécard G, Belausov E, Beeckman T, Dor E, Hershenhorn J, Koltai H (2011) Strigolactones affect lateral root formation and root-hair elongation in Arabidopsis. Planta **233:** 209-216

Kohlen W, Charnikhova T, Liu Q, Bours R, Domagalska MA, Beguerie S, Verstappen F, Leyser O, Bouwmeester H, Ruyter-Spira C (2011) Strigolactones are transported through the xylem and play a key role in shoot architectural response to phosphate deficiency in nonarbuscular mycorrhizal host Arabidopsis. Plant Physiology **155:** 974-987

Koltai H, Dor E, Hershenhorn J, Joel D, Weininger S, Lekalla S, Shealtiel H, Bhattacharya C, Eliahu E, Resnick N, Barg R, Kapulnik Y (2010) Strigolactones' effect on root growth and root-hair elongation may be mediated by auxin-efflux carriers. Journal of Plant Growth Regulation **29:** 129-136

Laskowski M, Grieneisen VA, Hofhuis H, Hove CAt, Hogeweg P, Marée AFM, Scheres B (2008) Root system architecture from coupling cell shape to auxin transport. PLoS Biol **6:** e307

Ledger SE, Janssen BJ, Karunairetnam S, Wang T, Snowden KC (2010) Modified CAROTENOID CLEAVAGE DIOXYGENASE8 expression correlates with altered branching in kiwifruit (*Actinidia chinensis*). New Phytologist **188:** 803-813

Leyser O (2006) Dynamic integration of auxin transport and signalling. Current Biology **16:** R424-R433

Lin H, Wang R, Qian Q, Yan M, Meng X, Fu Z, Yan C, Jiang B, Su Z, Li J, Wang Y (2009) DWARF27, an iron-containing protein required for the biosynthesis of strigolactones, regulates rice tiller bud outgrowth. Plant Cell **21:** 1512-1525

López-Bucio J, Hernandez-Abreu E, Sanchez-Calderon L, Nieto-Jacobo MF, Simpson J, Herrera-Estrella L (2002) Phosphate availability alters architecture and causes changes in hormone sensitivity in the Arabidopsis root system. Plant Physiology **129:** 244-256

López-Ráez JA, Charnikhova T, Gómez-Roldán V, Matusova R, Kohlen W, Vos RD, Verstappen F, Puech-Pages V, Bécard G, Mulder P, Bouwmeester H (2008) Tomato strigolactones are derived from carotenoids and their biosynthesis is promoted by phosphate starvation. New Phytologist **178:** 863-874

López-Ráez JA, Kohlen W, Charnikhova T, Mulder P, Undas AK, Sergeant MJ, Verstappen F, Bugg TDH, Thompson AJ, Ruyter-Spira C, Bouwmeester H (2010) Does abscisic acid affect strigolactone biosynthesis? New Phytologist **187:** 343-354

Lucas M, Guédon Y, Jay-Allemand C, Godin C, Laplaze L (2008) An auxin transport-based model of root branching in *Arabidopsis thaliana*. Plos One **3**

Ma Z, Baskin TI, Brown KM, Lynch JP (2003) Regulation of root elongation under phosphorus stress involves changes in ethylene responsiveness. Plant Physiology **131:** 1381-1390

Maillet F, Poinsot V, André O, Puech-Pagès V, Haouy A, Gueunier M, Cromer L, Giraudet D, Formey D, Niebel A (2011) Fungal lipochitooligosaccharide symbiotic signals in arbuscular mycorrhiza. Nature **469:** 58-63

Martín Rodriguez JÁ, León Morcillo R, Vierheilig H, Antonio Ocampo J, Ludwig-Müller J, García Garrido JM (2010) Mycorrhization of the *notabilis* and *sitiens* tomato mutants in relation to abscisic acid and ethylene contents. Journal of Plant Physiology **167:** 606-613

Matusova R, Rani K, Verstappen FWA, Franssen MCR, Beale MH, Bouwmeester HJ (2005) The strigolactone germination stimulants of the plant-parasitic *Striga* and *Orobanche spp*. are derived from the carotenoid pathway. Plant Physiology **139:** 920-934

Moubayidin L, Di Mambro R, Sabatini S (2009) Cytokinin-auxin crosstalk. Trends in Plant Science **14:** 557-562

Murakami Y, Miwa H, Imaizumi-Anraku H, Kouchi H, Downie JA, Kawaguchi M, Kawasaki S (2007) Positional cloning identifies Lotus japonicus NSP2, a putative transcription factor of the GRAS family, required for *NIN* and *ENOD40* gene expression in nodule initiation. DNA research **13:** 255-265

Nacry P, Canivenc G, Muller B, Azmi A, Van Onckelen H, Rossignol M, Doumas P (2005) A role for auxin redistribution in the responses of the root system architecture to phosphate starvation in Arabidopsis. Plant Physiology **138:** 2061-2074

Nelson DR, Schuler MA, Paquette SM, Werck-Reichhart D, Bak S (2004) Comparative Genomics of Rice and Arabidopsis. Analysis of 727 Cytochrome P450 Genes and Pseudogenes from a Monocot and a Dicot. Plant Physiology **135:** 756-772

Pérez-Torres C-A, Lopez-Bucio J, Cruz-Ramirez A, Ibarra-Laclette E, Dharmasiri S, Estelle M, Herrera-Estrella L (2008) Phosphate availability alters lateral root development in Arabidopsis by modulating auxin sensitivity via a mechanism involving the TIR1 auxin receptor. Plant Cell **20:** 3258-3272

Proust H, Hoffmann B, Xie X, Yoneyama K, Schaefer DG, Yoneyama K, Nogué F, Rameau C (2011) Strigolactones regulate protonema branching and act as a quorum sensing-like signal in the moss *Physcomitrella patens*. Development **138:** 1531-1539

Rahman A, Bannigan A, Sulaman W, Pechter P, Blancaflor EB, Baskin TI (2007) Auxin, actin and growth of the Arabidopsis thaliana primary root. The Plant Journal **50:** 514-528

Rani K, Zwanenburg B, Sugimoto Y, Yoneyama K, Bouwmeester HJ (2008) Biosynthetic considerations could assist the structure elucidation of host plant produced rhizosphere signalling compounds (strigolactones) for arbuscular mycorrhizal fungi and parasitic plants. Plant Physiology and Biochemistry **46:** 617-626

Rock C, Sun X (2005) Crosstalk between ABA and auxin signaling pathways in roots of *Arabidopsis thaliana* (L.) Heynh. Planta **222:** 98-106

Ruyter-Spira C, Kohlen W, Charnikhova T, van Zeijl A, van Bezouwen L, de Ruijter N, Cardoso C, López-Ráez JA, Matusova R, Bours R, Verstappen F, Bouwmeester H (2011) Physiological effects of the synthetic strigolactone analog GR24 on root system architecture in Arabidopsis: Another belowground role for strigolactones? Plant Physiology **155:** 721-734

Sánchez-Calderón L, Lopez-Bucio J, Chacon-Lopez A, Cruz-Ramirez A, Nieto-Jacobo F, Dubrovsky JG, Herrera-Estrella L (2005) Phosphate starvation induces a determinate developmental program in the roots of *Arabidopsis thaliana*. Plant Cell Physiology **46:** 174-184

Sharda J, Koide R (2008) Can hypodermal passage cell distribution limit root penetration by mycorrhizal fungi? New Phytologist **180:** 696-701

Smit P, Raedts J, Portyanko V, Debellé F, Gough C, Bisseling T, Geurts R (2005) NSP1 of the GRAS protein family is essential for rhizobial Nod factor-induced transcription. Science **308:** 1789-1791

Snowden KC, Simkin AJ, Janssen BJ, Templeton KR, Loucas HM, Simons JL, Karunairetnam S, Gleave AP, Clark DG, Klee HJ (2005) The *Decreased apical dominance 1/petunia hybrida carotenoid cleavage dioxygenase8* gene affects branch production and plays a role in leaf senescence, root growth, and flower development. Plant Cell **17:** 746-759

Sorefan K, Booker J, Haurogné K, Goussot M, Bainbridge K, Foo E, Chatfield S, Ward S, Beveridge C, Rameau C, Leyser O (2003) *MAX4* and *RMS1* are orthologous dioxygenase-like genes that regulate shoot branching in Arabidopsis and pea. Genes & Development **17:** 1469-1474

Stirnberg P, van de Sande K, Leyser HMO (2002) MAX1 and MAX2 control shoot lateral branching in Arabidopsis. Development **129:** 1131-1141

Taylor IB, Linforth RST, Al-Naieb RJ, Bowman WR, Marples BA (1988) The wilty tomato mutants *flacca* and *sitiens* are impaired in the oxidation of ABA-aldehyde to ABA. Plant, Cell & Environment **11:** 739-745

Troughton A (1977) The effect of phosphorus nutrition upon the growth and morphology of young plants of *Lolium perenne L*. Annals of Botany **41:** 85-92

Tsuchiya Y, Vidaurre D, Toh S, Hanada A, Nambara E, Kamiya Y, Yamaguchi S, McCourt P (2010) A small-molecule screen identifies new functions for the plant hormone strigolactone. Nature Chemical Biology **6:** 741-749

Umehara M, Hanada A, Magome H, Takeda-Kamiya N, Yamaguchi S (2010) Contribution of strigolactones to the inhibition of tiller bud outgrowth under phosphate deficiency in rice. Plant and Cell Physiology**:** 1118-1126

Umehara M, Hanada A, Yoshida S, Akiyama K, Arite T, Takeda-Kamiya N, Magome H, Kamiya Y, Shirasu K, Yoneyama K, Kyozuka J, Yamaguchi S (2008) Inhibition of shoot branching by new terpenoid plant hormones. Nature **455:** 195-200

Vieten A, Vanneste S, Wiśniewska J, Benková E, Benjamins R, Beeckman T, Luschnig C, Friml J (2005) Functional redundancy of PIN proteins is accompanied by auxin-dependent cross-regulation of PIN expression. Development **132:** 4521-4531

Vogel JT, Walter MH, Giavalisco P, Lytovchenko A, Kohlen W, Charnikhova T, Simkin AJ, Goulet C, Strack D, Bouwmeester HJ, Fernie AR, Klee HJ (2010) SlCCD7 controls strigolactone biosynthesis, shoot branching and mycorrhiza-induced apocarotenoid formation in tomato. The Plant Journal **61:** 300-311

Xie X, Yoneyama K, Yoneyama K (2010) The strigolactone story. Annual Review of Phytopathology **48:** 93-117

Yoneyama K, Takeuchi Y, Yokota T (2001) Production of clover broomrape seed germination stimulants by red clover root requires nitrate but is inhibited by phosphate and ammonium. Physiologia Plantarum **112:** 25-30

Yoneyama K, Yoneyama K, Takeuchi Y, Sekimoto H (2007) Phosphorus deficiency in red clover promotes exudation of orobanchol, the signal for mycorrhizal symbionts and germination stimulant for root parasites. Planta **225:** 1031-1038

Zou J, Zhang S, Zhang W, Li G, Chen Z, Zhai W, Zhao X, Pan X, Xie Q, Zhu L (2006) The rice *HIGH-TILLERING DWARF1* encoding an ortholog of Arabidopsis *MAX3* is required for negative regulation of the outgrowth of axillary buds. The Plant Journal **48:** 687-698

Summary

Strigolactones are carotenoid derived signaling molecules initially identified as germination stimulants for root parasites of the Orobanchaceae family and pre-symbiotic signal for arbuscular mycorrhiza (AM). They have been identified in the root extracts and exudates of many plant species. Recently, strigolactones – or their derivatives – were identified to be the branch inhibiting signal. This elusive signal is graft transmissible and originating - partly - from the root system. However, the exact origin of strigolactones in the shoot is unknown. Nevertheless, it is likely that strigolactones are transported to the shoot where they exert their shoot branching inhibiting effect in concert with auxin and cytokinins. However, reports of strigolactones in aerial parts of the plant are scarce.

Strigolactone biosynthesis is not fully elucidated. An unknown carotenoid substrate is sequentially cleaved by CAROTENOID CLEAVAGE DIOXYGENASE7 (CCD7) and CAROTENOID CLEAVAGE DIOXYGENASE8 (CCD8). In addition to this, two enzymes MORE AXILLARY GROWTH1 and DWARF27 are also involved in strigolactone biosynthesis. However, their precise role in strigolactone biosynthesis remains unknown.

In **chapter 1**, the root parasitic plants of the Orobanchaceae family and the problems they cause in agriculture are introduced. Furthermore, the role of strigolactones in the root parasite lifecycle as well as in AM symbiosis are addressed. In addition, the recently discovered strigolactone role in shoot architecture, their biosynthesis, hormonal signaling and the two theories on how strigolactones might be integrated into the apical dominance are described.

The first genuine strigolactone derived form the strigolactone biosynthetic pathway is thought to be 5-deoxystrigol. This strigolactone is postulated to be the precursor for all known strigolactones, which are believed to be derived from this compound through a number of different enzymatic and/or non-enzymatic steps. In **chapter 2**, the biosynthesis of solanacol in the roots of tomato (*Solanum lycopersicum)* is described. This strigolactone contains an aromatic A-ring and therefore its biosynthesis from the precursor 5-deoxystrigol is not obvious. On the basis of the presence of other strigolactones in tomato (orobanchol, orobanchyl acetate, two 7-hydroxy-orobanchol isomers, 7-oxo-orobanchol and four didehydro-orobanchol isomers) we postulate how solanacol can be derived from 5-deoxystrigol through a series of enzymatic hydroxylation-dehydroxylation reactions with migration of a methyl group and the introduction of double bonds.

In **Chapter 3** we report the cloning of a tomato *CAROTENOID CLEAVAGE DIOXYGENASE 8* (*SlCCD8*) and demonstrate that reduction of its expression leads to reduced strigolactone levels in root extracts, exudates and xylem sap. All lines display excessive lateral shoot branching, reduced plant height and increased numbers of nodes. We show that the severity of these phenotypes correlates with the level of orobanchol present in tomato xylem sap. Furthermore, we demonstrate that a mild reduction in strigolactone biosynthesis and concomitant secretion into the rhizosphere is sufficient to reduce root parasitism by *Phelipanche ramosa* by about 90% without compromising apical dominance or AM symbiosis establishment too much. We also report additional phenotypes in tomato reproductive development (such as smaller flowers, fruits and seeds) - normally associated with reduced auxin levels – to be present in these strigolactone-deficient transgenic lines. We demonstrate decreased levels of free auxin in these organs, indicating that these phenotypes might be the consequence of the removal of the down-regulating effect of strigolactones on auxin levels.

In addition to strigolactones, the - well described - phytohormone abscisic acid (ABA) is also derived from the carotenoid pathway. Earlier results in our group indicated that a mutation in 9-*cis*-

epoxycarotenoid dioxygenase (NCED) - an enzyme involved in ABA-biosynthesis - results in lower strigolactone levels. For this reason we investigated the relationship between ABA and strigolactones. Our findings are reported in **chapter 4**. We demonstrate that the carotenoid cleavage dioxygenase (CCD) inhibitor D2 reduces strigolactone but not ABA content of roots. However, in plants treated with abamineSG - an inhibitor of 9-*cis*-epoxycarotenoid dioxygenase (NCED) - and in the ABA mutants *Notabilis*, *Sitiens* and *Flacca* (mutants in two different enzymatic steps in ABA biosynthesis), both ABA and strigolactone levels were strongly reduced. Our results indicate a correlation between ABA levels and strigolactone biosynthesis, and suggest a role for ABA in the regulation of strigolactone biosynthesis.

In **chapter 5** the role of two GRAS-type transcription factors (NSP1 and NSP2) in the regulation of strigolactone biosynthesis is assessed. In legumes these transcription factors are essential for *Rhizobium* Nod factor induced nodulation. In this chapter we show that NSP1 and NSP2 are required for strigolactone biosynthesis in *Medicago truncatula* and rice. Hereto we have developed *M. truncatula* as a model for strigolactone analysis and identified its strigolactone composition to consist of didehydro-orobanchol (major) and orobanchol (minor). With this work we identify for the first time transcription factors that are regulating strigolactone biosynthesis. We demonstrate that NSP1 functions in strigolactone biosynthesis by regulating *DWARF27* expression. Our *in vitro* binding studies indicate that *MtDWARF27* is a primary target of MtNSP1. We also demonstrate that MtNSP2 is essential for conversion of orobanchol into didehydro-orobanchol. *NSP1* and *NSP2* are single copy genes in legumes, implying that the proteins they encode fulfill dual regulatory functions of different downstream targets: symbiotic and non-symbiotic. Since NSP1 and NSP2 are required for strigolactone biosynthesis in rice as well as Medicago and these two species represent distinct phylogenetic lineages that split ~150 million years ago, we postulate that regulation of strigolactone biosynthesis by NSP1 and NSP2 is an ancestral function conserved in higher plants.

In **chapter 6** strigolactone biosynthesis is assessed using *Arabidopsis thaliana* as a model. Strict control of environmental conditions and optimization of analytical protocols for strigolactone analysis enabled the detection of orobanchol, orobanchyl acetate and 5-deoxystrigol in Arabidopsis. In this chapter we demonstrate that the relation between phosphate starvation and the up-regulation of strigolactone biosynthesis is also present in this non AM species. Most land plants are mycorrhizal, which is believed to be the ancestral condition. Hence lack of AM symbiosis in Arabidopsis is likely to be a derived trait. We postulate that strigolactone exudation into the rhizosphere is a relic of this ancestral trait lost by Arabidopsis. However, our data show that strigolactone up-regulation in Arabidopsis under phosphorus deficient conditions serves to restrict the outgrowth of lateral shoot branches. We postulate that this represents an evolutionary advantage which could be the new driving force for the preservation of low phosphate induced strigolactone biosynthesis, as AM colonization no longer is in Arabidopsis. We demonstrate that orobanchol is transported through the xylem sap and that its concentration is elevated under phosphorus deficient conditions and we provide analytical evidence that MAX1 is required for orobanchol biosynthesis.

Recently, a novel function for strigolactones in the regulation of root system architecture (RSA) of tomato and Arabidopsis has been discovered. In **chapter 7** we show that reduced strigolactone biosynthesis or perception - as displayed by the *max1,2,4* mutants - leads to a reduction in the length of the primary root meristem. We demonstrate that application of the synthetic strigolactone analog GR24 is able to rescue this phenotype in all max mutants except the strigolactone insensitive mutant,

max2. Furthermore - when grown under sufficient phosphate conditions - GR24 application reduces the amount of lateral roots (LR) - arresting their development at phase five of lateral root primordia (LRP) initiation. We also show that higher concentrations of GR24 blocked LRP initiation completely and caused the primary root meristem to collapse. However, when GR24 application is accompanied by exogenous application of NAA, it has a stimulatory effect on lateral root development and outgrowth. Similarly, under phosphate-limiting conditions, up-regulation of endogenous strigolactones (**chapter 6**) present in wild type plants stimulated a more rapid outgrowth of lateral root primordia when compared with strigolactone-deficient mutants. In addition, we demonstrate that – under sufficient phosphate conditions - GR24 application to the root system of Arabidopsis leads to reduced auxin concentrations in the leaves. Combined, these results suggest that strigolactones are modulating local auxin gradients and hence influence changes in root architecture. Therefore, the net result of strigolactone action on root development depends on the auxin status of the plant. We postulate that a tightly balanced auxin-strigolactone interaction is the basis for the mechanism by which plants regulate their root to shoot ratio for example under phosphate limited conditions.

In **chapter 8** we summarize and discuss the most important results obtained from the work presented in this thesis and integrate these into the current knowledge on strigolactones, both as a plant hormone as well as rhizosphere signaling molecule. In this chapter we also consider the future perspectives of strigolactone research, especially related to the root parasitic weed problem.

Samenvatting

(Summary in Dutch)

Strigolactonen zijn van carotenoïden afkomstige signaalmoleculen, aanvankelijk geïdentificeerd als de kiemstimulantia voor wortelparasieten van de *Orobanchaceae* familie en pre-symbiotisch signaal voor arbusculaire mycorrhiza (AM) schimmels. Strigolactonen zijn aangetoond in de wortelextracten en exudaten van diverse plantensoorten. Recent zijn strigolactonen - of hun afgeleiden - geïdentificeerd als plantenhormoon betrokken bij de regulatie van de plantarchitectuur. Het lijkt erop dat strigolactonen vooral in de wortels worden geproduceerd, maar de exacte plaats van strigolacton biosynthese is onbekend. Niettemin is het waarschijnlijk dat strigolactonen vanuit de wortels naar de scheut worden getransporteerd waar zij hun remmende werking op okselknopuitgroei, in samenwerking met auxine en cytokinines, uitoefenen. Tot nu toe zijn strigolactonen in de scheut van planten niet of nauwelijks aangetoond.

Ook de biosynthese van strigolactonen is nog niet volledig opgehelderd. Een onbekend carotenoid substraat wordt opeenvolgend geknipt door CAROTENOID CLEAVAGE DIOXYGENASE 7 (CCD7) en CAROTENOID CLEAVAGE DIOXYGENASE 8 (CCD8). Hiernaast, zijn twee enzymen, MORE AXILLARY GROWTH 1 (MAX1) and DWARF 27 (D27), betrokken bij de biosyntheses van strigolactonen, maar hun exacte rol is onbekend.

In **hoofdstuk 1**, worden de wortelparasitaire planten van de Orobanchaceae familie en de problemen welke zij veroorzaken in de landbouw geïntroduceerd. Verder wordt de rol van strigolactonen in de levenscyclus van deze parasieten en in AM symbiose besproken. Daarnaast, wordt de recent ontdekte hormonale functie van strigolactonen in de plantarchitectuur, hun biosynthese, hormonale signalering en de twee gangbare theorieën over hoe strigolactonen een rol spelen bij apicale dominantie beschreven.

Van 5-deoxystrigol wordt gedacht dat dit het eerste echte strigolacton afkomstig van de strigolacton biosynthese route is. Aangenomen wordt dat 5-deoxystrigol via een aantal - al dan niet enzymatische - stappen de precursor is voor alle andere bekende strigolactonen. In **hoofdstuk 2**, wordt de biosynthese van solanacol in de wortel van tomaat (*Solanum lycopersicum)* beschreven. Solanacol heeft een aromatische A-ring en daardoor is de biosyntheses van dit strigolactone via 5-deoxystrigol niet voor de hand liggend. Op basis van de aanwezigheid van andere strigolactonen in tomaat (orobanchol, orobanchyl acetate, twee 7-hydroxy-orobanchol isomeren, 7-oxo-orobanchol en vier didehydro-orobanchol isomeren) speculeren wij hoe solanacol door een series van enzymatische hydroxylatie-dehydroxylatie reacties, de migratie van een methyl groep en de introductie van dubbele bindingen van 5-deoxystrigol afgeleid kan zijn.

In **hoofdstuk 3** bespreken we de klonering van een tomaat *CAROTENOID CLEAVAGE DIOXYGENASE 8* (*SlCCD8*) en demonsteren dat een reductie in CCD8 expressie leid tot een reductie van strigolactonen in de wortel extracten, exudaten en het xyleem sap. Alle lijnen tonen excessieve zijscheutgroei, zijn korter en hebben meer internodes. Ook demonstreren wij dat de sterkte van al deze fenotypes correleert met de concentratie orobanchol in het xyleem sap. Verder tonen we aan dat een milde reductie in strigolacton biosynthese en de gerelateerde secretie naar de rhizosphere voldoende is om parasitisme door *Phelipanche ramosa* met 90% te verminderen. Dit zonder de apicale dominantie of AM symbiose te sterk nadelig te beïnvloeden. Verder melden we enkele additionele fenotypes in de reproductieve ontwikkeling van tomaat (zoals kleinere bloemen, vruchten en zaden) - normaliter geassocieerd met gereduceerde auxine niveaus. We demonstreren verlaagde niveaus van vrij auxine in deze organen, wat er op wijst dat deze fenotypes mogelijk een consequentie zijn van het ontbreken van het regulerende effect van strigolactonen op het auxine niveau.

Het goed beschreven plant hormoon abscissine zuur (ABA) is net als de strigolactonen afkomstig van de carotenoïden. Eerdere experimenten binnen onze groep wezen uit dat een mutatie in 9-*cis*-epoxycarotenoid dioxygenase (NCED) – een sleutel enzym betrokken bij de ABA biosyntheses – leidt tot een reductie in de strigolacton productie. Dit gaf aanleiding tot onderzoek naar de relatie tussen ABA en strigolactonen. De resultaten van dit onderzoek worden omschreven in **hoofdstuk 4**. Wij demonstreren dat applicatie van de carotenoid cleavage dioxygenase (CCD) inhibitor D2 het strigolacton niveau verlaagt, maar geen effect heeft op de ABA concentraties. Echter, in planten behandeld met abamineSG – een remmer van de 9-*cis*-epoxycarotenoid dioxygenases (NCEDs) - en in de ABA deficiënte mutanten *notabilis*, *sitiens* en *flacca* (mutanten in twee verschillende enzymatische stappen van de ABA biosynthese), zijn de niveaus van zowel ABA als strigolactonen gereduceerd. Onze resultaten duiden op een correlatie tussen ABA niveaus en strigolacton biosynthese en wijzen op een mogelijke rol van ABA in de regulatie van strigolacton biosynthese.

In **hoofdstuk 5** wordt de rol van twee GRAS-type transcriptie factoren (*NSP1* en *NSP2*) in de regulatie van strigolacton biosynthese besproken. In peulvruchten hebben deze transcriptie factoren een essentiële rol in de door *Rhizobium* Nod factor geïnduceerde nodulatie. In dit hoofdstuk tonen we aan dat *NSP1* en *NSP2* ook vereist zijn voor de strigolactone biosynthese in *Medicago truncatula* (Medicago) en rijst. Hiervoor is Medicago opgezet als een modelplant voor stigolacton analyse. Ook tonen wij aan dat het strigolactonenmengsel van *M. truncatula* bestaat uit dedihydro-orobanchol (major) en orobanchol (minor). In dit werk identificeren we voor het eerst transcriptie factoren welke de biosynthese van strigolactonen reguleren. Wij tonen aan dat *NSP1* de strigolacton biosynthese reguleert door middel van de regulatie van de expressie van *D27*. Een *in vitro* binding studie toont dat *MtD27* een primair doel van MtNSP1 kan zijn. Verder tonen wij aan dat *MtNSP2* essentieel is voor de conversie van orobanchol naar dedihydro-orobanchol. Het feit dat *NSP1* en *NSP2* vereist zijn voor strigolacton biosynthese in zowel rijst als Medicago - soorten die twee verschillende fylogenetische geslachten vertegenwoordigen welke ongeveer 150 miljoen jaar geleden ontstaan zijn – brengt ons tot de aanname dat de regulatie van de strigolacton biosynthese door NSP1 en NSP2 als een voorouderlijke functie in hogere planten is geconserveerd.

In **hoofdstuk 6** bestuderen we strigolacton biosynthese in *Arabidopsis thaliana* (Arabidopsis). Strikte controle van de groeicondities en optimalisatie van de analytische protocollen voor strigolacton analyse maakte de detectie van orobanchol, orobanchyl acetaat en 5-deoxystrigol in Arabidopsis mogelijk. In dit hoofdstuk tonen wij aan dat de relatie tussen fosfaat tekort en de inductie van strigolacton biosynthes ook in deze soort aanwezig is. Dat is opmerkelijk omdat Arabidopsis geen AM symbiose aangaat in tegenstelling tot de meeste andere landplanten. Het ontbreken van AM symbiose in Arabidopsis is daarom mogelijk een verloren eigenschap. Wij speculeren dat de exudatie van strigolactonen naar de rhizosfeer – wat Arabidopsis zij het in lage hoeveelheden nog steeds doet - een overblijfsel is van deze voorouderlijke eigenschap welke door Arabidopsis verloren is. Echter, onze resultaten demonstreren dat de verhoging van de strigolacton biosynthese in Arabidopsis onder fosfaat tekort dient om de groei van de zijscheuten te verminderen onder deze suboptimale condities. Wij speculeren dat dit mogelijk een evolutionair voordeel schept welke de nieuwe stuwende kracht is voor het behoud van fosfaat-tekort geïnduceerde verhoging van de strigolacton biosynthese in Arabidopsis, aangezien AM symbiose niet meer aanwezig is. We tonen aan dat orobanchol getransporteerd wordt in het xyleem sap en dat de concentratie hiervan omhoog gaat onder fosfaat tekort. Verder leveren we analytisch bewijs dat MAX1 is vereist voor de biosynthese van orobanchol.

Een nieuwe functie van strigolactonen in de regulatie van wortelarchitectuur in tomaat en Arabidopsis is recent ontdekt. In **hoofdstuk 7** tonen we dat een reductie in strigolacton biosynthese en/of perceptie - als vertoond in de *max1,2,4* mutanten - leidt tot een reductie in de lengte van het primaire wortelmeristeem. We demonstreren dat toediening van het synthetische strigolacton GR24 dit fenotype in alle *max* mutanten - uitgezonderd de strigolacton ongevoelige mutant *max2* – kan herstellen. De toediening van GR24 onder toereikende fosfaat condities reduceert het totale aantal laterale wortels per plant - hun ontwikkeling wordt gestopt in fase vijf van de laterale wortel primordium initiatie. Ook tonen wij aan dat hogere concentraties GR24 de initiatie van deze laterale wortel primordia compleet blokkeren wat leidt tot het instorten van het primaire wortelmeristeem. Echter, als GR24 samen met exogeen auxine (NAA) wordt toegediend heeft het een stimulerend effect op de laterale wortelontwikkeling en -uitgroei. Daaraan analoog, onder fosfaatbeperkende condities stimuleert de verhoging van endogene strigolacton niveaus (**hoofdstuk 6**) in wild type planten een snellere uitgroei van laterale wortel primordia vergeleken met de strigolacton-deficiënte mutanten. Verder demonstreren wij dat – onder toereikende fosfaat condities - GR24 toediening aan het wortelsysteem van Arabidopsis leidt tot een lagere auxineconcentratie in de bladeren. Gecombineerd wijzen deze resultaten erop dat strigolactonen lokale auxine gradiënten modificeren en zo invloed uitoefenen op de wortel architectuur. Daardoor zal het netto resultaat van de strigolactone werking op de ontwikkeling van het wortelstelsel afhangen van de auxine status van een plant. Wij denken dat een uiterst fijn gereguleerde balans tussen auxine en strigolactonen de basis vormt voor het mechanisme dat de wortel-scheut ratio van een plant reguleert, bijvoorbeeld onder fosfaat limiterende condities.

Hoofdstuk 8 is een samenvatting en discussie van de meest belangrijke resultaten verkregen gedurende het werk gepresenteerd in dit proefschrift. Er wordt getracht de nieuw verkregen kennis te integreren met de huidige kennis van strigolactonen. Zowel op het gebied van hun hormonale eigenschappen als hun rol als rhizosfeer signaal. In dit hoofdstuk word verder vooruit gekeken naar de perspectieven van het onderzoek aan strigolactonen. Speciale aandacht wordt besteed aan de relatie met het probleem van de parasitaire planten.

Acknowledgements

Their is a cliché by which most of these acknowledgments start. This one will be no different. There are many people that were involved in the realization of this thesis, I thank them all. However, a few I would like to mention in person. Rumor has it that this is the part of the thesis that people do read, therefore I will try not to make a complete fool of myself.

I would like to start by thanking my promoter, Prof. dr. Harro Bouwmeester for giving me the opportunity to work on strigolactones for the last years. I remember when we first met. My first scientific job interview, I was nervous as hell. However, I somehow convinced you that I was the right candidate for the job as you offered it to me a few hours later. You know it has been difficult at times, my car accident, mother's illness and ultimately her death had a huge impact on me and my performance. I am grateful for your support.

My co-promoter, Carolien. Thank you for all your guidance, friendship and tough words when needed. I honestly believe that I would not have succeeded in my PhD if it wasn't for you. As you know, the first two years were pretty tough. You provided the structure that was absent for too long. At first it was difficult to accept your request for detailed formulation of my ideas, experiments and most of all planning. However, this gradually became more and more natural. I will never be as organized as you are but you definitely gave me a push in the right direction.

Juan Antonio from you I learned more than you taught me. I consider you one of my best friends, not just in the scientific world. I do not like that you now live on the other side of Europe, but we will keep planning joint congresses together! Still, I miss your Spanglish and look forward to my planned trip to Spain autumn of next year.

My favorite chemist Tanya, you always seem to work double shifts. You are the chemical analyst for the group and operate the most important piece of machinery we have at our disposal, the Waters Xevo tandem quadruple mass spectrometer equipped with an electrospray ionization source and coupled to an Acquity UPLC system. A real mouthful, isn't it. You do all the analysis and calculations for a large part of the group, not always getting the credit you deserve. In these few lines I would like to express my gratitude for this. At the same time you have your own postdoc projects that require your full attention as well. On a more personal note, you have no idea how much I started to dislike the word maybe with a Russian accent. Many times you told me that a peak was maybe strigolactone, which indicated it probably was not.

I would especially like to thank Francel. The true hidden hero of my project and I am sure several other PPH projects as well. I remember the evenings you either stayed late or came back to help me with my work. It didn't matter, if I needed help with sample collections in the greenhouse, auxin transport assays in the isotope lab or just exudate purification in the lab. If needed, you were there and didn't leave until the work was done, or we were kindly asked to leave by the security. The latter only happened two, maximum three times. Francel, thank you!

Ralph, you started as a student, became a college and now I consider you a friend. I deeply respect you and greatly value your opinion. I am confident that you will have a great scientific career. I very much appreciate our scientific discussions and am grateful we shared some of our frustrations. You know we were compared once to Waldorf and Statler and I am afraid I must concur with this comparison!

Peter, the man with colorful clothing. You are by far the most enthusiastic scientist I know. Your 'small' presentations are magic! Thank you for being part of my PhD experience.

Rada, you are one of the most straightforward people I know. Thank you for showing me it is okay to speak your mind. At one moment it seemed everybody was leaving. However, you came back (although only briefly).

I would like to thank my colleagues of the parasitic plant team (Catarina, Imran, Nasr, Xi, Yanxia, Carin and Jamil) and Plant Physiology (Ronny, Benyamin, Jimmy, Anna, Desalegn, Lydia, Rik, Liu Qing, Natalia, Manickam et al) for their value input and more important pleasant working atmosphere.

During my PhD I supervised several students (Tobia, Sebastiën, Laura, Bart, Ralph). You were all special in your individual way. Supervising you guys I really learned a lot, especially about myself. I hope you also learned a bit from me!

I would like to thank some (inter)national collaborators and supervisors for their wisdom and guidance. I really learned a lot working with you. I would especially like to mention Prof. dr. Titti Mariani, Wim Vriezen, Lisette Nitch, Prof. dr. Ottoline Leyser, Malgorzata (Gosia) Domagalska, Prof. dr. Binne Zwanenburg, Tobias Kretzschmar, Prof. dr. Enrico Marinoia, Efstathios (Stathis) Roumeliotis, Padraic Flood, Ruud de Maagd, Michiel Lammers, Norbert de Ruijter, Rene Geurts, Jonathan Vogel, Prof. dr. Harry Klee, Prof. dr. Ton Bisseling, Liu Wei, Davide Bulgarelli, Prof. dr. Paul Schulze-Lefert, Prof. dr. Maarten Koornneef and Prof dr. Klaus Theres.

My two oldest and dearest fiends Bas and Jim. I thank you for always being there, in good and in bad times. We had a lot of fun together (some times too much) and I promise you we will have a lot more in the future!

My mentor and friend Wil. Thank you for believing in me, especially when I did not. Your support and guidance were a beckon for me not only during my first study at the HAN. I am not sure, but I really hope that some day soon I will be able to finish what I started.

I thank my loving parents Marjorie† and Jan Kohlen. Thank you for your unlimited support and for giving me the ability to follow my own path wherever it takes me. The most precious gift you ever gave me is the opportunity to make my own mistakes.
Special thanks for my brother Martijn, you have no idea how much I admired you when we were growing-up and how long I lived in your shadow.
To my in-laws Herm and Marian I can be brief, thank you for your daughter! Oh, and all the free lunches, diners and breakfasts I ‘stole’ from you!

My sons, Quinten, Pepijn and Julian. First of all I would like to apologize to you for being late from work so many times. I would like to thank you for showing me the wonders of being young. The sheer unspoiled amazement you guys show at each new discovery makes me realize that this must be a vital quality for any researcher. I know you will grow-up and change, but please don’t rush on my account.

Finally, my lovely wife Petra. I would like to thank you for your companionship, warmth and love. With the words of John Denver “If I should live forever and all my dreams come true, my memories of love would be of you.”

Publication list

Publications related to this thesis

Research articles

Kohlen W*, Charnikhova T*, Qing L, Bours R, Domagalska MA, Beguerie S, Verstappen F, Leyser O, Bouwmeester HJ, Ruyter-Spira C (2010) Strigolactones are transported through the xylem and play a key role in shoot architectural response to phosphate deficiency in non-AM host Arabidopsis thaliana. Plant physiology 155(2): 974-987

* authors contributed equally to this publication

Ruyter-Spira C*, **Kohlen W***, Charnikhova T, Zeijl van A, Bezouwen van L, de Ruijter N, Cardoso C, Lopez-Raez JA, Matusova R, Bours R, Verstappen F, Bouwmeester HJ (2010) Physiological effects of the synthetic strigolactone analogue GR24 on root system architecture in Arabidopsis: Another below-ground role for strigolactones? Plant physiology 155(2): 721-734

* authors contributed equally to this publication

Malik H, **Kohlen W**, Jamil M, Rutjes FPJT, Zwanenburg B (2010) Aromatic A-ring analogues of orobanchol, new germination stimulants for seeds of parasitic weeds. Organic & Biomolecular Chemistry 9: 2286-2293

López-Ráez JA*, **Kohlen W***, Charnikhova T, Mulder P, Undas AK, Sergeant MJ, Verstappen F, Bugg TDH, Thompson AJ, Ruyter-Spira C, Bouwmeester HJ (2010) Does abscisic acid affect strigolactone biosynthesis? New Phytologist 187: 343-354

* authors contributed equally to this publication

Vogel JT, Walter MH, Giavalisco P, Lytovchenko A, **Kohlen W**, Charnikhova T, Simkin AJ, Goulet C, Strack D, Bouwmeester HJ, Fernie AR, and Klee HJ (2010) SlCCD7 controls strigolactone biosynthesis, shoot branching and mycorrhiza induced apocarotenoid formation in tomato. Plant Journal 61(2): 300-311

López-Ráez JA, Charnikhova T, Mulder P, **Kohlen W**, Bino R, Levin I, Bouwmeester HJ (2008) Susceptibility of the tomato mutant *high pigment-2dg* (*hp-2dg*) to Orobanche spp. Infection. Journal of Agricultural and Food Chemistry 56: 6326-6332

López-Ráez JA, Charnikhova T, Gómez-Roldán V, Matusova R, **Kohlen W**, Vos RD, Verstappen F, Puech-Pages V, Bécard G, Mulder P, Bouwmeester HJ (2008) Tomato strigolactones are derived from carotenoids and their biosynthesis is promoted by phosphate starvation. New Phytologist 178: 863-874

Kohlen W*, López-Ráez JA*, Tobia Pollina, Michiel Lammers, Peter Toth, Tatsiana Charnikhova, Ruud de Maagd, María J. Pozo, Carolien Ruyter-Spira and Harro Bouwmeester (2011) The tomato *CAROTENOID CLEAVAGE DIOXYGENASE8 (SlCCD8)* is regulating, rhizosphere signaling, plant architecture and reproductive development through strigolactone biosynthesis. (submitted, the Plant journal)

* authors contributed equally to this publication

Liu W, **Kohlen W**, Lillo A, Camp op den R, Ivanov S, Hartog M, Limpens E, Jamil M, Smaczniak C, Kaufmann K, Yang WC, Hooiveld G, Charnikhova T, Bouwmeester HJ, Bisseling T and Geurts R (2011) Strigolactone biosynthesis requires the sybiotic gras-type transcription factors NSP1 and NSP2 (accepted, the Plant Cell)

Kretzschmar T, **Kohlen W**, Sasse J, Schlegel M, Bachelier JB, Bours R, Harro J. Bouwmeester, Martinoia E. (2011) A petunia ABC protein controls strigolactone-dependent symbiotic signaling and branching (under review, Nature)

Reviews articles

Kohlen W, Ruyter-Spira C and Bouwmeester HJ (2011) Strigolactones. A new musician in the orchestra of plant hormones (Accepted, Botany)

López-Ráez JA, Matusova R, Cardoso C, Jamil M, Charnikhova T, **Kohlen W**, Ruyter-Spira C, Verstappen F and Bouwmeester HJ (2009) Strigolactones: ecological significance and use as a target for parasitic plant control. *Pest Management Science* 65, 471-477

Kohlen W and Bouwmeester HJ (2007) Ondergrondse communicatie: de driehoeksrelatie gastheerplant, parasitaire plant en mycorrhiza-schimmel Gewasbescherming 38(4): 145-149

Other publication

Madsen O, Kortum TT, Hupkes M, **Kohlen W**, van Rheede T, de Jong WW (2010) Loss of octarepeats in two processed prion pseudogenes in the red squirrel, *Sciurus vulgaris*, Journal of molecular evolution 71:356-363

Nitsch L, Oplaat C, Michieli T, **Kohlen W**, Charnikhova T, Bouwmeester HJ, Mariani C and Vriezen WH (2011) ABA-deficiency in *notabilis* and *flacca* mutants and the *notabilis-flacca* double mutant results in reduced plant and fruit size. (Submitted, Journal of Plant Physiology)

Curriculum vitae

Wouter Kohlen was born on the 26th of March 1975 in Venlo. In 1994 he obtained his secondary school diploma (HAVO, Thomas college Venlo). In that same year he started a bachelor environmental hygiene in Deventer, but switched to a bachelor biology teaching at the Hogeschool van Arnhem en Nijmegen in 1995. After his graduation he worked as a biology teacher for almost one year. In 2000 he joint Cap Gemini Ernst & Young as an educational consultant, a position he held for four years. In this period he gained insight in several programming languages, technologies and management skills. However, as he felt something was missing in his life he quit his job on the 31st of December 2004 to return to his first love, biology. As it seemed impossible to work in this field on an academic level with only a bachelor in biology teaching, a master in biology was started at the Radboud University Nijmegen. A three year training program was custom designed, which he finished in two years. In 2007, a position as a PhD student on the VICI project “Underground communication” under supervision of Prof. dr. Harro Bouwmeester took his interest, he applied and got hired. Results from this research were presented at different institutes in Europe and at the international IPGSA conference in Tarragona (Spain, 2010). Part of the research was conducted at the Max Planck Institute for Plant Breeding, Cologne (Germany) under supervision of Dr. Davide Bulgarelli and Prof. dr. Paul Schulze-Lefert. In addition, several (inter)national collaborations were established.

Appendix

Supplemental data

Supplemental data Chapter 3

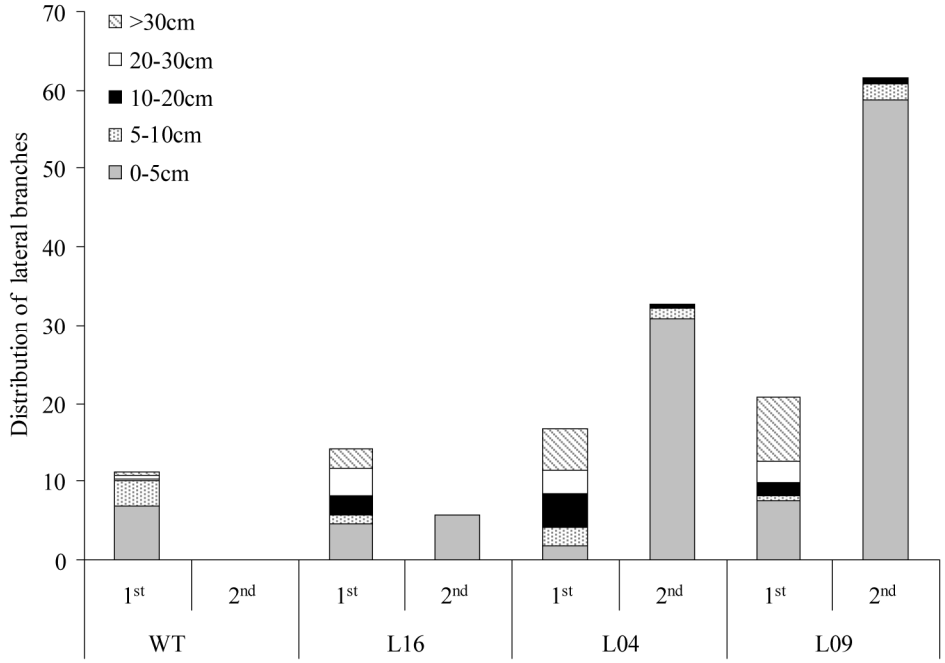

Figure S3.1 Dispersion of lateral branch of 1st and 2nd order of tomato cv. Craigella (wild-type) and three independent *SlCCD8* RNAi lines (L16, L04, and L09). Bars represent means of 5 replicates.

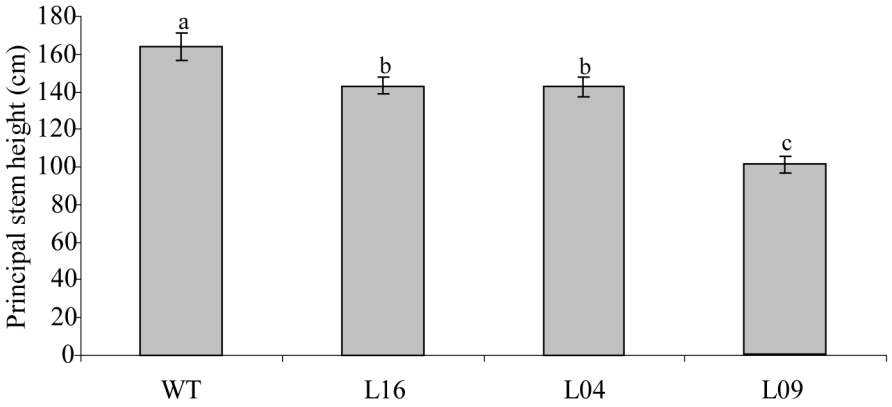

Figure S3.2: Average principal stem height of tomato cv. Craigella (wild-type) and three independent *SlCCD8* RNAi lines (L16, L04, and L09). 8-week old plants grown hydroponically and lateral branches were frequently removed. Bars represent means of 5 replicates ± s.e. Bars with a different letter differ significantly; $P < 0.05$.

Figure S3.3: Adventitious root formation on the principle stem (60% relative humidity).

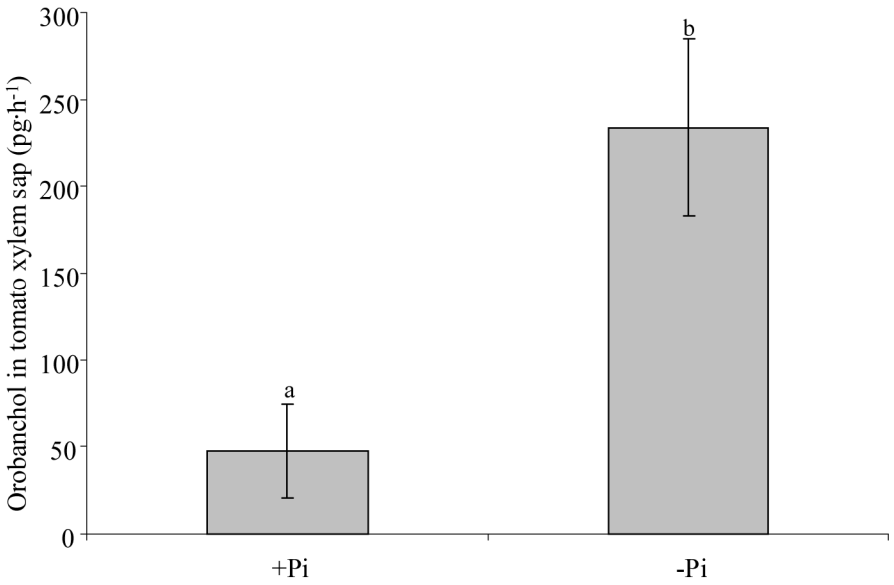

Figure S3.4: Analysis of the effect of treatments with sufficient phosphate (+Pi) and limiting phosphate (–Pi) on orobanchol content in tomato xylem sap. Bars represent means of 3 replicates ± s.e. Bars with a different letter differ significantly; $P < 0.05$.

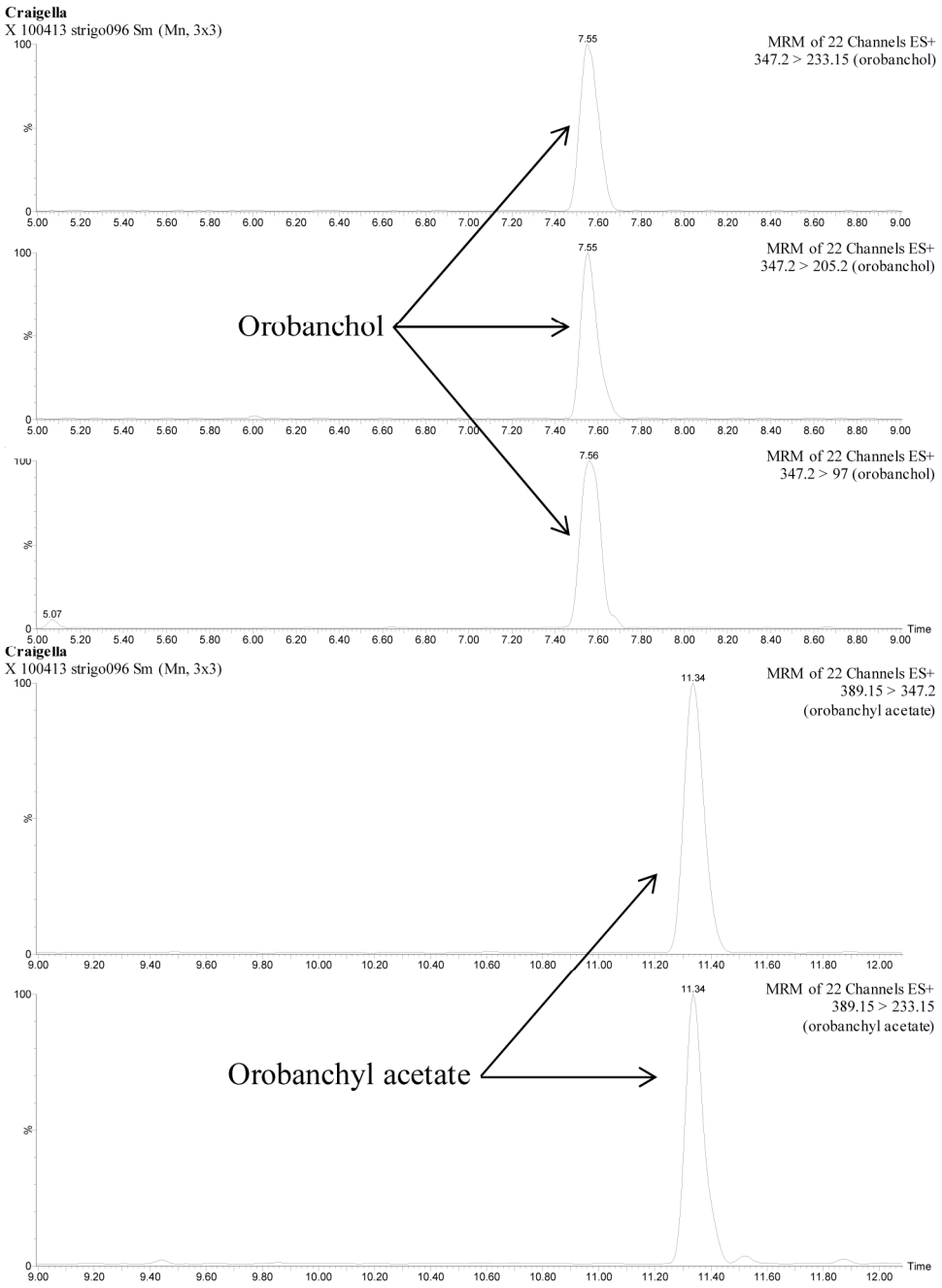

Figure S3.5: MRM-LC-MS/MS analysis of tomato xylem sap.
(a) transitions 347 > 233, 347 > 205 and 347 > 96.8 for orobanchol.
(b) transitions 389.2 > 347 and 389.2 > 233 for orobanchyl acetate.

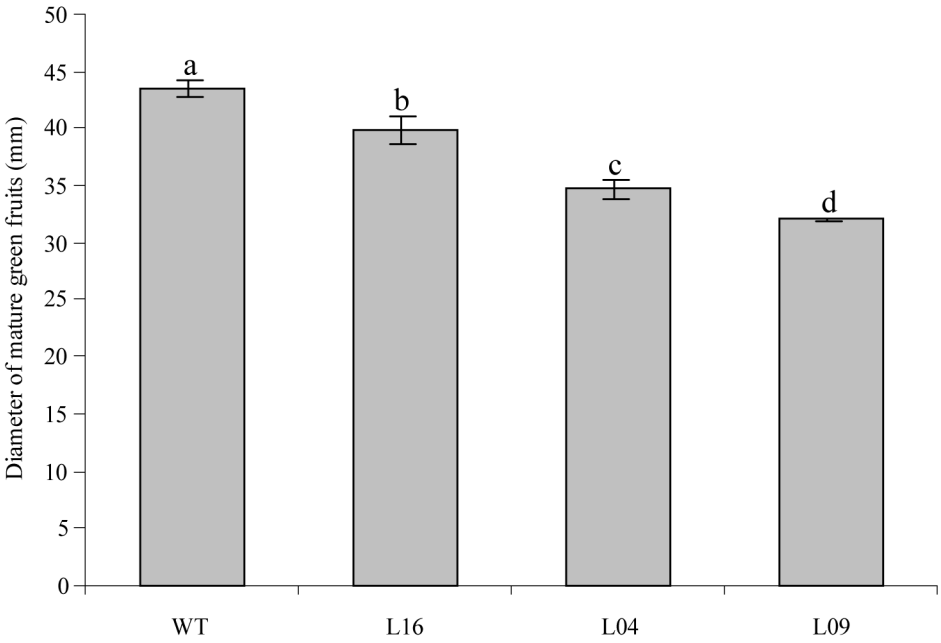

Figure S3.6: Fruit diameter of tomato cv. Craigella (wild-type) and three independent *SlCCD8* RNAi lines (L16, L04, and L09) in mm (mature green, 40 days after pollination (DAP). Plants grown hydroponically and lateral branches were frequently removed. Bars represent means of 10 replicates ± s.e. Bars with a different letter differ significantly; $P < 0.05$.

Table S3.1. *SlCCD8* complete nucleotide sequence

ATGGCTTCTCTTGCTTCTTCAACAACCAAAATTTATTGTAACAAGATCCTTCCTGACATGTTTGATCA
TGGCAAACATGAATCTCATCTTGGATCAAAGTTGAAAAACAACGAAAAAAACAAGAAAAAATTGGACT
TGAAATTGGTTACAAAGGTTGCTAACCAATTGCCTGTAATAGTTCCACCACCAGATCAAGAGGTGATT
AGTAAGGAGAAAAAGCTTGCTGCATGGACTAGCGTACGCCAAGAAAGATGGGAAGGAGAACTCGTCGT
TGAAGGCGAGTTACCATTGTGGCTGAATGGCACGTACCTAAGAAATGGTCCAGGACAATGGCACATAG
GTGACTACAATTTTCGTCACCTTTTCGATGGCTACGCTACCTTAGTCCGTCTTCATTTCGAAAATGGA
CGATTAATCATGGGTCATAGACAAATCGAATCGGACGCATATAAAGCAGCAAAAATCAGTAAGAAAAT
ATGTTACAGAGAATTTTCAGAAGTACCTAAAGTAGACAATTTCTTATCCTACATAGGTGACATGGCAA
AATTACTCTCCGGTGCATCCCTAACCGATAATGCTAACACTGGAGTCGTTAAACTTGGGGATGGACGC
GTAGTCTGCTTAACTGAGACGATAAAAGGTTCCATTGTAATTGATCCGAACACCCTAGATACAATTGG
GAAATTTGAATATAGTGACTCGTTAGGTGGATTGATTCATTCAGCTCATCCAGTGGTTACGGACAGTG
AGTTCATAACGTTGATTCCGGATTTAATGAACCCGGGATATACGGTGGTGAGAATGGAGGCAGGGACA
AATGAGAGGAAGTATATAGGGAGAGTGAGTTGTAGAGGAGGACCAGCACCAGGATGGGTTCATTCATT
TCCTGTTACAGAAAATTATGTTATTGTGCCTGAGATGTCACTAAGGTATTGTGCAAAAAATTTGTTGA
AGGCTGAGCCAACACCACTGTATAAGTTTGAGTGGCATCCTGATTCTAAAGCATTTGTACATGTTATG
TGTAAAGCCAGTGGCAACATTGTGGCAAGTGTAGAAGTGCCATTATACGTGACATTCCACTTCATCAA
TGGATACGAAGAAAAAGACGAAGATGGAAGAGTTACCGCTGTGATTGCAGATTGCTGTGAGCATAGCG
CAGACACCACCATCCTTGACAAGCTCCGCCTTGAGAATCTTCGTTCCTTCAACGGCAAGGATGTCTTA
CCTGATGCAAGGGTTGGAAGATTCAGAATACCATTAGATGGAAGTCCATATGGAGAATTAGAAGCAGC
ATTGGATCCAAATGAACATGGAAAAGGCATGGATATGTGCAGTATGAATCCTGCTTATTTAGGCAAGA
AATACAGATATGCTTATGCTTGTGGTGCTAAGAGGCCTTGTAATTTCCCCAACACCCTCACCAAGATT
GATTTATTTGATAAGAAGGCAAAGAATTGGTATGATGAAGGTGCTGTGCCTTCTGAACCATTCTTTGT
GGCTCGACCCGGTGCAACCGAAGAAGATGATGGTGTTGTAATCTCAATGATCAGTGACAAGAATGGAG
AAGGATATGCTCTAATACTGGATGGATCAACATTTGAAGAAATTGCAAGAGCTAAATTTCCTTATGGT
CTCCCCTATGGGCTACATGGTTGTTGGGTTCCAAAGATATAG

Table S3.2. SlCCD8 complete amino acid sequence

MASLASSTTKIYCNKILPDMFDHGKHESHLGSKLKNNEKNKKKLDLKLVTKVANQLPVIVPPPDQEVI
SKEKKLAAWTSVRQERWEGELVVEGELPLWLNGTYLRNGPGQWHIGDYNFRHLFDGYATLVRLHFENG
RLIMGHRQIESDAYKAAKISKKICYREFSEVPKVDNFLSYIGDMAKLLSGASLTDNANTGVVKLGDGR
VVCLTETIKGSIVIDPNTLDTIGKFEYSDSLGGLIHSAHPVVTDSEFITLIPDLMNPGYTVVRMEAGT
NERKYIGRVSCRGGPAPGWVHSFPVTENYVIVPEMSLRYCAKNLLKAEPTPLYKFEWHPDSKAFVHVM
CKASGNIVASVEVPLYVTFHFINGYEEKDEDGRVTAVIADCCEHSADTTILDKLRLENLRSFNGKDVL
PDARVGRFRIPLDGSPYGELEAALDPNEHGKGMDMCSMNPAYLGKKYRYAYACGAKRPCNFPNTLTKI
DLFDKKAKNWYDEGAVPSEPFFVARPGATEEDDGVVISMISDKNGEGYALILDGSTFEEIARAKFPYG
LPYGLHGCWVPKI

Table S3.3. Sequence homology of *SlCCD8*

Species	Amino acid	Nucleotide
Petunia hybrida	89%	86%
Pisum sativum	75%	78%
Medicago truncatula	74%	74%
Oryza sativa b	68%	61%
Sorghum bicolor	67%	62%
Zea mays	67%	62%
Arabidopsis thaliana	61%	68%
Oryza sativa a	57%	58%

Supplemental data Chapter 4

(a)

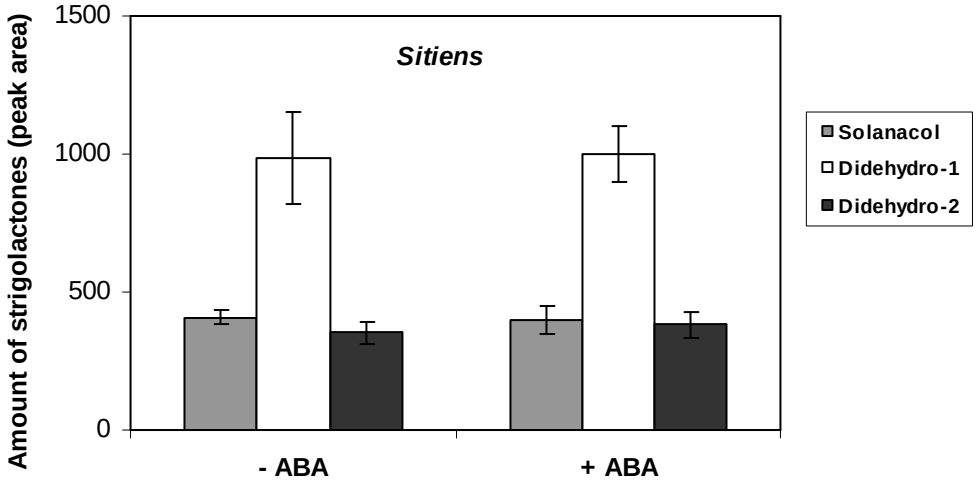

(b)

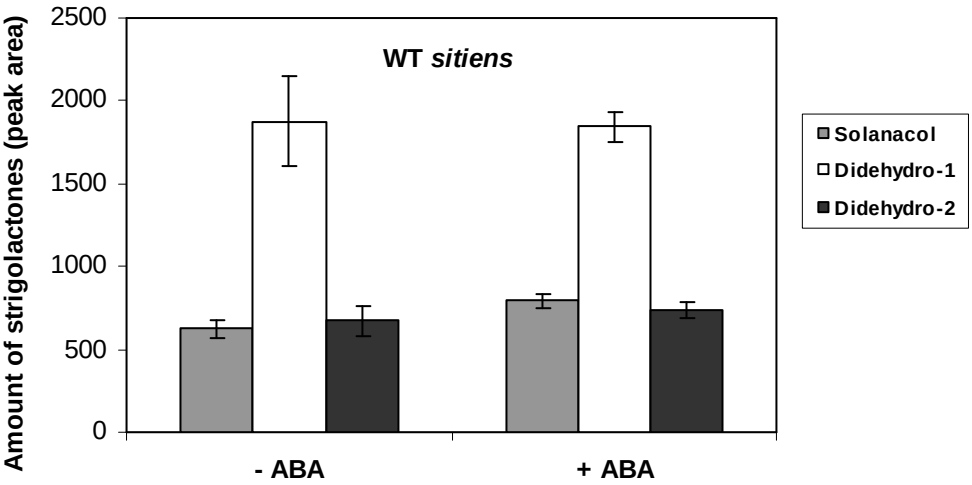

Figure S4.1: Strigolactone content in the root exudates of the tomato ABA-deficient mutant *sitiens* (a), and corresponding wild-type (WT) (b) after ABA (10 µM) application. The amount (according to the peak area) of the strigolactone solanacol and the didehydro-orobanchol isomers 1 and 2 (Didehydro-1 and Didehydro-2) was quantified. Strigolactone content was analysed using LC-MS/MS. Bars represent the average of 4 independent replicates ± SE.

(a)

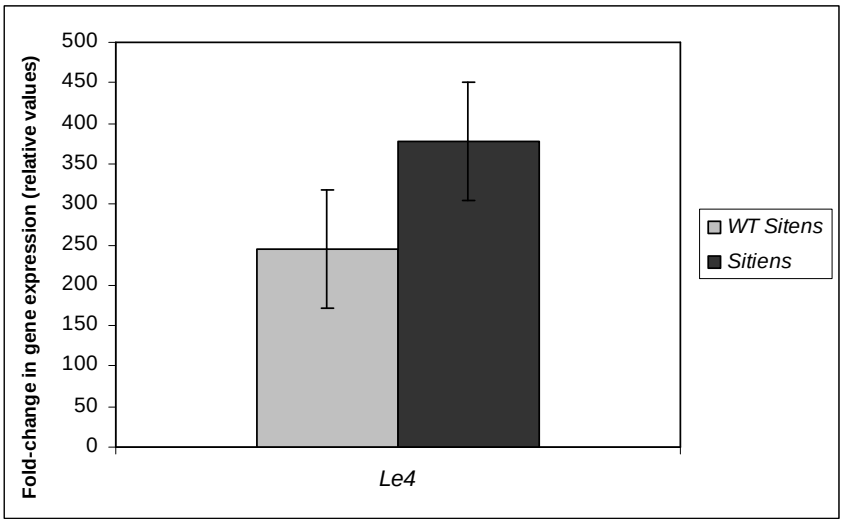

(b)

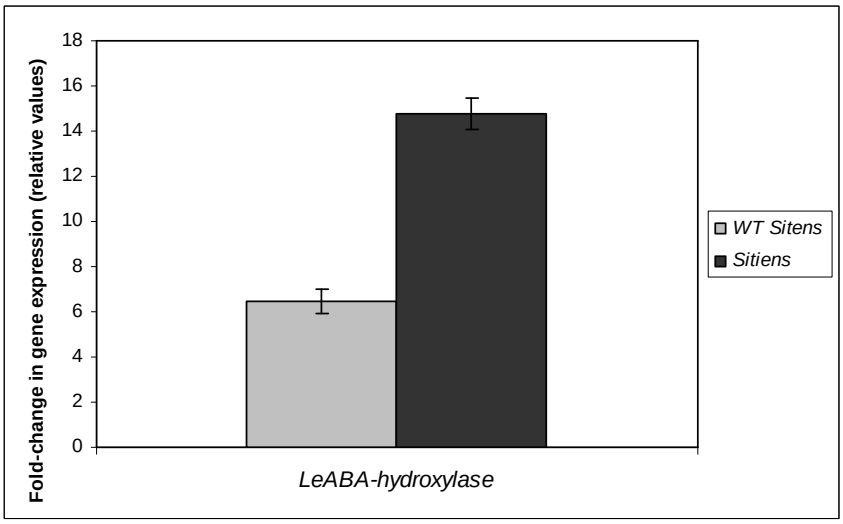

Figure S4.2: Gene expression analysis by real time qPCR of *Le4* (a) and ABA-8'-hydroxylase (*SlCYP7070A1*) (b) upon ABA application (10 µM) to *sitiens* (black bars) and corresponding wild-type (Reinlands Rhum, WT) (grey bars) for 48 hours. Real time qPCR was based on the Ct values as described in Materials and Methods. Ct values were normalized using the gene *LeActin* as an endogenous control gene. The expression for each gene is given relative to the expression of the same gene in plants not treated with ABA. Bars represent mean values ± SE of 3 independent biological replicates.

Supplemental data Chapter 5

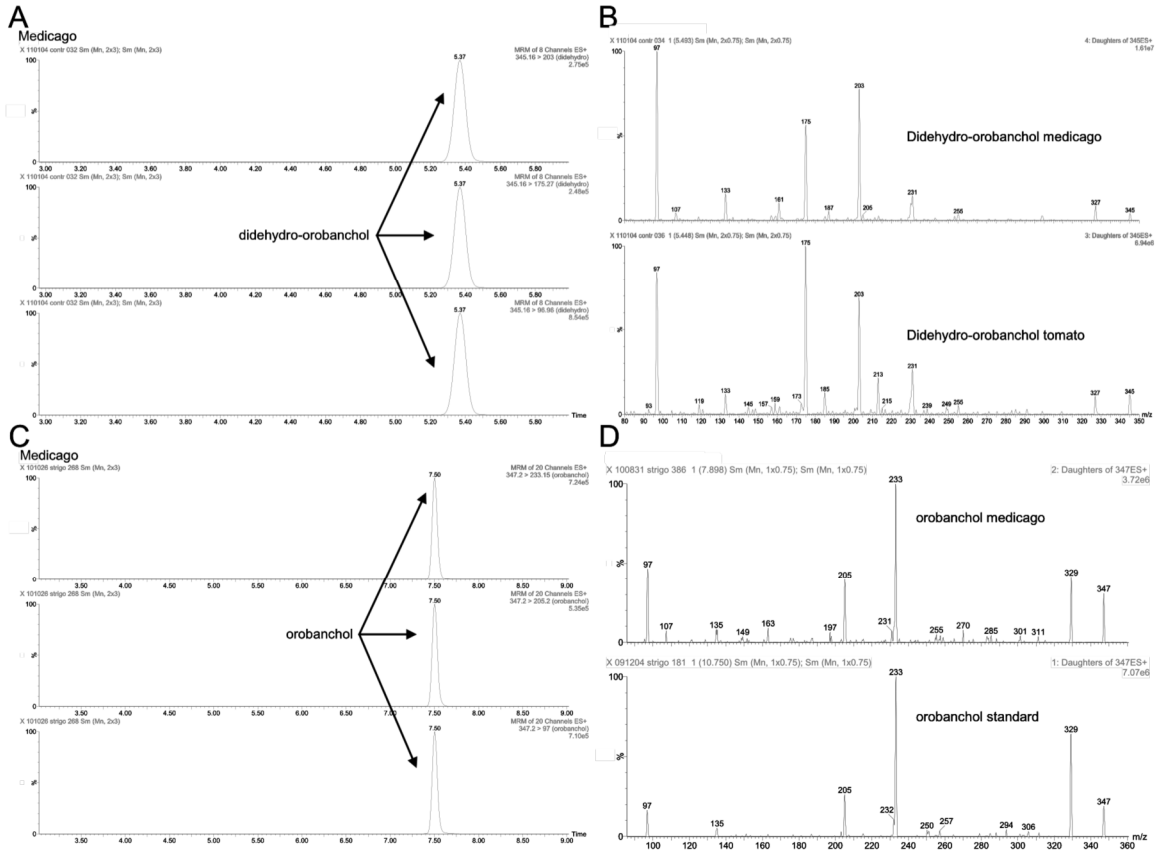

Figure S5.1: MRM-LC-MS/MS analysis of Medicago root exudates. **(a)** Transitions 345 > 203, 345 > 175 and 345 > 96.8 for didehydro-orobanchol. **(b)** Full daughter ion scan MS/MS spectrum of didehydro-orobanchol in Medicago exudate and didehydro-orobanchol in tomato (*Solanum lycopersicum*). **(c)** Transitions 347 > 233, 347 > 205 and 347 > 96.8 for orobanchol. **(d)** Full daughter ion scan MS/MS spectrum of orobanchol in Medicago exudate and orobanchol standard.

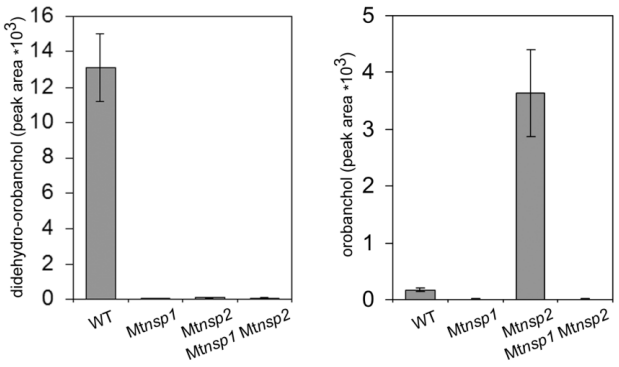

Figure S5.2: Amount of didehydro-orobanchol and orobanchol in Medicago root exudates of wild type (A17), *Mtnsp1*, *Mtnsp2* and *Mtnsp1Mtnsp2* mutants (n=6). Data are means ± s.e.

A

>Mt*D27* promoter region

-921

acaactgttc ccagcgcagt cttgtggtta gctatcacac tagcacctta tatcttcata acaagttctt

ttgttcaaag ttttatAATT Taagaatcgg ttgttagagt atgtcattat tagattaaaa tataactaag

aaccatcctt aacacAATTT tcatgatttg cactatttta agtagtgatt AATTTaaagt tcttaaaggg

gtgtattgac cgagggacgc aattctctgc ctacattatt ttaataacat gaatggttaa tagcagttgc

tttatcagaa ttaaagtgtc aagttttcta ttcttAATTT ctacaaacca aagtcttctt tcttatgAAT

TTttttggtt tagttctttt tgtgttcaac tAATTTtagc ttaaacagaa gctgatgcaa tcacttgcta

gttcaaagtt agacttgagt gaagttcacc gacttgt*AAA TT*ctatttat tttctttttg gataatcagt

tgaaatatgt agttatatag tatcatacaa atataagcca caatatattt tcac*AAATT*a tcttaaaaag

cgtatgaaag taagccaaaa atagtatatg tacacgtcac atgtttttat aaactctcat aaaacccaac

cggcctaaat agttgacatt taaaacaaaa taaggggaac attggtagtg gaacacAATT Tgtgaccgaa

gcattagaca taagttacta aagaatacta gaatcatgtc acatcatttc gatagaactg gaagtaccac

cataagccaa caaataaagc atctagagag tcacaaaaca gaatcatgag taagagcttt gtgctaagat

gcttttcatg cactatttgt ccttattaat cccctcctat ataaagctcc tttcacatga aaatcaataa

ctactcacaa ATG +3

B

Mt*D27* promoter

PBE-1:

-845 caaagttttatAATTTaagaatcggttgttagagtatgtcattattagattaaaatataactaagaaccatccttaacacAATTTtcatgatttg -751

PBE-2:

-775 tccttaacacAATTTtcatgatttgcactattttaagtagtgattAATTTaaagttcttaaaggggtgtattgaccgagggacgcaattctctgcctac -677

PBE-3:

-681 cctacattattttaataacatgaatggttaatagcagttgctttatcagaattaaagtgtcaagttttctattcttAATTTctacaaaccaaag -588

PBE-4:

-648 gcagttgctttatcagaattaaagtgtcaagttttctattcttAATTTctacaaaccaaagtcttctttcttatgAATTTttttggtttag -558

PBE-5:

-583 ctttcttatgAATTTttttggtttagttctttttgtgttcaactAATTTtagcttaaacagaagctgatgcaatcacttgctagttcaaagttagacttg -484

Mt*ENOD11* promoter

PBE-C1:

-411 agacacttaAATTTgagggtcataataacataaaataattgcaggcctaaagctattattttaccagcctttAATTTgacctgccatg -323

PBE-C3:

-256 tctagatttcctAATTTtcctaaaacattctaaaaagtaagaagtttttacatttttgaAAATTattccacaacag -181

Figure S5.3: Putative NRE-like cis regulatory binding elements for *NSP1* in the promoter region of Medicago *MtD27* and rice *OsD27*. **(a)** Medicago *MtD27* promoter region (-920+3 bp). Nine putative MtNSP1 binding elements are marked in uppercase and shaded. Seven elements are present in the forward strand (marked in normal case) and 2 in the reverse strand (marked in Italic). **(b)** Putative binding element (PBE) probes used in EMSA analysis originating from the MtD27 and MtENOD11 promoter regions. Given numbers mark position in promoter. The AATTT elements are shown in uppercase letters. **(c)** In the rice *OsD27* promoter (-1780+3), 11 putative NSP1 binding elements are present (marked in uppercase letters and shaded). Six of these are localized in the forward chain (marked in normal case) and 5 are localized in the reverse chain (marked in Italic). Predicted transcription start sites (TSS) are underlined.

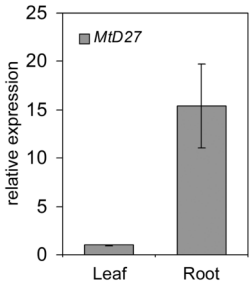

Figure S5.4: Expression analysis of *MtD27* in Medicago root and shoot tissue determined by qRTPCR.

Table S1: Medicago probe sets representing genes down-regulated in root tissue of the Medicago Mt*nsp1* and Mt*nsp2* knockout mutant. Expression determined based on microarray analysis.

	FC		Target Description	ID	Homolog(s) in *A. thaliana*
	nsp1	***nsp2***			
Mtr.32254.1.S1_at	-7.8	-10.1	C2H2 type Zinc finger protein 6	AW686309	At1g67030
Mtr.12833.1.S1_at	-7.7	-7.7	Unknown protein	TC146803	Legume specific
Mtr.9516.1.S1_at	-6.1	-5.4	Dirigent-like protein	TC158536	At1g22900 At5g42500
Mtr.25451.1.S1_at Mtr.10522.1.S1_s_at	-5.5 -3.3	-4.7 -3.4	Alanine-tRNA ligase	TC144165	At1g50200
Mtr.4797.1.S1_s_at Mtr.11343.1.S1_at	-5.1 -3.2	-6.2 -3.4	DWARF27	TC158596	At1g03055 At1g64680
Mtr.36679.1.S1_s_at	-4.7	-2.8	Unknown protein with homolog	TC158127	At5g66780
Mtr.34371.1.S1_at	-4.6	-7.8	Unknown protein	TC162100	Legume specific
Mtr.48470.1.S1_s_at	-3.7	-3.7	OB-fold Replication protein A1	NP7269740	Legume specific
Mtr.20927.1.S1_at	-3.6	-3.5	Calmodulin binding protein	TC143830	At3g13600
Mtr.11099.1.S1_at	-3.6	-3.7	1-cys peroxiredoxin	TC146236	At1g48130
Mtr.32982.1.S1_at	-3.5	-4.5	Nudix hydrolase	TC153996	At2g01670 At1g14860
Mtr.45041.1.S1_at	-3.4	-2.8	Abnormal gametophytes (AGM)	TC163978	At4g19950 At1g31130
Mtr.22664.1.S1_at	-3.3	-3.3	Avr9/Cf-9 rapidly elicited protein 146	TC168023	At1g52140 At4g29110
Mtr.2114.1.S1_at	-3.3	-3.7	Unknown protein	TC152884	Legume specific
Mtr.12358.1.S1_at	-3.2	-3.0	Seed maturation protein LEA 4	TC147896	At5g06760
Mtr.28502.1.S1_at	-3.0	-2.9	Gypsy-like retrotransposon protein	BG647160	At4g21420
Mtr.15641.1.S1_at	-2.9	-2.3	unknown protein	NP7273282	Legume specific
Mtr.11744.1.S1_at	-2.8	-2.5	(+)-abscisic acid 8'-hydroxylase	TC165592	At1g19630 At4g19230
Mtr.40725.1.S1_at	-2.5	-2.3	Mannose-6-phosphate isomerase	TC143057	At3g02570
Mtr.12616.1.S1_at	-2.5	-2.3	MAX1	TC143057	At2g26170
Mtr.42432.1.S1_at Mtr.12200.1.S1_at	-2.5 -2.1	-2.5 -2.2	Carotenoid isomerase	TC170207 TC165115	At1g06820
Mtr.38430.1.S1_at	-2.5	-2.6	CIPK4	TC165047	At3g23000 At4g14580

Mtr.17478.1.S1_at	-2.5	-2.4	26S proteasome subunit RPN5b	TC143513	At5g09900 At5g64760
Mtr.40755.1.S1_at	-2.4	-2.1	ERD7	TC160548	At2g17840 At3g51250
Mtr.33914.1.S1_at	-2.4	-2.3	Gibberellin 2-oxidase	BI273162	At1g78440 At1g30040
Mtr.42587.1.S1_at	-2.4	-2.5	Heat shock transcription factor-like protein	TC153611	At5g03720 At5g16820
Mtr.17298.1.S1_at	-2.4	-2.5	NAD+ ADP-ribosyltransferase	NP7267637	At1g23550 At1g70440
Mtr.43078.1.S1_s_at	-2.4	-2.5	Cytokinin-specific binding protein	TC161067	-
Mtr.13426.1.S1_at	-2.3	-2.4	β-glucan-binding protein 4	TC145129	At5g15870 At1g18310
Mtr.28846.1.S1_at	-2.2	-2.7	ARR6	BQ124080	At5g62960
Mtr.50800.1.S1_at	-2.2	-2.3	2OG-Fe(II) oxygenase	TC144924	At1g06620 At2g30840
Mtr.38432.1.S1_at	-2.2	-2.0	Temperature stress-induced lipocalin	TC147968	At5g58070
Mtr.27101.1.S1_at	-2.1	-2.7	Unknown protein	AW559488	Legume specific
Mtr.37912.1.S1_at	-2.1	-2.0	Allyl alcohol dehydrogenase	TC159212	At5g16970
Mtr.7947.1.S1_at	-2.1	-2.8	Pherophorin-S precursor	BG447806	Legume specific
Mtr.30981.1.S1_at	-2.1	-2.7	Unknown protein	TC145768	Legume specific
Mtr.7136.1.S1_at	-2.0	-3.0	Nine-cis-epoxycarotenoid dioxygenase 4	CX549419	At4g19170
Mtr.7138.1.S1_at	-2.0	-2.4	Short-chain alcohol dehydrogenase	CX549464	At3g26770 At1g52340
Mtr.10681.1.S1_s_at	-2.0	-4.1	USP1-like protein	TC151489	At3g62550

Table S2

	Fold Change nsp2-A17	Target Description
Mtr.43502.1.S1_at	-774.5	TC95479 /20S proteasome subunit alpha-5
Mtr.12315.1.S1_x_at	-434.0	TC94362 /Glutathione S-transferase GST 8
Mtr.13115.1.S1_at	-374.5	TC96958 /MLO-like protein 1
Mtr.12577.1.S1_s_at	-120.4	TC95279
Mtr.29613.1.S1_at	-113.8	TC98883
Mtr.38864.1.S1_at	-91.6	TC103695
Mtr.1122.1.S1_s_at	-72.4	F-box protein
Mtr.12577.1.S1_at	-70.6	TC95279
Mtr.42066.1.S1_at	-68.0	TC110677 /Phytase
Mtr.14020.1.S1_at	-45.7	TC99986 /Protein phosphatase
Mtr.29721.1.S1_at	-39.4	AL367580
Mtr.27518.1.S1_at	-36.8	BE203734 / Cell surface protein
Mtr.2291.1.S1_at	-35.2	BG584884 / P-type R2R3 Myb protein
Mtr.7710.1.S1_at	-32.5	AL367581
Mtr.38507.1.S1_at	-25.1	TC102945 /Ser/Thr protein phosphatase BSL1
Mtr.17523.1.S1_at	-17.5	Protein of unknown function
Mtr.13843.1.S1_at	-15.3	TC99351
Mtr.569.1.S1_s_at	-15.0	hypothetical protein
Mtr.38949.1.S1_x_at	-13.1	TC103888 /Albumin 2
Mtr.8470.1.S1_s_at	-12.8	TC100295 /Strictosidine-O-beta-D-glucosidase
Mtr.23596.1.S1_s_at	-11.8	AC146756
Mtr.7635.1.S1_at	-11.3	AJ548095 /Anther-specific protein
Mtr.42093.1.S1_at	-11.2	TC110744
Mtr.19517.1.S1_at	-10.9	Ribulose bisphosphate carboxylase
Mtr.13269.1.S1_at	-10.5	TC97491
Mtr.42093.1.S1_x_at	-10.4	TC110744
Mtr.2135.1.S1_s_at	-10.1	BF640276
Mtr.1666.1.S1_at	-9.9	AW694130
Mtr.43424.1.S1_at	-9.7	TC95281
Mtr.5739.1.S1_at	-9.2	BF646806 / LRR protein
Mtr.35945.1.S1_at	-9.0	TC99852 /UDP-glycose:flavonoid glycosyltransferase
Mtr.45231.1.S1_at	-8.8	TC99117 /Nodulin
Mtr.44995.1.S1_at	-7.9	TC98565
Mtr.7459.1.S1_at	-7.6	TC112501 /Resistance protein MG55
Mtr.38949.1.S1_at	-6.8	TC103888 /Albumin 2
Mtr.38494.1.S1_at	-6.7	TC102920
Mtr.33112.1.S1_at	-6.7	BF642307 /Patatin homolog
Mtr.38508.1.S1_at	-6.5	TC102946 /Serine/threonine protein phosphatase BSL1
Mtr.25451.1.S1_s_at	-6.3	alanine--tRNA ligase
Mtr.48470.1.S1_at	-6.2	AC119409
Mtr.41147.1.S1_at	-6.1	TC108815
Mtr.13904.1.S1_at	-6.0	TC99584/ 4-coumarate-CoA ligase
Mtr.1810.1.S1_at	-5.8	BE202654
Mtr.31788.1.S1_at	-5.8	AL380233 /F-box protein
Mtr.11820.1.S1_x_at	-5.7	TC111162 /UDP-glycosyltransferase
Mtr.48675.1.S1_s_at	-5.6	Purple acid phosphatase
Mtr.52163.1.S1_at	-5.3	hypothetical protein
Mtr.43310.1.S1_at	-5.3	TC95027 /blight resistance protein RGA1
Mtr.8426.1.S1_at	-5.0	TC100135 /Chlorophyll a/b binding protein
Mtr.48681.1.S1_at	-5.0	hypothetical protein
Mtr.40279.1.S1_at	-4.8	TC106943 /glutathione S-transferase
Mtr.10626.1.S1_at	-4.7	TC107414 /SRG1-like protein
Mtr.33562.1.S1_at	-4.5	BG453865 /type II keratin subunit protein
Mtr.10681.1.S1_at	-4.3	TC107596 /USP1-like protein

Mtr.13908.1.S1_at	-4.3	TC99593
Mtr.42339.1.S1_at	-4.2	TC111274
Mtr.35078.1.S1_at	-4.2	CX532386 /ATPase 2
Mtr.10604.1.S1_at	-4.2	TC107357 /Nitrate reductase
Mtr.8517.1.S1_at	-4.2	TC100462 /mannitol dehydrogenase
Mtr.45148.1.S1_at	-4.1	TC98922 /
Mtr.31557.1.S1_at	-4.1	AL370071
Mtr.11695.1.S1_at	-4.1	TC110748
Mtr.10450.1.S1_at	-4.0	TC106817
Mtr.25731.1.S1_at	-3.9	plastocyanin-like domain containing protein
Mtr.2334.1.S1_at	-3.9	BG586672
Mtr.21972.1.S1_at	-3.7	hypothetical protein
Mtr.13183.1.S1_at	-3.5	TC97194
Mtr.6718.1.S1_at	-3.5	CX519518
Mtr.47199.1.S1_at	-3.5	Calcineurin-like phosphoesterase-like
Mtr.35681.1.S1_at	-3.5	TC111048 /Metal-dependent amidase
Mtr.33530.1.S1_at	-3.5	BG453035
Mtr.47631.1.S1_s_at	-3.5	Transposase
Mtr.34638.1.S1_at	-3.5	BQ157221 /glutaredoxin-like protein
Mtr.42692.1.S1_at	-3.4	TC112168 /Glutaredoxin-like protein
Mtr.43831.1.S1_at	-3.4	TC96132 /F-box protein
Mtr.35757.1.S1_at	-3.4	TC112048 /Short chain alcohol dehydrogenase
Mtr.48064.1.S1_at	-3.3	hypothetical protein
Mtr.43048.1.S1_at	-3.3	TC94419 /Early nodulin 12A precursor
Mtr.31645.1.S1_at	-3.3	AL373660 /Deoxycytidine deaminase
Mtr.21112.1.S1_at	-3.3	Myb
Mtr.10545.1.S1_at	-3.3	TC107140
Mtr.30965.1.S1_at	-3.3	CX550363
Mtr.15275.1.S1_at	-3.2	lectin
Mtr.38954.1.S1_at	-3.2	TC103902 /Ferric-chelate reductase
Mtr.7244.1.S1_at	-3.2	TC104280
Mtr.37288.1.S1_at	-3.1	TC100298 /Beta-primeverosidase
Mtr.26939.1.S1_at	-3.1	AL379176
Mtr.12428.1.S1_at	-3.1	TC94767 /Anther-specific protein
Mtr.2631.1.S1_at	-3.1	BI311272 /Caffeic acid O-methyltransferase II
Mtr.34470.1.S1_s_at	-3.1	BQ148677 /Ca2+/H+ exchanger
Mtr.11820.1.S1_at	-3.1	TC111162 /UDP-glycosyltransferase
Mtr.11364.1.S1_at	-3.0	TC109714 /cytochrome P450
Mtr.38932.1.S1_at	-3.0	TC103858 /Malate synthase
Mtr.28845.1.S1_at	-3.0	BQ123925 /Cystinosin
Mtr.32209.1.S1_at	-3.0	AW684842
Mtr.41195.1.S1_at	-3.0	TC108916
Mtr.37084.1.S1_at	-2.9	TC112271
Mtr.5456.1.S1_at	-2.9	BE325502 /Valine--tRNA ligase
Mtr.37624.1.S1_s_at	-2.9	TC101083 /3-beta-hydroxysteroid dehydrogenase
Mtr.25691.1.S1_s_at	-2.9	TNP2-like transposon protein
Mtr.7052.1.S1_at	-2.9	CX537932 /Histone H1
Mtr.26276.1.S1_at	-2.9	1499.m00024 /CER1 protein
Mtr.41805.1.S1_at	-2.9	TC110159
Mtr.8612.1.S1_at	-2.9	TC100798
Mtr.4665.1.S1_at	-2.8	AL374081
Mtr.13947.1.S1_x_at	-2.8	TC99709 /EIX receptor 1
Mtr.28586.1.S1_at	-2.8	BI266323
Mtr.42446.1.S1_at	-2.8	TC111556 / Nitrate reductase
Mtr.40084.1.S1_at	-2.8	TC106463 /Sulfate transporter protein
Mtr.15010.1.S1_s_at	-2.7	Myb

Mtr.34799.1.S1_at	-2.7	CX524988
Mtr.17954.1.S1_s_at	-2.7	hypothetical protein
Mtr.39139.1.S1_at	-2.7	TC104268 /Pathogenesis-related protein 4A
Mtr.39091.1.S1_at	-2.7	TC104170 /Beta-glucan binding protein
Mtr.10175.1.S1_at	-2.6	TC105774 /Cytochrome P450
Mtr.9660.1.S1_at	-2.6	TC103997
Mtr.37623.1.S1_at	-2.6	TC101082 /3-beta-hydroxysteroid dehydrogenase
Mtr.7818.1.S1_at	-2.6	AW684444
Mtr.22108.1.S1_x_at	-2.6	EIX receptor 1
Mtr.44349.1.S1_at	-2.6	TC97188 /Zinc transporter
Mtr.13237.1.S1_at	-2.6	TC97378 /protein integral membrane protein
Mtr.39664.1.S1_at	-2.5	TC105397
Mtr.41148.1.S1_at	-2.5	TC108816 /Ca2+/H+ exchanger
Mtr.27598.1.S1_at	-2.5	BE239791 /WRKY transcription factor 33
Mtr.48991.1.S1_s_at	-2.5	hypothetical protein
Mtr.43078.1.S1_at	-2.5	TC94480 /Histone H1
Mtr.2200.1.S1_at	-2.5	BG455696
Mtr.37751.1.S1_at	-2.5	TC101337 /Isoflavone-7-O-methytransferase 9
Mtr.37989.1.S1_at	-2.5	TC101850
Mtr.47546.1.S1_at	-2.5	Albumin 1 precursor
Mtr.33270.1.S1_at	-2.5	BF648401 /cytochrome P450
Mtr.10187.1.S1_at	-2.5	TC105821 /LEXYL1
Mtr.31998.1.S1_at	-2.4	AL388370 /Epoxide hydrolase
Mtr.42265.1.S1_at	-2.4	TC111090 /Transmembrane protein kinase
Mtr.1405.1.S1_at	-2.4	AL370412
Mtr.11212.1.S1_s_at	-2.4	TC109255 /Isoflavonoid glucosyltransferase
Mtr.40085.1.S1_s_at	-2.4	TC106466 /18S ribosomal RNA gene
Mtr.1495.1.S1_at	-2.4	AW171775
Mtr.37578.1.S1_at	-2.4	TC100962
Mtr.20215.1.S1_at	-2.4	hypothetical protein
Mtr.10019.1.S1_at	-2.4	TC105283
Mtr.27663.1.S1_at	-2.4	BE940981
Mtr.3180.1.S1_at	-2.4	CX542025
Mtr.13527.1.S1_at	-2.4	TC98264 /Cytochrome b
Mtr.6640.1.S1_at	-2.4	BQ152527
Mtr.8550.1.S1_s_at	-2.4	TC100587 Leghemoglobin 29
Mtr.50032.1.S1_at	-2.4	Nucleoside phosphatase
Mtr.1532.1.S1_at	-2.4	AW267858
Mtr.13887.1.S1_at	-2.4	TC99521 /Tropinone reductase-I
Mtr.20804.1.S1_at	-2.3	serine/threonine protein kinase
Mtr.42525.1.S1_x_at	-2.3	TC111746
Mtr.27041.1.S1_at	-2.3	AW256402 /Salicylic acid-binding protein 2
Mtr.44643.1.S1_at	-2.3	TC97782
Mtr.35515.1.S1_at	-2.3	TC105090 / Leucoanthocyanidin dioxygenase-like protein
Mtr.44610.1.S1_at	-2.3	TC97710 /Valine--tRNA ligase
Mtr.43046.1.S1_at	-2.3	TC94416 / Early nodulin 12A precursor
Mtr.45331.1.S1_at	-2.3	TC99400
Mtr.15215.1.S1_at	-2.3	hypothetical protein
Mtr.34408.1.S1_s_at	-2.3	BQ147176
Mtr.38872.1.S1_at	-2.3	TC103704
Mtr.48196.1.S1_at	-2.3	F-box protein
Mtr.15199.1.S1_at	-2.3	hypothetical protein
Mtr.20427.1.S1_at	-2.3	Disease resistance protein
Mtr.27572.1.S1_at	-2.3	BE205155 /AtHVA22a
Mtr.41956.1.S1_at	-2.3	TC110457
Mtr.32765.1.S1_at	-2.3	BE321908 /Serine/threonine protein phosphatase BSL1

Mtr.35562.1.S1_at	-2.3	TC105695
Mtr.19822.1.S1_at	-2.2	hypothetical protein
Mtr.25950.1.S1_at	-2.2	ACC oxidase
Mtr.18528.1.S1_at	-2.2	Cyclin-like F-box
Mtr.44900.1.S1_at	-2.2	TC98362
Mtr.13654.1.S1_at	-2.2	TC98687 / Tyrosine aminotransferase
Mtr.8284.1.S1_s_at	-2.2	Leghemoglobin
Mtr.37708.1.S1_at	-2.2	TC101252 /Sulfate transporter
Mtr.3883.1.S1_at	-2.2	BM813684 /Beta-cyanoalanine synthase
Mtr.8783.1.S1_at	-2.2	TC101370 /RNA helicase
Mtr.28700.1.S1_at	-2.2	BI310751 /Pyrogallol hydroxytransferase small subunit
Mtr.7637.1.S1_at	-2.2	AJ548187 /Prostatic spermine-binding protein precursor
Mtr.29716.1.S1_at	-2.2	AL367132
Mtr.30879.1.S1_at	-2.2	CB893428 /Permease protein of ABC transporter
Mtr.46001.1.S1_s_at	-2.2	C2 calcium/lipid-binding
Mtr.34929.1.S1_at	-2.2	CX528280 /Zinc finger protein CONSTANS-LIKE 16
Mtr.22096.1.S1_at	-2.2	EIX receptor 1
Mtr.39963.1.S1_at	-2.2	TC106180
Mtr.7380.1.S1_at	-2.1	TC110898
Mtr.35316.1.S1_at	-2.1	CX542483 / Beta-xylosidase
Mtr.47087.1.S1_at	-2.1	Glucan 1,3-beta-glucosidase
Mtr.31558.1.S1_at	-2.1	AL370072
Mtr.13396.1.S1_at	-2.1	TC97887
Mtr.12729.1.S1_at	-2.1	TC95749 /Pr1-like protein
Mtr.49098.1.S1_at	-2.1	hypothetical protein
Mtr.11251.1.S1_at	-2.1	TC109352 /protein integral membrane protein
Mtr.41982.1.S1_at	-2.1	TC110501 /sulfate transporter ATST1
Mtr.40836.1.S1_at	-2.1	TC108150 /MYB-related transcription factor PHAN1
Mtr.13947.1.S1_at	-2.1	TC99709 /EIX receptor 1
Mtr.40342.1.S1_at	-2.1	TC107088
Mtr.9281.1.S1_at	-2.1	TC102903 /NOI protein
Mtr.7670.1.S1_at	-2.1	AJ846785 /Albumin 1 precursor
Mtr.13919.1.S1_s_at	-2.1	TC99619
Mtr.35701.1.S1_at	-2.1	TC111297 /N7 protein
Mtr.50231.1.S1_at	-2.1	P-type trefoil
Mtr.10130.1.S1_at	-2.1	TC105614
Mtr.33808.1.S1_at	-2.1	BI270332 / two-component response regulator
Mtr.12712.1.S1_at	-2.1	TC95685 /Alpha-expansin
Mtr.46868.1.S1_s_at	-2.1	Lipoxygenase
Mtr.2633.1.S1_s_at	-2.1	BI311333
Mtr.41817.1.S1_at	-2.0	TC110184 /sulfate transporter ATST1
Mtr.29083.1.S1_at	-2.0	CA917785
Mtr.32904.1.S1_s_at	-2.0	BF633401 / Phosphoglycerate kinase
Mtr.30266.1.S1_at	-2.0	BG580434
Mtr.5630.1.S1_at	-2.0	BF640372
Mtr.40866.1.S1_at	-2.0	TC108215 / Hydrolase-like protein
Mtr.39948.1.S1_at	-2.0	TC106137
Mtr.33147.1.S1_at	-2.0	BF644066
Mtr.37455.1.S1_at	-2.0	TC100688 /Glucosyltransferase-13
Mtr.23540.1.S1_at	-2.0	Nodule-specific protein Nlj70
Mtr.26318.1.S1_at	-2.0	hypothetical protein
Mtr.27985.1.S1_at	-2.0	BF641475
Mtr.3806.1.S1_at	-2.0	BG645951
Mtr.11200.1.S1_at	-2.0	TC109191 /Zinc finger protein

Table S3

	primer name	sequence (5'-3')
qRT-PCR primers	Mtr.32254.1.S1_at-F	CATTTCCTCGCCAATGCTC
	Mtr.32254.1.S1_at-R	AAAAACTCCCGAACCTGCTG
	Mtr.43078.1.S1_s_at-F	TGCTCAGTCCAAGGATATCACC
	Mtr.43078.1.S1_s_at-R	CCCTCCATCCCCTTCAATTAC
	Mtr.9516.1.S1_at-F	GCCAATCCGTTGAATCTCAC
	Mtr.9516.1.S1_at-R	GACGAGGTTGGTTTGGTTTG
	Mtr.4797.1.S1_s_at-F	GAGATGATATTCGGCCAGGAAC
	Mtr.4797.1.S1_s_at-R	GCATGGTTTTTCTTAGCCTTGC
	Mtr.11343.1.S1_at-F	TCAAGCAGCAACAGGAATCAG
	Mtr.11343.1.S1_at-R	AAATTTCTGTGAAGCCACGGTAG
	Mtr.12616.1.S1_at-F	TTGGGTTTGGTTAGCCCTTG
	Mtr.12616.1.S1_at-R	CGCAGTTAGGGTCAAACCTTTC
	Mtr.42432.1.S1_at-F	AAAGCCGGAATTGTGAGCTG
	Mtr.42432.1.S1_at-R	AGCCCCTGACTCCCAAAATAG
	Mtr.40725.1.S1_at-F	TTGGGTTTGGTTAGCCCTTG
	Mtr.40725.1.S1_at-R	CGCAGTTAGGGTCAAACCTTTC
	Mtr.12833.1.S1_at-F	GCATCGATCAGATGTTGTTAGGG
	Mtr.12833.1.S1_at-R	TTCATCCATGTCGTGAAGACG
	Mtr.25451.1.S1_at-F	CCCCGAGCTAAAGCAAAATG
	Mtr.25451.1.S1_at-R	ATGGGACAACTCAAACGCTACC
	Mtr.34371.1.S1_at-F	CGAGGAAATTCTGGGAATAAGC
	Mtr.34371.1.S1_at-R	TTCCTTCCTTTCAGGCTTCC
	Mtr.11099.1.S1_at-F	GAACATGGATGAAGTGCTGAGG
	Mtr.11099.1.S1_at-R	TTCCAGTTAGCAGGGGTTGC
	Mtr.32982.1.S1_at-F	TTGCAGCGCTACAGAAAAGG
	Mtr.32982.1.S1_at-R	TTGCCCCTAAGGAAGTTTGG
	Mtr.45041.1.S1_at-F	TAACGAGGCCCCAAAGAATG
	Mtr.45041.1.S1_at-R	AATTGGACACAGGATCGTTCG
	Mtr.12358.1.S1_at-F	GGAGGAGCAAAGAAAACAGGAG
	Mtr.12358.1.S1_at-R	TCTCTTGAAATGTGGCCTTGG
	Mtr.37912.1.S1_at-F	AACCTCGAAAGGGTGAAACG
	Mtr.37912.1.S1_at-R	CAGCACAGCCAACAACATAGC
	Mtr.7136.1.S1_at-F	CTTTGCTCCTGTGGAAGAGTTG
	Mtr.7136.1.S1_at-R	CACCCTCTGGAAAATCATTCG
	Mtr.12200.1.S1_at-F	CACATGGGGGTTAAAGCAGAG
	Mtr.12200.1.S1_at-R	CCATATGGTTCCTCCAAACTGG
	qMtNSP1-F	GCGATTTCGCCACTGGATTC
	qMtNSP1-R	CAGCCTCGCCTTCCATCATT
	qMtD27-F	GAGATGATATTCGGCCAGGAAC
	qMtD27-R	GCATGGTTTTTCTTAGCCTTGC
	qMtUBQ-F	CCCTTCATCTTGTCCTTCGTCTG
	qMtUBQ-R	CACCTCCAATGTAATGGTCTTTCC
	qMtPTB-F	CGCCTTGTCAGCATTGATGTC
	qMtPTB-R	TGAACCAGTGCCTGGAATCCT
	qOsNSP1-F	GTGTCCTTCTGCTCGCTGTG
	qOsNSP1-R	CACGCCGTAGCGCTTAGTAAC
	qOsNSP2-F	TCAGCTGCTTCAACCACAGC
	qOsNSP2-R	TGTTGGGACCCGTCTCCTC
construct and genotyping primers	MtNSP1-t	CTTGTGCTGTAGCCATAAC
	MtNSP1-b	ACAGTAAGGCGAACAAGAG
	MtNSP2-5F	CAATGACCTCCACTTCTCTG
	MtNSP2-7R	TAAAAAGCCCTAACAACAGC
	OsNSP1-f	GGG *CTCGAG* GGCGCAGCAGGATGACA
	OsNSP-mf	GAGGCCGGCAACCTGTCGGTGCTACGCGTGGGGCGA
	OsNSP-mr	TCGCCCCACGCGTAGCACCGACAGGTTGCCGGCCTC
	OsNSP2-r	CGGGGTGGGAGCCGTCGA
EMSA primers	PBE-1F	CAAAGTTTTATAATTTAAGAATCGG
	PBE-1R	CAAATCATGAAAATTGTGTTAAG
	PBE-2F	TCCTTAACACAATTTTCATGATTTG
	PBE-2R	GTAGGCAGAGAATTGCGTC
	PBE-3F	CCTACATTATTTTAATAACATGAATG
	PBE-3R	CTTTGGTTTGTAGAAATTAAGAATAG
	PBE-4F	GCAGTTGCTTTATCAGAATTAAAG
	PBE-4R	CTAAACCAAAAAAATTCATAAGAAAG
	PBE-5F	CTTTCTTATGAATTTTTTTGGTTTAG
	PBE-5R	CAAGTCTAACTTTGAACTAG
	PBE-C1F	AGACACTTAAATTTGAGGGTC
	PBE-C1R	CATGGCAGGTCAAATTAAAAGG
	PBE-C2F	TCTAGATTTCCTAATTTTCCTAAAAC
	PBE-C2R	CTGTTGTGGAATAATTTTCAAAAATG
	biotin-F	biotin*CATGGCCGCGGGATT
	biotin-R	biotin*GCGGCCGCACTAGTGATT
	cMtNSP1-NcoI-F	GGG *CCATGG* ATGACTATGGAACCAAATCCAAC
	cMtNSP1-ClaI-R	GGG *ATCGAT* CTACTCTGGTTGTTTATCCAGTTTCC

Supplemental data Chapter 6

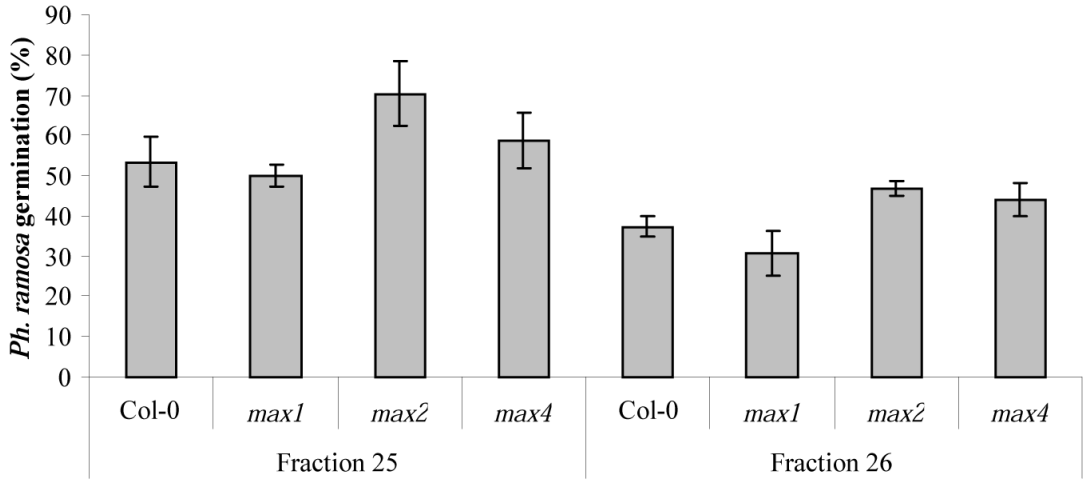

Figure S6.1: Germination of Phelipanche ramosa seeds induced by HPLC fractions 25 and 26 of Arabidopsis (Col-0, max1-1, max2-1 and max4-1) root exudates. Bars represent the average of 3 independent biological replicates ± SE.

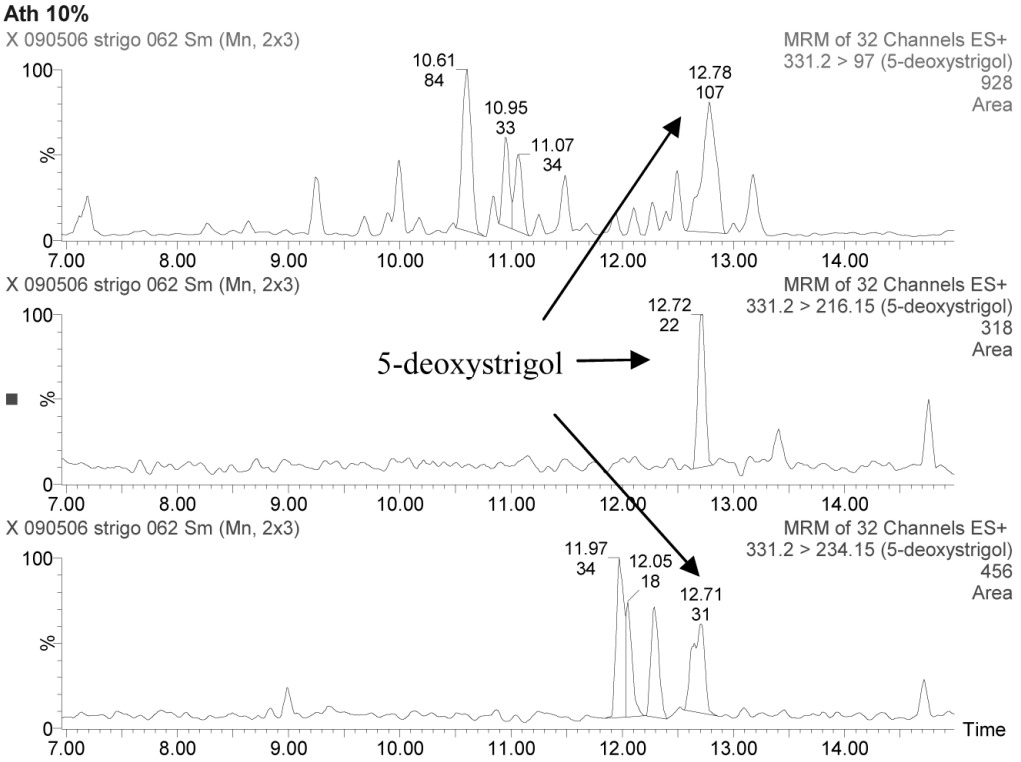

Figure S6.2: MRM-LC-MS/MS analysis of Arabidopsis root exudates from plants grown under phosphate starvation, showing transitions 331.2 > 97, 331.2 > 216.15 and 331.2 > 234.15 for 5-deoxystrigol.

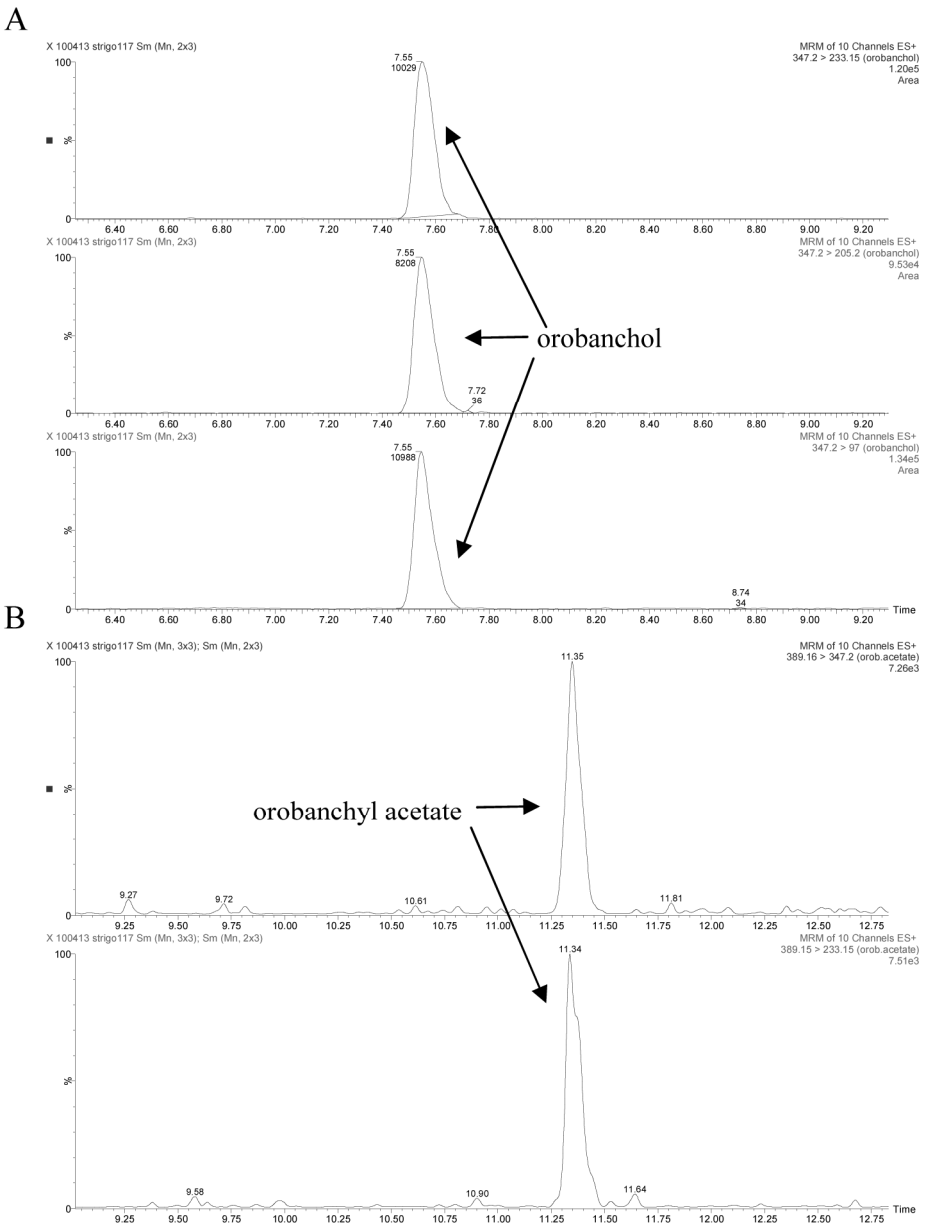

Figure S6.3: MRM-LC-MS/MS analysis of Arabidopsis root extracts from plants grown under phosphate starvation. A, showing transitions 347 > 233, 347 > 205 and 347 > 96.8 for orobanchol. B, showing transitions 389.2 > 233 and 389.2 > 347 for orobanchyl acetate

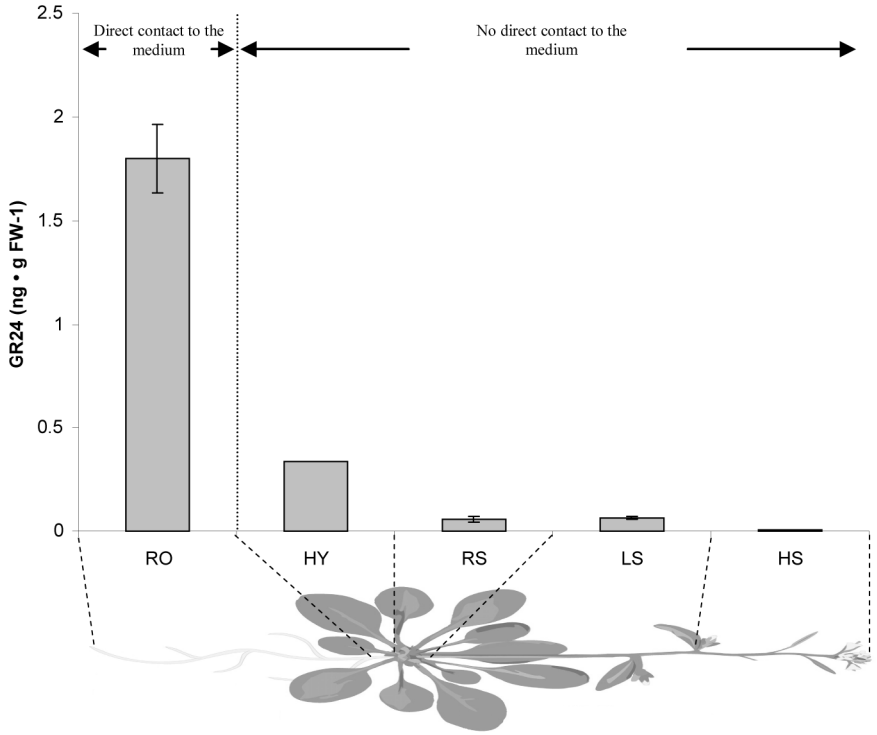

Figure S6.4: MRM-LCMS/MS analysis of GR24 uptake and accumulation by Arabidopsis thaliana tissues (RO = root system, HY = hypocotyl, RS = rosette stem, LS = lower stem and HS = higher stem).

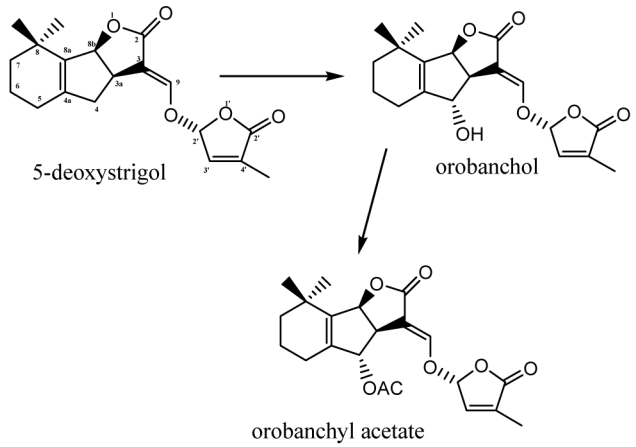

Figure S7.5: Postulated biosynthetic scheme for the strigolactones formation in Arabidopsis (modified from Rani et al., 2008)

Table S1. HPLC fractioned strigolactone standards

Strigolactone standard	HPLC fraction
7-hydroxyorobanchol	11
7-oxoorobanchol	14
7-hydroxyorobanchyl acetate	17
solanacol	17
7-oxoorobanchyl acetate	19
epiorobanchol	20
orobanchol	20
strigol	20
sorgumol	20
GR24	22
orobanchyl acetate	26
sorgolactone	27
5-deoxystrigol	28

Supplemental data Chapter 7

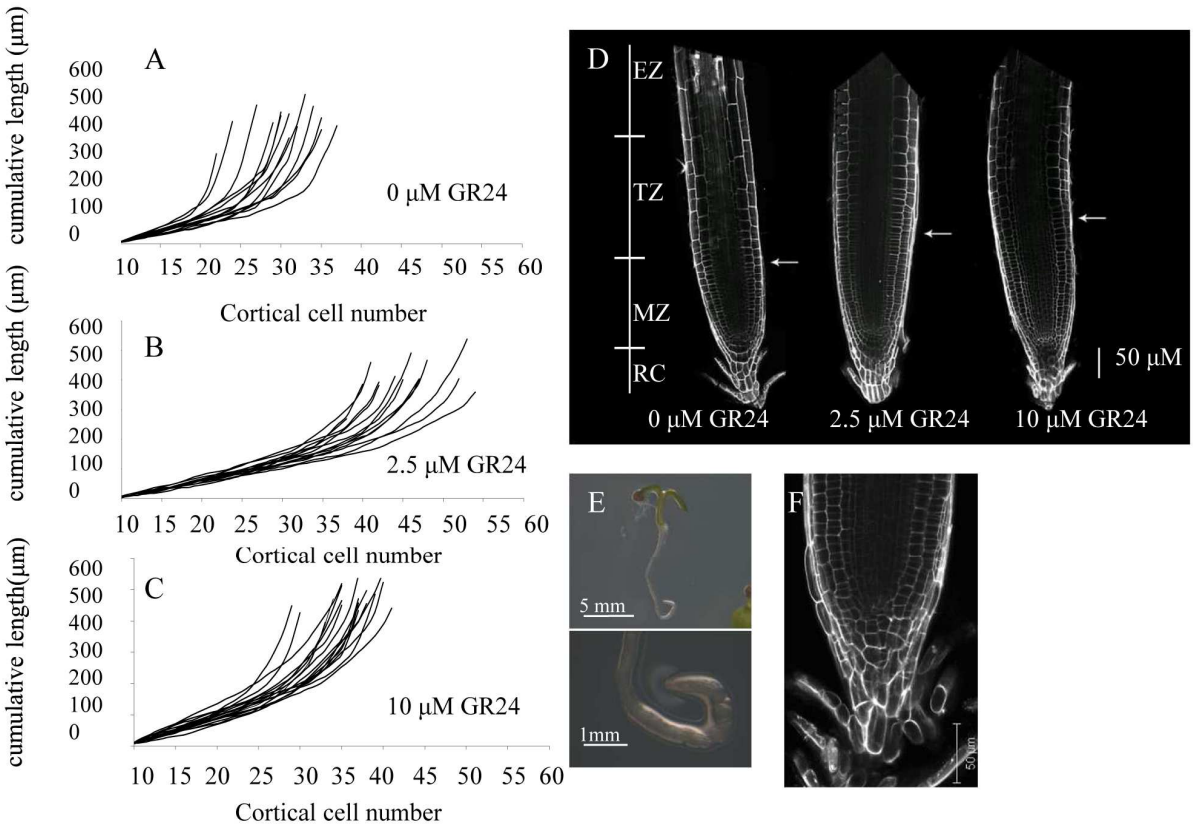

Figure S7.1: Application of GR24 affects cortical root cell dynamics of the proliferation and transition zone in a concentration dependent way. **(a-c),** Cumulative root cortical cell length as a response to different concentrations of GR24 as measured in one cell file starting from the 10th cell above the quiescent centre plotted against the cell number. Lines represent the values of individual 7 day old Arabidopsis wild type plants. The linear, left part of the curves, reflects the meristematic zone in which cells have a relatively constant length.The change in the slope is indicative for the transition from meristematic to elongation zone. **(d)**, Primary root images (confocal microscopy) of propidium iodide stained, untreated and 2.5 resp. 10 µM GR24 treated 7 day old plants. EZ=elongation zone, TZ= transition zone, MZ= meristem zone, RC= columella root cap as observed for the untreated plant. Arrows indicate the approximate start of the transition zones. **(e)**, GR24 induced root curvature in 6 day old Arabidopsis seedlings grown on 1x MS plates in the presence of 5 µM GR24. **(f)**, Confocal microscopy image of the tip of a curved primary root.

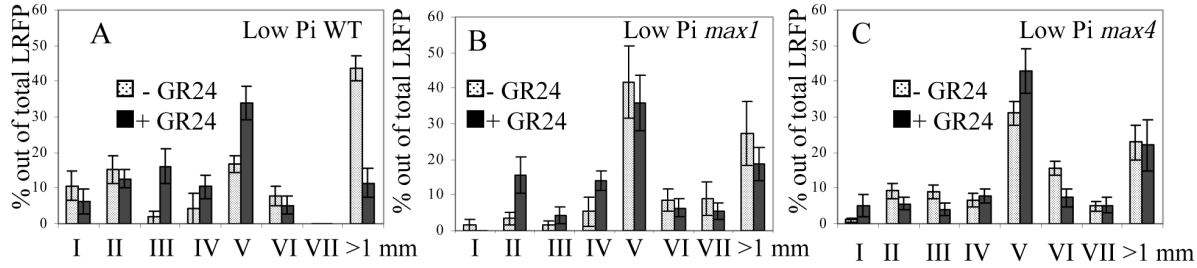

Figure S7.2: The inhibitory effect of GR24 application on LRP development is decreased in plants grown under phosphate limiting conditions. Wild type (WT) **(a)**, *max1-1* **(b)** and *max4-1* **(c).** Plants were pre-grown on vertical MS plates containing sufficient levels (1.5 mM) of Pi. After 5 days, plants were transferred to Pi limiting (20 µM) MS plates supplemented with or without 2.5 µM GR24. When plants were 12 days old, LR developmental stages were characterised according to the scheme of Malamy and Benfey (1997). The yaxis represents the % of each developmental stage out of the total LRFP. Data are means ± SE (n= 15-20).

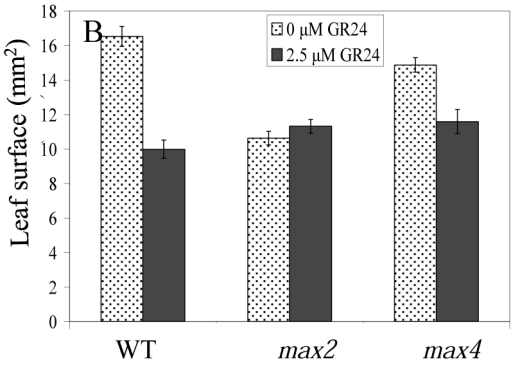

Figure S7.3: GR24 treatment results in a decrease in leaf surface. Leaf surface was decreased by GR24 application in a MAX2 dependent way. Data are means ± SE (n=50-75).

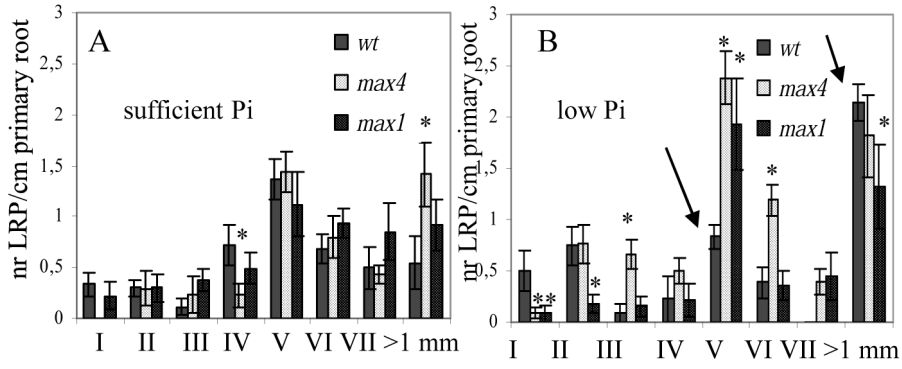

Figure S7.4: The effect of endogenous strigolactones on lateral root development in Pi sufficient **(a)** and Pi limiting conditions **(b)**. **(a-b)**, Density (LRP per cm primary root) for each category of LRP developmental stage, characterised according to the classification scheme of Malamy and Benfey (1997), of 12 day old wild type (wt), *max1-1* and *max4-1* plants carrying the DR5-GUS transgene. Plants were pre-grown for 5 days on vertical MS plates containing sufficient Pi levels (1.5 mM) after which all plants were transferred to either Pi deficient (20 µM Pi) or Pi sufficient MS plates. Arrows indicate the decrease in LRP V and the increase in LR density which is specific for wild type plants. Data are means ± SE (n=15-20). Asterisks indicate significant (P<0.05) differences between max mutant and wild type plants as determined by Student's t-test.

Education Statement of the Graduate School
Experimental Plant Sciences

Issued to: Wouter Kohlen
Date: 7 October 2011
Group: Laboratory of Plant Physiology, Wageningen University & Research Centre

1) Start-up phase	date
► **First presentation of your project**	
The hormonal regulation of strigolactone biosynthese	Feb 18, 2008
► **Writing or rewriting a project proposal**	
The hormonal regulation of axillary meristem formation and development in higher plants (EMBO)	Feb 15, 2011
► **Writing a review or book chapter**	
Kohlen W, Bouwmeester HJ (2007) Ondergrondse communicatie: de driehoeksrelatie gastheerplant, parasitaire plant en mycorrhiza-schimmel. Gewasbescherming 38 (4). - p. 145 - 149.	2007
Kohlen W, Ruyter-Spira CP, Bouwmeester HJ (2011) Strigolactones. A new musician in the orchestra of plant hormones, Canadian Journal of Botany (in press)	2011
► **MSc courses**	
► **Laboratory use of isotopes**	
Subtotal Start-up Phase	*13.5 credits**

2) Scientific Exposure	date
► **EPS PhD Student Days**	
EPS PhD student day, Wageningen University	Sep 13, 2007
EPS PhD student day, Leiden University	Feb 26, 2009
EPS PhD student day, Utrecht University	Jun 01, 2010
► **EPS theme symposia**	
Ecology and Experimental Plant Sciences: From Molecules to Multitrophic Interactions, Wageningen University	Mar 23, 2007
EPS theme 1 symposium 'Developmental Biology of Plants', Leiden University	Jan 30, 2009
EPS theme 3 symposium 'Metabolism and Adaptation', University of Amsterdam	Feb 18, 2009
EPS theme 1 symposium 'Developmental Biology of Plants', Wageningen University	Jan 28, 2010
EPS theme 3 symposium 'Metabolism and Adaptation', Leiden University	Feb 19, 2010
EPS theme 4 symposium 'Genome Biology', Wageningen University	Dec 10, 2010
EPS theme 1 symposium 'Developmental Biology of Plants', Leiden University	Jan 20, 2011
EPS theme 3 symposium 'Metabolism and Adaptation', Wageningen University	Feb 10, 2011
► **NWO Lunteren days and other National Platforms**	
ALW meeting 'Experimental Plant Sciences', Lunteren	Apr 02 & 03, 2007
ALW meeting 'Experimental Plant Sciences', Lunteren	Apr 07 & 08, 2008
ALW meeting 'Experimental Plant Sciences', Lunteren	Apr 24 & 25 2009
ALW meeting 'Experimental Plant Sciences', Lunteren	Apr 19 & 20 2010
ALW meeting 'Experimental Plant Sciences', Lunteren	Apr 04 & 05 2011
► **Seminars (series), workshops and symposia**	
Seminar: Guillaume Bécard	2007
Seminar: Hiroo Fukuda	2007
Semina: Jaakko Kangasjärvi	Mar 13, 2008
Seminar: Zhenbiao Yang	Jun 23, 2008
Seminar: Jian Kang Zhu	Nov 03, 2008
Seminar: Sjef Smeekens	Nov 27, 2008
Seminar: Jan de Ruijter	2009
Seminar: Wim Soppe	Oct 20, 2009
Seminar: Adam Prize	2009
Seminar: Otoline Leyser	Aug 28, 2009
Seminar: Koichi Yoneyama	Jun 25, 2010
Seminar: Takahito Nomura	Jun 25, 2010
Seminar: Adam Prize	Sep 17, 2010
Seminar: Eric Visser	Dec 08, 2010
► **International symposia and congresses**	
Auxin 2008 conference, Marrakesh, Morocco	Oct 04-09, 2008
IPSGA conference 2010, Tarragona, Spain	Jun 28-Jul 02, 2010
► **Presentations**	
Poster presentation "EPS Assessment Report, Peer Review 2003-2008"	Jun 2009
Oral presentation lunteren "Strigolactones play a key role in shoot architectural response to Phosphorous deficiency in non-AM host Arabidopsis	Apr 20, 2010
Oral presentation seminar "Strigolactones are transported through the xylem and play a key role in shoot architectural response to Phosphorous	Jun 25, 2010
Poster presentation IPGSA 2010	Jun 28, 2010
Oral presentation Max Planck institute Cologne "The role of strigolactones in plant development"	Jan 11, 2011
Oral presentation EPS theme 1	Jan 20, 2011
	May 09, 2011
Oral presentation Università di Roma 'La Sapienza' "The regulation of strigolactone biosynthesis, transport and their effect on plant development"	
► **IAB interview**	Dec 04, 2009
► **Excursions**	
Subtotal Scientific Exposure	*18.7 credits**

3) In-Depth Studies	date
► **EPS courses or other PhD courses**	
PhD Summerschool “Environmental signaling: Arabidopsis as a model”	Aug 27-29, 2007
PhD Summerschool “Environmental Signaling”	Aug 24-26, 2009
PhD course 'Basic STATISTICS'	May 26 - June 02 2010
► **Journal club**	
PPH journal club	2008
► **Individual research training**	
Introduction into convocal microscopy (PCB, wageningen university)	May 2009
Tomato transformation at Plant Reasearch International (Plant Research International, Wageningen)	Mar-Jun 2010
Root microbiome experiments (Max Planck, Cologne)	Jun 2011
Subtotal In-Depth Studies	*7.1 credits**

4) Personal development	date
► **Skill training courses**	
Communication with the Media and the General Public	Oct 07-08 & Nov 02, 2010
► **Organisation of PhD students day, course or conference**	
Co-organisation theme 3 day 2011	Feb 10, 2011
Co-organisation mini-symposium "Parasitic plants and strigolactones more than rhizosphere communication"	Oct 07, 2011
► **Membership of Board, Committee or PhD council**	
Subtotal Personal Development	*3.0 credits**

TOTAL NUMBER OF CREDIT POINTS*	**42.3**

Herewith the Graduate School declares that the PhD candidate has complied with the educational requirements set by the Educational Committee of EPS which comprises of a minimum total of 30 ECTS credits

** A credit represents a normative study load of 28 hours of study.*

Lay-out: Wouter Kohlen
Cover image: *Phelipanche ramosa* grown on *Arabidopsis thaliana max1* (Photograph Peter Tóth)